Università
Ca'Foscari
Venezia

Scuola Dottorale di Ateneo
Graduate School

Dottorato di ricerca
in Scienze Chimiche
Ciclo XXIX
Anno di discussione 2015/2016

Continuous-flow procedures for the chemical upgrading of glycerol

SETTORE SCIENTIFICO DISCIPLINARE DI AFFERENZA: CHIM/06
Tesi di Dottorato di Sandro Guidi, matricola 808541

Coordinatore del Dottorato

Prof. Maurizio Selva

Tutore del Dottorando

Prof. Maurizio Selva

Co-tutore del Dottorando

Prof. Alvise Perosa

Abstract

In the past twenty years, the biodiesel industry has cogenerated enormous quantity of glycerol as a byproduct. This situation lead to two important consequences: i) with the steady growth of the biodiesel production, the market experienced an unprecedented excess of glycerol whose price collapsed worldwide. During 2000-2010, In the EU (the main biodiesel producer), the decline was almost by a factor of 10: from 4000 USD/ton to 450 USD/ton; ii) the overabundance of glycerol, as a low-cost source of renewable carbon, has fueled a huge interest in both the academy and industry toward research programs for the conversion of glycerol and its derivatives in energy and especially in high value added chemicals. The latter aspect was the subject of the PhD thesis.

The experimental work was divided in three main areas which common denominator was the use of continuous flow synthesis techniques (CF).

- The development of new methodologies for the upgrading of glycerol to cyclic acetals. The glycerol acetals, in particular light ones deriving from formaldehyde and acetone, are compounds of interest especially in the field of green solvents. The reaction of acetalization was studied by comparing two types of catalysts such as Amberlyst resins and $AlF_3 \cdot 3H_2O$, the latter never previously investigated for this reaction. Although the acid resins proved to be more active respect to $AlF_3 \cdot 3H_2O$, the most interesting result of this study was that the aluminum fluoride has been able to effectively catalyze the acetalization of crude-like glycerol, i.e. contaminated glycerol with common impurities (water, methanol and inorganic salts) resulting from the production of biodiesel in the biorefinery processing. On the other hand, the same crude reagent rapidly and irreversibly deactivate the Amberlyst system. XRD characterization studies of $AlF_3 \cdot 3H_2O$ shown that the active phase of the catalyst is conceivably a solid solution of the formula $Al_2[F_{1-x}(OH)_x]6(H_2O)_y$ as a component of the investigated commercial sample.

- This part of the thesis work has been developed at The University of Nottingham in the laboratories of the Clean Technology Group (CTG). The GTG in collaboration with a leading company in the processes and technologies for

the use of niobium, is studying and developing new applications of niobium oxides as catalysts. In this context the idea was to investigate continuous flow methodologies for the dehydration of glycerol in the presence of a strong acid such as niobium phosphate ($NbOPO_4$). The thesis work has therefore focused on the Skraup reaction for the conversion of glycerol into quinoline, with the aim of replacing the conventional catalyst (concentrated H_2SO_4) with such oxide. The reaction was initially studied with aniline as a model amine and then extended to a variety of aromatic amines. In all cases, niobium phosphate have proven to be a catalyst for the Skraup condensation.

- The thermal synthesis with organic carbonates (OCs). The OCs, in particular the lightest terms of the series dimethyl carbonate and diethyl carbonate (DMC and DEC) are non-toxic compounds considered among the most promising green reagents for both the alkylation reactions and transesterification. In the thesis work, the thermal transesterification was particularly investigated (without catalyst) in a continuous flow of DMC, DEC and dibenzyl carbonate, with glycerol and its acetals. This unconventional method has proved to be very effective. Not only the feasibility of the thermal reaction is demonstrated, but the optimization of the main parameters (T, p, and flow rate of the reagents) has allowed to isolate transesterification derivatives with excellent yields. In the absence of any catalyst, the flow in the reaction can be performed virtually indefinitely, with simplified downstreaming operations for the purification of the products with high productivity.

List of abbreviations

A15	Amberlyst-15
A36	Amberlyst-36
ACS	American Chemical Society
AF	Aluminum fluoride trihydrate ($AlF_3 \cdot 3H_2O$)
AFc	$AlF_3 \cdot 3H_2O$ calcined in air at 500 °C for 5h
APR	Aqueous phase reforming
BFB	Bubbling fluidised bed
BPR	Back pressure regulator
CBMM	Companhia Brasileira de Metalurgia e Mineração
CF	Continuous flow
CFB	Circulating fluidised bed
CG	Crude glycerol
CSTR	Continuous stirred tank reactor
DAlCs	Dialkyl carbonates
DBE	Dibenzyl ether
DBnC	Dibenzyl carbonate
DEC	Diethyl carbonate
DEG	Diethylene glycol
DFT	Density functional theory
DFT	Density functional theory
DMC	Dimethyl carbonate
DME	1,2-dimethoxyethane
EC	Ethylene carbonate
ECN	Energy research Centre of the Netherlands
EG	Ethylene glycol

FAEE	Fatty acid ethyl esters
FAGCs	Fatty acid glycerol carbonate monoesters
FCCX	Food Chemicals Codex
FDA	Food and Drug Administration
FEMA	Flavor and Extract Manufacturers Association
FFA	Free fatty acid
FICFB	Fast Internal Circulation Fluidised Bed
FPR	Flow photochemical reactors
GAs	Glycerol acetals
GCI	Green Chemistry Institute
GFR	Gas flow reactor
GHG	Greenhouse gases
GHSV	Gas hourly space velocity
GK	Glycerol ketal
GlyC	Glycerol carbonate
GlyF	Glycerol formal
GMEs	Glycerol Monoethers
GRS	Generally Recognized As Safe
HEEPM	High Efficiency Electro-Pressure Membrane
HVLV	High-value low-volume
ICSD	Inorganic Crystal Structure Database
IEA	International Energy Agency
IFP	Institut Francais du Pétrole
LCF	Lignocellulose feedstock
LDH	Layered double hydroxides
LHSV	Liquid hourly space velocity

LVHV	Low-value high-volume
MDA	4,4'-methylenedianiline
MONG	Matter organic non-glycerol
MR	Microreactor
NA	Nicotinic acid
NbP	Niobium phosphate
NBS	N-Bromosuccinimide
NREL	National Renewable Energy Laboratory
OCs	Organic carbonates
PBR	Packed bed reactor
PC	Propylene carbonate
PDO	Propanediols
PEI	Potential environmental impact
PFR	Plug flow reactor
PNNL	Pacific Northwest National Laboratory
Qui	Quinoline
SS	Solid solution
SV	Space velocity
TBDMS	Tert-butyldimethylsilyl
TDS	Total dissolved solids
TGs	Triacylglycerols or triglycerides
THP	Tetrahydropyranyl
US DOE	United States Department of Energy
USP	United States Pharmacopeia
WGS	Water–gas shift
WHSV	Weight hourly space velocity

XRD	X-ray diffraction
XRPD	X-ray powder diffraction
YTD	Year to date

INDEX

1 INTRODUCTION

1.1 The energy supply

Energy is indispensable for human life and a secure supply is crucial for the sustainability of modern societies. In the last two centuries, the growth of the world population from 1 to 7 billion people has brought about an increase of global energy consumption from 20 to over 500 exajoules in 2010 (Figure 1.1). [1]

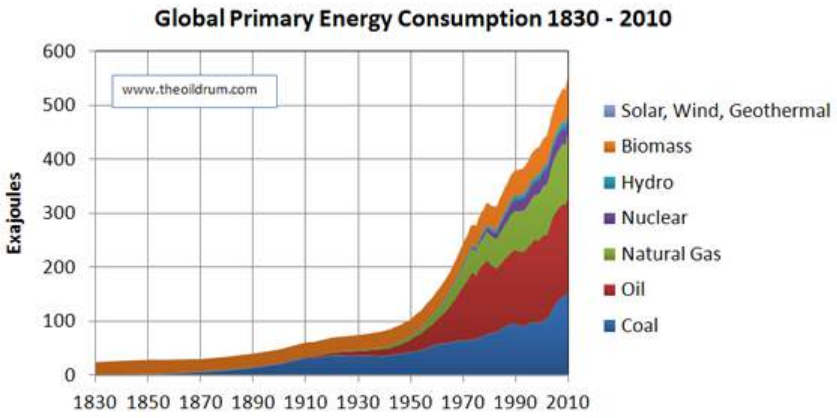

Figure 1.1. Stacked graph of the global primary energy consumption[2]

Not surprisingly, this hunger for energy is the most critical aspect dealing with the survival of our Planet and one of the great issues that the current energy business has to cope with is how best to sustain basic operations including heat, light, transportation and services as well as the production of necessary goods. According to the U.S. Department of Energy, fossil fuels and nuclear power account for nearly 90% and 5% of the world energy, respectively, while only a minor residual share is offered by alternative renewable sources.[3] Both private and public sectors have been and are debating on solutions to not deplete fossil sources, but the answer still seems a long way off with all the consequent implications from social and environmental standpoints. At present, the only certainty is that the global fossil fuel consumption is expected to further increase by 2020.

1.1.1 Crude oil and related issues

Historically, wood was the first energy source used by mankind, but it then appeared that coal and fossil fuels were more convenient: they were not only very stable and

abundant, but also much more effective to satisfy human needs. These two sources were so used for centuries. With the advent of the industrial revolution in 19th century, as the mankind creativity exceeded expectations, liquid fossil fuels saw an apex on their consumption because they proved to be more active and flexible with respect to their solid counterparts. Furthermore, also gaseous (fossil) fuels started to be used to produce energy and implement new technologies. This transition from wood to coal, and then to oil-derived liquids and gases wrote the eras of the different traditional fossil fuels.[4]

Today, there is no doubt about the leading role preserved by oil for both the energy production and the chemical manufacture of plastics, solvents, fertilizers, pesticides and pharmaceutics, etc.[5] Of the major advantages, the three most consistent aspects include:

- *High Energy Density*. Oil has one of the highest energy density among the known sources, which means that a small amount of oil can produce a large amount of energy. This makes oil the most convenient choice to prepare transportation fuels.
- *Availability.* Oil is widely distributed in several geographic regions of the Earth both in emerged lands and deep seas. A massive infrastructure network including ships, pipelines and tankers, exists to transport oil from drilling wells to the refineries plants.
- *Constant quality and flexible uses.* Unlike solar and wind energies, oil can produce power through highly reliable supplying services, most often operating on a 24/7 basis. Moreover, no other sources can compete with oil for the synthesis of chemicals as well as for the manufacture of many items of daily life.

On the other hand, the use of oil has also some remarkable undesirable consequences. Two of them are of utmost importance:

- *Fluctuating price.* The fluctuation of crude oil price largely depended on the historical events which involved oil-producing Countries and/or the major upheavals of financial markets (Figure 1.2). Such an instability caused severe economic problems over the years: for example, according to some analysts, the variability of the oil price was one of the large contributors to the Euro crisis that hit southern Europe in 2007-08.[6]

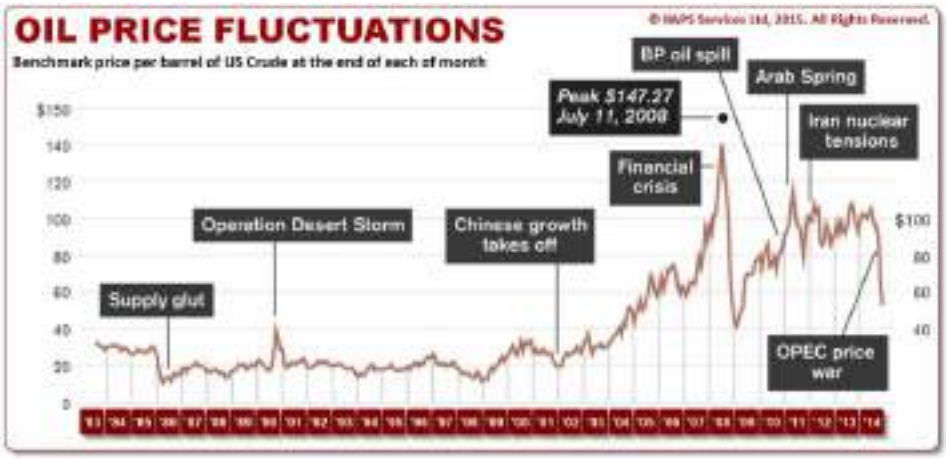

Figure 1.2. Oil price fluctuations and related events.[7]

It should be noted that changes of the crude oil price affect primarily the energy generation and transports, but they also impact on many other subsidiary businesses and service trades.

- *The environmental issue.* Looking at the crude oil issues only from the economic point of view, one risks to miss the real-world problem which is simply summarized by the fact that our World is finite. The Earth cannot offer infinite resources nor it has the unlimited ability to handle the excess pollution deriving from the exploitation of fossil fuels. Crude oil, coal and natural gas are by their own nature not renewables meaning that they cannot be regenerated once oxidized by combustion processes, and even most importantly, the burning of hydrocarbons emits immense amounts of greenhouse gases (GHG) in the Earth atmosphere. Scientific investigations leave no doubts that the rapid growth of GHG is raising the Earth's temperature and it is changing the climate with many potential catastrophic consequences.[8] If the model case of CO_2 (the most important GHG) is considered,[9] in 2013, the atmospheric concentration of this gas reached a level of 396 ppm which corresponded to a growth of about 42% compared to the pre-industrial era.[10] Anthropogenic CO_2 emissions are the largest contributor (63.5%) to the global warming (Figure 1.3), and due to fossil fuel combustion, they are expected to rise of about 32% from 2007 to 2030.[11]

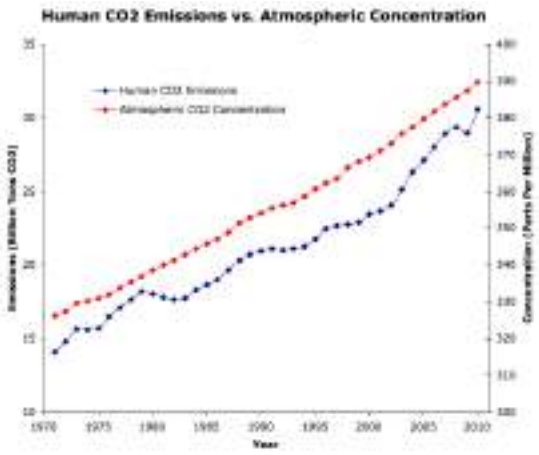

Figure 1.3. Anthropogenic CO_2 emission and atmospheric CO_2 trend.[12]

Starting from the Kyoto Protocol (December 1997) followed by 15th Conference of Parties to the United Nations Framework Convention on Climate Change (Copenhagen, December 2009), and the recent COP-21 (Paris 2015),[13] massive efforts have been addressed to limit GHG emissions through policies agreed from Governments of many different Countries. These strategies have marked important turning points aimed at lowering GHG via a gradual increase of the use of renewable energies which are intrinsically beneficial to the Environment,[14] may reduce healthcare costs,[15] and make non-producer Countries less dependent on fluctuations of oil prices caused by geopolitical factors.

The GHG release is not the only environmental issue to be considered. Oil spills from oil tanks and drilling wells represent another concern which may literally devastate entire ecosystems. Only to cite few cases, the disasters of the sinking of Exxon Valdez (Prince William, Alaska, 1979) and Haven tankers (Genoa, Italy, 1991) and the explosion of semi-submersible offshore oil drilling rig Deepwater Horizon (Gulf of Mexico, USA, 2010) are among the most sadly famous examples.[16]

Ultimate solutions to these critical problems are far from being established. Nonetheless, a perspective may be offered by the use of biomass-derived feedstocks.

1.1.2 Biomass vs fossils: carbon footprint and renewability

Most abundant and widespread types of biomass come from plants including wood, crops (wheat, maize, rice, etc) and agricultural wastes, while a minor source (about 10% of the total available amount) of organic decomposable matter derives from food waste and manure.[17] By its own nature, biomass is an immense carbon sink: if fully combusted for the production of energy, the direct carbon emission in the form of CO_2 produced from

(vegetable) biomass is offset by the carbon fixation during photosynthetic processes involved in the growing stage of plants.[18] Though, the entire cycle cannot be considered truly carbon-neutral since a net carbon footprint is caused by the indirect carbon emission generated along the supply chain of biomass, especially by transportation activities.[19]

The concepts of the carbon cycle and quasi-zero carbon emissions offer important marking points to distinguish the characteristics of biomass from fossil resources. Another fundamental feature stands on the renewability of biomass which is its capability of being continuously replaced and indefinitely available within a natural ecologic cycle occurring in the human lifetime. Biomass belongs to resources that will not deplete the earth wealth for the future generations as they can be continually regrown or regenerated at a rate higher or equal than that they are consumed.[20] Since renewability implies the replication of Nature's processes, the occurrence and use of biomass share both the strength and weakness of natural transformations and events. Biomass is obviously intrinsically eco-compatible, but it possesses a low energy density (energy per unit volume) and a high specific land use (energy per unit area). Moreover, i) vagaries of Nature including storms and floodings do not allow to secure a steady production of biomass, and ii) biomass resources are often available only in remote locations which means that building infrastructures, to transfer biomass energy over long distances to urban settings, would tend to increase its cost.

On balance however, the use of biomass must be explored and implemented especially in those regions (*e.g.* in Europe) where it is imperative to reduce the dependence on foreign imports of crude oil and natural gas. Beyond the energy supply, biomass may become also an excellent feedstock for the production of a variety of chemicals from lubricants, to plastics, building materials, etc.[21]

Of the different types of biomass, two categories can be considered of major importance:

Lignocellulose and starch. As already stated, photosynthetic processes allow plants to combine solar energy, carbon dioxide and water to form mainly carbohydrate building blocks $(CH_2O)_n$. Carbohydrates are stored in plant cells in the form of polymeric structures such as cellulose which is comprised of glucose units linked via β-glycosidic bonds, and hemicellulose which is a copolymer composed of C_6 and C_5 sugars (*e.g.* xylose and arabinose).[22] The relative proportions of these two polymers depend on the type of plant and they usually range from 30-60 wt% for cellulose and 10-40 wt% for hemicellulose.

Another significant component is lignin. This is the third most abundant structural polymeric material found in plant cell walls comprising up to 20-30% of vegetable biomass (Figure 1.4).[23] Lignin is non-carbohydrate polymer based on an aromatic crosslinked structure derived principally from coniferyl alcohol. The major function of lignin is to bind hemicellulose and cellulose together in plant cell walls and shields, thereby protecting the cell from enzymatic and chemical degradation. Lignin is also the only known renewable source of aromatic compounds.

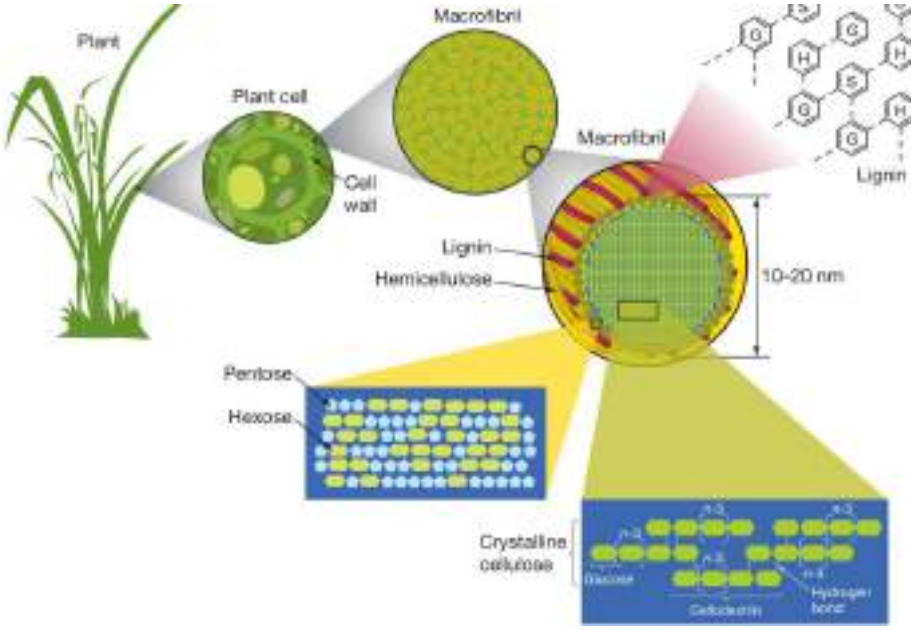

Figure 1.4. Membrane structure of plat biomass.[23]

Plants are also able to produce starches which are another important family of substances designated to energy storage. Similarly to cellulose, starches are biopolymer based on glucose units, but in this case, the single monomers are linked via α-glycosidic bonds. This peculiarity imparts a non-rigid crystal structure to starches that, unlike cellulose, can be easily hydrolyzed.

Lipids. Different kinds of plants including palm, soybeans, sunflower, rapeseed and microalgae are excellent sources of triglycerides (triacylglycerols, TGs), which are the main components of oils or fats (lipids).[24] Lipids are a broad group of naturally water-insoluble molecules, which includes fatty acids, waxes, sterols, oil-soluble vitamins, phospholipids, terpenes and others. TGs are formally esters of glycerol with three different (or identical) molecules of fatty acids. This structure makes them high-energy density materials which beyond common uses for cooking, food purposes, lubricants and raw materials for detergents and chemicals, find remarkable applications also in the biofuels sector.

1.2 The Biorefinery: definition, current status and perspectives

As above mentioned, biomass derived feedstocks represent the best option to both reduce the consumption of fossil fuels and mitigate climate changes. A biorefinery is the facility able to integrate processes and equipment for the conversion of almost all the types of natural feedstocks into different classes of transportation biofuels, power, and chemicals.[25] Similarly to oil-based refineries, where many energy and chemical products are produced from crude oil, biorefineries will produce many different industrial products from biomass (Figure 1.5). [26]

Figure 1.5. Comparison of petro-refinery vs biorefinery.[26]

Among the several definitions of biorefinery, one of the most exhaustive description was recently coined by the International Energy Agency (IEA) Bioenergy Task 42: "Biorefining is the sustainable processing of biomass into a spectrum of marketable products and energy".[27]

It should however be noted that main biobased products are today obtained from conversion of biomass to basic products like starch, oil and cellulose, and most of the existing biofuels and biochemicals (*e.g.* lactic acid, amino acids, etc.) are currently produced in single production chains. This means that the manufacture does not occur within the concept of an integrated biorefinery, and it often requires materials that may be in competition with the food and feed industry. If a forward looking approach is the stepwise conversion of large parts of the global economy and industry into a sustainable biobased society having bioenergy, biofuels and biobased products as main pillars, then new synergies among biological, physical, chemical and technical sciences must be developed to improve the exploitation of biomass-derived feedstocks and generate the bio-industries of the future.[28] For example, through a better use of lignocellulosic crops which, in comparison with conventional crops, are able to: i) reduce the competition for fertile land since they may be grown on lands not suitable for agricultural crops; ii) rely on larger yields of biomass per

hectare since the whole crop is available as a feedstock. Moreover, technologies for the conversion of biomass must be designed to be totally (or for the most part) carbon neutral, meaning that they must avoid/minimize the consumption of non-renewable energy resources and the related environmental impacts during biorefinery processing.[29] To cope with these objectives, biorefineries are expected to develop as dispersed industrial complexes able to revitalize rural areas. Unlike oil refinery, which almost invariably means very large plants, biorefineries will most probably encompass a whole range of different-sized installations able to process different flows of raw materials in order to maximize the use of all biomass components. The overall setup will take advantage of the implementation of a series of task-specific unit operations in each bio-plant which will favor an integrated bio-industrial systems, where the residue from one bio-industry (*e.g.* lignin from a lignocellulosic ethanol production plant) becomes an input for other factories.[30] Accordingly, high-value low-volume (HVLV) will enhance profits, while low-value high-volume (LVHV) compounds will be converted into fuels to help the global energy demand through renewable feedstocks.

Going back to the current situation, even if the biorefinery world is relatively young, it has already evolved since its first formulation. This progress has been dictated by the need of improving both the conversion of the starting materials and the flexibility of bio-factories. The first model was the so called phase 1 biorefinery: this was designed to receive a single input (*i.e.* only one bio-feedstock) and produce a single output (a defined product) through a single well-defined process (Figure 1.6, top).

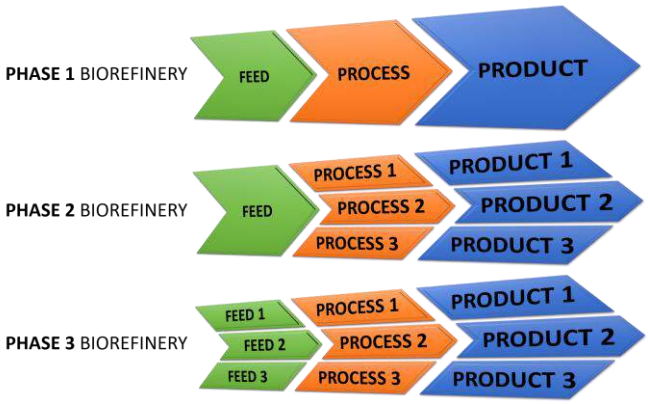

Figure 1.6. Evolution of the Biorefinery.

A dry mill ethanol plant, illustrated in Figure 1.7, is an example of a phase 1 biorefinery which produces a fixed amount of ethanol, other feed products, and carbon dioxide and has almost no processing flexibility.[30]

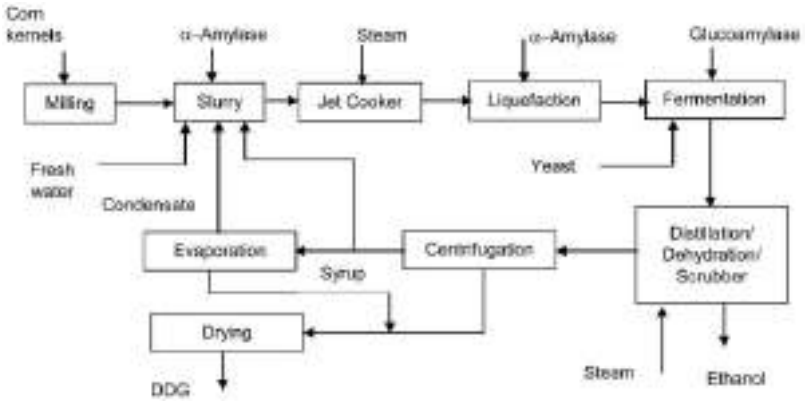

Figure 1.7. Representation of a dry mill ethanol process plant. [30]

Such an approach however, was neither versatile nor economically sustainable. The natural advancement was the establishment of phase 2 biorefineries in which different processes could be implemented to produce more than one product from a single feed (Figure 1.6, mid). A remarkable commercial example of such an installation is the Novamont plant which is operating in Italy for the conversion of starch (from corn and other crops) to a range of chemical products, producing annually over 80000 tons of biodegradable polyesters (Origo-Bi), biodegradable and compostable bioplastics (Mater-bi) and biolubricants (Matrol-bi).[31] However, considering that the nature and availability of bio-feedstocks may be rather discontinuous depending on seasons and local harvesting, an ideal refinery should be able to process different sources, also including bio-wastes. Such a facility in which a mix of biomass feedstocks may be treated by several processes to obtain an array of products identifies the phase 3 biorefinery (Figure 1.6, bottom).[26]

A phase 3 biorefinery must obviously employ a combination of technologies to obtain higher-value chemicals and co-produce fuels (*e.g*. ethanol) to be used either for the operation of the plant or sold in the market.[30] Phase 3 biorefineries, namely, *whole-crop*, *green*, and *lignocellulose feedstock* (LCF) biorefineries, have been already designed, but the complexity of such arrangements is so high that these plants still do not have a commercial exploitation. To cite an example, Figure 1.8 depicts the flow-chart of a *whole-crop* biorefinery where raw materials such as wheat, rye, triticale, and maize can be used as input in different unit operations. The overall conversion process initiates by the mechanical separation of biomass (cereals and corn) into different components that are then treated separately. The

straw undergoes high-temperature decomposition and gasification to produce lignin, cellulose, and syngas, respectively. While, starch may be either mechanically treated to yield bio-plastics, binders, adhesives, etc., or chemically/biochemically converted to produce sugars and other derivatives along with ethanol as a bio-fuel. Syngas may be further used for the synthesis of fuels and methanol through the Fischer Tropsch process.

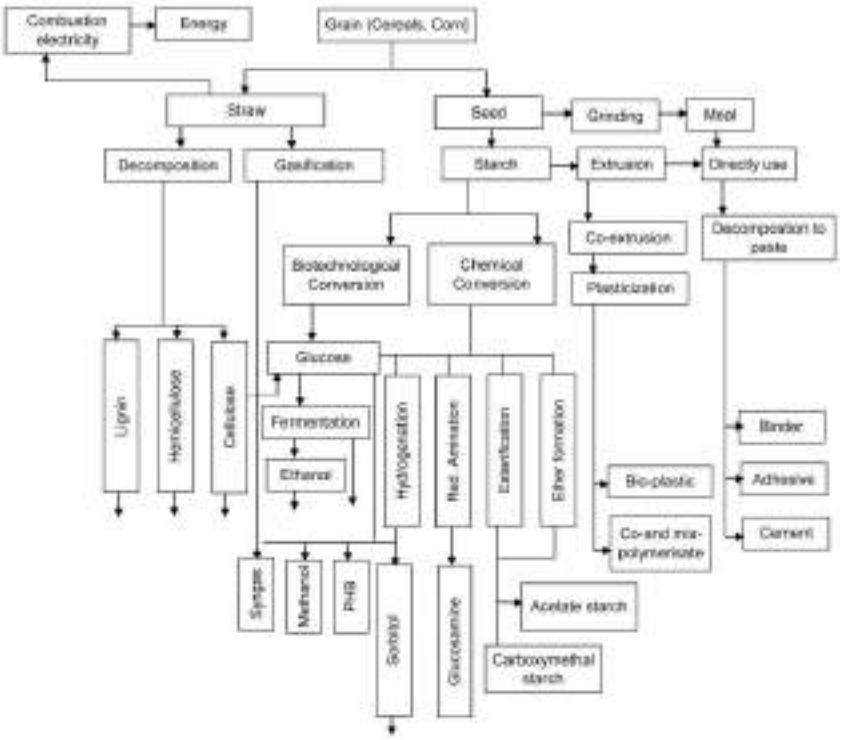

Figure 1.8. Representation of *whole-crop* biorefinery process and products.[30]

1.2.1 Biorefinery feedstocks and their processing

A crucial step of any biorefinery system is the availability of a renewable, consistent and regular supply of raw materials (feedstocks). A general initial evaluation is often required to increase the energy density of feedstocks by reducing their transportation, handling and storage costs. Then, a further distinction is between feedstocks coming from dedicated crops, residues from agricultural, forestry and industrial activities, which can be available without upstream concerns. The technological approaches that are used for the treatment of such materials aim at the depolymerization and the deoxygenation of the biomass components. Even though these (approaches) must be often jointly applied, they can be divided in four main groups (a-d):

a) *Thermochemical*. There are three main thermochemical biomass transformation processes to obtain energy and chemical products (Figure 1.9).

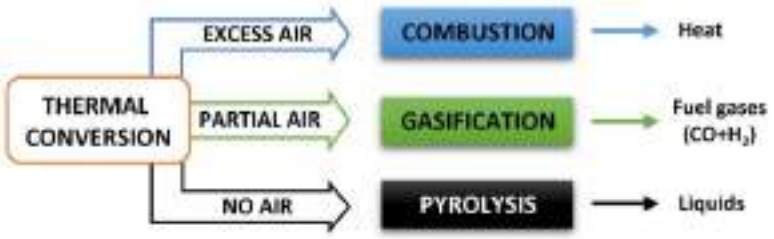

Figure 1.9. Thermal biomass conversion processes.

The combustion treatment burns the organic matter in the presence of an overstoichiometric oxidant (normally oxygen) to produce primarily carbon dioxide and water. Heat is the final desired outcome.

The pyrolysis is the second thermochemical pathway which uses moderate temperatures (300–600 °C) in the complete absence of oxygen. A set of complex reactions convert the feedstock into liquid oil (or bio-oil), solid charcoal and light gases similar to syngas[32] including hydrocarbon gases, hydrogen, carbon monoxide, carbon dioxide, tar and water vapor. A model flexible system used for the pyrolysis of cedar sawdust, coffee bean residues and rice straw is shown in Figure 1.10.[33]

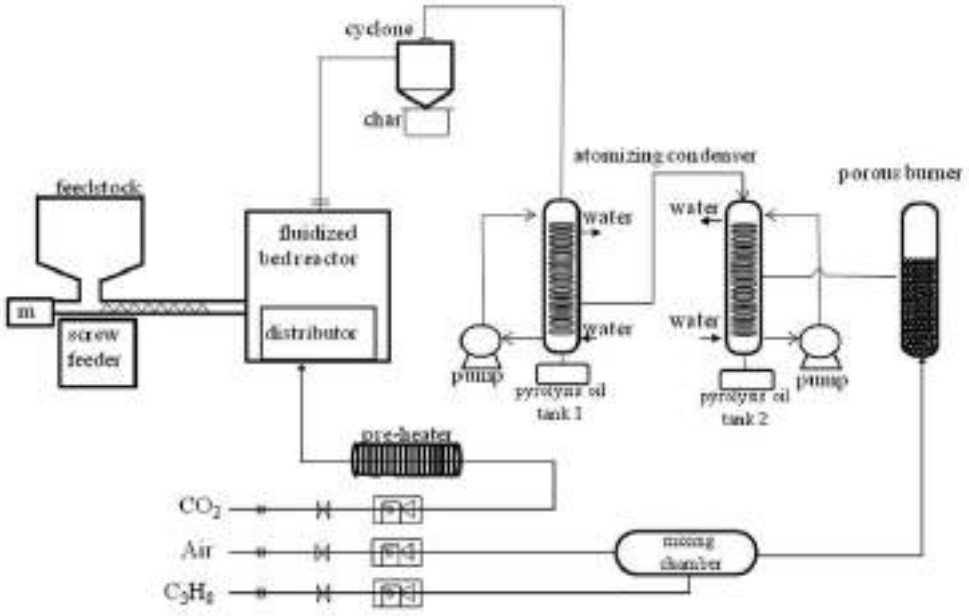

Figure 1.10. Example of biomass pyrolysis system.[33]

The pyrolysis yields vary with process conditions, but for the biorefinery purposes, the most desirable treatment should maximize the production of bio-oil (pyrolysis oils: tanks 1 and 2).

The gasification is the third thermochemical treatment by which at very high temperatures (700-1000 °C), biomass produces syngas (H_2 and CO), CO_2 and CH_4.[34] The process can be further differentiated in direct (autothermal) and indirect (allothermal) operating modes which are identified as: i) fixed-bed updraft, ii) fixed-bed downdraft, iii) fluidised bed (bubbling and circulating, i.e. BFB and CFB) and iv) indirect fluidised bed (steam-blown). For most biomass applications, the gasifiers are operated with air which affords a product gas diluted with nitrogen. If a nitrogen-free gas is required for advanced uses, this can be produced by an oxygen-blown gasification or by alternative indirect processes including Fast Internal Circulation Fluidised Bed (FICFB) based systems. The latter technology (FICFB) represents the most attractive option since a N_2-free gas is generated from the gasification of biomass in the complete absence of oxygen. The basic idea of this reactor is to separate the gasification and combustion and increase the calorific value of the product gas without using oxygen. Biomass fuel is fed into the gasification zone where it devolatilizes and gasifies in the presence of steam fed through the bottom of the bubbling fluidised bed. Residual char from these reactions circulates with bed material into the combustion zone where it is combusted with air in a circulating fluidised bed, heating the bed material. Combustion gases are separated from the hot bed material, which is circulated into the gasification zone, without mixing of the combustion and gasification product gases, providing the heat for the endothermic gasification reactions.[35] Under such conditions, the conversion is generally complete, whereas, direct processes often produce carbon-containing ashes. Examples of FICFB-processes have been developed by the Vienna University of Technology,[36] the SilvaGas process based on the Batelle development,[37] and the MILENA gasifier developed at the Energy research Centre of the Netherlands (ECN, Figure 1.11).[38]

Figure 1.11. Schematic representation of the MILENA gasifier (left) and the 5 kg/h lab scale MILENA indirect gasification reactor at ECN.[38]

Syngas from FICFB-processes can be directly used as a stationary biofuel or can be used as an intermediate (platform) to produce a wide range of chemicals such as alcohols, organic acids, ammonia, methanol, etc.

b) *Biochemical.* The most common types of biochemical treatments are fermentation and anaerobic digestion. These both occur at lower temperatures and have lower reaction rates than thermochemical processes. The fermentation uses microorganisms or enzymes to convert organic substrates into different products, usually alcohols or organic acids. Ethanol is currently the most required fermentation product of sugars, specifically of hexoses. Also, the fermentation of pentoses, glycerol and other hydrocarbons has been investigated through customized micro-organisms.[39] Anaerobic digestion involves the bacterial breakdown of biodegradable organic material in the absence of oxygen at temperatures of 30-65 °C. The major end product of these processes is biogas (a mixture of methane, CO_2 and other impurities), which can be upgraded up to >97% of methane content and used as a surrogate of natural gas.[40]

c) Mechanical/physical. Mechanical processes are usually applied before the utilization of the biomass: these treatments do not change the chemical composition of the starting materials, but only perform a size reduction or a separation of the feedstock components.[41] For example, the split of lignocellulosic biomass into cellulose, hemicellulose and lignin falls within this category, even if some hemicellulose is partially hydrolyzed to the sugars components.[42]

d) *Chemical processes.* The most common chemical processes for the conversion of biomass are based on hydrolysis and transesterification reactions. Both transformations are

carried out in the presence of different catalysts including acids, bases or enzymes: hydrolysis is used to depolymerize polysaccharides and proteins into their component sugars (e.g. glucose from cellulose) or other derivatives (e.g. levulinic acid from glucose),[42] while transesterification is primarily employed in the manufacture of biodiesel from natural oils (see later on this chapter). Among other chemical reactions used in the processing of biomass derived feedstocks are Fisher–Tropsch synthesis, methanisation, and steam reforming.

1.2.2 Platform chemicals from biomass

Biomass is an exceptional source of chemical diversity from simple molecules to highly polyfunctionalized substrates. A not trivial issue is therefore the identification of the most promising products or families of compounds towards which research and investments should be addressed. In the past fifteen years, of the many analyses performed to sort out this complex scenario, the extensive work commissioned by the US Department of Energy in 2004 to the National Renewable Energy Laboratory (NREL) and the Pacific Northwest National Laboratory (PNNL) and its revision in 2010 probably represent the best guidelines in this field.[43,44] These studies have proposed for the first time, a systematic and detailed classification of bio-based chemicals by adopting concepts and selection conditions employed in traditional petrochemical industry flow-charts. Starting from an initial list of over 300 candidates, the use of screening criteria including the type of raw material, the estimated processing costs, the estimated selling price, the chemical functionality, the potential use and development in the market, etc., allowed to identify a restricted list of compounds or building blocks, the so called top platform chemicals, which were grouped according to the categories shown in Figure 1.12.

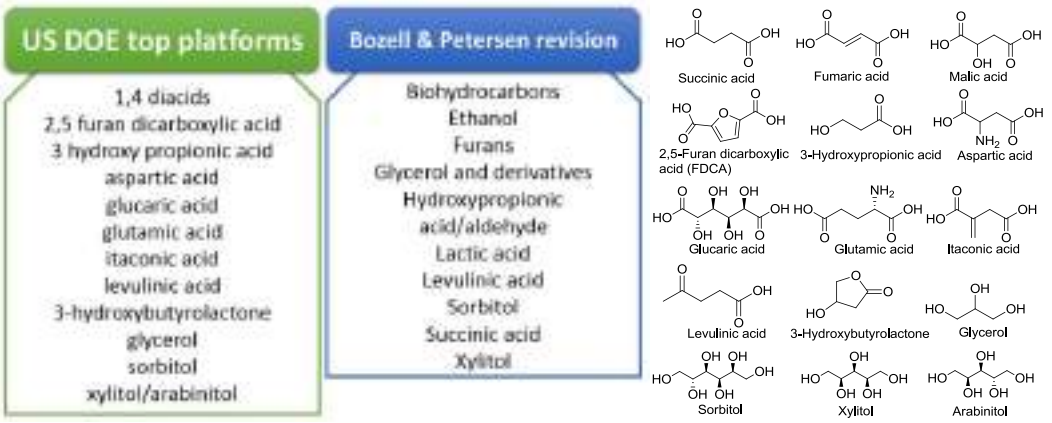

Figure 1.12. Comparison between US DOE's and Bozell & Petersen's top bio-derived chemicals

This approach has been further refined over the years,[45] but current platform compounds from biomass include most of structures of the original Top 10 list, particularly mono- and di-carboxylic functionalized acids, 3-hydroxybutyrolactone, a bunch of bio-hydrocarbons derived from isoprene, glycerol and derivatives, and few other sugars as sorbitol and xylitol.

Interestingly, the selection criteria for the "revisited top 10" included (Table 1.1):[44] i) significant attention in the literature; ii) the occurrence of technologies that could be adapted to the production of the desired product but also for several other compounds; iii) the possibility for a direct substitution of existing petrochemicals; iv) the involvement of a technology for a high volumes production; v) the potentiality as a platform chemical, *i.e.* a compound serving as starting materials for many other derivatives; vi) the engineering scale-up or the existence of pilot and demo plants for that product; vii) the occurrence of the product as an already existing commercial intermediate or commodity; viii) the role of the product as a primary building block like olefins, BTX, methane, and CO in petrochemistry; and, ix) the occurrence of a manufacturing process already recognized within the industry.

Table 1.1. Revisited top chemicals

Compound	Extensive recent literature	Multiple product applicability	Direct substitute	High volume product	Platform potential	Industrial scaleup	Existing commercial product	Primary building block	Commercial biobased product
Ethanol	+++	+++	+++	+++	+++	+++	+++	+++	+++
Furfural	++++	++	+	++	+	+	+++	++	+++
HMF[a]	+++	++	+	+	++	+	+	++	+
FDCA[a]	+++	+	+	+++	++	+	+	+	+
Glycerol	+++	+++	+++	+++	+++	+++	+++	+++	+++
Isoprene	+++	++	+++	+++	+	+++	+++	+	+
BHC[a]	++++	++	+++	+	+	+	+	++	+
Lactic acid	+++	+++	+	+++	++	+	++	+	+
Succinic acid	+++	+++	+	+	+++	+++	+	+	+
HPA[a]	+++	+	+++	+++	++	+	+	+	+
Levulinic acid	+++	++	+++	++	+++	+++	+	+++	+
Sorbitol	+++	+++	+++	+++	+++	+++	+++	+++	+++
Xylitol	+++	+++	+	+	+++	+	++	+++	++

[a] HMF=Hydroxymethylfurfural; FDCA=Furan-2,5-dicarboxylic acid; BHC=Biohydrocarbons; HPA= 3-hydroxypropionaldehyde. +++: high; +:low.

Although authors clearly stated that such an analysis included a degree of subjectivity due to the rapid change and expansion of the biorefining industry, a peculiarity was that, in analogy to previous DOE report, the "revisited Top 10" identified only three compounds with full marks (triple star) with respect to all the selection criteria: ethanol, sorbitol and glycerol.

On this basis and for the specific interest of this Thesis, the next paragraphs will briefly review the current situation of biofuels, particularly of biodiesel, to best introduce the case of glycerol and its derivatives.

1.2.3 Biofuels: some general aspects

The production of transportation biofuels is considered one the main driver for the growth of the biorefinery market.[46,47] Thanks to their similarity to the common liquid hydrocarbon fuels, biofuels do not require dramatic changes to transportation infrastructures nor to combustion engines in which they are employed.[48] Biofuels generate significantly less GHG emission respect to their fossil counterparts: at best, they can even be almost GHG neutral if efficient methods for their production are developed.[49] A well-known chronological classification describes 1st, 2nd and 3rd generation biofuels in which the two main families, *i.e.* bioethanol and biodiesel, are recognized (Figure 1.13).

First generation biofuels are obtained from seeds and grain such as wheat, corn and rapeseed. Notwithstanding the high oil content of these materials and their easy conversion to biofuels,[25] the production of such biofuels poses ethical and political concerns that strongly discourage, if not prevent at all (at least in some regions), the use of edible sources for any scope, except for food. By contrast, 2nd generation biofuels are produced from non-edible biomass including wastes and lignocellulose, and they are currently seen as a genuine sustainable alternative to both fossil fuels and conventional biofuels.[25] 2nd generation feedstocks are based on several non-edible oil plants such as miscanthus, switchgrass, sweet sorghum, jatropha, karanja, tobacco, mahua, neem, rubber, sea mango, castor, and cotton.[50] These belong to the so-called "sustainable energy crops" which are grown specifically for use as fuels from a low cost and a low maintenance harvest with high biomass yield even in infertile land.[49,51]

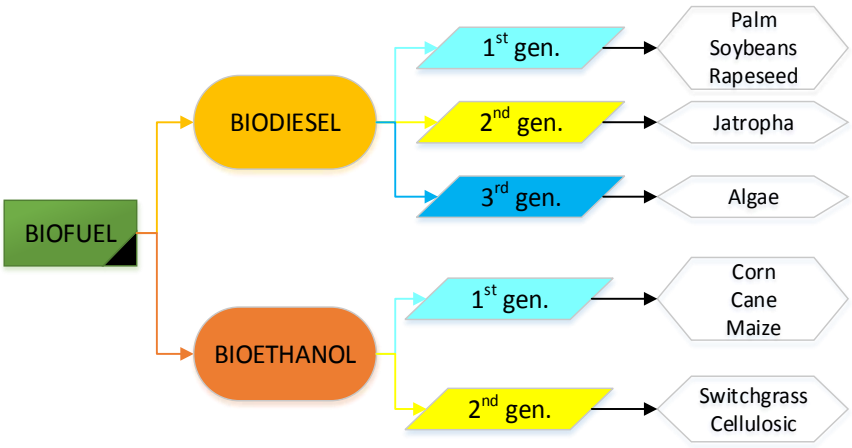

Figure 1.13. First, second and third generation of biofuels[52]

More recently, also algae have been considered as a raw material for 3rd generation biofuels. Due to an outstanding capability to convert solar energy into cellular structures, algae are a highly productive source of TGs: for example, *Botryococcus* and *Chlorella* have a lipid content as high as 50-80 wt%,[53] and they can double their biomass in a few days unlike land crops that can be harvested only once or twice a year. The exploitation of algae however, is still limited due to investment costs for harvesting and treatment of such feedstocks.[54]

Bioethanol obtained by the fermentation of sugar is the most abundantly produced biofuel. It accounted for more than 90% of total biofuel usage in 2006[55] and its consumption boosted up by 44% in the period 2006-2009. At present, albeit at a slower rate, the production of bioethanol continues to rise led by increases from Asia Pacific, South & Central America and North America (Figure 1.14).[56]

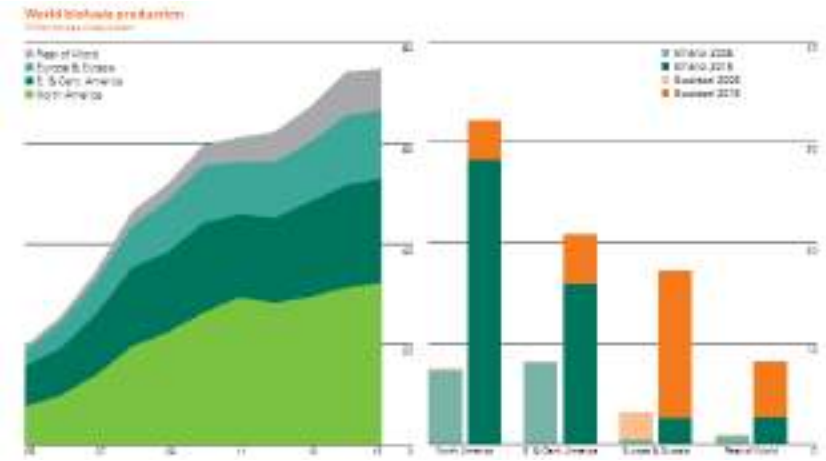

Figure 1.14. Trend of the global production (millions of tonnes of oil equivalent) of bioethanol and biodiesel from 2005 to 2015.[55]

The preferred feedstocks for this biofuel still remain food crops, particularly sugarcane in Brazil and corn in the USA, but a great deal of research is devoted to improve the production of the second generation bioethanol from waste biomass by optimizing the pretreatment of cellulosic feedstocks.[48]

Biodiesel is the second most abundant renewable liquid fuel. The largest producer of such a fuel is the European Union, accounting for 53% of all world's production in 2010 (Figure 1.14).[51,55] Biodiesel also represents ~80% of the total production of European biofuels.[57] Although this manufacture is dominantly based on rapeseed as a feedstock, accepted raw materials for biodiesel of second generation include jatropha and cottonseed. Stringent environmental regulations have stimulated a large interest in biodiesel not only for safety, renewability, non-toxicity and biodegradability in water, but also for the low sulfur content and high flashing point that allows the biofuel to reduce vehicular emissions with respect to conventional diesel.[58] Supported by Governments which strive to increase energy independence and meet the rising energy demand, the biodiesel market is expected to further increase in 2020 especially in the US and Brazil which are currently ramping up production at a faster rate than Europe. Surprisingly, the biodiesel price tracks very closely with petroleum derived diesel prices. Accordingly with analysts, this is one of the main reasons that can explain to increasing biodiesel production.[59]

Chemically speaking, biodiesel is prepared by a rather simple transesterification of TGs with light alcohols, more often methanol and ethanol, in the presence of a base (e.g. KOH, NaOH, $NaOCH_3$, etc.)[60] or even an acid catalyst (Scheme 1.1).[61] The process consists in three consecutive and reversible reactions were TGs are stepwise converted to diglycerides, monoglycerides and finally to glycerol, while 3 moles of a fatty acid ester are produced. Depending on the catalyst nature (acid or alkali), the reaction rate may follow first order or second order kinetics, or even a combination of both.[62] Colza, soybean and palm oils have the most suitable physicochemical characteristics for transformation into biodiesel, particularly for the proportion between saturated and unsaturated alkyl chains (R_1, R_2, and R_3) in the starting TGs.[60]

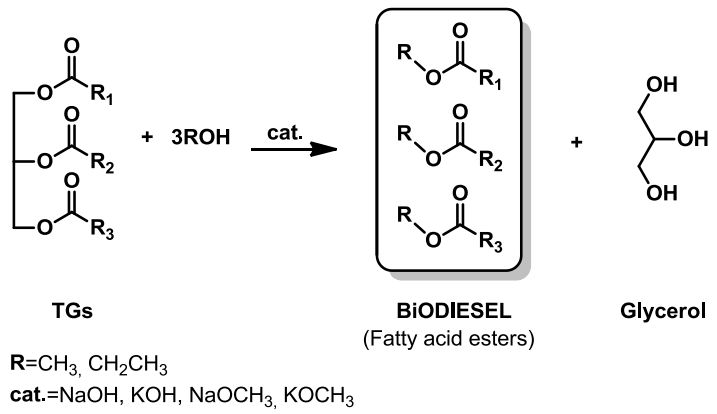

Scheme 1.1. Biodiesel production through catalytic transesterification of TGs

Notwithstanding its simplicity on paper, the biodiesel manufacturing has a number of drawbacks, including: i) the soap formation (caused by the base catalyst); ii) the use of an excess alcohol which has to be separated and recycled; iii) the need of neutralization of homogeneous catalysts which produces additional wastes; iv) the expensive separation of products from the reaction mixture, and v) the relatively high investment and operating costs. Of the many available solutions to cope with these problems, two deserve a mention for their innovation and efficiency.

The first one was patented in 2005 by the Institut Francais du Pétrole (IFP) that disclosed a novel biodiesel process called Esterfif (Figure 1.15).[63] Starting from vegetable oils, the transesterification step was conducted using methanol in the presence of a mixed Zn–Al oxide as a solid catalyst. The process was carried out at higher temperature and pressure than conventional homogeneous methods, by employing two reactors and two separators to shift the methanolysis equilibrium. At each stage, the excess methanol is removed and recycled by partial evaporation, while the esters (biodiesel) and pure glycerol (>98%) are separated in a settler.[64]

The second configuration was developed in 2006 by Gadi Rothenberg's group at the University of Amsterdam, and it was licensed to the Yellow Diesel BV Company. This plant was especially suited to mixed feedstocks with high free fatty acid (FFA) content such as used cooking oil, low grade grease, and in general, low-quality oils, waste oils and fats.[65] The process combined the reaction and the separation in a single step by using a reactive distillation system.[66]

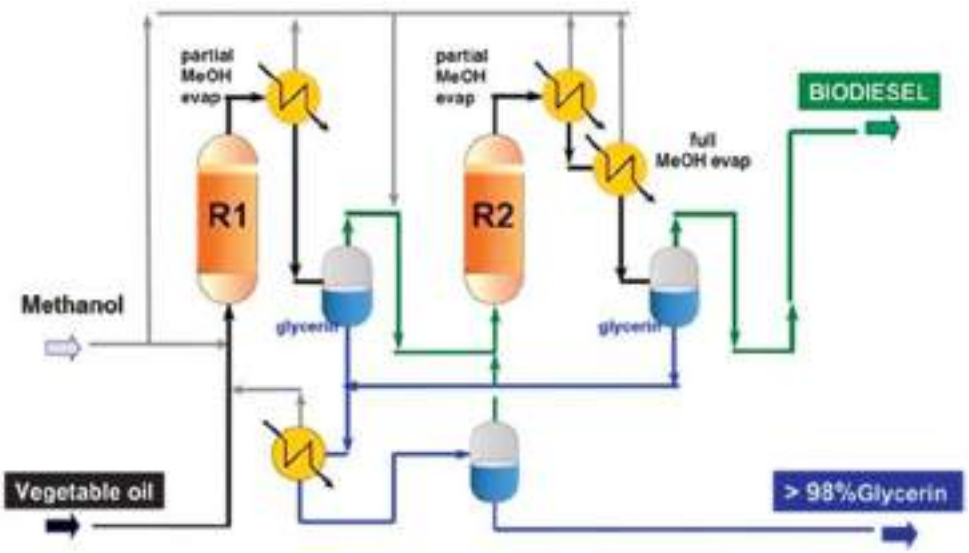

Figure 1.15. Simplified schematic of the IFP Esterfif biodiesel process based on two consecutive reactor–separator stages

Whichever the technology used for the preparation of biodiesel, the reaction stoichiometry of Scheme 1.1 shows that the amount of glycerol formed as a by-product is equivalent to approximately 10 wt% of the total biodiesel. This evidence implied two remarkable consequences: i) in the past fifteen years, as the biodiesel production steadily grew, the market experienced an unprecedented glut of glycerol whose price collapsed all over the World. In the EU (the major producer of biodiesel), the fall was almost by a factor of 10, from \$4000/tonn to \$450/tonn, respectively, in the 2000-2010 decade.[67,68] ii) the overabundance of a low cost source of renewable carbon fuelled an enormous interest from both Academia and Industry towards research programs for the conversion of glycerol and its derivatives into energy and most of all, high-added value chemicals. This aspect largely contributed to the ranking of glycerol on the above described Top 10 list (Table 1.1).

The upgrading of glycerol and its derivatives into chemical products has been also the leitmotif of the present Thesis.

1.3 **Glycerol**

Glycerol was accidentally discovered in 1779 by the Swedish chemist K. W. Scheele while he was heating a mixture of olive oil and litharge (lead monoxide). Scheele called this new liquid the "sweet principle of fat",[69] and shortly after, the compound was named *glicerine* after the Greek word *glykys* meaning sweet. In 1824, Pelouze announced the empirical formula $C_3H_8O_3$. The immense potential of glycerol went largely untapped and did

not become economically or industrially significant until dynamite was invented in 1866. Although liquid nitroglycerine had already been invented by the Italian chemist Ascanio Sobrero in 1846, the discovery that the mixing of nitroglycerine with silica (kieselguhr) could turn the liquid into a malleable paste was of Alfred Nobel. This invention became the first worldwide technical application for glycerol and thrusted it into economic and industrial development.

Today, the vital role of glycerol is well established: it is a component of living cells and natural energy reservoirs such as TGs which constitute vegetable and animal fats and oils, and it occurs naturally in wines, beers, bread, and other fermentation products of grains and sugars. Glycerol is also an outstanding versatile compound with more than a thousand of applications and uses:[70] the key of its success is a unique combination of physical and chemical properties, compatibility with many other substances, and easy handling. Physically, glycerol is a high boiling, water-soluble, clear, colorless, odorless, viscous and hygroscopic liquid. Chemically, it is a trihydric alcohol, capable of being reacted as an alcohol yet stable under most conditions.

1.3.1 Production of glycerol

1.3.1.1 Synthetic glycerol from propene

At the beginning of the last century, DuPont was the leading producer of dynamite which derived from the soap manufacture. After the end of the World War I, the US Government decided to implement the production of dynamite based on high yield reactions using petroleum feedstock. However, only 25 years later, the first process was put on stream, following the discovery that propylene could be efficiently converted to glycerol.[71] The reaction of propylene may actually occur through three different routes which involve the intermediate stages summarized in Scheme 1.2: 1) allyl chloride-epichlorohydrin; 2) acrolein-allyl alcohol-glycidol, and 3) propene oxide-allyl alcohol-glycidol.

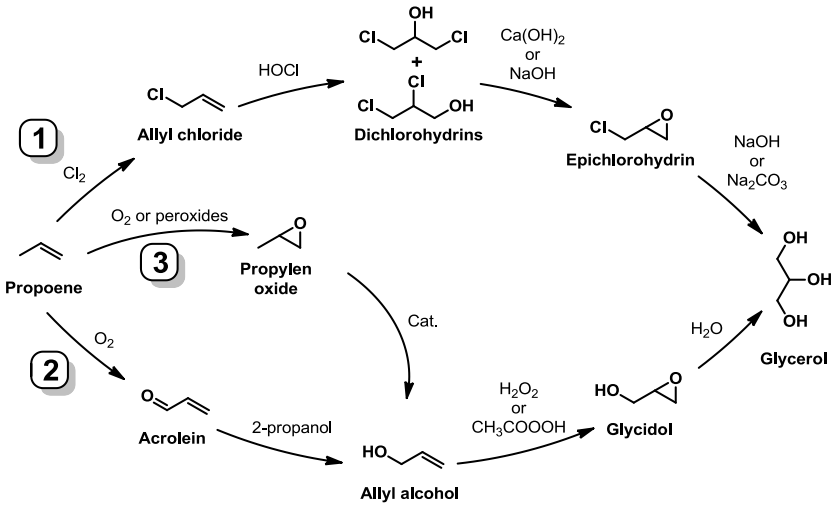

Scheme 1.2. Glycerol synthetic routes starting from propene

Interestingly, because of war (World War II) priorities, the first synthetic glycerol from allyl chloride was not produced by US industries, but rather, by the German factory I. G. Farben in Oppau and Hydebreck in 1943 (Scheme 1.2, route 1). This method became available once the high-temperature chlorination of propene to allyl chloride (300-600 °C) could be properly controlled. Allyl chloride was then oxidized with hypochlorite to dichlorohydrin under mild conditions (25-50 °C). This first step yielded a mixture of 1,2-dichloropropanol and 1,3-dichloropropanol in about 30% and 70% amount, respectively. In a further reaction, 1,2-dichloropropanol was converted to the 1,3-isomer which without isolation, underwent a ring closing process to epichlorohydrin: the reaction was promoted by calcium or sodium hydroxide at 50-90 °C. Epichlorohydrin was finally hydrolyzed with basic aqueous solution of sodium hydroxide or sodium carbonate at 80-200 °C.

In 1948, a similar production was begun also by Shell in Houston, Texas. However, a major drawback of the allyl chloride-epichlorohydrin process was the co-generation of large amounts of wastewater contaminated not only by inorganic, but also by toxic organic chlorinated compounds such as 1,2- and 1,3-dichloropropane, 1,2,3-trichloropropane, penta- and hexachlorohexane (Scheme 1.3).[72] When Dow Chemical adopted the same process in the late 70's,[73] the production of polluted wastewater was of 45000 tons/y. In 2006, the same Company considered the process no more economically viable and the plant was shut down.[74]

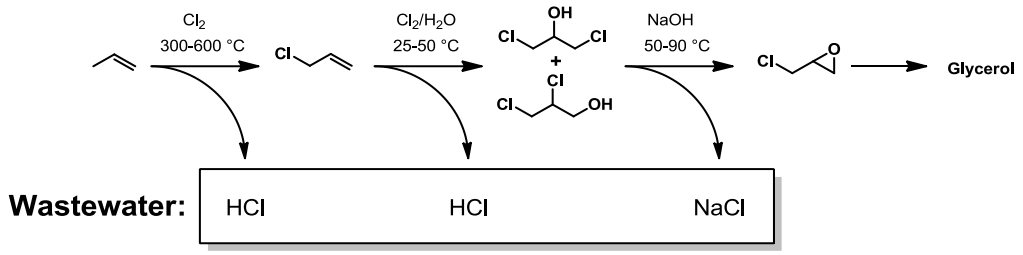

Scheme 1.3. The traditional industrial process via epichlorohydrin based on high temperature chlorination of propene

The acrolein process for the production of glycerol was developed by Shell and implemented in 1958 in a plant operating in Norco, Louisiana (Scheme 1.2, route 2). The major breakthrough was that the Shell process did not require the use of chlorine.[75] The initial reaction was the oxidation of propene to acrolein, followed by the reduction of the aldehyde to the corresponding allyl alcohol thorough the well-known mechanism of the Meerwein-Ponndorf-Verley reaction.[76] The allyl alcohol was then epoxidized to glycidol and finally, hydrolyzed to glycerol. Eventually, at the beginning of 60's, a third synthetic route for the synthesis of glycerol was invented by the French Society Progil.[77] The process started from the direct epoxidation of propene to propene oxide and proceeded with the isomerization of the epoxide to allyl alcohol in the presence of Lithium orthophosphate as a catalyst (Scheme 1.2, route 3). The overall procedure then continued according to the same chemistry of the previously described Shell manufacture.

Today, the technologies of Scheme 1.2 are considered obsolete. Even the production of epichlorohydrin does not come anymore through the use of propylene, but rather from glycerol as a starting material.[78,79] Several Companies including Dow Chemical, Solvay and Spolchemie have proposed to manufacture epichlorohydrin from the catalytic hydrochlorination of glycerine followed by an internal nucleophilic displacement on (1,3-dichloro)-*i*-propanol (Scheme 1.4).

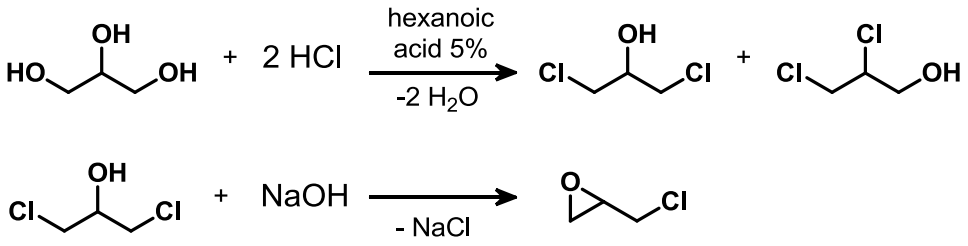

Scheme 1.4. Modern routes proposed for the manufacture of epichlorohydrin from glycerol

This trend is obviously the result of the surplus of glycerol created by the transesterification of fats and oils during the production of biodiesels. The transesterification reaction along with the hydrolysis of natural oils and fats used in the preparation of soaps, have almost completely replaced previous synthetic methods based on propene. *Native* or *natural* glycerol is the term coined to identify the product derived from petrochemistry-free routes.

1.3.1.2 Native glycerol

Besides the already discussed production of glycerol from biodiesel (Scheme 1.1, paragraph 1.2.3), native glycerol is also obtained from hydrolytic reactions carried out by high-pressure splitting processes (Scheme 1.5).

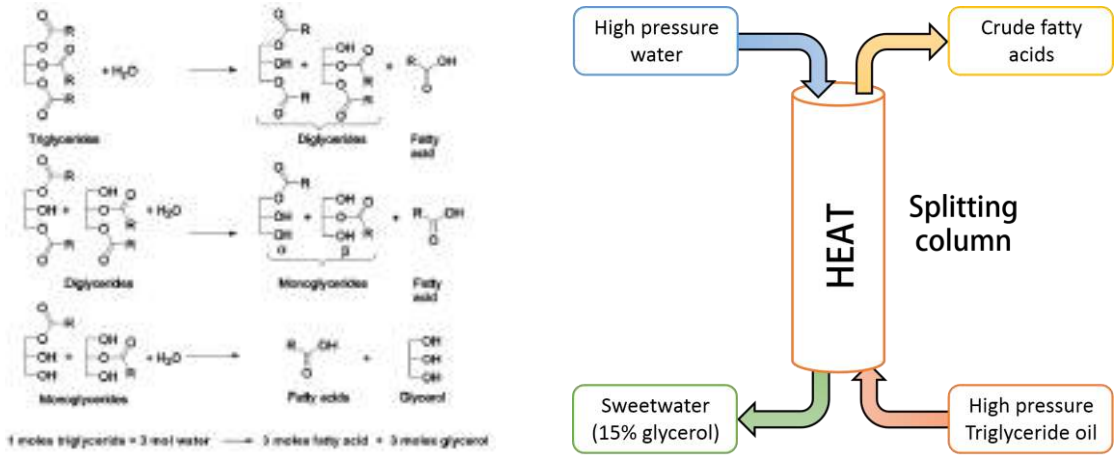

Scheme 1.5. Hydrolysis of TGs for the production of native glycerol (top). Single-stage countercurrent splitting process (bottom)

These transformations are more often performed under continuous-flow conditions. In a typical configuration, water and the organic feedstock (oil or fat) are fed into a splitting column in countercurrent fashion at 2-6 MPa and 220-260 °C: once the splitting has occurred (with high pressure steam), fatty acids are discharged from the top of the splitter and an aqueous solution of glycerol (~15-18 wt%), known as sweet water, is recovered at the bottom. Such glycerol is extremely low in ash: a typical value is ca. 0.1% or less of inorganic salts.[71,80] Also, lipases such as *Candida Rugosa* or *Aspergillus Niger* can be used to help the hydrolytic step.[81]

Native glycerol, although encountered only in small quantities, is also obtained from the saponification (splitting) of neutral oils carried out in the presence of caustic alkali and alkali carbonates.[82]

Two other - far less used – methods for the production of native glycerol include: i) the fermentation of alcohols.[83] The fermentation can be interrupted at the glyceraldehyde 3-phosphate stage by using sodium carbonate or alkali or alkali-earth sulfites. After reduction to glycerol phosphate, glycerol is obtained in yield up to 25% by hydrolysis. ii) High temperature hydrogenations of natural polyalcohols such as cellulose, starch, or sugar in the presence of several type of catalysts such as Ru/magnetite.[84]

According to some market researches, the Asia-Pacific region is the largest world producer of native glycerol: major manufactures are Malaysia, Indonesia, and the Philippines which use palm oil and coconut oil as feedstocks.[85] The second and third producers are Western Europe and the United States, that obtain glycerol from biodiesel refineries, vegetable oils, fats and animal tallow. These Countries were responsible for ~90% of world production of glycerol in 2007.[86] In 2010, it was forecasted that the global production of refined glycerin should have more than doubled by 2015, thereby reaching 2 million tons (Figure 1.16).[87]

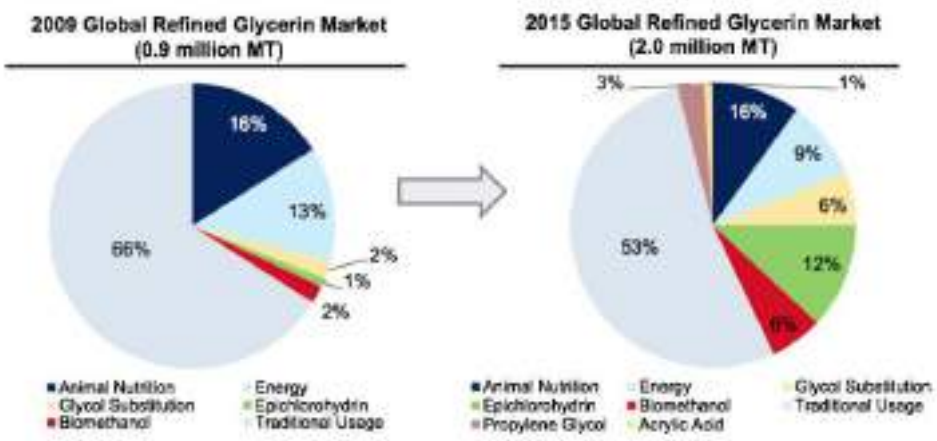

Figure 1.16. A perspective for the global market of refined glycerol starting from 2009

Although updated market investigations are hardly available, a recent (2016) outlook indicates that, unlike expectations, the refined glycerol imports in the US have decreased by 14% year to date (YTD) through October year on year (data from the US International Trade Commission).[88] The picture of US imports, in tonnes, is shown in Table 1.2.

Table 1.2. US refined glycerine imports

	YTD 2014	YTD 2015
Malaysia	49259	55977
Indonesia	45246	32043
Argentina	26103	13129
Total	132913	114457

A lack of demand from China and South America, the desire to export some out of Europe and the need for the Asian producers to put additional product into the US market have been considered as possible reasons for this trend.

The price of glycerol has also seen remarkable fluctuations over the years. Since 2003 the rapidly increasing glycerol oversupply caused a dramatic fall in the price of both refined and crude glycerol. As mentioned above, the value of refined glycerol decreased to less than 450 $/ton in early 2010, while crude glycerol went almost to 0 $/ton.[67] Despite several conservative predictions, in the early 2012, the price started to rise: in the US, it was recorded at 838-1014 $/ton with good global demand across several key end-uses (food-grade and pharmaceutical applications). Eventually, in late 2013 the prices in the US were around 900 $/ton and Asia's vegetable refined glycerol prices were reported at an average of 965 $/ton due to higher feedstock prices.[67] Thanks to the combination of new applications, market expansion in traditional sectors and replacement of other polyols, the price of glycerol partly recovered since the 2009 historic lows. In 2014 in the US, pharmaceutical grade could be bought for 900 $/ton, whereas crude glycerol was sold at 240 $/ton.[89]

1.3.2 Purification

A remarkable drawback of native glycerol prepared by any of the above described reactions is its rather low purity which may vary depending on the TGs source and on the type of processing, but it is generally around or below 60%.[60] For example, in a biodiesel refinery, the glycerol side-stream contains methanol, water, inorganic salts (catalyst residue), FFA and their esters, unreacted mono-, di-, and TGs, and other ''matter organic non-glycerol'' (MONG) in varying proportions:[90] a typical mixture may be comprised of <65 wt% glycerol, 15-50 wt% MeOH, 10-30 wt% water, 2-7 wt% salts (primarily NaCl and KCl derived from the catalyst neutralization), and minor amounts of organics.

Crude glycerol must therefore be purified and the degree of purity depends on the type of application and and potential end use of the product. Particularly, a very high purity is required in the food and pharmaceutical sectors. Refined glycerol found in the market is of three different qualities: i) technical grade (>90%); ii) United States Pharmacopeia (USP, up to 99.7%) and iii) Food Chemical Codex (FCCX, 95-100%).[91] Technical grade is mainly used (when possible) as a reagent or a solvent/additive. USP glycerol is usually derived from animal fat or vegetable oil and it is suitable for both pharmaceutical and food products, while FCCX glycerin, still derived from vegetable oils, is appropriate for the food industry.

The technology developed for purification of glycerol derived from biodiesel is mainly adapted from existing soap making industry: vacuum distillation and other treatments including ion exchange and neutralization reactions and use of activated carbon, are generally employed. As a rule of thumb, the purification is comprised of the steps shown in Figure 1.17.[92]

Figure 1.17. General stages in the glycerol purification process. [92]

The first step involves the removal of FFA and some salts which may precipitate during neutralization. The next step is finalized at concentrating the solution by evaporation. This operation eliminates the residual alcohol (methanol or ethanol) from the glycerol stream. The final refining step is often achieved by a combination of vacuum distillation, ion exchange, and membrane separation and adsorption. As an example, a crude glycerol stream may be purified by a combined set of electrodialysis and nanofiltration. Such a system has been patented by EET Corporation that implemented a High Efficiency Electro-Pressure Membrane (HEEPM) device able to operate in a batch, semi-batch, or continuous flow mode.[92] Major specifications of this system include: i) capacities from 2 to 5000 m^3/day; ii) feed water salinity in the range 100-50000 ppm; iii) product purity to 2 ppm total dissolved solids (TDS) ;[93] iv) 99+% water recovery with 99.9+% salt removal. After polishing, the recovered glycerol easily meets USP glycerol standards (Figure 1.18).[94]

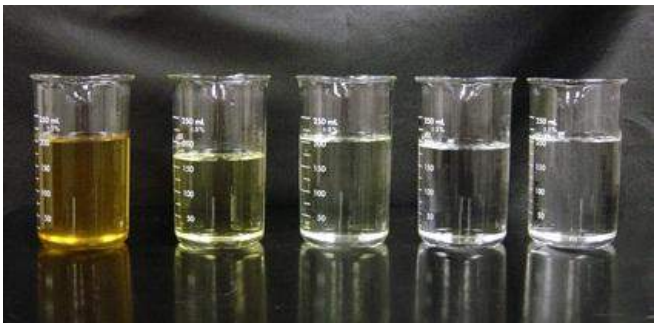

Figure 1.18. Purification stages with the HEEPM device.[94]

This membrane-based technique avoids evaporation, distillation and problems such as foaming, carry-over of contaminants and limited recovery.

Whichever the method used, the purification of glycerol always involves rather expensive operations or instruments. This implies that most often, the chemical upgrading of glycerol (as a platform chemical) becomes economically viable only on condition that very high-added value products are synthesised. Otherwise, the refining of glycerol might be a cost not worth paying. Alternative routes should then be conceived for the straightforward transformation of raw glycerol followed by the isolation of the obtained products. This sequence may be more difficult to accomplish, but it is often cheaper and simpler than refining the crude reagent and then proceeding with its upgrading.

1.3.3 Physico-chemical properties and major applications

Glycerol is a sweet-tasting, colorless, odorless, hygroscopic and viscous liquid at room temperature. It possesses a highly flexible molecule able to form both intra- and inter-molecular hydrogen bonds. There are 126 possible conformers of glycerol, all of which have been characterized in a study using density functional theory (DFT) methods.[95] In condensed phases, the hydrogen bonding is responsible for a high degree of association of glycerol: a molecular dynamics simulation suggests that on average 95% of molecules in the liquid are connected.[96] This network is very stable and only rarely, especially at high temperature, releases a few short-living (less than 0.5 ps) monomers, dimers or trimers. In the glassy state, a single hydrogen bonded network is observed involving 100% of the molecules present. A highly branched network of molecules connected by hydrogen bonds exists in all phases and at all temperatures.

Major physicochemical properties of glycerol are shown in Table 1.3. In its pure anhydrous condition, glycerol has a melting point of 18.2 °C and a boiling point of 290 °C at

atmospheric pressure, accompanied by decomposition. At low temperatures glycerol may form crystals which melt at 17.9 °C. This crystalline state, however, is seldom reached because of a strong tendency toward supercooling.

Table 1.3. Major physicochemical properties of glycerol at 20 °C

Molecular mass	92.09382 g/mol
Density	1.261 g/cm^3
Viscosity	1.5 Pa·s
Melting point	18.2 °C
Boiling point	290 °C
Food energy	4.32 kcal/g
Flash point	160 °C (closed cup)
Surface tension	64.00 mN/m

Because of its three hydroxyl groups, glycerol has properties similar to those of water and simple aliphatic alcohols (methanol, ethanol, propanol, butanol, and pentanol) with which is fully miscible. The liquid-vapor equilibria of glycerol-water solutions have been carefully investigated for their importance in distillation and fractionation operations,[97] and suitable theoretical methods are also available to predict the behavior of aqueous mixtures of glycerol.[98] Other properties of such solutions including the freezing point, density, viscosity, compressibility and refractive index have been detailed in the literature.[99] Glycerol is also completely miscible with phenol, glycol, propanediols, and several amines (*e.g.,* pyridine, quinoline), while it displays a limited solubility in acetone, diethyl ether, and dioxane, and it is almost insoluble in hydrocarbons, long-chain aliphatic alcohols, fatty oils, and halogenated solvents such as chloroform. Glycerol also forms azeotropes with different substances and ternary systems including glycerol-water-phenol and glycerol-ethanol-benzene shows significant temperature- dependent miscibility gaps.[100]

Overall, glycerol possesses a unique combination of properties that makes it an attractive compound for many industrial branches.[101,102] Traditional applications currently involve about 160000 tons of glycerol per year, of which pharmaceuticals, toothpaste and cosmetics account for around 28%, while the manufacture of tobacco, foodstuffs and urethanes represent 6, 11, and 11%, respectively. The remainder includes lacquers,

varnishes, inks, adhesives, plastics (alkyd resins), regenerated cellulose, explosives (nitroglycerine) and other miscellaneous uses (Figure 1.7).[103]

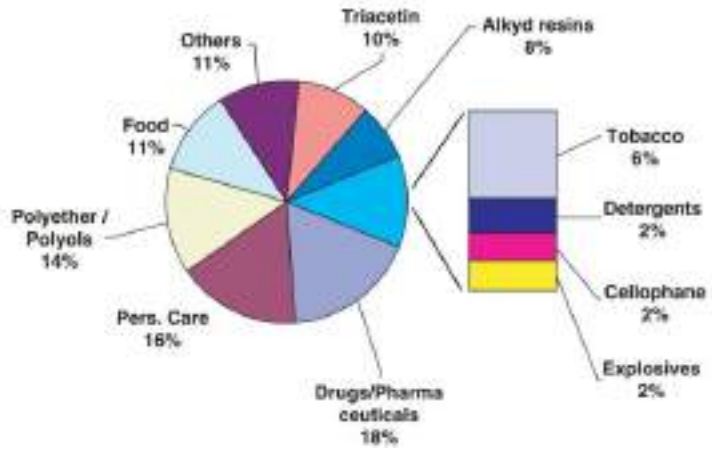

Figure 1.19. Market for glycerol. [103]

Glycerol is also increasingly used as a substitute for propylene glycol. Most of the glycerol marketed today meets the stringent requirements of the USP and the FCCX. However, technical grades of glycerol - not certified as USP or FCCX quality - are also available.

Food industry. Glycerol is a non-toxic and easily digested compound largely used as a sugar-free sweetener. In this sector, sorbitol is facing particularly stiff competition from glycerol since the latter contains only 27 calories per teaspoonful and it is 60% as sweet as sucrose. Moreover, glycerol does not raise blood sugar levels, nor does it feed the bacteria that cause plaque and dental cavities.

Drugs, cosmetics, and tobacco. In the drug sector, glycerol is either a component of medical preparations including anesthetics as the glycerin phenol solution, or it may be used as the starting material for tranquilizers and vasodilators as the well-known nitroglycerine. In cosmetics, glycerol is used as an ingredient of tinctures, elixirs, jellies and ointments, and creams and lotion as a skin softener and moisturizer. It is also the basic medium to impart smoothness, viscosity and brilliance to toothpastes. In this respect, it must be noted that glycerol is similar in appearance, smell and taste to the toxic and cheap diethylene glycol (DEG). This has often caused fatal accidents due to the fraudulent replacement of glycerol with DEG.[104] One of the last episodes dates back to 2007. The FDA blocked shipments of toothpaste from China entering US via Panama.[18] The toothpaste contained DEG which causes the death of at least 100 people. DEG was produced by a Chinese factory which deliberately falsified records to allow exports. Eventually, a batch of contaminated

toothpaste also reached the EU market, and a number of poisoning cases were reported in southern Europe.

Glycerin and other flavoring agents are sprayed on tobacco leaves before they are shredded and packed. These additives account for about 3% of the tobacco weight and they prevent the leaves from becoming friable and crumbling during the tobacco processing.

Miscellaneous uses. Glycerin can be used as a lubricant for applications where oils and common lubricants can fail. For example, it is recommended for oxygen compressors because it is more resistant to oxidation than mineral oils, and it is also used to lubricate pumps and bearings exposed to fluids such as gasoline and benzene, which would dissolve conventional oil-based lubricants.

Glycerol is a component of heat casings and special types of papers, such as glassine and grease proof paper, which need a plasticizer to give them pliability and toughness. It is also used in the cements production, embalming fluids, masking, shielding, soldering, cleaning, ceramics, photographic, leather, wood treatments, adhesives, etc. Also, some recently reported applications include the use of glycerol as a building block for polyethers used too in rigid urethane foams.

1.3.4 The chemical reactivity and the major derivatives of glycerol

Chemically speaking, glycerol exhibits the typical reactivity of alcohols: the two terminal primary hydroxyl groups are slightly more reactive than the internal secondary hydroxyl group.

Several technologies are presently available for the chemical conversion of glycerol into value added products.[105,106] The most investigated ones are focused on esterification,[107] etherification,[108] cyclization,[68,109,110] oligomerization,[111] oxidation,[112,113] hydrogenolysis,[114] fermentation,[115] and aqueous-phase reforming (APR).[116] The reactions and the corresponding products are summarized in Scheme 1.6.

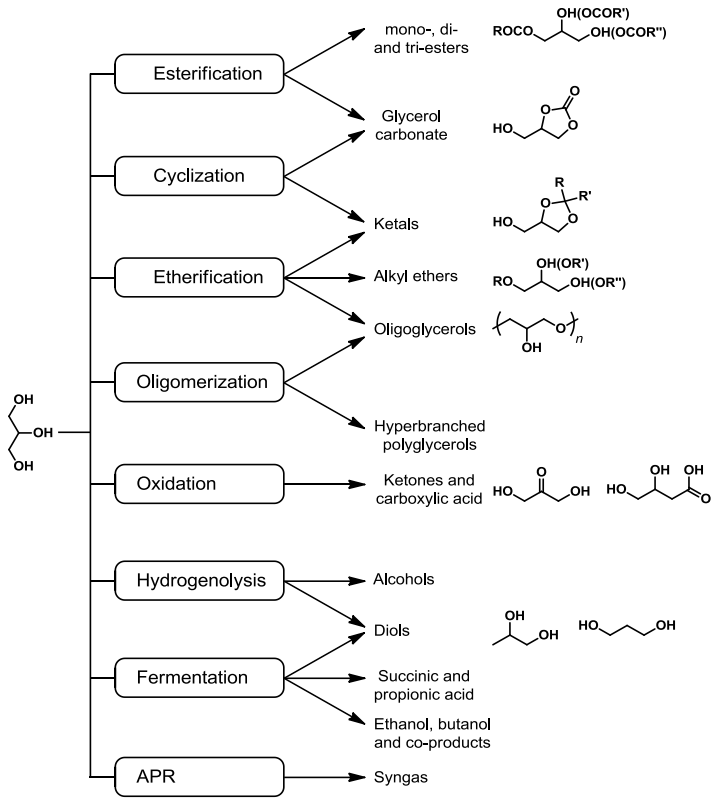

Scheme 1.6. Most investigated chemical transformations of glycerol

The following section surveys reactions and products of Scheme 1.6 with a major focus on topics that have been investigated in this PhD thesis: particularly, on (trans)esterification and acetalization (cyclisation) processes and on derivatives such as glycerol carbonate and glycerol acetals (further details will be given in chapters 2 and 4). Other reactions will only briefly mentioned.

Esterification and Cyclisation. Glycerol carbonate [4-(hydroxymethyl)-1,3-dioxolan-2-one: GlyC] is one of the top derivatives obtained by both transesterification and cyclization reactions of glycerol. Physicochemical properties of GlyC are in between those of propylene carbonate and glycerol.[117] It shows an unusually large liquid range from -69 °C to 354 °C, a flashing point of 190 °C, and a high solvency which makes it an excellent medium even for inorganic salts.[118] Moreover, GlyC exhibits a flexible reactivity due to its structure in which three electrophilic and one nucleophilic sites are simultaneously present (a carbonyl carbon, two alkylene carbons, and a hydroxyl oxygen, respectively). An interesting study has demonstrated that a valuable multi-electrophilic synthon can be achieved through the substitution of the hydroxyl group of GlyC by a tosyl function (Scheme 1.7).[119]

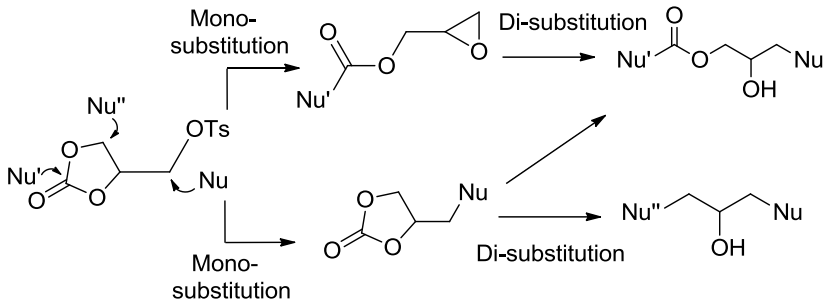

Scheme 1.7. The flexible electrophilic reactivity of tosylated GlyC

In the presence of O-nucleophiles, the reaction of the tosylated glycerol carbonate (Ts-GlyC) follows the HSAB principle:[120] under basic conditions, hard alkoxides generated by alcohols (as reactants) are able to regioselectively attack the carbonyl center of Ts-GlyC to produce alkyl glycidyl carbonates (Scheme 1.7, top), while softer phenolate ions (from phenols) form aryl ethers by replacing the TsO group (Scheme 1.7, bottom).

The versatile reactivity, the non-toxicity and the good glycerol-like biodegradability of GlyC,[121] account for the wide range of direct and indirect applications of this compound as a green solvent[122,123,124] an electrolyte carrier, a curing agent, a plasticizer/humectant for cosmetics,[125,126,127,128] a starting material for glycidol and epichlorohydrin,[129] and hyperbranched polyethers, polycarbonates and non-isocyanate polyurethanes.[130,131,132] (Figure 1.20).

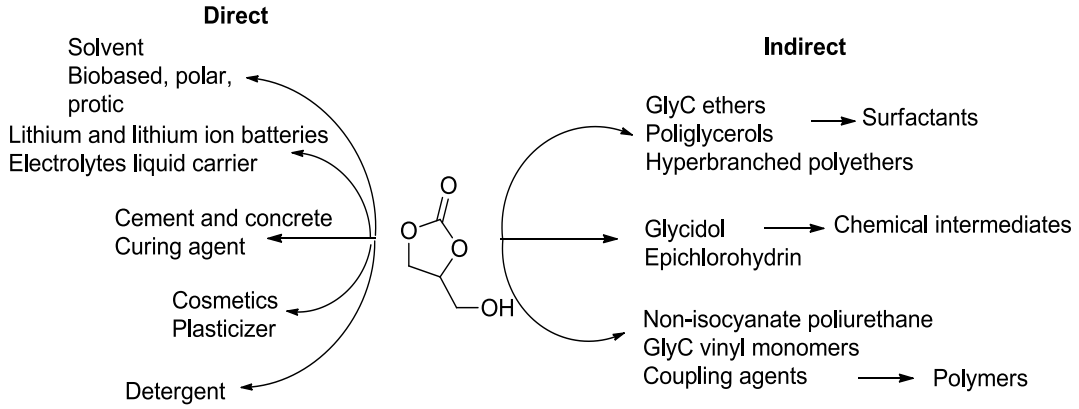

Figure 1.20. Major applications of GlyC

Although this is not an exhaustive list, it clearly indicates how the chemistry of GlyC discloses a great potential that it is far from being fully understood and exploited. The strategies for the synthesis of glycerol carbonate from glycerol are summarized in Figure 1.21.[133]

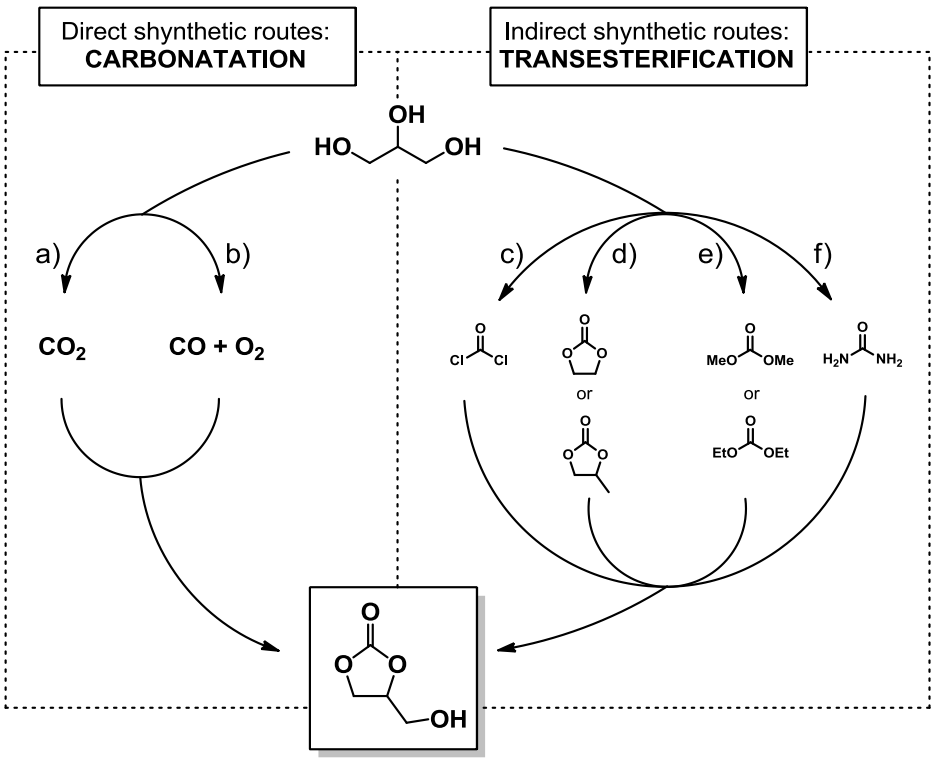

Figure 1.21. Major strategies for the synthesis of GlyC from glycerol

In the following discussion, only catalytic reactions able to avoid/minimize (toxic) reagents, solvents and wastes, and improve the process safety will be commented [paths a), d), e), and f)]. Procedures involving harmful reactants such as phosgene and CO-derived starting materials will not be considered [paths b) and c)].

The carbonation of glycerol by CO_2 appears as the most obvious sustainable route (path a): it is a highly atom economic process (AE: 87%) which involves renewable, safe, and cheap reactants. However, thermodynamics limits the reaction:[109,134,135,136] the best reported yield of GlyC is of only 34% by using Bu_2SnO and methanol as catalyst and solvent, respectively.[137]

The transcarbonation of urea with glycerol affords high conversions (>80%) and complete selectivity towards GlyC in the presence of ZnO or $ZnSO_4$ as catalysts.[138,139] (path f). The Zn-based systems however, dissolve in the reaction mixture making both their recovery and the purification of GlyC quite difficult. Moreover, sizeable amounts of by-product ammonia hinder a large scale implementation of the reaction.

The catalytic transesterification of either ethylene carbonate (EC) or dimethyl carbonate (DMC) with glycerol has also been extensively investigated [paths d) and e)]. At rather low temperatures (50-80 °C), several basic heterogeneous catalysts successfully lead

to a conversion of EC as high as 85-100%, and good-to-excellent selectivities of 84-99% towards GlyC.[140,141] The main issue however, is the purification of the product from viscous and high boiling liquids such as unconverted EC and ethylene glycol (EG) which forms as a reaction by-product. This makes rather problematic the work up (mostly distillation and filtration steps) of final reaction mixtures. Therefore, although the reaction of glycerol with EC occurs under milder conditions with respect to DMC,[142,143] the latter is becoming the preferred reactant for the synthesis of GlyC. Both the unreacted DMC and the co-product methanol (bp: 90 °C and 64.5 °C, respectively) are easily removed and recycled after the reaction is complete. Base catalysts including homogeneous (K_2CO_3, triethylamine, ionic liquids)[110] and heterogeneous (CaO, MgO, hydrotalcites)[144,145,146,147] systems, have been mostly used to the scope.[148] The mechanism accepted for such reactions is outlined in Scheme 1.8: [149]

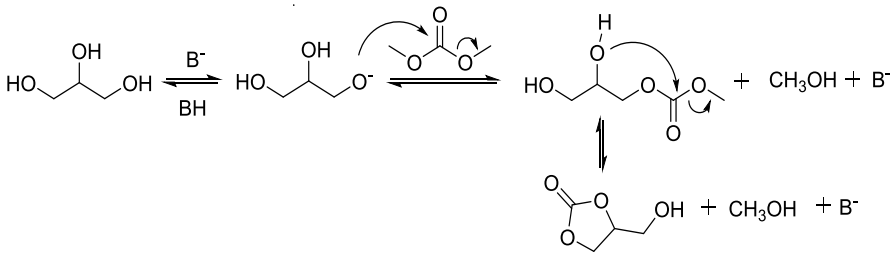

Scheme 1.8. The general mechanism for the base-catalysed transesterification of glycerol with DMC

In the first step, the base catalyst activates the reacting glycerol by deprotonation of a primary hydroxyl groups forming a glycerolate anion. This nucleophile attacks the carbonyl carbon of DMC leading to methyl glyceryl carbonate and a methoxide leaving group ($B_{Ac}2$ substitution). An acid-base reaction restores the original base (B) and produces methanol. In the last step, a secondary hydroxyl group is deprotonated and the stable cyclic product GlyC forms through an intramolecular ($B_{Ac}2$) nucleophilic displacement.

Cyclisation. Acetals obtained by acid-catalysed condensations of glycerol with light (up to C_4) aldehydes and ketones are the most known cyclic derivatives of glycerol. More specifically, glycerol formal and solketal resulting from the simplest aldehyde and ketone (formaldehyde and acetone) respectively, have received a great deal of attention in this field (**Scheme 1.9**).[150,151] Both acetals are obtained in the presence of different homogeneous and heterogeneous acid catalysts such as hydrochloric acid, acetic acid, amberlysts, transition metals oxides and complexes and others.[152,153,154,155]

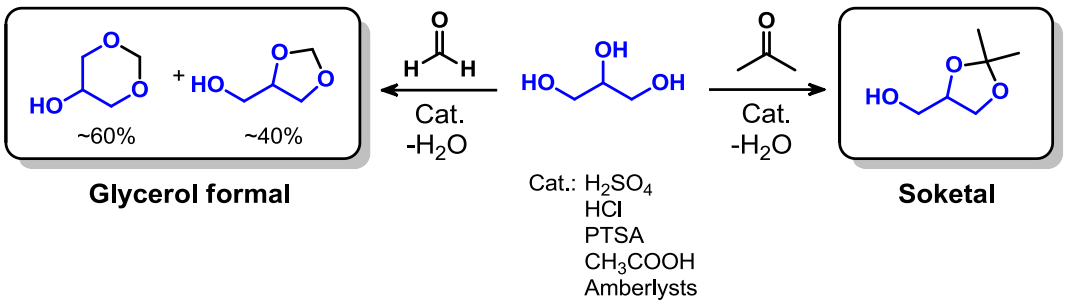

Scheme 1.9. Most common cyclic acetals derived from glycerol. Glycerol formal (a 60:40 mixture of six- and five-membered ring isomers) and solketal.

In particular, the acid amberlyst resins represent an interesting catalytic system. Being a heterogeneous catalyst, they are suitable for CF processes and furthermore they can promote the acetalization reaction of glycerol in mild conditions (rt-40 °C). Glycerol acetals are viscous, dense, non-toxic and thermally stable liquids and can find application as solvet for injectable preparations, paints, plastifying agents, insecticide delivery systems and flavors.[153]

Etherification. Glycerol Monoethers (GMEs) are perhaps the most interesting etherification products. As witnessed by the over 7000 patents in the last two decades,[156] GMEs have an impressive number of applications mostly as intermediates and additives for personal care products, pharmaceuticals, surfactants, fuels and lubricants.[157,158] (Figure 1.22).

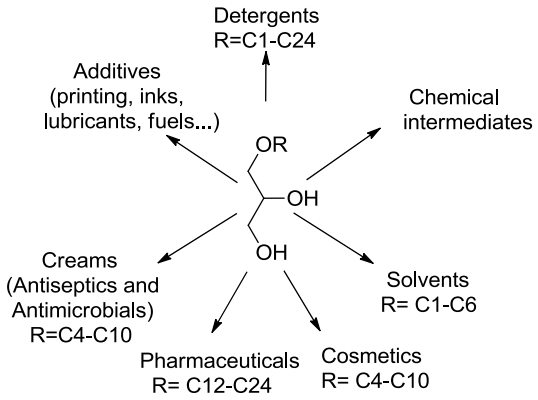

Figure 1.22. Applications of glycerol monoethers (GMEs)

Three approaches (a-c) have been used for the synthesis of GMEs from glycerol.

a) The first one is based on the straightforward alkylation of glycerol. However, under the typical (basic) conditions of the Williamson reactions,[159,160] the selectivity is limited by the similar pKa and reactivity of the three hydroxyl groups of glycerol which bring to the

concurrent formation of di- or three-ethers as by-products. Other issues are the use of toxic alkylating agents (*i.e.* alkyl halides or dialkyl sulphates) and the co-generation of salts to be disposed of. In this respect, more promising alkylating reagents are alcohols which offered excellent glycerol conversion and GMEs selectivity up to ~80% and 90%, respectively, in the presence of Amberlyst 15 and 35 resins as catalysts (Scheme 1.10).[161,162]

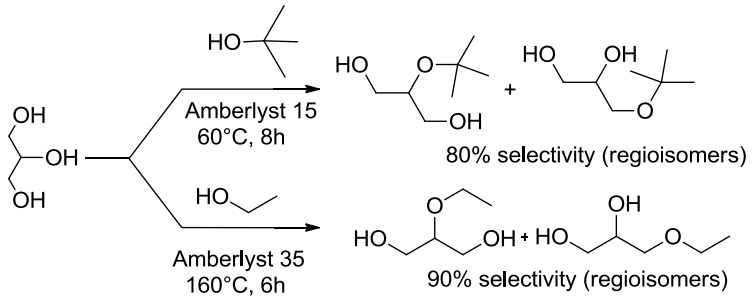

Scheme 1.10. Synthesis of GMEs through the alkylation of glycerol by alcohols

b) The second strategy makes use of protection/deprotection sequences which usually involve three steps: i) the synthesis of glycerol acetals; ii) the O-alkylation of acetals, and iii) the removal of protective acetal group. Scheme 1.11 reports the sequence for the model case of solketal.

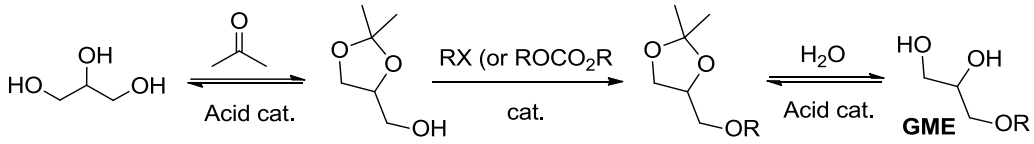

Scheme 1.11. Synthesis of terminal GMEs through a protection/deprotection sequence

Once the acetal is prepared, the OH-capped tether (hydroxyl methylene group of solketal) undergoes a catalytic etherification reaction with both alkyl, tosyl, mesyl halides (RX) and dialkyl carbonates ($ROCO_2R$), respectively.[163,164,165,166,167] Finally, the O-alkylated acetal is hydrolysed under acid conditions to provide the desired GME.

c) A third innovative route has been reported through the use of glycerol carbonate (GlyC) to produce glycerol ethers. In this case, a K_2CO_3-catalysed multicomponent reaction of glycerol, phenol(s) and diethylcarbonate allows the formation of GlyC as an intermediate which evolves to glycerol monoaryl ethers in very good yields (> 80%, Scheme 1.12).[168]

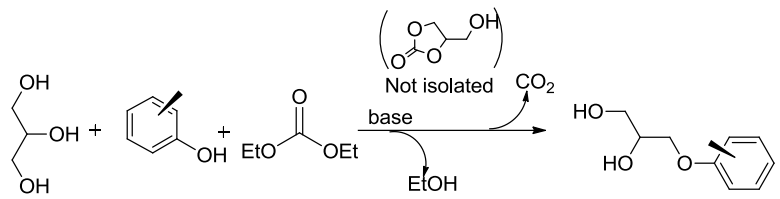

Scheme 1.12. Synthesis of GMEs by a multicomponent reaction involving glycerol carbonate as an intermediate

Oligomerisation. Several studies refers to the conversion of glycerol to oligomers as etherification reaction. To avoid confusion, the reaction pathways of glycerol with itself to form oligomers and polymers is better designated as oligomerization or polymerization. Often, oligomers with 2-4 glycerol units are viewed as polyglycerols without a strict differentiation where the oligomers end and the polyglycerol begins. Diglycerols finds wide application in the cosmetics, food industry and polymer industry.[169] For laboratory-scale production of pure diglycerol, several direct syntheses routes were described.[170,171] A polyglycerol is a highly branched polyol and is specifically produced by either anionic or cationic polymerization of glycidol.[172,173] Hyperbranched polyglycerol possesses an inert polyether scaffold. Each branch ends in a hydroxyl function, which renders hyperbranched polyglycerol a highly functional material.

Oxidation. The dehydration/oxidation of glycerol yields a variety of products whose formation depends upon the reaction conditions. Terminal carbons are more easily oxidized than the central carbon atom:[113] Accordingly, acrolein and hydroxypropionaldehyde are favored over hydroxyacetone. All these compounds however, are precursors for polymers, flavour enhancers, and intermediates in pharmaceuticals and cosmetics.[53,174,175] Acrolein is also synthesized by the biochemical oxidation of glycerol.[71]

Hydrogenolysis. The hydrogenolysis of glycerol into 1,2- and 1,3-PDO (propandiols) finds remarkable industrial applications. In fact, millions tons of both diols are produced annually and used as chemicals and solvents: plants have been put in operation by ADM, Cargill, Virent and DOW.[106] In this respect, biochemical transformations allows the synthesis of 1,3-PDO that is a highly added-value component in the polymer industry: an outstanding example is the sorona fiberTM by DuPont, a co-polymer of 1,3-PDO and terephthalic acid.[176]

Fermentation. Availability, low price, and high degree of reduction make glycerol an attractive carbon source for the production of fuels and reduced chemicals. Glycerol's

reduced state enables synthesis of reduced products at higher yields compared to common sugars. Although the number of organisms able to use this reduced carbon source under fermentative conditions is limited, *K. pneumoniae*, *C. pasteurianum*, and *C. butyricum* have been exploited to produce several industrially relevant compounds at high yields and titers including 1,3-PDO and n-butanol. In addition to these products, microorganisms naturally producing compounds such as propionic acid and succinic acid have also been utilized to produce these products through the anaerobic fermentation of glycerol.[115]

APR: syngas. From both industrial and innovation viewpoints, one of the major achievements of the new chemistry of glycerol is the APR process,[177] in which glycerol is converted to syngas (H_2 and CO mixture) over a Pt–Re catalyst operating at 225-300 °C.[178] The overall process takes advantage of a favorable water–gas shift (WGS) thermodynamics which allows a far less energy intensive reaction with respect to the traditional methane reforming.[179] Major features are shown in Figure 1.23. In the biorefineries, the production of syngas is crucial not only to provide fuel for services, but also as a reactant for the Fischer–Tropsch synthesis.[180]

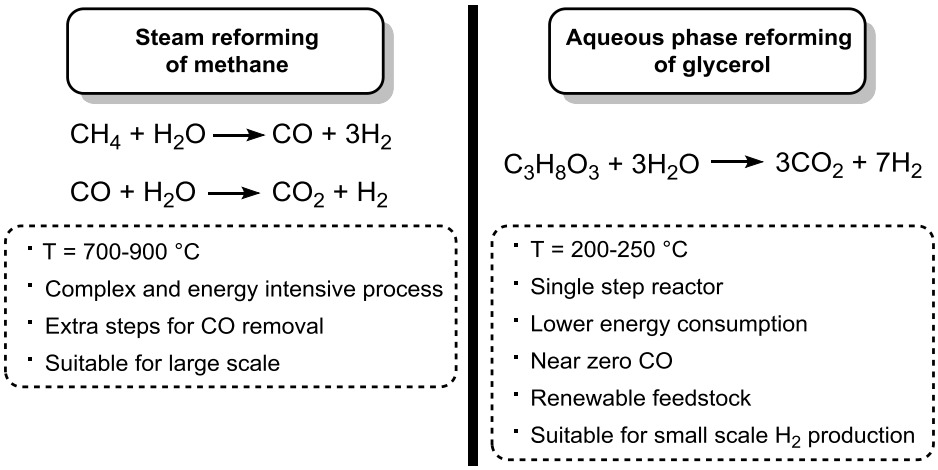

Figure 1.23. Production of syngas. Comparison between aqueous phase reforming of methane (left) and steam reforming of glycerol (right)

1.4 Continuous-flow techniques: a greener perspective

In the past two decades, a significant amount of research has been addressed to the development of 'green' techniques aimed at improving the environmental impact of chemical syntheses not only by using clean reagents, solvents and catalysts, but also through the choice of reaction conditions.[181] To cite an initiative that probably acted as a driver in this field, in 2007, the Green Chemistry Institute (GCI) as a part of the American Chemical

Society (ACS), set up a roundtable in conjunction with a series of global pharmaceutical key areas to facilitate the identification and development of sustainable manufacturing.[182] The panel of experts soon acknowledged the importance of continuous-flow (CF) processing which was ranked as one the pillar technologies for research in Green Chemistry. Consequently, many 'big pharma' looked towards new CF-techniques for green research and production with a renewed interest.[183] This trend has certainly continued and it has expanded over the years until today.[184]

The same philosophy has also inspired a significant part of this PhD Thesis in which CF-based procedures have been used as a tool to conceive and implement new green processes for the upgrading of glycerol and its derivatives.

"Flow chemistry" encompasses a wide range of chemical processes taking place in a continuous mode by allowing a reactants stream to flow through a reactor in which a catalyst is often, but not always, placed. A simplified scheme of a CF-system for chemical reactions is shown in Figure 1.24.

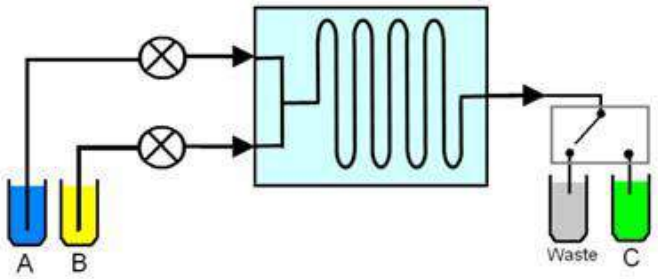

Figure 1.24. A general scheme for a CF-apparatus.

The apparatus is generally composed of the following components: i) one or more fluid control devices (pumps) which deliver solutions of different reactants (A and B) to the reactor section (light blue zone); ii) the reactor in which reactions occur under a precise control of temperature and pressure iii) devices (oven/thermostate and back pressure regulator) for the control of the temperature and the pressure of the reactor, and iv) an analyzer for the monitoring of the reaction, and vi) suitable reservoirs to collect products, and eventually disposed of wastes.

1.4.1 Flow reactors

CF-reactors can be divided into the following categories.[185]

Continuous stirred tank reactor (CSTR). Also known as vat- or backmix reactor, it is primarily used for liquid phase reactions (Figure 1.25). [186]

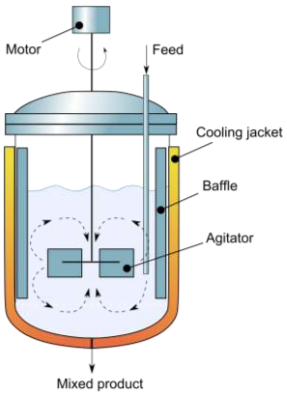

Figure 1.25. Cross-sectional diagram of a CSTR. [186]

In an ideal CSTR, reactants are perfectly mixed and the temperature and the reactants/products concentration are identical at every point inside the reactor. Thus, the exit stream is modeled as being the same as that inside the reactor. This approximation allows an easy calculation of the volume V necessary to convert the entering flow rate of species j to the exit flow rate.

Tubular Reactor. It consists of a cylindrical pipe which normally operates under steady state conditions, as is the CSTR. Reactants are continually consumed as they flow down the length of the reactor with the concentration that varies continuously in the axial direction through the length of the reactor. If one assumes that the flow has no radial variation, the system can be approximated to the plug flow reactor (PFR) (Figure 1.26).

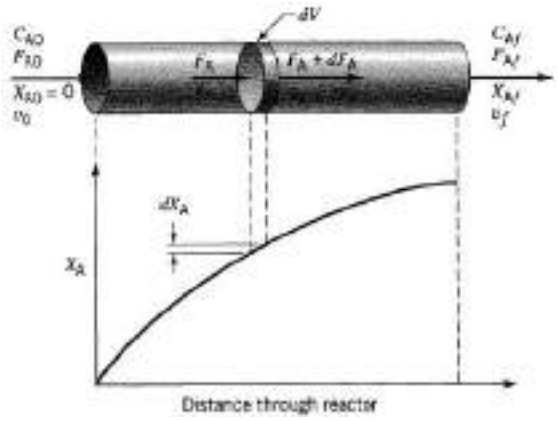

Figure 1.26. The plug flow approximation.[187]

In PFR model, the velocity of the fluid is constant across any cross-section of the pipe and no back mixing occurs. Also for their simple arrangement, ubular reactors find a number of excellent applications.[188,189]

Packed-Bed Reactor. A packed bed reactor (PBR) is a hollow tube, pipe, or other vessel that is filled with a packing material. The packing more often consists of small objects like raschig rings or else appropriate designed solids (spheres, extrudates, etc.) which serve to improve contact between reactants. Packed beds may also be made of catalyst particles or adsorbents such as zeolite pellets, granular activated carbon, etc. Unlike homogeneous reactions taking place in a PFR, in a PBR fluid-solid heterogeneous reactions occur at the surface of the catalyst if used. Consequently, the reaction rate is based on mass of solid catalyst, rather than on the simple reactor volume, and it may be sensitive to solid-liquid mass transport phenomena. Several example can be found in the literarure.[190,191] The efficiency of a continuous flow process is frequently described by the space velocity (SV) which is the quotient of the entering volumetric flow rate of the reactants divided by the reactor catalyst amount (or the volume if there no catalyst is used). SV indicates how many reactor volumes of feed can be treated in a unit time.[192] Depending on the physical nature of the reactants, SV can be calculated by considering the reactant liquid, gas or mass flow rate using Liquid-, Gas- or Weight hourly space velocity (LHSV, GHSV and WHSV respectively). For instance, WHSV is calculated with the following equation.[193]

$$WHSV\ (\mathrm{h}^{-1}) = \frac{F_A\ (\mathrm{g/h})}{W_{cat}\ (\mathrm{g})} \qquad \text{Eq.(1)}$$

where F_A is the flow of the reactant A and W_{cat} is the amount of catalyst loaded in the reactor.

An intriguing recent example of industrial importance is the CF-preparation of Aliskiren developed by the Novartis-MIT Center for Continuous Manufacturing. Aliskiren is a drug belonging to the class renin inhibitors and it is used to treat high blood pressure (Figure 1.27).[194] The flow synthesis of this molecule takes place in a continuous end-to-end manufacturing plant: the process starts with the chemical intermediate **1** that is melted and pumped into a tubular reactor (R1) at 100 °C, where it is mixed with amine **2** and acid catalyst **3**, and reacts reversibly to compound **4**. The process residence time is nominally 47 h. The two-phase stream is separated using a membrane-based liquid–liquid separator (S1): the organic phase contains only **1** and **4**, whereas the aqueous phase removes **2** and **3**. The separated organic phase is fed into a two-stage, mixed suspension, mixed product removal (MSMPR) crystallization process (Cr1 and Cr2). Intermediate **4** then goes into the second CF-tubular reactor (R2) where the removal of the Boc protecting group (Boc=*tert*-butoxycarbonyl) takes place in the presence of concentrated

HCl as a catalyst. Compound **5** is achieved and it is purified by microfiltration membranes (S4) a packed column (S5) of molecular sieves to remove water. A reactive crystallization is eventually performed to create and purify the final salt **6**. The overall CF-plant exemplifies a platform to test newly developed continuous technologies in a fully integrated production system, and to investigate the performance of multiple interconnected units.

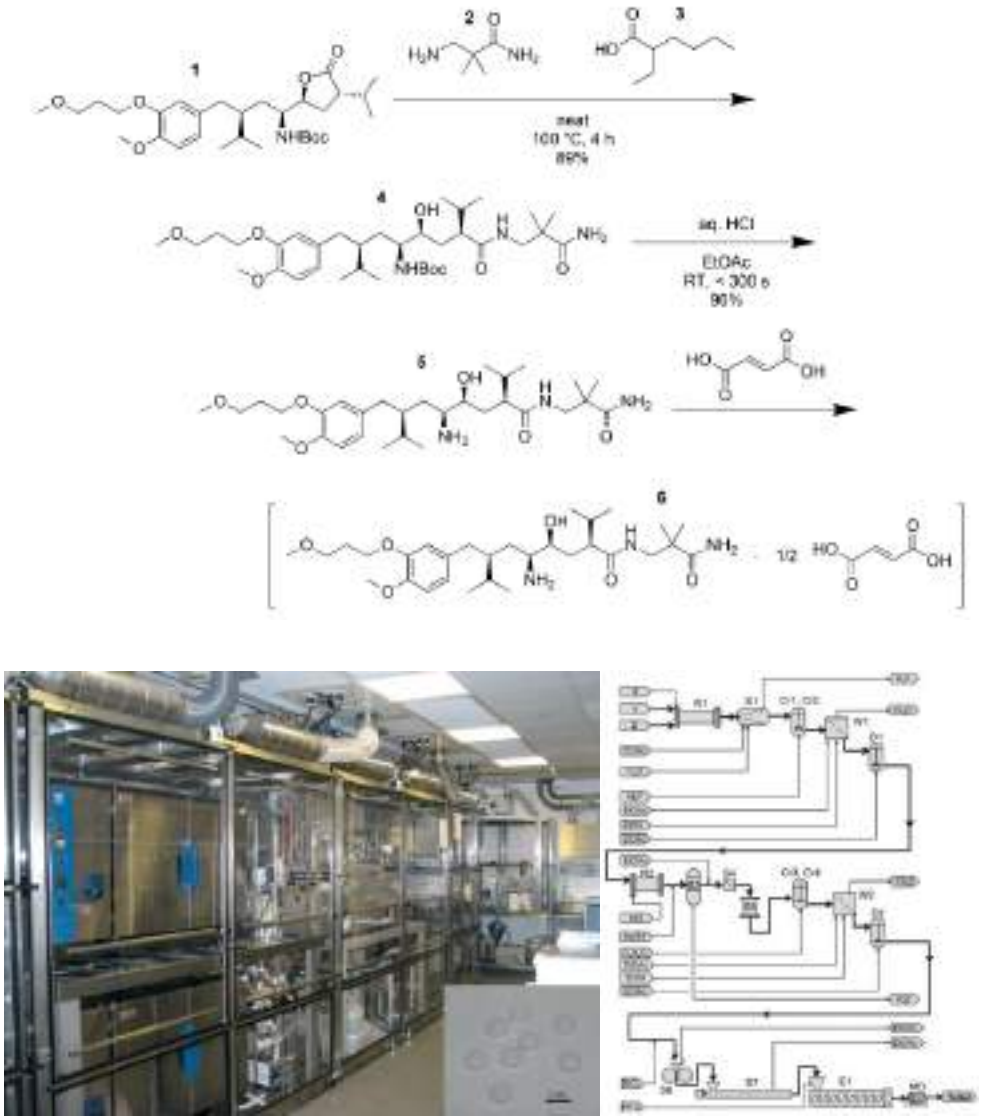

Figure 1.27. Top: Synthetic steps of CF-synthesis of Aliskiren from intermediate 1 to aliskiren hemifumarate (6). Bottom. Left: continuous manufacturing plant for the synthesis of Aliskiren. The inset shows the formulated tablets. Right: process flow diagram including the major unit operations.[194]

Other reactors. Several types of gas flow reactors (GFR) have been designed to deal with continuous processes in the presence of gaseous reagents.[195,196] Particularly interesting is the case of the tube-in-tube system which uses a semi-permeable membrane able to control the solubilization of gaseous reagents into a reactant liquid stream (Figure 1.28).[197]

Figure 1.28. Visual concept of tube-in-tube gas reactor.[198]

Flow photochemical reactors (FPR) have also revolutionized the way chemists deal with either small- or large-scale reactions promoted by light.[199,200,201]

Continuous triphasic processes can be run with trickle bed reactors in which various gas and liquid feeds are delivered to a fixed bed packed with a solid catalyst.[202,203]

The use of micro-reactors for CF-reactions has also been expanded considerably in recent years. Micro-reactors (MR) are generally comprised of channels having volumes from 10 to 1000 µL.[204] MR are usually planar objects roughly the size of a deck of playing cards or a small dinner plate (Figure 1.29).

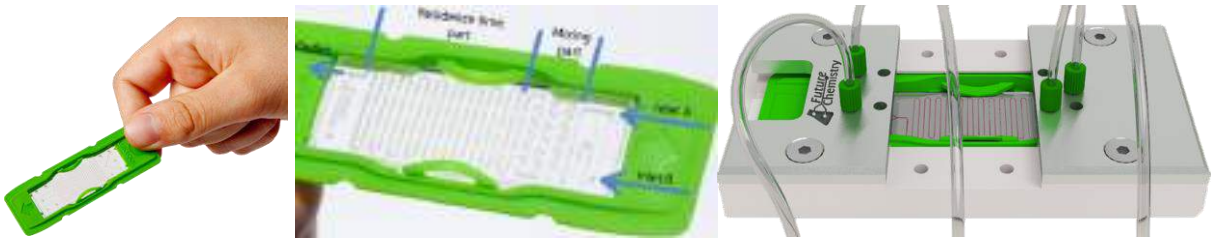

Figure 1.29. A CF-microreactor.[205]

The very low volume (per channel) allows the MR technology to be very effective in gathering a large amounts of data with small amounts of material. Moreover, investigations of chemical reactions on a small scale usually minimize issues with mixing and heat transfer. Unlike the macroscale equipment, fluid behavior is dominated by non-convective, laminar flow wherein only diffusion affects the mixing.

1.4.2 Flow advantages

With respect to batch reactions, CF-processes offers significant improvements in mixing and heat management, scalability, energy efficiency, waste generation, safety, access to a wider range of reaction conditions and unique opportunities in heterogeneous catalysis, multistep synthesis, and more.[206,207,208,209]

Efficient Mixing and Heat Transfer. Both micro- and meso- reactors possess a high surface to volume ratio which allows to absorb heat created from a reaction much more efficiently than any batch reactor. Moreover, a high quality and precision of the mixing regime is obtained in small path length (of few cm). This holds particularly true for micro-scale reactor. Figure 1.30 shows the profiles of heat and mixing distribution for the model exothermic neutralization reaction between HCl and NaOH.[210] In the batch reactor, the exothermic reaction brings about a strong temperature gradient since the cooling takes place only at the surface of the reactor (left, top); by contrast, a much lower gradient – almost at the detection limit - is noted in the MR (left, bottom). A similar behavior is observed also for the reagent mixing.

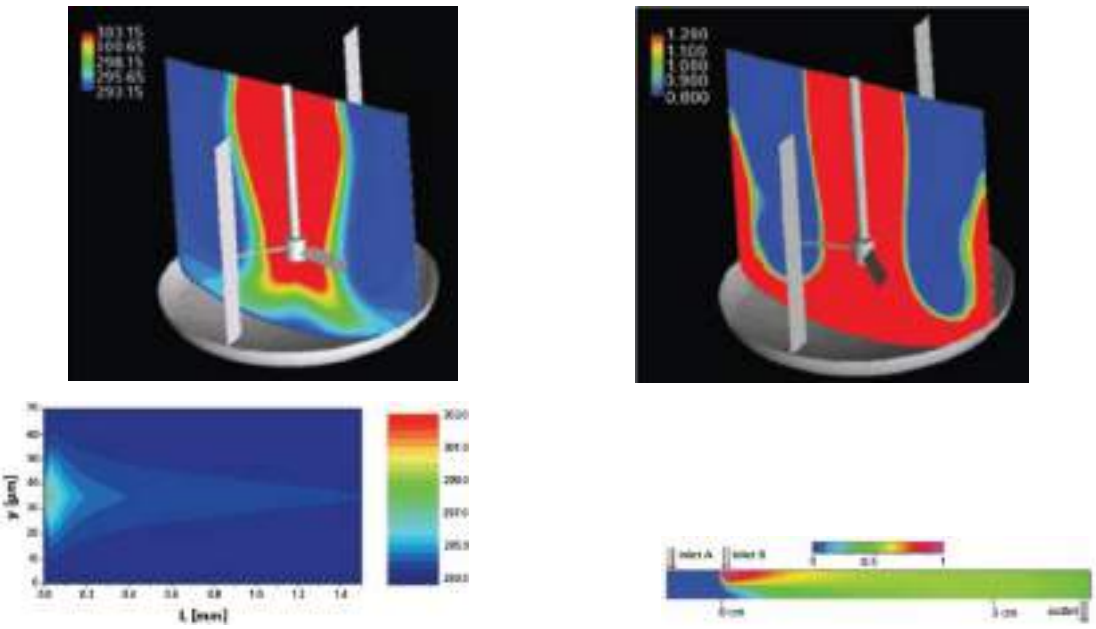

Figure 1.30. Exothermic neutralization reaction of HCl with NaOH: heath distribution in a batch reactor (top-left) and in a microreactor (bottom-left); mixing efficiency in a batch reactor (top-right) and in a microreactor (bottom-right).[210]

Reaction efficiency and product intensification. Batch reactions are often limited by the atmospheric boiling point of the solvent or reagents. By contrast, flow reactors allow to safely manipulate pressure and temperature far beyond atmospheric conditions, resulting in improved energy, time, and space efficiency.[211] An example is offered by the comparison of methylation protocols carried out with conventional hazardous reagents such as methyl iodide (MeI) or dimethyl sulfate (DMS), and the non-toxic dimethyl carbonate (DMC) as a green alternative. Consider for instance, the O-methylation of naphthol (Scheme 1.13).

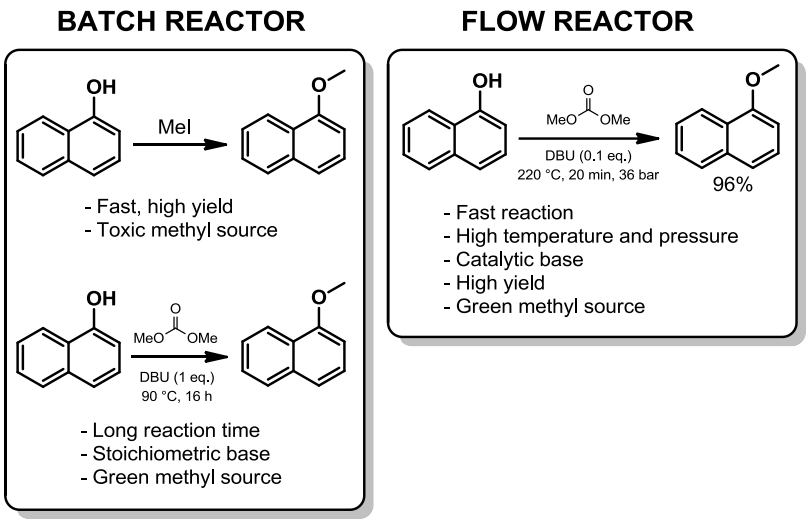

Scheme 1.13. Naftol methylation. Batch vs flow conditions

With respect to methyl iodide or dimethyl sulfate, batch methylations by DMC are limited by the lower reactivity of the carbonate: at the normal boiling point (90 °C), undesired long reaction times are necessary (left). An autoclave must be used to access higher temperature and faster rates, but this implies remarkable costs and scale-up issues. On the other hand, the same reaction (DMC+naphthol) may be run on a simple CF-setup which allows quantitative yields and reaction times as short as ten minutes.[212] Although more energy is required to reach elevated temperatures, the CF-system is well suited to insulation to prevent heat loss, and to the recycling of the energy given off from exothermic reactions. These aspects greatly contribute to improve efficiency on a commercial scale.[213]

In batch reactors, rapid and exothermic reactions are tricky and the corresponding quenching operations are scale dependent.[214] As mentioned above, the effective heat transfer of flow reactors allows to run reactions at higher concentrations than in batch systems with a major benefit in term of product intensification. The material production may often increase by a factor of 200-250 at identical reactor volumes.

Handling of poorly stable intermediates. Flow chemistry techniques allow to easily deal with unstable intermediates without loss of yields and side-reaction runaways. A model example is the Moffat-Swern CF-oxidation of alcohols carried out in a MR (Scheme 1.14).[215]

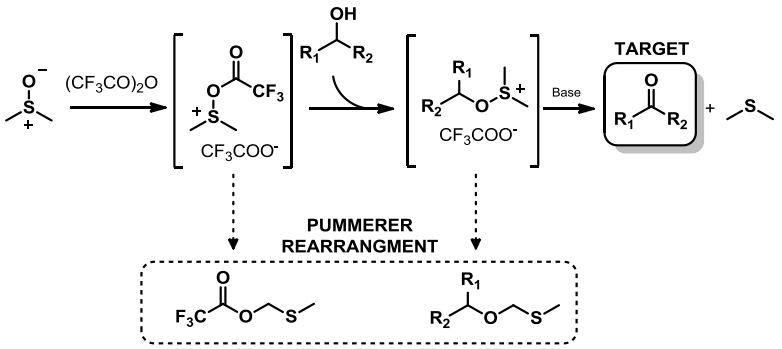

Scheme 1.14. Moffat-Swern alcohols oxidation (top); undesired Pummerer rearrangements (bottom).

The flow reaction operates with a short residence time which ensures a double advantage: i) the minimization of undesired side-reactions such as Pummerer rearrangements (bottom). Unstable sulfonium intermediates proceed straight to the target ketone; ii) the use of remarkably higher temperatures (0-20°C) in comparison with batch reactions requiring cryogenic temperatures (-70°C). In this case, the MR provides a narrow temperature profiles (closer to the ideal one) limiting the access to multiple reaction pathways.[216]

H*eterogeneous catalysis and recycling*. In a continuous process, the (heterogeneous) catalyst is usually confined in the reactor and the reagent mixture is allowed to flow over it. This is the best configuration to combine the reaction and the product separation in a single step and, at the same time, to reactivate and recycle the catalyst. Moreover, the catalyst may have improved lifetime due to decreased exposure to the environment and reaction rates enhanced through the use of high concentrations of the catalyst.[217]

Telescoping multistep reactions. The synthesis of fine chemicals sometimes requires multistep sequences involving extractions, additions of several agents (quenching, drying etc.), filtration, evaporation, purification, distillation and/or recrystallization. These procedures require significant input of energy and materials that ultimately end up as large amounts of waste. Continuous processing is particularly suitable for 'telescoping' reaction sequences by integrating several operations into one (or a few) continuous process.[218] This strategy is well exemplified by the previously described synthesis of Aliskiren (Figure 1.27).

Scale-up. Continuous techniques allow to scale-up syntheses from grams to kilograms without variations in yields, purities and safety. Three main configurations may serve to the scope (Figure 1.31): i) a single flow reactor used for an extended time; ii) multichannel parallel reactors (numbering-up process), or iii) a larger flow reactor by which an increase of the total flow rate is allowed.

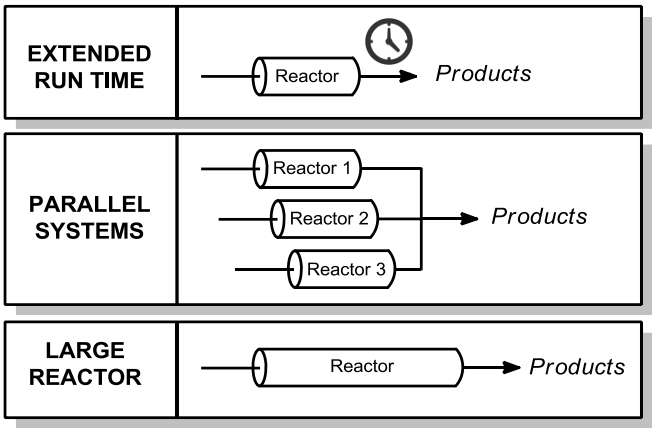

Figure 1.31. The reaction scale-up under flow conditions: three possible configurations

Continuous processing has demonstrated a great flexibility for both laboratory and pilot-plant scale-up of pharmaceuticals and fine chemicals.[219] Particularly, the MR approach has proved efficient for the scale-up of chemical reactions.[220]

Table 1.4 gives an exemplary comparison for an investment decision into a chemical development pilot unit. In this calculation a MR array is invested in place of a 50 L batch vessel in a pilot plant environment.[221].

Table 1.4. Comparison of cost for production in a batch vessel and in a microreactor.

Parameter	50 L batch vessel	Microreactors array
Investment	96632 €	430782 K€
Scale-up effort	10 man days	0 man days
Mean yield	90%	93%
Solvent consumption	10.0 L/Kg	8.3 L/Kg
Personnel per facility	2 men	1 men
Production rate	427 Kg/y	536 Kg/y
Production cost	7227 €/y	2917 €/y
Cost advantage		2308529 €/y
Return on investment		0.14 y

Albeit a higher initial investment is required, the MR plant saves scaling efforts, requires fewer operating personnel, increases yields and reduces (moderately) the consumption of solvent. Also, since MR-based technologies operate with very small volumes, they allow to minimize safety concerns in the case of dangerous reactions involving explosive or toxic reagents (diazo compounds, azides, etc.).[222]

1.5 Aim and brief summary of the Thesis

The present Thesis work has been mainly carried out at the Università Ca' Foscari Venezia in the laboratories of the Green Organic Synthesis Team (GOST). A part of the work has been done at the University of Nottingham (UK) in collaboration with the Clean Technology Group. Both the research groups have a long standing interest in the green and sustainable chemistry.

The general aim of the project has been the development of green continuous-flow synthesis for the chemical upgrading of glycerol and some of its derivatives into high added-value products. Two different approaches were investigated for the implementation of CF-protocols: in the first one, the reaction of glycerol with both ketones and aniline were explored over solid (heterogeneous) catalytic systems, while in the second line, catalyst-free reactions of glycerol and its acetals with organic carbonates were studied. The results have been described and discussed into three chapters.

- ***Chapter 2: Glycerol acetalization***

The continuous-flow acetalization of glycerol with model ketons was studied in the presence of commercial heterogeneous catalysts such as Amberlyst resins and $AlF_3 \cdot 3H_2O$, the latter being never previously explored for this reaction (Scheme 1.15).

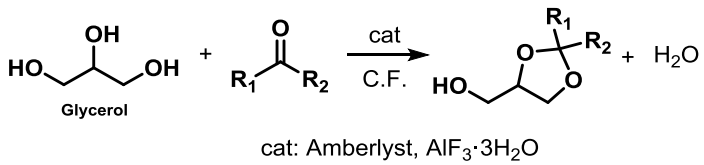

Scheme 1.15. Continuous flow glycerol acetalization with commercial $AlF_3 \cdot 3H_2O$

Although organic resins (particularly Amberlyst-36) were more active than $AlF_3 \cdot 3H_2O$, the major achievement of the study was that aluminium fluoride could efficiently catalyse the acetalization of crude-like glycerol, *i.e.* glycerol contaminated by the common impurities (water, methanol and inorganic salts) deriving from the biodiesel manufacturing in biorefinery plants. By contrast, the same crude-like starting reactant rapidly and irreversibly deactivated the Amberlyst system. XRD characterization studies of $AlF_3 \cdot 3H_2O$ proved that the catalytic active phase was most plausibly a solid solution of formula $Al_2[F_{1-x}(OH)_x]_6(H_2O)_y$ present as a component of the investigated commercial sample.

- ***Chapter 3: Glycerol aromatization with anilines***

This part of the Thesis work was developed at the University of Nottingham where the Clean Technology Group in collaboration with a leader Company in Niobium-based processes and technologies (CBMM: Companhia Brasileira de Metalurgia e Mineração) was exploring applications of niobium oxides and phosphate as catalysts. As a part of this project, the idea of investigating CF-methods for the dehydration of glycerol in the presence of strong acidic niobium oxides and phosphate was considered. The Skraup reaction was therefore studied by replacing the conventional catalyst, *i.e.* concentrated H_2SO_4,[223] by such Nb-derivatives (Scheme 1.16).

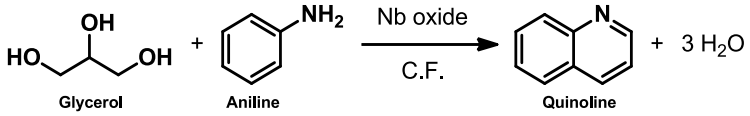

Scheme 1.16. Modified Skraup reaction by using niobium oxide in the continuous-flow mode

- ***Chapter 4: Catalyst-free transesterification with organic carbonates***

Organic carbonates (OCs), particularly the non-toxic light terms of the series such as dimethyl- and diethyl- carbonate (DMC and DEC, respectively) are considered among the most promising green reagents for both alkylation and transesterification reactions. In this thesis, the CF-transesterification of OCs including DMC, DEC, and dibenzyl carbonate, with both glycerol and its acetals was investigated under thermal (catalyst-free) conditions. This non-conventional method proved particularly effective: not only the CF-thermal reaction was feasible, but the tuning of major parameters (T, p, and flow rates) allowed to isolate the desired transesterification derivatives with excellent yields (up to 85-90%) and selectivity (up to 99%), respectively. Scheme 1.10 shows some representative examples for the model case of dimethyl carbonate (DMC).

Of note, in the absence of any catalyst, the CF-reaction could be run virtually indefinitely, downstream operations for the purification of products were simplified, and a high productivity (up to 68 mg min^{-1} compared to a CF-reactor of a capacity as low as 1 mL) was achieved.

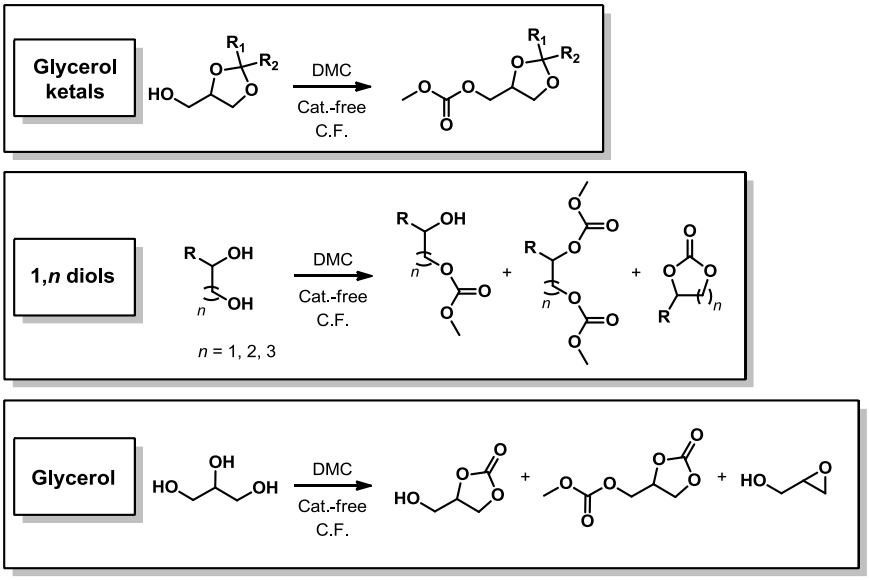

Scheme 1.17. Thermal (catalyst-free) continuous-flow transformation of glycerol ketals, 1,*n* diols and glycerol glycerol. The scheme show the main products obtained.

1.6 Bibliography

[1] V. Smil, Energy transitions: history, requirements, prospects. Praeger, **2010**, ABC-CLIO, LLC

[2] http://praxacap.blogspot.it/2012/02/human-energy-consumption-moves-beyond.html (last access: 2016/12/08)

[3] http://smallbusiness.chron.com/renewable-energy-vs-fossil-fuel-5257.html Renewable Energy Vs. Fossil Fuel (Last access: 2016/07/10)

[4] M. Asif and T. Muneer, Energy supply, its demand and security issues for developed and emerging economies, *Renew. Sust. Energ. Rev.*, **2007**, 11, 1388-1413

[5] http://www.greenworldinvestor.com/2011/07/07/ Advantages and disadvantages of oil cons disregarded by powerful lobbies/ (last access: 2016/07/10)

[6] J. D. Hamilton, *Causes and Consequences of the Oil Shock of 2007-08*, Brookings Papers on Economic Activity, **2009**

[7] http://www.iiaps.org/blog/?tag=oil-gas Wow to manage sourcing in declining markets - will it be any different in oil & gas this time around? (last access: 2016/07/10)

[8] T. M. L. Wigley, R. Richels and J. A. Edmonds, Economic and environmental choices in the stabilization of atmospheric CO2 concentrations, *Nature*, **1996**, 379, 240-243.

[9] R. F. Service, Bringing Fuel Cells Down to Earth, *Science*, **1999**, 285, 682-685.

[10] www.eea.europa.eu Atmospheric Greenhouse Gas Concentrations, Copenaghen, (last access: 2016/09/01)

[11] A. D. Leakey, Rising atmospheric carbon dioxide concentration and the future of C4 crops for food and fuel, *Proceedings. Biological sciences / The Royal Society*, **2009**, 276, 2333-2343.

[12] http://www.skepticalscience.com/co2-increase-is-natural-not-human-caused.htm (Last access: 2016/12/08)

[13] United Nations, *Adoption of the Paris Agreement*, Co.t. Parties Editor, Paris, **2015**

[14] N. Y. Amponsah, M. Troldborg, B. Kington, et al., Greenhouse gas emissions from renewable energy sources: A review of lifecycle considerations, *Renew. Sust. Energ. Rev.*, **2014**, 39, 461-475.

[15] B. Machol and S. Rizk, Economic value of U.S. fossil fuel electricity health impacts, *Environ. Int.*, **2013**, 52, 75-80.

[16] http://www.popularmechanics.com/science/energy/g1765/biggest-oil-spills-in-history/?slide=1 Biggest Oil Spills in History (last access: 2016/07/26)

[17] D. Klemm, B. Heublein, H. P. Fink, et al., Cellulose: fascinating biopolymer and sustainable raw material, *Angew. Chem. Int. Ed. Engl.*, **2005**, 44, 3358-3393.

[18] K. T. Tan and K. T. Lee, A review on supercritical fluids (SCF) technology in sustainable biodiesel production: Potential and challenges, *Renew. Sust. Energ. Rev.*, **2011**, 15, 2452-2456.

[19] H. L. Lam, P. Varbanov and J. Klemeš, Minimising carbon footprint of regional biomass supply chains, *Res. Cons. Recycling*, **2010**, 54, 303-309.

[20] Heinberg, R. *The Party's Over*, 2nd ed., New Society Publishers, **2005**.

[21] National Research Council, *Biobased Industrial Products: Priorities for Research and Commercialization.* National Accademy Press, Washington, DC, **2000**.

[22] I. Kögel-Knabner, The macromolecular organic composition of plant and microbial residues as inputs to soil organic matter, *Soil Biol. Biochem.*, **2002**, 34, 139-162.

[23] E. M. Rubin, Genomics of cellulosic biofuels, *Nature*, **2008**, 454, 841-845.

[24] D. L. Nelson and M. M. Cox in *Lehninger, Principles of Biochemistry*,3rd ed., Worth Publishing, New York, **2000**.

[25] F. Cherubini, The biorefinery concept: Using biomass instead of oil for producing energy and chemicals, *Energy Convers. Manage.*, **2010**, 51, 1412-1421.

[26] J. Clark, F. Deswarte, *The Biorefinery Concept–An Integrated Approach* in *Introduction to Chemicals from Biomass*, Chap. 1. Wiley, **2008**.

[27] http://www.biorefinery.nl/ieabioenergy-task42/ IEA Bioenergy Task 42 (last access: 2016/07/19)

[28] B. Kamm, M. Kamm, P.R. Gruber et al., *Biorefinery systems – an overview. In Industrial processes and products* vol. 1. Wiley-VCH, **2006**.

[29] R. T. L. Ng, D. H. S. Tay and D. K. S. Ng, Simultaneous Process Synthesis, Heat and Power Integration in a Sustainable Integrated Biorefinery, *Energy & Fuels*, **2012**, 26, 7316-7330.

[30] S. Fernando, S. Adhikari, C. Chandrapal, et al., Biorefineries: Current Status, Challenges, and Future Direction, *Energy & Fuels*, **2006**, 20, 1727-1737.

[31] http://www.novamont.com Novamont - Chimica vivente per la qualità della vita (last access: 2016/09/01)

[32] A. V. Bridgwater and G. V. C. Peacocke, Fast pyrolysis processes for biomass, *Renew. Sust. Energ. Rev.*, **2000**, 4, 1-73.

[33] S. I. Yang, M. S. Wu and C. Y. Wu, Application of biomass fast pyrolysis part I: Pyrolysis characteristics and products, *Energy*, **2014**, 66, 162-171.

[34] P.L. Spath, D.C. Dayton, *Preliminary screening – technical and economic assessment of synthesis gas to fuels and chemicals with emphasis on the potential for biomass-derived syngas*, NREL, **2003**.

[35] H. Hofbauer, G. Veronik, T. Fleck, et al., in *Thermochemical Biomass Conversion*: Volume 2, Springer Netherlands, Dordrecht, **1997**.

[36] H. Hofbauer, R. Rauch, K. Bosch et al., *Biomass CHP Plant Güssing – A Success Story*, Expert Meeting on Pyrolysis and Gasification of Biomass and Waste, Strasbourg, October **2002**.

[37] M.A. Paisley and R.P. Overend, *The Silvagas Process from Future Energy Resources – a commercialisation success*; 12th European Conference and Technology Exhibition on Biomass for Energy, Industry and Climate Protection, Amsterdam, June **2002**.

[38] A. van del Drift, C. M. van der Meijden and H. Boerrigter, *MILENA gasification technogy for high efficient SNG production from biomass*, 14th European Biomass Conference & Exhibition, Paris, October **2005**

[39] C. N. Hamelinck, G. v. Hooijdonk and A. P. C. Faaij, Ethanol from lignocellulosic biomass: techno-economic performance in short-, middle- and long-term, *Biomass Bioenergy*, **2005**, 28, 384-410.

[40] H. Roubík, J. Mazancová, J. Banout, et al., Addressing problems at small-scale biogas plants: a case study from central Vietnam, *Journal of Cleaner Production*, **2016**, 112, 2784-2792.

[41] H.-J. Huang, S. Ramaswamy, U. W. Tschirner, et al., A review of separation technologies in current and future biorefineries, *Sep. Purif. Technol.*, **2008**, 62, 1-21.

[42] Y. Sun and J. Cheng, Hydrolysis of lignocellulosic materials for ethanol production: a review, *Bioresour. Technol.*, **2002**, 83, 1-11.

[43] US DOE, T. Werpy, G. Petersen, *Top Value Added Chemicals From Biomass; Volume I: Results of Screening for Potential Candidates from Sugars and Synthesis Gas*, **2004**.

[44] J. J. Bozell and G. R. Petersen, Technology development for the production of biobased products from biorefinery carbohydrates—the US Department of Energy's "Top 10" revisited, *Green Chem.*, **2010**, 12, 539.

[45] T. J. Farmer and M. Mascal, in Introduction to Chemicals from Biomass, 2nd ed., J. Clark and F. Deswarte, Eds., John Wiley & Sons, Ltd, Chichester, UK, **2015**.

[46] EU. Biofuels in the European Union - a vision for 2030 and beyond. Final report of the biofuels research advisory council, **2006**.

[47] J. Clark and F. Deswarte, *Introduction to Chemicals from Biomass*, Wiley, **2008**.

[48] D. M. Alonso, J. Q. Bond and J. A. Dumesic, Catalytic conversion of biomass to biofuels, *Green Chem.*, **2010**, 12, 1493.

[49] G. W. Huber, S. Iborra and A. Corma, Synthesis of Transportation Fuels from Biomass: Chemistry, Catalysts, and Engineering, *Chem. Rev.*, **2006**, 106, 4044-4098.

[50] I. B. Banković-Ilić, O. S. Stamenković and V. B. Veljković, Biodiesel production from non-edible plant oils, *Renew. Sust. Energ. Rev.*, **2012**, 16, 3621-3647.

[51] G. Koçar and N. Civaş, An overview of biofuels from energy crops: Current status and future prospects, *Renew. Sust. Energ. Rev.*, **2013**, 28, 900-916.

[52] http://www.oilgae.com/ref/report/venture_capital/venture_capital.html Algae Fuels Presents an Investing Opportunity You Cannot Afford to Ignore (last access: 2016/07/13)

[53] J. A. Costa and M. G. de Morais, The role of biochemical engineering in the production of biofuels from microalgae, *Bioresour. Technol.*, **2011**, 102, 2-9.

[54] T. M. Mata, A. A. Martins and N. S. Caetano, Microalgae for biodiesel production and other applications: A review, *Renew. Sust. Energ. Rev.*, **2010**, 14, 217-232.

[55] M. Balat, H. Balat and C. Öz, Progress in bioethanol processing, *Prog. Energy Combust. Sci.*, **2008**, 34, 551-573.

[56] http://www.bp.com/en/global/corporate/energy-economics/statistical-review-of-world-energy.html Statistical Review of World Energy (last access: 2016/09/01)

[57] https://www.iea.org/publications/freepublications/publication/iea-energy-technology-essentials-biofuel-production.html IEA Energy Technology Essentials – Biofuel Production, (last access: 2016/09/01)

[58] A. P. Vyas, J. L. Verma and N. Subrahmanyam, A review on FAME production processes, *Fuel*, **2010**, 89, 1-9.

[59] http://www.afdc.energy.gov/uploads/publication/alternative_fuel_price_report_april_2016.pdf The US DOE Clean Cities program: clean cities alternative fuel price report April 2016 (last access: 2016/07/29)

[60] D. Y. C. Leung, X. Wu and M. K. H. Leung, A review on biodiesel production using catalyzed transesterification, *Appl. Energy*, **2010**, 87, 1083-1095.

[61] E. Lotero, Y. Liu, D. E. Lopez, et al., Synthesis of Biodiesel via Acid Catalysis, *Ind. Eng. Chem. Res.*, **2005**, 44, 5353-5363.

[62] B. Freedman, R. O. Butterfield and E. H. Pryde, Transesterification kinetics of soybean oil 1, *Journal of the American Oil Chemists' Society*, **1986**, 63, 1375-1380.

[63] L. Bournay, D. Casanave, B. Delfort, et al., New heterogeneous process for biodiesel production: A way to improve the quality and the value of the crude glycerin produced by biodiesel plants, *Catal. Today*, **2005**, 106, 190-192.

[64] G. Rothenberg, *Catalysis: Concepts and Green Applications*, Weinheim, Wiley–VCH, **2008**.

[65] A. A. Kiss, A. C. Dimian and G. Rothenberg, Solid Acid Catalysts for Biodiesel Production –-Towards Sustainable Energy, *Adv. Synth. Catal.*, **2006**, 348, 75-81.

[66] F. Omota, A. C. Dimian and A. Bliek, Fatty acid esterification by reactive distillation: Part 2—kinetics-based design for sulphated zirconia catalysts, *Chem. Eng. Sci.*, **2003**, 58, 3175-3185.

[67] R. Ciriminna, C. D. Pina, M. Rossi, et al., Understanding the glycerol market, *Eur. J. Lipid Sci. Technol.*, **2014**, 116, 1432-1439.

[68] G. Vicente, J. A. Melero, G. Morales, et al., Acetalisation of bio-glycerol with acetone to produce solketal over sulfonic mesostructured silicas, *Green Chem.*, **2010**, 12, 899.

[69] C. S. Miner and N. N. Dalton, *Glycerol, American Chemical Society Monograph Series*. Reinhold Publishing Company, New York, **1953**.

[70] M. Pagliaro and M. Rossi, *Chlorination* in *The Future of Glycerol*, Chap. 4, 2nd Ed. Royal Society of Chemistry, **2010**.

[71] R. Christoph, B. Schmidt, U. Steinberner, et al., *Glycerol* in *Ullmann's Encyclopedia of Industrial Chemistry*, Wiley-VCH Verlag GmbH & Co. KGaA, **2006**.

[72] W. Dilla, H. Dillenburg, E. Ploenissen et al., Solvay Deutschland GmbH, US5393428, Process for treating waste water containing chlorinated organic compounds from production of epichlorohydrin, **1993**.

[73] T. S. Boozalis, J. B. Ivy, G. D. Willis, US4319062, Allyl Chloride Process, The Dow Chemical Company, **1978**.

[74] M. McCoy, Glycerin surplus, *Chem. Eng. News*, **2006**, 84, 7.

[75] B. A. De and H. D. V. FinchShell, US2779801, Aluminum alkoxide reduction of alpha methylidene alkanals, **1957**.

[76] M. B. Smith and J. March, in *March's Advanced Organic Chemistry: Reactions, Mechanisms, and Structure*, 6th ed., John Wiley & Sons, **2007**.

[77] A. Thizy, M. E. Degeorges and E. Charles, PROGIL French Body Corporate, FR1271563, **1961**.

[78] B. M. Bell, J. R. Briggs, R. M. Campbell, et al., Glycerin as a Renewable Feedstock for Epichlorohydrin Production. The GTE Process, *CLEAN - Soil, Air, Water*, **2008**, 36, 657-661.

[79] A. Almena and M. Martín, Technoeconomic Analysis of the Production of Epichlorohydrin from Glycerol, *Ind. Eng. Chem. Res.*, **2016**, 55, 3226-3238.

[80] NIIR Board of Consultants & Engineers, *The Complete Technology Book on Soaps*, 2nd Revised ed., Asia Pacific Business Press Inc., **2016**.

[81] K. W. Anderson, A. L. Hall and D.A. Oester, K.T. Zilch, Henkel Corporation, improved fat splitting process, EP19940900377, **1996**.

[82] K. Schumann, K. Siekmann, Soaps in *Ullmann's Encyclopedia of Industrial Chemistry*, Wiley-VCH, Weinheim, **2000**.

[83] G. G. Freeman and G. M. S. Donald, Fermentation Processes Leading to Glycerol: I. The Influence of Certain Variables on Glycerol Formation in the Presence of Sulfites, *Applied Microbiology*, **1957**, 5, 197-210.

[84] A. Negoi, I. T. Trotus, O. Mamula Steiner, et al., Direct synthesis of sorbitol and glycerol from cellulose over ionic Ru/magnetite nanoparticles in the absence of external hydrogen, *ChemSusChem*, **2013**, 6, 2090-2094.

[85] C. A. G. Quispe, C. J. R. Coronado and J. A. Carvalho Jr, Glycerol: Production, consumption, prices, characterization and new trends in combustion, *Renew. Sust. Energ. Rev.*, **2013**, 27, 475-493.

[86] https://www.ihs.com/products/glycerin-chemical-economics-handbook.html Glycerin (last access: 2016/08/01).

[87] http://www.prweb.com/releases/glycerin_natural/oleo_chemicals/prweb4714434.htm Global Glycerin Market to Reach 4.4 Billion Pounds by 2015, According to a New Report by Global Industry Analysts (last access: 2016/08/01).

[88] http://www.icis.com/resources/news/2015/12/31/9952515/outlook-16-us-glycerine-market-faces-long-supply/ OUTLOOK '16: US glycerine market faces long supply (last access: 2016/08/16)

[89] *OPIS Ethanol & Biodiesel Information Service*, March 24, Vol. 11, **2014**.

[90] Y. Xiao, G. Xiao and A. Varma, A Universal Procedure for Crude Glycerol Purification from Different Feedstocks in Biodiesel Production: Experimental and Simulation Study, *Ind. Eng. Chem. Res.*, **2013**, 52, 14291-14296.

[91] M. S. Ardi, M. K. Aroua and N. A. Hashim, Progress, prospect and challenges in glycerol purification process: A review, *Renew. Sust. Energ. Rev.*, **2015**, 42, 1164-1173.

[92] N. Sdrula, A study using classical or membrane separation in the biodiesel process, *Desalination*, **2010**, 250, 1070-1072.

[93] Total dissolved solids (TDS) is a measure of the combined content of all inorganic and organic substances contained in a liquid in molecular, ionized or micro-granular (colloidal sol) suspended form.

[94] http://www.eetcorp.com/heepm/glycerine.htm Glycerol Purification (last access: 2016/09/01)

[95] C. S. Callam, S. J. Singer, T. L. Lowary, et al., Computational Analysis of the Potential Energy Surfaces of Glycerol in the Gas and Aqueous Phases: Effects of Level of Theory, Basis Set, and Solvation on Strongly Intramolecularly Hydrogen-Bonded Systems, *J. Am. Chem. Soc.*, **2001**, 123, 11743-11754.

[96] R. Chelli, P. Procacci, G. Cardini, et al., Glycerol condensed phases Part II.A molecular dynamics study of the conformational structure and hydrogen bonding, *Phys. Chem. Chem. Phys.*, **1999**, 1, 879-885.

[97] D. F. Stedman, The vapour equilibrium of aqueous glycerin solutions, *Trans. Faraday Soc.*, **1928**, 24, 289-298.

[98] R. C. Reid, I. M. Prausnitz, T. K. Sherwood, *The Properties of Gases and Liquids*, 3rd ed., McGraw-Hill, New York **1977**.

[99] C. S. Miner and N. N. Dalton in *Glycerol*, Reinhold Pub. Corp., New York, **1953**.

[100] L. H. Horsley, Table of Azeotropes and Nonazeotropes, *Anal. Chem.*, **1947**, 19, 508-600.

[101] M. Pagliaro and M. Rossi, *Glycerol: Properties and Production* in *The Future of Glycerol*, Chap. 1, 2nd Ed. Royal Society of Chemistry, **2010**.

[102] http://www.sbioinformatics.com/design_thesis/Glycerol/Glycerol.htm Production of Glycerol (last access: 2016/09/01)

[103] https://www.frost.com/sublib/display-market-insight.do?id=77264824 R&D Creating New Avenues for Glycerine (last access: 2016/09/01)

[104] http://www.the-scientist.com/?articles.view/articleNo/35714/title/The-Elixir-Tragedy--1937/ The Elixir Tragedy, 1937 (last access: 2016/09/01)

[105] C. Len and R. Luque, Continuous flow transformations of glycerol to valuable products: an overview, *Sustain. chem. process.*, **2014**, 2, 1.

[106] A. Behr, J. Eilting, K. Irawadi, et al., Improved utilisation of renewable resources: New important derivatives of glycerol, *Green Chem.*, **2008**, 10, 13-30.

[107] X. Liao, Y. Zhu, S.-G. Wang, et al., Producing triacetylglycerol with glycerol by two steps: Esterification and acetylation, *Fuel Process. Technol.*, **2009**, 90, 988-993.

[108] R. S. Karinen and A. O. I. Krause, New biocomponents from glycerol, *Appl. Catal., A*, **2006**, 306, 128-133.

[109] M. Aresta, A. Dibenedetto, F. Nocito, et al., A study on the carboxylation of glycerol to glycerol carbonate with carbon dioxide: The role of the catalyst, solvent and reaction conditions, *J. Mol. Catal. A: Chem.*, **2006**, 257, 149-153.

[110] P. U. Naik, L. Petitjean, K. Refes, et al., Imidazolium-2-Carboxylate as an Efficient, Expeditious and Eco-Friendly Organocatalyst for Glycerol Carbonate Synthesis, *Adv. Synth. Catal.*, **2009**, 351, 1753-1756.

[111] S. Cassel, C. Debaig, T. Benvegnu, et al., Original Synthesis of Linear, Branched and Cyclic Oligoglycerol Standards, *Eur. J. Org. Chem.*, **2001**, 2001, 875-896.

[112] D. Tongsakul, S. Nishimura and K. Ebitani, Platinum/Gold Alloy Nanoparticles-Supported Hydrotalcite Catalyst for Selective Aerobic Oxidation of Polyols in Base-Free Aqueous Solution at Room Temperature, *ACS Catalysis*, **2013**, 3, 2199-2207.

[113] R. Garcia, M. Besson and P. Gallezot, Chemoselective catalytic oxidation of glycerol with air on platinum metals, *Appl. Catal., A*, **1995**, 127, 165-176.

[114] Y. Nakagawa, X. Ning, Y. Amada, et al., Solid acid co-catalyst for the hydrogenolysis of glycerol to 1,3-propanediol over Ir-ReOx/SiO2, *Appl. Catal., A*, **2012**, 433-434, 128-134.

[115] J. M. Clomburg and R. Gonzalez, Anaerobic fermentation of glycerol: a platform for renewable fuels and chemicals, *Trends Biotechnol.*, **2013**, 31, 20-28.

[116] D. A. Boga, F. Liu, P. C. A. Bruijnincx, et al., Aqueous-phase reforming of crude glycerol: effect of impurities on hydrogen production, *Catal. Sci. Technol.*, **2016**, 6, 134-143.

[117] M. O. Sonnati, S. Amigoni, E. P. Taffin de Givenchy, et al., Glycerol carbonate as a versatile building block for tomorrow: synthesis, reactivity, properties and applications, *Green Chem.*, **2013**, 15, 283-306.

[118] J. H. Clements, Reactive Applications of Cyclic Alkylene Carbonates, *Ind. Eng. Chem. Res.*, **2003**, 42, 663-674.

[119] J. Rousseau, C. Rousseau, B. Lynikaite˙, et al., Tosylated glycerol carbonate, a versatile bis-electrophile to access new functionalized glycidol derivatives, *Tetrahedron*, **2009**, 65, 8571-8581.

[120] W. L. Jolly in *Modern Inorganic Chemistry*, McGraw-Hill, New York, 1984.

[121] C. Ursin, C. Hansen, J.Van Dyk et al., Permeability of commercial solvents through living human skin. *Am. Ind. Hyg. Assoc. J.*, **1995**, 56*,* 651-660.

[122] B. Schäffner, F. Schäffner, S. P. Verevkin, et al., Organic Carbonates as Solvents in Synthesis and Catalysis, *Chem. Rev.*, **2010**, 110, 4554-4581.

[123] P. Lameiras, L. Boudesocque, Z. Mouloungui, et al., Glycerol and glycerol carbonate as ultraviscous solvents for mixture analysis by NMR, *Journal of magnetic resonance*, **2011**, 212, 161-168.

[124] G. Ou, B. He and Y. Yuan, Design of biosolvents through hydroxyl functionalization of compounds with high dielectric constant, *Appl. Biochem. Biotechnol.*, **2012**, 166, 1472-1479.

[125] P. K. Varshney and S. Gupta, Natural polymer-based electrolytes for electrochemical devices: a review, *Ionics*, **2011**, 17, 479-483.

[126] C. Magniont, G. Escadeillas, C. Oms-Multon, et al., The benefits of incorporating glycerol carbonate into an innovative pozzolanic matrix, *Cem. Concr. Res.*, **2010**, 40, 1072-1080.

[127] K. Ueno and H. Mizushima, US2005033122(A1), Glycerol carbonate glycoside, **2005**.

[128] A. Murase, US4801331(A), Nail lacquer remover composition, **1989**.

[129] C. L. Bolívar-Diaz, V. Calvino-Casilda, F. Rubio-Marcos, et al., New concepts for process intensification in the conversion of glycerol carbonate to glycidol, *Applied Catalysis B: Environmental*, **2013**, 129, 575-579.

[130] J. Geschwind and H. Frey, Poly(1,2-glycerol carbonate): A Fundamental Polymer Structure Synthesized from CO2and Glycidyl Ethers, *Macromolecules*, **2013**, 46, 3280-3287.

[131] M. S. Kathalewar, P. B. Joshi, A. S. Sabnis, et al., Non-isocyanate polyurethanes: from chemistry to applications, *RSC Advances*, **2013**, 3, 4110.

[132] H. Zhang and M. W. Grinstaff, Synthesis of atactic and isotactic poly(1,2-glycerol carbonate)s: degradable polymers for biomedical and pharmaceutical applications, *J. Am. Chem. Soc.*, **2013**, 135, 6806-6809.

[133] J. R. Ochoa-Gómez, O. Gómez-Jiménez-Aberasturi, C. Ramírez-López, et al., A Brief Review on Industrial Alternatives for the Manufacturing of Glycerol Carbonate, a Green Chemical, *Org. Proc. Res. Dev.*, **2012**, 16, 389-399.

[134] A. Dibenedetto, A. Angelini, M. Aresta, et al., Converting wastes into added value products: from glycerol to glycerol carbonate, glycidol and epichlorohydrin using environmentally friendly synthetic routes, *Tetrahedron*, **2011**, 67, 1308-1313.

[135] M. Aresta, A. Dibenedetto, C. Pastore, et al., Cerium(IV)oxide modification by inclusion of a hetero-atom: A strategy for producing efficient and robust nano-catalysts for methanol carboxylation, *Catal. Today*, **2008**, 137, 125-131.

[136] M. Aresta, A. Dibenedetto, C. Pastore, et al., Influence of Al2O3 on the performance of CeO2 used as catalyst in the direct carboxylation of methanol to dimethylcarbonate and the elucidation of the reaction mechanism, *J. Catal.*, **2010**, 269, 44-52.

[137] J. George, Y. Patel, S. M. Pillai, et al., Methanol assisted selective formation of 1,2-glycerol carbonate from glycerol and carbon dioxide using nBu2SnO as a catalyst, *J. Mol. Catal. A: Chem.*, **2009**, 304, 1-7.

[138] L. Wang, Y. Ma, Y. Wang, et al., Efficient synthesis of glycerol carbonate from glycerol and urea with lanthanum oxide as a solid base catalyst, *Catal. Commun.*, **2011**, 12, 1458-1462.

[139] M. J. Climent, A. Corma, P. De Frutos, et al., Chemicals from biomass: Synthesis of glycerol carbonate by transesterification and carbonylation with urea with hydrotalcite catalysts. The role of acid–base pairs, *J. Catal.*, **2010**, 269, 140-149.

[140] A. Takagaki, K. Iwatani, S. Nishimura, et al., Synthesis of glycerol carbonate from glycerol and dialkyl carbonates using hydrotalcite as a reusable heterogeneous base catalyst, *Green Chem.*, **2010**, 12, 578.

[141] H.-J. Cho, H.-M. Kwon, J. Tharun, et al., Synthesis of glycerol carbonate from ethylene carbonate and glycerol using immobilized ionic liquid catalysts, *Journal of Industrial and Engineering Chemistry*, **2010**, 16, 679-683.

[142] J. Li and T. Wang, Chemical equilibrium of glycerol carbonate synthesis from glycerol, *The Journal of Chemical Thermodynamics*, **2011**, 43, 731-736.

[143] M. Selva, A. Perosa and M. Fabris, Sequential coupling of the transesterification of cyclic carbonates with the selective N-methylation of anilines catalysed by faujasites, *Green Chem.*, **2008**, 10, 1068-1077.

[144] M. G. Álvarez, A. M. Frey, J. H. Bitter, et al., On the role of the activation procedure of supported hydrotalcites for base catalyzed reactions: Glycerol to glycerol carbonate and self-condensation of acetone, *Applied Catalysis B: Environmental*, **2013**, 134-135, 231-237.

[145] M. Malyaadri, K. Jagadeeswaraiah, P. S. Sai Prasad, et al., Synthesis of glycerol carbonate by transesterification of glycerol with dimethyl carbonate over Mg/Al/Zr catalysts, *Appl. Catal., A*, **2011**, 401, 153-157.

[146] M. G. Alvarez, A. M. Segarra, S. Contreras, et al., Enhanced use of renewable resources: Transesterification of glycerol catalyzed by hydrotalcite-like compounds, *Chem. Eng. J.*, **2010**, 161, 340-345.

[147] F. S. H. Simanjuntak, T. K. Kim, S. D. Lee, et al., CaO-catalyzed synthesis of glycerol carbonate from glycerol and dimethyl carbonate: Isolation and characterization of an active Ca species, *Appl. Catal., A*, **2011**, 401, 220-225.

[148] M. Tudorache, L. Protesescu, S. Coman, et al., Efficient bio-conversion of glycerol to glycerol carbonate catalyzed by lipase extracted from Aspergillus niger, *Green Chem.*, **2012**, 14, 478.

[149] J. R. Ochoa-Gómez, O. Gómez-Jiménez-Aberasturi, B. Maestro-Madurga, et al., Synthesis of glycerol carbonate from glycerol and dimethyl carbonate by transesterification: Catalyst screening and reaction optimization, *Appl. Catal., A*, **2009**, 366, 315-324.

[150] N. Suriyaprapadilok and B. Kitiyanan, Synthesis of Solketal from Glycerol and Its Reaction with Benzyl Alcohol, *Energy Procedia*, **2011**, 9, 63-69.

[151] P. Manjunathan, S. P. Maradur, A. B. Halgeri, et al., Room temperature synthesis of solketal from acetalization of glycerol with acetone: Effect of crystallite size and the role of acidity of beta zeolite, *J. Mol. Catal. A: Chem.*, **2015**, 396, 47-54.

[152] C. Gonzalez-Arellano, R. A. D. Arancon and R. Luque, Al-SBA-15 catalysed cross-esterification and acetalisation of biomass-derived platform chemicals, *Green Chem.*, **2014**, 16, 4985-4993.

[153] V. R. Ruiz, A. Velty, L. L. Santos, et al., Gold catalysts and solid catalysts for biomass transformations: Valorization of glycerol and glycerol–water mixtures through formation of cyclic acetals, *J. Catal.*, **2010**, 271, 351-357.

[154] H. Yamamoto and K. Ishihara, in *Acid catalysis in modern organic Synthesis*. Wiley Online Library, Vol. 1, **2008**.

[155] G. S. Nair, E. Adrijanto, A. Alsalme, et al., Glycerol utilization: solvent-free acetalisation over niobia catalysts, *Catalysis Science & Technology*, **2012**, 2, 1173.

[156] M. Sutter, E. D. Silva, N. Duguet, et al., Glycerol Ether Synthesis: A Bench Test for Green Chemistry Concepts and Technologies, *Chem. Rev.*, **2015**, 115, 8609-8651.

[157] C. J. A. Mota, C. X. A. da Silva, N. Rosenbach, et al., Glycerin Derivatives as Fuel Additives: The Addition of Glycerol/Acetone Ketal (Solketal) in Gasolines, *Energy & Fuels*, **2010**, 24, 2733-2736.

[158] C. D. Driscoll and R. Valentine, Developmental toxicity of diglyme by inhalation in the rat. *Drug. Chem. Toxicol.*, **1998**, 21, 119-136.

[159] L. J. Stegerhoek and P. E. Verkade, Esters derived from batyl alcohol, *Recl. Trav. Chim. Pays-Bas*, **1956**, 75, 143-163.

[160] O. Sirkecioglu, B. Karliga and N. Talinli, Benzylation of alcohols by using bis[acetylacetonato]copper as catalyst, *Tetrahedron Lett.*, **2003**, 44, 8483-8485.

[161] M. P. Pico, A. Romero, S. Rodríguez, et al., Etherification of Glycerol bytert-Butyl Alcohol: Kinetic Model, *Ind. Eng. Chem. Res.*, **2012**, 51, 9500-9509.

[162] S. Pariente, N. Tanchoux and F. Fajula, Etherification of glycerol with ethanol over solid acid catalysts, *Green Chem.*, **2009**, 11, 1256.

[163] S. Gupta and F. Kummerow, Notes- An Improved Procedure for Preparing Glycerol Ethers, *The Journal of Organic Chemistry*, **1959**, 24, 409-410.

[164] E. Baer, L.J. Rubi and; H.O.L. Fischer, Naturally occuring glycerol ethers. Synthesis of selachyl alcohol. *J. Biologic. Chem.*, **1944**. 155, 447-457.

[165] E. Baer and H.O.L. Fischer, Studies on acetone-glyceraldehyde, and optically active glycerides. Configuration of the natural batyl, chimyl and selachyl alcohols, *J. Biological Chem.*, **1941**, 140, 397-410.

[166] M. Selva, V. Benedet and M. Fabris, Selective catalytic etherification of glycerol formal and solketal with dialkyl carbonates and K2CO3, *Green Chem.*, **2012**, 14, 188-200.

[167] M. Selva, S. Guidi and M. Noè, Upgrading of glycerol acetals by thermal catalyst-free transesterification of dialkyl carbonates under continuous-flow conditions, *Green Chem.*, **2015**, 17, 1008-1023.

[168] A. M. Truscello, C. Gambarotti, M. Lauria, et al., One-pot synthesis of aryloxypropanediols from glycerol: towards valuable chemicals from renewable sources, *Green Chem.*, **2013**, 15, 625.

[169] A. Martin and M. Richter, Oligomerization of glycerol - a critical review, *Eur. J. Lipid Sci. Technol.*, **2011**, 113, 100-117.

[170] H. Wittcoff, J. R. Roach and S. E. Miller, Polyglycerols. I. The Identification of Polyglycerol Mixtures by the Procedures of Allylation and Acetonation: Isolation of Pure Diglycerol1, *J. Am. Chem. Soc.*, **1947**, 69, 2655-2657.

[171] H. Wittcoff, J. R. Roach and S. E. Miller, Polyglycerols. II. Syntheses of Diglycerol, *J. Am. Chem. Soc.*, **1949**, 71, 2666-2668.

[172] A. Sunder, R. Hanselmann, H. Frey, et al., Controlled Synthesis of Hyperbranched Polyglycerols by Ring-Opening Multibranching Polymerization, *Macromolecules*, **1999**, 32, 4240-4246.

[173] A. Dworak, W. Walach and B. Trzebicka, Cationic polymerization of glycidol. Polymer structure and polymerization mechanism, *Macromol. Chem. Phys.*, **1995**, 196, 1963-1970.

[174] A. Talebian-Kiakalaieh, N. A. S. Amin and H. Hezaveh, Glycerol for renewable acrolein production by catalytic dehydration, *Renew. Sust. Energ. Rev.*, **2014**, 40, 28-59.

[175] H. Krauter, T. Willke and K. D. Vorlop, Production of high amounts of 3-hydroxypropionaldehyde from glycerol by Lactobacillus reuteri with strongly increased biocatalyst lifetime and productivity, *New biotechnology*, **2012**, 29, 211-217.

[176] C. S. Lee, M. K. Aroua, W. M. A. W. Daud, et al., A review: Conversion of bioglycerol into 1,3-propanediol via biological and chemical method, *Renew. Sust. Energ. Rev.*, **2015**, 42, 963-972.

[177] M. Pagliaro and M. Rossi, *Reforming* in *The Future of Glycerol*, Chap. 2, 2nd ed. Royal Society of Chemistry, **2010**.

[178] R. R. Soares, D. A. Simonetti and J. A. Dumesic, Glycerol as a source for fuels and chemicals by low-temperature catalytic processing, *Angew. Chem. Int. Ed. Engl.*, **2006**, 45, 3982-3985.

[179] R. D. Cortright, R. R. Davda and J. A. Dumesic, Hydrogen from catalytic reforming of biomass-derived hydrocarbons in liquid water, *Nature*, **2002**, 418, 964-967.

[180] A. de Klerk, Fischer–Tropsch Process in *Kirk-Othmer Encyclopedia of Chemical Technology*, John Wiley & Sons, Inc., **2000**.

[181] C. J. Li and B. M. Trost, Green chemistry for chemical synthesis, *Proc Natl Acad Sci U S A*, **2008**, 105, 13197-13202.

[182] C. Jiménez-González, P. Poechlauer, Q. B. Broxterman, et al., Key Green Engineering Research Areas for Sustainable Manufacturing: A Perspective from Pharmaceutical and Fine Chemicals Manufacturers, *Org. Proc. Res. Dev.*, **2011**, 15, 900-911.

[183] V. Hessel, D. Kralisch and U. Krtschil, Sustainability through green processing – novel process windows intensify micro and milli process technologies, *Energy Environ. Sci.*, **2008**, 1, 467.

[184] K. S. Elvira, X. Casadevall i Solvas, R. C. Wootton, et al., The past, present and potential for microfluidic reactor technology in chemical synthesis, *Nature chemistry*, **2013**, 5, 905-915.

[185] H. S. Fogler in *Continuous-Flow Reactors* in *Essentials of Chemical Reaction Engineering*, chap. 1.4, Prentice Hall, **2010**.

[186] https://en.wikipedia.org/wiki/Continuous_stirred-tank_reactor Picture of a continuous stirred-tank reactor (last access: 2016/08/03)

[187] http://pyomark.tistory.com/224 (Last access: 2016/12/08)

[188] D. Ghislieri, K. Gilmore and P. H. Seeberger, Chemical assembly systems: layered control for divergent, continuous, multistep syntheses of active pharmaceutical ingredients, *Angew. Chem. Int. Ed. Engl.*, **2015**, 54, 678-682.

[189] S. H. Lau, A. Galvan, R. R. Merchant, et al., Machines vs Malaria: A Flow-Based Preparation of the Drug Candidate OZ439, *Org. Lett.*, **2015**, 17, 3218-3221.

[190] C. Battilocchio, F. Feist, A. Hafner, et al., Iterative reactions of transient boronic acids enable sequential C–C bond formation, *Nature chemistry*, **2016**, 8, 360-367.

[191] M. Chen, S. Ichikawa and S. L. Buchwald, Rapid and efficient copper-catalyzed Finkelstein reaction of (hetero)aromatics under continuous-flow conditions, *Angew. Chem. Int. Ed. Engl.*, **2015**, 54, 263-266.

[192] For instance, a reactor with a space velocity of 7 h^{-1} is able to process feed equivalent to seven times the reactor volume per hour.

[193] P. Harriott, Ideal Reactors, in *Chemical Reactor Design*, chap. 3, Marcel Dekker, Inc. New York, USA, **2003**.

[194] S. Mascia, P. L. Heider, H. Zhang, et al., End-to-end continuous manufacturing of pharmaceuticals: integrated synthesis, purification, and final dosage formation, *Angew. Chem. Int. Ed. Engl.*, **2013**, 52, 12359-12363.

[195] F. Levesque and P. H. Seeberger, Continuous-flow synthesis of the anti-malaria drug artemisinin, *Angew. Chem. Int. Ed. Engl.*, **2012**, 51, 1706-1709.

[196] F. Mastronardi, B. Gutmann and C. O. Kappe, Continuous Flow Generation and Reactions of Anhydrous Diazomethane Using a Teflon AF-2400 Tube-in-Tube Reactor, *Org. Lett.*, **2013**, 15, 5590-5593.

[197] M. Brzozowski, M. O'Brien, S. V. Ley, et al., Flow chemistry: intelligent processing of gas-liquid transformations using a tube-in-tube reactor, *Acc. Chem. Res.*, **2015**, 48, 349-362.

[198] http://www.leygroup.ch.cam.ac.uk/research/medicinal-chemistry/gas-reactors tube-in-tube flow gas reactor (last access: 2016/08/03)

[199] J. P. Knowles, L. D. Elliott and K. I. Booker-Milburn, Flow photochemistry: Old light through new windows, *Beilstein Journal of Organic Chemistry*, **2012**, 8, 2025-2052.

[200] J. F. B. Hall, R. A. Bourne, X. Han, et al., Synthesis of antimalarialtrioxanesvia continuous photo-oxidation with1O2in supercritical CO2, *Green Chem.*, **2013**, 15, 177-180.

[201] K. G. Maskill, J. P. Knowles, L. D. Elliott, et al., Complexity from simplicity: tricyclic aziridines from the rearrangement of pyrroles by batch and flow photochemistry, *Angew. Chem. Int. Ed. Engl.*, **2013**, 52, 1499-1502.

[202] T. Ouchi, C. Battilocchio, J. M. Hawkins, et al., Process Intensification for the Continuous Flow Hydrogenation of Ethyl Nicotinate, *Org. Proc. Res. Dev.*, **2014**, 18, 1560-1566.

[203] T. Ouchi, R. J. Mutton, V. Rojas, et al., Solvent-Free Continuous Operations Using Small Footprint Reactors: A Key Approach for Process Intensification, *ACS Sustainable Chem. Eng.*, **2016**, 4, 1912-1916.

[204] K. Geyer, J. D. Codee and P. H. Seeberger, Microreactors as tools for synthetic chemists-the chemists' round-bottomed flask of the 21st century?, *Chem. Eur. J.*, **2006**, 12, 8434-8442.

[205] http://futurechemistry.com/flow-chemistry-technology/flow-chemistry-applications/ (Last access: 2016/12/08)

[206] S. G. Newman and K. F. Jensen, The role of flow in green chemistry and engineering, *Green Chem.*, **2013**,15,

1456-1472.

[207] C. Wiles and P. Watts, Continuous flow reactors: a perspective, *Green Chem.*, **2012**, 14, 38-54.

[208] S. V. Ley, On being green: can flow chemistry help?, *Chem. Rec.*, **2012**, 12, 378-390.

[209] J. Yoshida, H. Kim and A. Nagaki, Green and sustainable chemical synthesis using flow microreactors, *ChemSusChem*, **2011**, 4, 331-340.

[210] http://www.sigmaaldrich.com/technical-documents/articles/chemfiles/microreactor-technology.html#ref Microreactor Technology (last access 2016/08/10).

[211] T. Razzaq and C. O. Kappe, Continuous flow organic synthesis under high-temperature/pressure conditions, *Chem. Asian J.*, **2010**, 5, 1274-1289.

[212] U. Tilstam, A Continuous Methylation of Phenols and N,H-Heteroaromatic Compounds with Dimethyl Carbonate, *Org. Proc. Res. Dev.*, **2012**, 16, 1974-1978.

[213] S. Huebschmann, D. Kralisch, V. Hessel, et al., Environmentally Benign Microreaction Process Design by Accompanying (Simplified) Life Cycle Assessment, *Chem. Eng. Technol.*, **2009**, 32, 1757-1765.

[214] R. L. Hartman, J. P. McMullen and K. F. Jensen, Deciding whether to go with the flow: evaluating the merits of flow reactors for synthesis, *Angew. Chem. Int. Ed. Engl.*, **2011**, 50, 7502-7519.

[215] J. J. M. v. d. Linden, P. W. Hilberink, C. M. P. Kronenburg, et al., Investigation of the Moffatt–Swern Oxidation in a Continuous Flow Microreactor System, *Org. Proc. Res. Dev.*, **2008**, 12, 911-920.

[216] D. Ferenc, H. Volker and D. György, in *Flow chemistry Volume 1: Fundamentals* ,De Gruyter, **2014**.

[217] C. G. Frost and L. Mutton, Heterogeneous catalytic synthesis using microreactor technology, *Green Chem.*, **2010**, 12, 1687.

[218] D. Webb and T. F. Jamison, Continuous flow multi-step organic synthesis, *Chem. Sci.*, **2010**, 1, 675-680.

[219] N. G. Anderson, Practical Use of Continuous Processing in Developing and Scaling Up Laboratory Processes, *Org. Proc. Res. Dev.*, **2001**, 5, 613-621.

[220] L. Ducry and D. M. Roberge, Dibal-H Reduction of Methyl Butyrate into Butyraldehyde using Microreactors, *Org. Proc. Res. Dev.*, **2008**, 12, 163-167.

[221] T. Schwalbe, V. Autze and G. Wille, Chemical Synthesis in Microreactors, *Chimia*, **2002**, 56, 636-646.

[222] X. Zhang, S. Stefanick and F. J. Villani, Application of Microreactor Technology in Process Development, *Org. Proc. Res. Dev.*, **2004**, 8, 455-460.

[223] S. A. Yamashkin and E. A. Oreshkina, Traditional and modern approaches to the synthesis of quinoline systems by the Skraup and Doebner-Miller methods. (Review), *Chemistry of Heterocyclic Compounds*, **2006**, 42, 701-718.

2 GLYCEROL ACETALIZATION

2.1 Introduction

Linear and cyclic acetals are usually prepared by the condensation of an aldehyde or a ketone with an alcohol (or a diol/polyol) in the presence of an acid catalyst. Owing to their stability to aqueous and non-aqueous bases, to nucleophiles including powerful reactants such as organometallic reagents, and to hydride-mediated reductions, acetals are among the best known protecting groups for carbonyl compounds. Acetals however, may be of interests also for their use as such. This happens for the case of native glycerol (co-generated in the production of biodiesel) for which a promising route for its exploitation is the conversion to the corresponding cyclic acetals (GAs: glycerol acetals). Well-known examples are the two simplest GAs, i.e. solketal (**2.1a**) and glycerol formal (GlyF, mixture of isomers **2.2a** and **2.2a'**), deriving from the reaction of glycerol with acetone and formaldehyde, respectively (Figure 2.1).

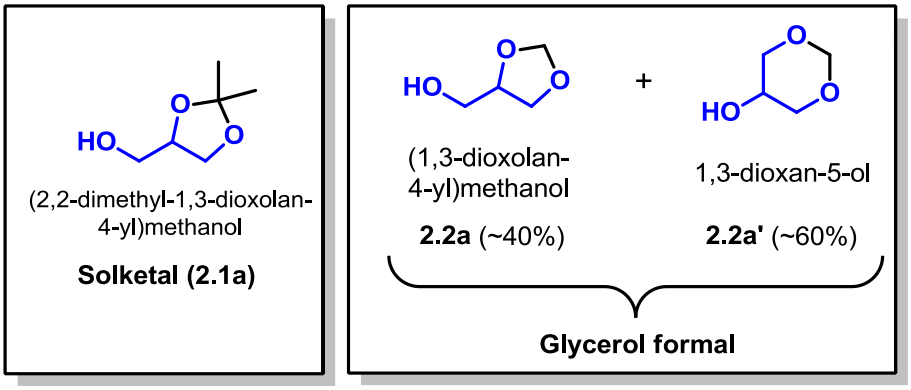

Figure 2.1. Most common cyclic acetals derived from glycerol. Glycerol formal is a 3:2 mixture of six- and five-membered ring isomers.

Like glycerol, GAs are viscous, dense, non-toxic and thermally stable liquids with boiling points in the proximity and over 200 °C.[1,2] However, since they are obtained by the formal protection of two OH groups of glycerol, they possess polarity, hydrophobicity and hydrogen bond ability that make them more similar to simple aliphatic alcohols.[3,4] These aspects account for major applications of GAs as safe solvents and additives in the formulation of injectable preparations, paints, plastifying agents, insecticide delivery systems and flavors.[5]

The stability of GAs to oxidative conditions and their miscibility with biodiesel blends, have been a key feature to investigate their potential as renewable diesel additives.[6] Diesel can be blended with GAs, up to 10% v/v to fulfill the diesel specifications,[7,8] improving some properties of the fuel. For example, Table 2.1 lists the viscosity, flash point and pour point of some diesel blends obtained by the addition of different amounts of two GAs: 4-methylpentan-2-one glycerol ketal (GK) and 4-methylpentan-2-one glycerol ketal octanoate (EGK).[9] Data are compared to a diesel fuel as such.

Table 2.1. Characteristics of diesel blends with GAs

Blend label	Acetal (wt.%)	Density (Kg/m³ at 15 °C)	Viscosity (mm²/s at 40	Flash point (°C)	Pour point (°C)
Diesel	0	842	2.70	61.1	-10
GK	1	839	2.63	61.2	-14
	3	843	2.65	61.5	-15
	6	848	2.68	62.1	-17
	9	849	2.71	62.6	-19
EGK	1	841	2.66	62.4	-17
	3	844	2.69	63.2	-19
	6	855	2.70	64.7	-20
	9	859	2.72	66.3	-22

All the GAs blends possess higher flash points respect to pure diesel making them suitable additives. Open and patent literature reports that with respect to other additives, such as the glycerol ter-butyl ethers (GTBE, see also introduction), the incorporation of GAs in fuels can improve the quality of both standard (petrochemical-based) and bio-diesels by reducing particulate emissions, pour point[10] and viscosity.[6,11,12]

GAs find also remarkable applications in the field of scents or flavors. Examples are the products obtained by the reactions of glycerol with phenylacetaldehyde and vanillin, which lead to hyacinth and vanilla fragrances, in the presence of strong acids such as PTSA, HCl, H_3PO_4 and acidic divinylbenzene-styrene resins. (Scheme 2.1).[13] These fragrances are included in the list of the Flavor and Extract Manufacturers Association (FEMA-GRAS) which offers naturally occurring or synthetically produced flavoring substances regulated by the Food and Drug Administration (FDA).[14]

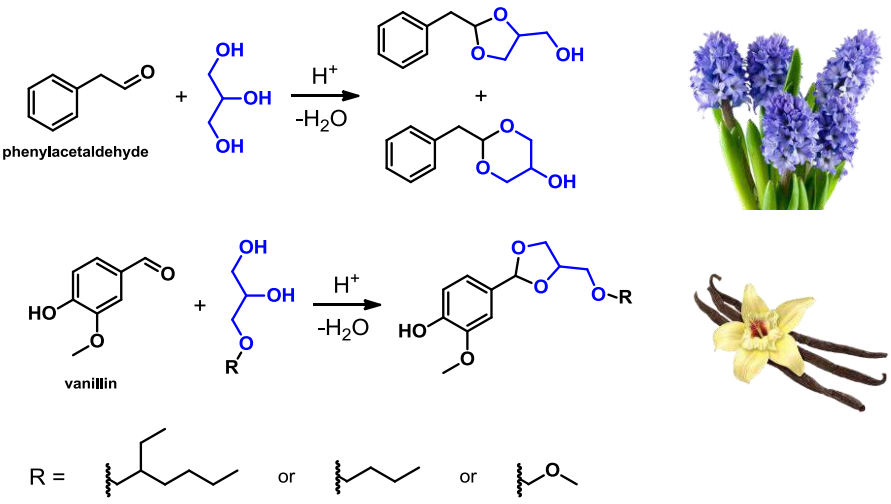

Scheme 2.1. Reaction of phenylacetaldehyde and vanillin with glycerol and its derivatives for the production of fragrances.

GAs can be used as solvents for pharmaceutical, veterinary, and agrochemicals applications. In particular, GlyF (**2.2a**+**2.2a'**) is one of the few solvents which can be used for injectables in veterinary medicine due to his very low toxicity. It possess a good solvent power making it capable to dissolve APIs like ivermectine, oxytetracycline, and sulfamethoxazole. In this field, a representative Company is Lambiotte & Cie that since 1970 has developed the use of formaldehyde as a reagent for the production of both linear or cyclic acetals including GlyF.[15] It should be noted that many of these compounds possess low toxicity and ecotoxicity, thereby showing good profiles from both health, safety and environment standpoints.

Among other uses, GAs based on long-chain carbonyl compounds have been reported for the synthesis of surfactants with interesting biodegradability features.[16,17,18]

Last, but not least, GAs possess a short OH-capped tether (hydroxymethylene group) which provides synthetic access to a number of other derivatives, mainly ethers, esters, and carbonates.[19]

2.1.1 Acetalization Catalysts

The broad spectrum of applications and interests for GAs has triggered research towards improving the performance of acetalization catalysts. Besides the most common acidic conditions, cases are reported in which the reaction is performed in a neutral or even a basic medium.[20] The following section reviews the acetalization process starting from the less conventional systems.

2.1.1.1 Neutral catalysts/conditions

The synthesis of cyclic acetals of polyhydric alcohols, can be performed under neutral conditions by using fluorinated ketones. The reaction can be carried in two different ways, that is by: i) heating a mixture of a halogenated ketone and the cyclic carbonate (Scheme 2.2), or ii) reacting an halogenated ketone with an alcohol or water to produce a hemiacetal (or a hydrate) which in turn, is converted to a cyclic acetal

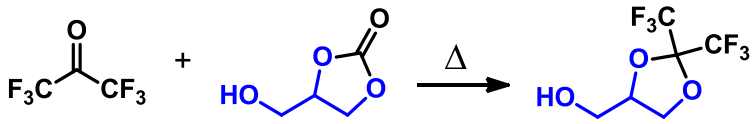

Scheme 2.2. Example of acetal formation using a halogenated ketone

In the presence of acid-sensitive substrates such as aliphatic tetrahydropyranyl (THP) or tert-butyldimethylsilyl (TBDMS) ethers, N-Bromosuccinimide (NBS) may act as a chemoselective catalyst for 1,3-dioxanation of various types of carbonyl compounds (Scheme 2.3).[21]

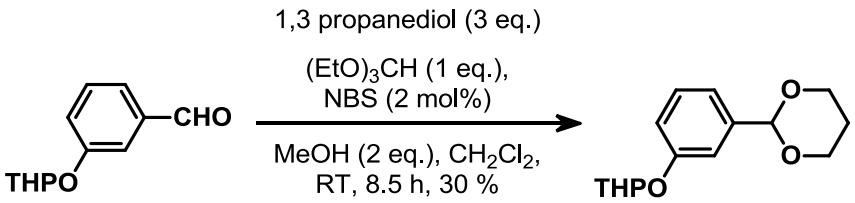

Scheme 2.3. Example of acetal formation using NBS

The synthesis of acetals under neutral conditions occurs also in the presence of the dimethylformamide/dialkyl sulfate adduct.[20]

2.1.1.2 Base catalysts

The base-catalyzed acetalization of glycerol has been recently achieved by using layered double hydroxides (LDH) under microwave assisted conditions.[22] Both 5- and 6-membered ring acetals have been obtained (Scheme 2.4). Mg-Al-LDH was the best system: interestingly, the spent catalyst could be rejuvenated through rehydration cycles carried out also under microwave irradiation.

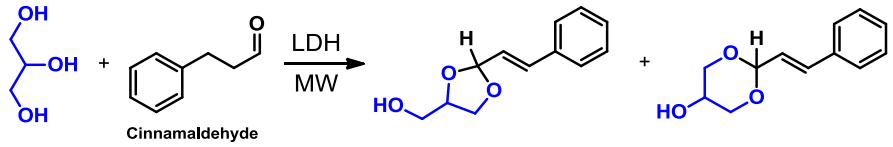

Scheme 2.4. Example of acetal formation using LDH

Strongly electron deficient substrates such as α- or α,β-halo- aldehydes and ketones undergo acetalization in basic medium. In the presence of a strong base such as sodium methoxide, α-hydroxyacetals or epoxyacetals, are obtained (Scheme 2.5).[20]

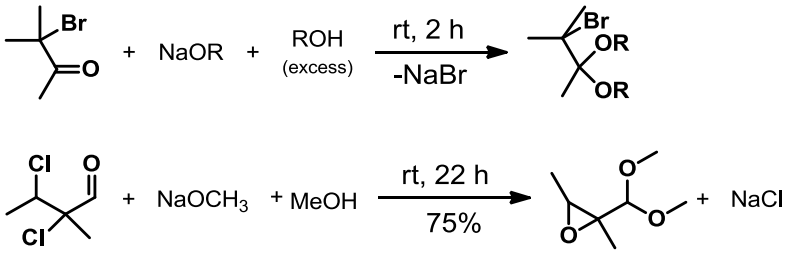

Scheme 2.5. Example of acetal formation using sodium alkoxide

2.1.1.3 Acid catalysts

Acetalization reactions are most often carried out with strong mineral acid catalyst such as sulfuric, hydrohalic, and *p*-toluenesulfonic (PTSA) acid. [20,23,24]

Homogeneous catalysts. Strong homogeneous acids such as dry HCl catalyze quantitative and chemoselective acetalization processes. Scheme 2.6 exemplifies the case of a cortisone-based steroid: notwithstanding the presence of two carbonyls, only the more reactive aldehyde group is converted to the corresponding acetal.[25]

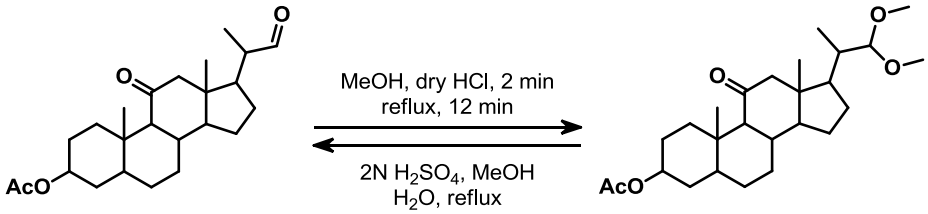

Scheme 2.6. Example of acetal formation using HCl

Recent literature and patents report the use of PTSA[26] or H_2SO_4[27] also for the preparation of GAs. Figure 2.1 shows a flow chart of this process which highlights how the hydrophilicity of reactants and products and the nature of the catalyst impose time-consuming and expensive steps of neutralization and distillation of the co-product water. Moreover, water decreases the conversion by weakening the acid strength and solvating

glycerol; not to mention, issues due acid corrosion.[28,29] The azeotropic removal of water with hydrocarbons or halogenated solvents offers a solution,[30] but it is rather uneconomic and dangerous for large scale preparations, and it becomes impracticable when low boiling carbonyl reactants (e.g. acetone) are used.[31]

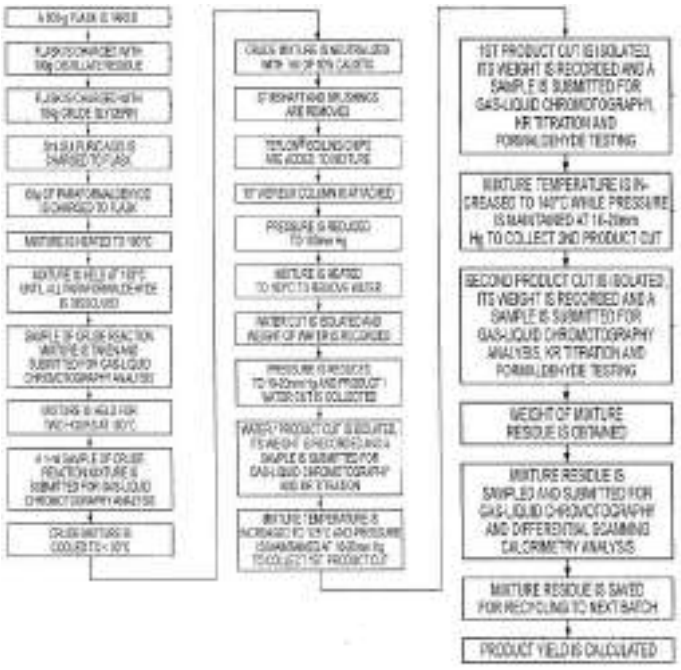

Figure 2.2. Flow chart of a step-by-step bench process for the preparation of GlyF from paraformaldehyde and glycerol using H_2SO_4 as catalyst.

Of the many other homogeneous systems able to act as both Lewis acid catalysts and dehydrating agents, inorganic Fe- and B-based salts and transition metal complexes should be mentioned.[32] Also, Brønsted acidic ionic liquids (e.g., *N*-butyl- pyridinium bisulfate, [BPy][HSO_4]) have been recently introduced as water-removal micro catalytic reactors for the synthesis of Gas.[33]

Heterogeneous catalysts. Elegant syntheses of GAs can be performed under heterogeneous conditions which avoid both costly neutralization steps and the generation of wastewater.

Different solid catalysts have been described for the model acetalization of glycerol with acetone. For example, TiO_2–SiO_2 mixtures prepared by sol–gel methods, have been activated by the adsorption of water followed by a high temperature calcination.[34] These catalytic systems display a high density of Brønsted acidic sites which are responsible for excellent glycerol conversion and selectivity towards solketal of 95% and 90%, respectively, at 70 °C and ambient pressure. Also, mixtures of mesoporous oxides of Ni and Zr (1% and

5%, respectively) on activated carbon have been reported for the same reaction.[35] Very mild (45 °C, 1 atm) and solventless conditions can be used. The intercalation and dispersion of porous NiO and ZrO_2 species into the structure of activated carbon account for the catalytic activity of these systems: at quantitative conversion of glycerol, solketal is achieved in up to 93% amount.

Another class of heterogeneous catalysts based on zeolites have been claimed for the acetalization of glycerol with butanal.[36] These solids can be differentiated by either their pore structures and their acidity. Beta zeolite proves the best among the tested systems, though all catalysts exhibited a selectivity to the five-membered ring acetal product as high as 77–82%.

The reaction of glycerol with different carbonyl compounds including formaldehyde, benzaldehyde, and acetone has been investigated also on Al-SBA-15.[37] Not only an effective preparation of acetals was reported, but also a peculiar switch of selectivity was noticed from a 6-membered product using paraformaldehyde to 5-membered acetals when benzaldehyde or furfural were used. Authors invoked both a kinetic control and the occurrence of a torsional effect in 6-membered rings of cyclic and aromatic substrates.

Other solid acids for the preparation of GAs are sulfonated polystyrene-based resins (Figure 2.3).

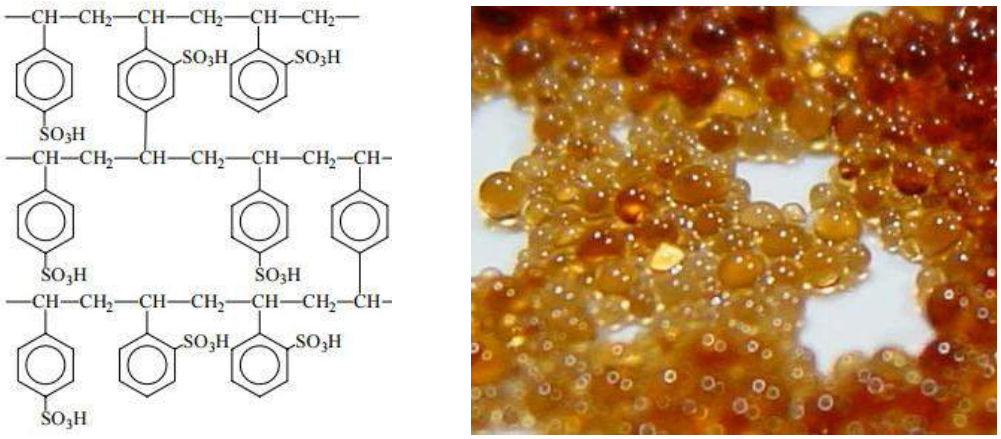

Figure 2.3. Example of polystyrene sulfonated structure of an acid exchange resin (left) and a representative picture of the resin beads (right)

Commercial Amberlyst-15 (A15) and Amberlyst-36 (A36) are perhaps the most used of such resins. Some of their properties are reported in Table 2.2.[38,39] These solids are usually available in the form of porous small beads (0.5-1 mm diameter) with a high surface area. Ion-exchange properties make the resins suitable for separation, purification, and

decontamination processes, while the high acidity can be exploited for catalysis purposes. For example, at T≤ 70 °C, A15 has been reported to catalyze the reaction of glycerol with butanal or acrolein with very high selectivities to the corresponding acetals (>90%), while at 50–110 °C, A36 is active for a high yield synthesis of GlyF from glycerol and formaldehyde.[40]

Table 2.2. Comparison of the major properties of Amberlyst-15 and Amberlyst-36

Parameter	Amberlyst-15	Amberlyst-36
Ionic form	H^+ form	H^+ form
Concentration of active sites	≥ 4.7 meq/g	>5.4 meq/g
Moisture holding capacity	52 to 57%	51-57%
Particle size	0.600-0.850 mm	<0.425 mm
Average pore diameter	300 Å	240 Å
Total pore volume	0.40 mL/g	0.20 mL/g
Maximum operating temperature	120 °C	150 °C

Amberlyst resins have been the first ever described catalysts for CF acetalization methods, particularly for the preparation of Solketal (Scheme 2.7).[41,42,43]

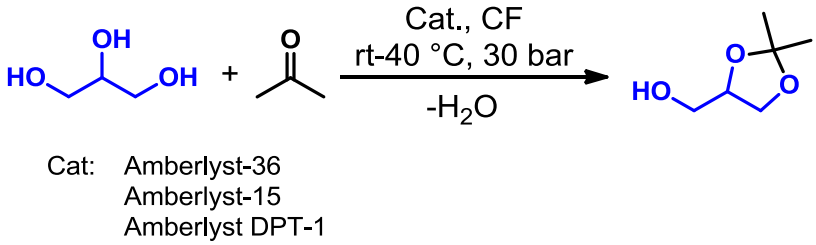

Scheme 2.7. CF shyntesis of solketal with Amberlyst resins

However, to the best of our knowledge, the CF-preparation of GAs still represents a largely unexplored area. The few reported papers prove the efficiency of Amberlyst resins as well as conventional acid catalysts (as sulfuric acid),[40,41,42,44,45] but they also highlight major drawbacks including clogging of reactors and deterioration/deactivation of the apparatus and catalytic beds, due to the viscosity of reactants and products and the co-formation of water. These problems have pushed to engineering improvements of the CF-technologies through the use of semi-batch or corrosion-resistant glass reactors, co-solvents and even subcritical reagents.

The same reaction has been investigated also in this Thesis work to compare the activity of Amberlyst resins to that of an unprecedented catalyst such as $AlF_3 \cdot 3H_2O$.

2.1.2 $AlF_3 \cdot 3H_2O$ as a catalyst for continuous-flow reactions

As a part of the research program of this PhD Thesis, the attention has been focused on the acetalization of glycerol aimed at achieving a catalytic and robust continuous-flow method able to be not only competitive to the above described procedures (Scheme 2.7), but also to overcome their problems. In this respect, the choice of the catalyst has been obviously the core issue.

A literature survey suggested to consider the commercially available aluminum fluoride trihydrate ($AlF_3 \cdot 3H_2O$, AF) as a potential new catalyst for the formation of GAs in CF-mode. AF as such, or its dehydrated-, partly hydroxylated-, nano- and supported-forms were already reported as acid catalysts for several processes such as halide exchanges on hydrochlorocarbons,[46,47] aromatic alkylations,[48,49] hydrocarbon isomerizations[50] and condensation processes.[51] Moreover, AF is a safe,[52] highly thermally (up to 400 °C), mechanically stable, and relatively inexpensive compound. At present, the major use of AF is as an additive to the cryolite employed in the electrolytic preparation of aluminum.[53] China dominates the world market of AF with over 50% of its production (in 2010).[54]

The study was articulated through two lines: i) in the first part of the work, the feasibility of using $AlF_3 \cdot 3H_2O$ to catalyze acetalization reaction was investigated and most of all, the performance of AF was compared to that of already known acetalization catalysts, particularly Amberlyst resins; ii) in the second step, an in-depth analysis of AF was carried out aimed at further exploring its potential and limitations in the synthesis of GAs.

The results of this study have been the object of a publication on the MDPI Open Access Journal *Molecules* which, for the part developed within this Thesis work, is described in the following paragraphs.[55]

2.2 Results

2.2.1 CF-synthesis of Solketal: comparison of AF to Amberlyst resins

The model acetalization of glycerol with acetone was the reaction of choice to begin the investigation (Scheme 2.8).

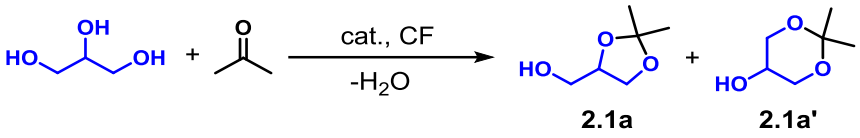

Scheme 2.8. CF-acetalization of glycerol with acetone

The experimental apparatus used for the investigation of CF-acetalyzation reactions was similar to that described in previous works of our research group.[56,57] It was composed of twin HPLC pumps for the separate delivery of liquid reactants, a thermostated oven, a static mixer, a reactor and a back pressure regulator. A detailed description of the overall system is given in the experimental paragraph (see later on this chapter).

2.2.1.1 Catalysts comparison for the upgrading of different types of glycerol

The acetalization of glycerol with acetone was initially investigated in the presence of Amberlyst resins which were reported as the most active catalysts for the process. Particularly, Amberlyst 36 (A36) was used to set up the CF-system. $AlF_3 \cdot 3H_2O$ was then considered to verify whether it could act as a reaction catalyst, and in the case, to compare its performance to that of A36. A wide range of conditions were explored starting from tests on different grades of glycerol: pure and blended with MeOH, variable amounts of water and NaCl. The relative proportion of each additive was chosen not only to operate with homogeneous solutions, but also to simulate the composition of crude glycerol (CG) deriving from processes.[58,59,60] In fact, typical CG compositions include <65 wt % glycerol, 15-50 wt % MeOH, 10-30 wt% water and 2-7% salts (primarily NaCl and KCl coming from the neutralization of catalysts for the biodiesel manufacture). Table 2.3 summarizes the six types of glycerols used in this investigation. For convenience, such reactants were labelled as **Glyc1-Glyc6**.

Due to solubility limitations, the use of pure glycerol (**Glyc1**) required a 40 molar excess of acetone to achieve a homogeneous solution at rt. For **Glyc2-5** and **Glyc6**, the acetone:glycerol molar ratio (Q) was set to 4 and 8, respectively.

Table 2.3. Different types of glycerols used

Entry	Glycerol:additive molar ratio (wt% composition)[a]				Label
	Gly	MeOH	H_2O	NaCl	
1	(100)	-	-	-	**Glyc1**
2	1 (70)	1.2 (30)	-	-	**Glyc2[b]**
3	1 (68)	1.2 (28)	0.3 (4)	-	**Glyc3[b]**
4	1 (53)	1.2 (22)	2.4 (25)	-	**Glyc4[b]**
5	1 (49.5)	1.2 (22)	2.4 (25)	0.08 (2.5)	**Glyc5[b]**
6	1 (44.3)	0.3 (4.4)	5.6 (49)	0.08 (2.3)	**Glyc6[b]**

ACS grade glycerol was used in all experiments. [a] Glycerol:additive molar ratio. The wt.% composition of the reactant glycerol is shown in parenthesis. [b] Relative proportions of MeOH, water, and NaCl were adjusted based on references 57-59.

Other conditions were adjusted according to those described in previous papers:[43] tests were carried out at temperature and pressure from 25 to 100 °C, and 2 to 35 bar, respectively.[61] Screening experiments allowed to choose the size of the reactor, the catalyst loading, and the weight hourly space velocity (WHSV).[62] These indicated that reactions could be conveniently carried out using a cylindrical steel reactor (V= 0.875 mL; L= 12 cm; Ø = 1/4“) filled with the catalyst (A36: 0.90 g; AF: 0.67 g), and fed in the upright position with the reactant mixture at a WHSV of 2 [$g_{glycerol}\ h^{-1}\ g_{cat}^{-1}$]. Since the acid loading of A36 was 5.1 meq/g (from Sigma-Aldrich), AF was used in a molar amount comparable to the acid equivalents available in the resin. All experiments were monitored periodically for 24 hours analyzing the samples by GC and GC/MS in order to evaluate both the glycerol conversion and the product distribution. Each test was triplicated to check for reproducibility.[63]

Figures Figure 2.4a-c report the result obtained for the CF-acetalization of **Glyc1-5** with acetone over A36 (0.9 g). Except for Figures Figure 2.4b, conversions and selectivity were determined after 24 hours.

A36 was a highly efficient catalyst: at 25 °C, we noticed that it was active also operating at a lower pressure (10 bar) than that previously reported (30 bar).[42,45,43] Under such conditions, a substantially quantitative process was observed when either pure glycerol or an almost equimolar glycerol/MeOH mixture were used (Figure 2.4a: **Glyc1** and **Glyc2**, respectively). A still satisfactory conversion of 82-85% was reached even in the presence of sizeable amounts of water (from 4 up to 24 wt%) in the reactant stream (**Glyc3** and **Glyc4**,

respectively). The overall selectivity, defined as the percentage ratio of the desired acetalization product (total of isomers **2.1a** and **2.1a'**) with respect to the conversion, was always >99%: isomeric acetals **2.1a** (solketal, preferred) and **2.1a'** were obtained in a rather steady relative ratio of ~50 (dashed green profiles of Figure 2.4a-c).

The structures of products (**2.1a** and **2.1a'**) were assigned by GC/MS analyses and by comparison to an authentic commercial sample of solketal (**2.1a**). GC and GC/MS records also indicated that both the conversion and the product distribution did not undergo any appreciable change from the first two hours up to the end (24 h) of each CF-reaction. Moreover, additional experiments – not shown here - with both **Glyc2** and **Glyc4** proved that the catalytic bed could be reused for at least 48 hours without loss of activity or selectivity.

However, the catalytic performance of A36 was dramatically affected by the addition of NaCl. The CF-acetalization of **Glyc5** that contained only 2.5 wt% of NaCl, showed a progressive drop of the reaction conversion from 82 to ~5% in 22 hours (Figure 2.4b). After that time, the catalyst was no longer effective. Any attempt to improve such an outcome by using a fresh catalytic bed of A36 at higher temperature and pressure proved unsuccessful (Figure 2.4c): even at 100 °C and 30 bar, the glycerol conversion never exceeded 7% and it was comparable to that observed during blank runs carried out in the absence of any catalyst. As reported also by other Authors,[31,64] the reaction could not be thermally controlled. On the other hand, reported procedures for the reactivation the Amberlyst resin by mineral acids (*e.g.* H_2SO_4) were not only time-consuming and corrosive, but also incapable of restoring the initial performance of the catalyst.[42]

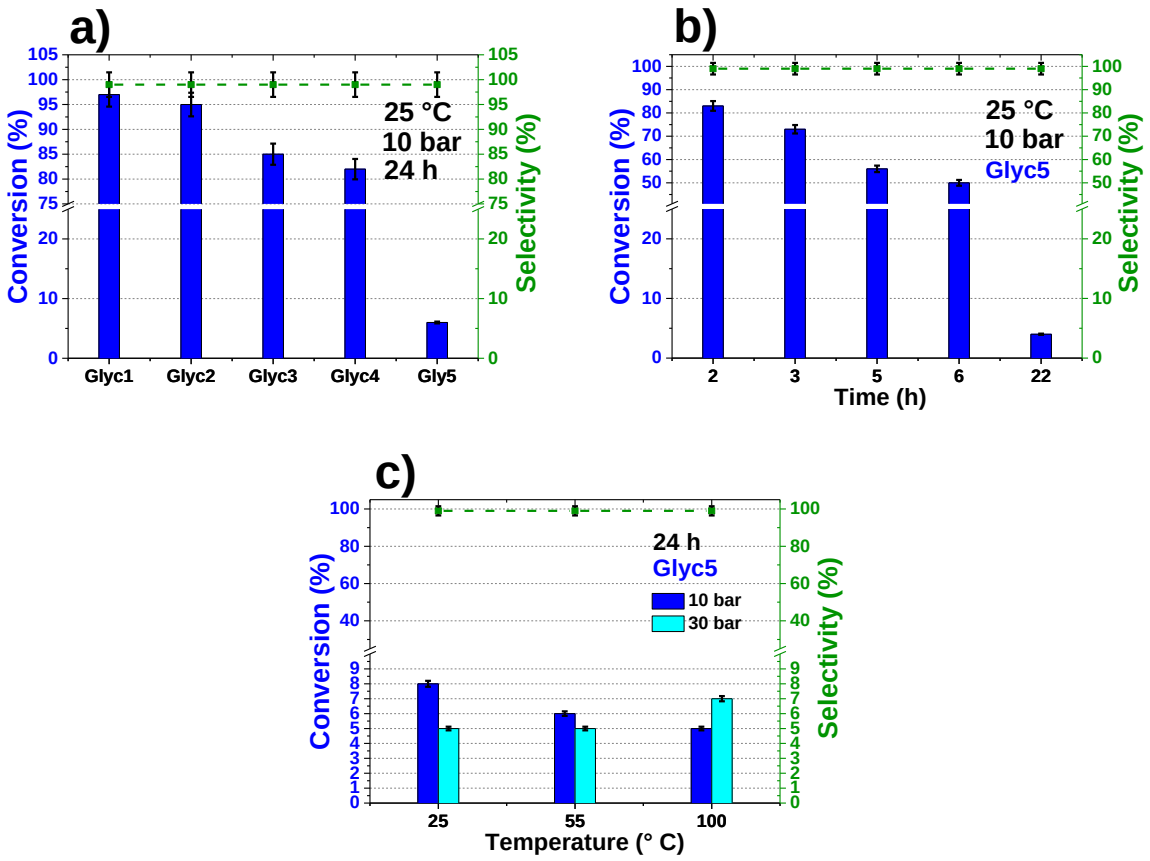

Figure 2.4. CF-acetalization of glycerol with acetone using A36 (0.9 g) as catalyst. **a)** Conversion of glycerol and selectivity toward the isomer products (**2.1a** and **2.1a'**) achieved after 24 h, at 25 °C and 10 bar, by feeding different types of reactant **Glyc1**-5; **b)** profile of the glycerol conversion vs time obtained at 25 °C and 10 bar with the use of **Glyc5** as the reagent; **c)** Effect of temperature and pressure on the conversion of **Glyc5** after 24 hours. Other conditions: WHSV = 2; molar ratio acetone:glycerol was 40 and 4 for **Glyc1** and **Glyc2-5**, respectively.

AF was then tested. Commercial $AlF_3 \cdot 3H_2O$ (0.67 g, from Aldrich) was used as such and after calcination in air at 500 °C for 5 h carried out according to an already reported procedure:[65] the two samples were labelled as AF and AF_c, respectively. Although AF had never been previously reported as an acetalization catalyst, experiments demonstrated that in its presence, the investigated reaction was feasible. Figure 2.5a-c reports the results. By contrast, the calcined compound AF_c proved totally inefficient.

Two major facts emerged by the comparison of AF to A36: i) AF was less active than the amberlyst resin when both pure and wet glycerol (**Glyc1-4**) were used. Consider for example, the model acetalization of **Glyc3** with acetone. Under the same set of conditions (25 °C, 10 bar, WHSV=2, molar ratio acetone:glycerol=4, 24 h), the glycerol conversion was 3% and 85% over AF and A36, respectively (compare Figure 2.4a and Figure 2.5a). Only by rising the temperature up to 100 °C, the reaction proceeded further to reach a steady 84%

conversion also over the AF catalyst (Figure 2.5a). A further experiment carried out by using the same catalytic bed for additional 30 hours, proved that both conversion (of **Glyc3**) and selectivity did not alter with time (83 and >99%, respectively), thereby confirming the robustness of the AF system. ii) Notwithstanding the demand for a higher reaction temperature (100 °C), AF was able to induce not only the acetalization of **Glyc1-4**, but also that of **Glyc5**: in all cases, the glycerol conversion was in the range of 78-84% (Figure 2.5b) with >99% selectivity towards products **2.1a** and **2.1a'** (dashed green profile). Regardless of conditions and composition of the reactant mixture, the **2.1a**/**2.1a'** ratio was rather constant (~40) and comparable to that achieved with A36. Such results were confirmed by both prolonging the reaction of **Glyc5** up to a time-on-stream of 48 hours and by reusing the same catalytic bed for 3 subsequent tests under the conditions of Figure 2.5b. This proved that AF allowed a stable and reproducible protocol, and it was a far superior catalyst than A36 for the transformation of wet glycerol contaminated by NaCl (**Glyc5**).

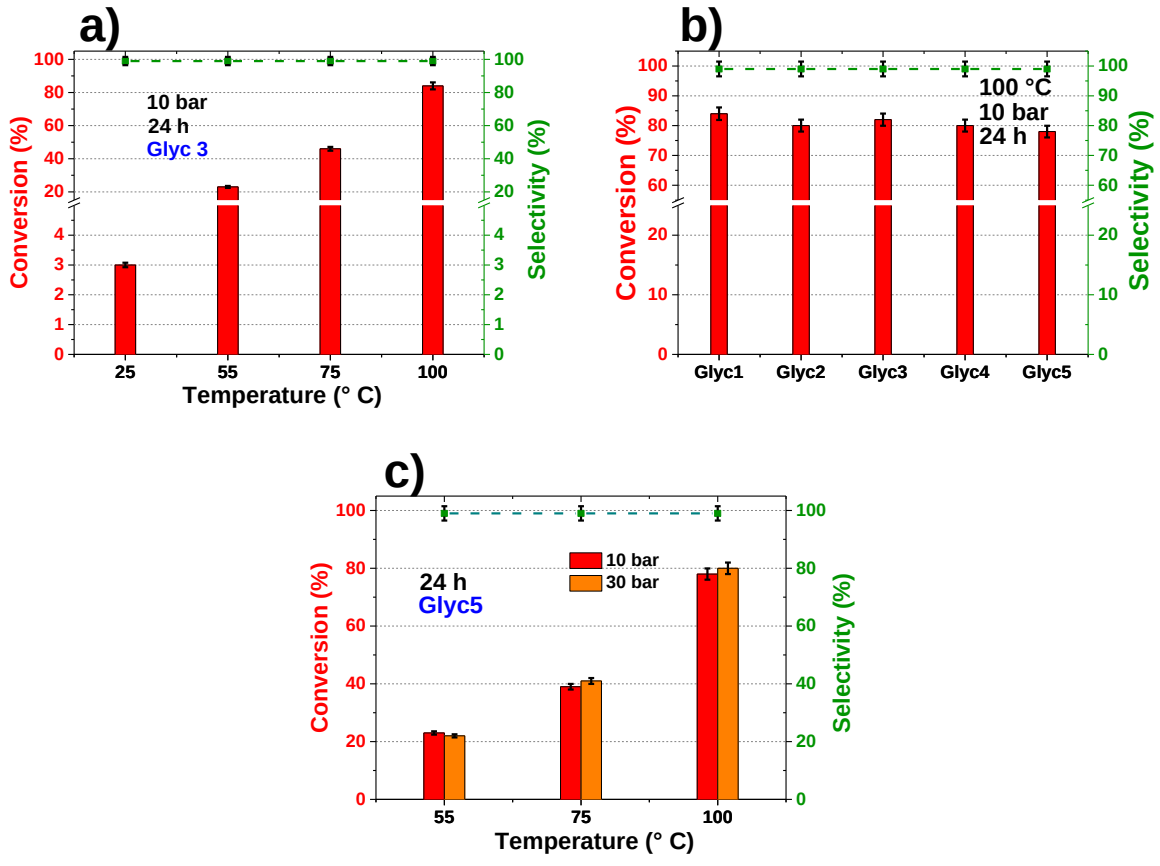

Figure 2.5. CF-acetalization of glycerol with acetone using AF as a catalyst. **a)** Profile of the glycerol conversion vs temperature obtained at 10 bar, after 24 hours, with the use of **Glyc3** as the reagent; **b)** Conversion of glycerol achieved after 24 h, at 100 °C and 10 bar, by feeding different types of reactant **Glyc1-5** to the reactor; **c)** Effect of T and p on the conversion of **Glyc5** achieved after 24 hours. Other conditions: WHSV = 2;, molar ratio acetone:glycerol = 4.

Additional experiments also demonstrated that in the presence of AF catalyst, the reaction of **Glyc5** with acetone was improved by an increase of the temperature in the same way described for **Glyc3** (compare Figure 2.5a and c in the interval between 55 and 100 °C); though, the conversion profiles did not change when the pressure was raised from 10 to 30 bar (Figure 2.5c), this effect resembling that shown in Figure 2.4c.

Mixtures recovered after the acetalization of **Glyc3** over AF were subjected to ICP and ionic chromatography analyses for the determination of Al and fluoride contents (details of the used procedures are given later in the experimental paragraph). For comparison, the same measure (Al and F contents) were carried out also on a blank sample obtained by flowing the reactants through the CF-system in the absence of the catalyst. Table 2.4 shows the results.

Table 2.4. ICP and ionic liquid chromatography analyses for the estimation of the Aluminium and fluoride content in the mixture recovered at the reactor outlet stream.

Entry[a]		Aluminium content (µg/L)	Fluoride content (mg/L)
1	**Glyc3**	201.1	2.808
2	**Blank**	137.4	0.274

[a] Entry 1: after the reaction of **Glyc3** over AF; entry 2: test in the absence of any catalyst.

The Al and fluoride concentrations were found to be ~64 ppb and ~2.5 ppm, respectively, corresponding to a mass loss of the catalytic bed of maximum 620 µg per 40 working hours (8 h/day per one week), with an insignificant incidence on the overall process.[66]

Overall, the use of AF allowed unprecedented good results, otherwise not possible with the Amberlyst resin, for the reaction of a crude-like glycerol such as **Glyc5** with acetone to produce the corresponding acetal (solketal) via a straightforward CF-mode.

The study was then continued to further explore the potential of AF as an acetalization catalyst.

2.2.1.2 Reaction productivity with AF

The reaction of the two crude-like glycerols **Glyc5** and **Glyc6** was compared by using different acetone:glycerol (Q) molar ratios, WHSVs and catalyst loadings. In order to increase the Q ratio, the content of MeOH and water of **Glyc6** were adjusted to both lower and higher values, respectively, with respect to **Glyc5** (Table 2.3): this choice allowed to

overcome limitations of mutual solubility of reactants and to operate with up to 8 molar equivs. excess of acetone (Q=8) with respect to glycerol. Experiments were all carried out at 100 °C, 10 bar, and for 24 hours. The total volumetric flow rate (F) was in the range of 0.1 to 1.18 mL/min, and the corresponding WHSV was from 2 to 6. Two catalyst loadings of 0.67 g (same as for Figure 2.5) and 4.2 g were considered. In the latter case, a different reactor size was used (L=12 cm, Ø=3/8", inner volume=3.5 cm^3) (see experimental). For a more convenient comparison, the reaction productivity (P), expressed as the mass of product (total of isomers **2.1a** and **2.1a'**) obtained per hour and per mass unity of the catalyst [g of (**2.1a**+**2.1a'**)/(g_{cat} h)] is indicated.

Table 2.5. Acetalization of **Gly5** and **Gly6** with acetone catalyzed by AF

Entry	Reactant	AF (g)	Q (mol:mol)[a]	WHSV	Conversion (%)	P[b]
1	**Gly5**	0.67	4	2	78	2.2
2			4	4	67	3.8
3			4	6	65	5.6
4		4.2	4	2	75	2.2
5	**Gly6**	0.67	4	2	30	0.86
7			8	2	60	1.7
8			8	4	71	4
6		4.2	8	2	54	1.6

[a] Molar ration acetone:glycerol
[b] Productivity expressed [g of (2.1a+2.1a')/(gcat h)]

The reaction of **Glyc5** showed that by keeping all the other conditions unaltered with respect to Figures Figure 2.5c, an almost linear rise of the productivity from 2.2 to 5.6 h^{-1} was observed when the WHSV was tripled (entries 1-3). Although no other increments of WHSV were tested, it was plausible that the catalytic bed was still not operating at its maximum capacity. The result led to conclude that the process could be efficiently intensified and the yield of solketal could be further improved. However, at a constant WHSV of 2, the productivity remained steady at 2.2 h^{-1} even if the catalyst loading was 6-fold increased (from 0.67 to 4.2 g; compare entries 1 and 4). This proving that the reaction reached an equilibrium conversion not exceeding 78%.

A similar behaviour was observed for the acetalization of **Glyc6**, though with a lower productivity: under the same conditions, P of 2.2 and 0.86 h^{-1} were obtained for **Glyc5** and **Glyc6**, respectively (compare entries 1 and 5). Only by doubling the amount of acetone

(Q=8), P was improved up to values comparable to those achieved for **Glyc5** (compare entries 1-2 to 6-7). Also in this case however, operating at a constant WHSV of 2, the increase of the catalyst loading had no substantial effects on the rate of formation of the product (entries 6 and 8: P=1.7 and 1.6 h^{-1}, respectively). The poorer performance of the catalyst observed with the use of **Glyc6** was plausibly due to the higher water content (49 wt%) of this reagent with respect to **Glyc5** (24 wt%). Notwithstanding this, the catalytic bed proved robust and able to offer stable and reasonably good conversions over time.

Data of Table 2.5 were validated by the mass balance: as an example, after the reaction of entry 3, the vacuum distillation of the mixture allowed to isolate the product (as a mixture of isomer acetals **2.1a** and **2.1a'**) in a 59% yield. This compound as such was of ACS grade (>99%) and no additional purification steps were required.

2.2.2 Acetalization with butanone

The acetalization of Gly with 2-butanone was examined to extend the synthetic scope of the investigated protocol (Scheme 2.9).

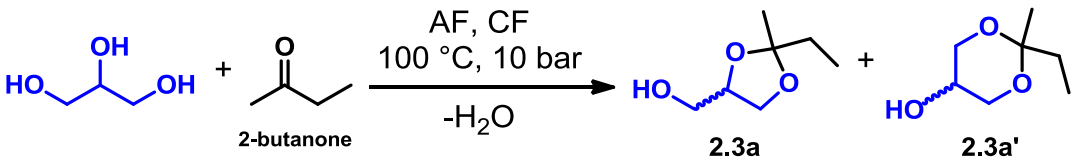

Scheme 2.9. The reaction of glycerol with 2-butanone

Experiments were carried out according to conditions of Figure 2.5b) and Table 2.5, by using **Glyc1** and **Glyc6** as reagents. Since the solubility of pure glycerol in 2-butanone was lower than that in acetone, the reactant molar ratio (Q) 2-butanone:**Glyc1** was set to 60 to achieve a homogeneous mixture. For the same reason, the reaction of **Glyc6** required additional MeOH (0.5 extra mL of MeOH for each mL of **Gly6**) as a co-solvent. Experiments were carried for 24 hours at 100 °C, 10 bar and WHSV = 2. Each test was triplicated to check for reproducibility.[63] Results are reported in Table 2.6.

Table 2.6. Acetalization of **Gly1** and **Gly6** with 2-butanone catalyzed by AF

Entry	Reactant	Q[a]	WHSV	Conversion (%)[b]	P[c]
1	**Glyc1**	60	2	85	2.7
2	**Glyc6**	4	2	45	1.3

[a] molar ratio 2-butanone:**Glyc1** or 2-butanone:**Glyc6**.
[b] Conversion of glycerol after 24 h (the reported value did not differ from that measured after the first two hours of reaction).
[C] Productivity expressed [g of (**2.3a**+**2.3a'**)/(g_{cat} h)]

A steady conversion of 85 and 45% was achieved for the acetalization of **Glyc1** and **Glyc6**, respectively, and the corresponding productivity (P) was 2.7 and 1.3 g (**2.3a**+**2.3a'**)/(g_{cat} h) on the total formation of isomer products **2.3a** and **2.3a'**. The process was not further optimized, but the results proved the concept: AF was an efficient catalyst also for the reaction of other carbonyl compounds with crude-like glycerol. The productivity with 2-butanone was apparently lower than that with acetone; however, a direct comparison between the reactivity of two ketones could not be inferred since different reactant molar ratios as well as amounts of MeOH must be used in the tests of Figure 2.5, Table 2.5, and Table 2.6.

As far as the product distribution, the reaction of 2-butanone could in principle, afford the following isomer products (Scheme 2.10).

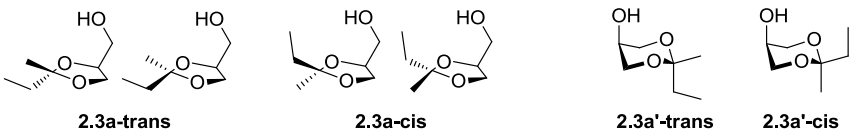

Scheme 2.10. Conformational isomers for the reaction of glycerol with 2-butanone

In the five-membered ring compound **2.3a**, the C2 and C4 asymmetric carbons of the dioxolane ring could give rise to a DL-isomers pair, while two *cis-trans* isomers of acetal **2.3a'** were possible due to the relative axial and equatorial positions of ethyl and methyl substituents at the C5 of the dioxane ring. Accordingly, experiments of Table 2.6 showed the formation of almost equimolar amounts of **2.3a-*cis*** and **2.3a-*trans*** as major products along with two other minor compounds which were plausibly the *cis* and *trans* isomers **2.3a'**. Derivatives **2.3a** (*cis+trans*) could not be separated from each other, but their (1:1) mixture was isolated and characterized by NMR and MS. By contrast, any attempt to obtain isomers **2.3a'** (*cis+trans*, either separately or in mixture) failed because they formed in low amounts.

The structure of such compounds was hypothesized from GC/MS analyses of final reaction mixtures.[67,68] (Further details are reported in the experimental and SM sections).

2.2.3 Catalyst characterization

A total of four catalyst samples were considered for XRD characterization analyses: fresh, calcined, and two used catalysts (Table 2.7).

X-ray powder diffraction (XRPD) analysis of the fresh catalyst AF_f is shown in Figure 2.6. The profile showed that the sample was comprised of three phases: $AlF_3 \cdot 3H_2O$, $Al_2[(OH)_xF_{(1-x)}]_6(H_2O)_y$ and β-AlF_3 which were in the relative weight amount of 83%, 13%, and 4%, respectively. Rietveld analysis[69] of the X-ray diffraction (XRD) data was used to obtain the quantitative fractions of all phases. Results are reported in Figure 2.7.

Table 2.7. Different AF samples considered for characterization analyses: fresh, calcined and used.

Entry	Label	AF condition	Reactant used	Time on stream (h)
1	AF_f	fresh	-	-
2	AF_c	calcined[a]	-	-
3	AF_1	after used[b]	**Gly1-4**	30[c]
4	AF_2	after used[b]	**Gly5-6**	90[c]

[a] AF_c was obtained by calcination of AF in air at 500 °C and 5 h.
[b] Catalyst used for the reaction of glycerol with acetone under the conditions described in Table 2.5 and Table 2.5.
[c] Total time of use of the catalyst in the acetalization of **Glyc1-4** and **Glyc5-6** with acetone.

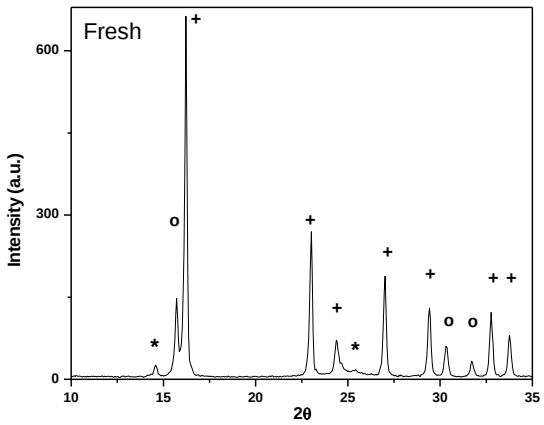

Figure 2.6. Diffraction pattern of the AF_f sample: (+) $AlF_3(H_2O)_3$ ICSD (Inorganic Crystal Structure Database) 416689 (83 wt%); (o) $Al_2[(OH)_xF_{(1-x)}]_6(H_2O)_y$ COD 1000086 (13 wt%) and (*) β-AlF_3 ICSD 202681 (4 wt%).

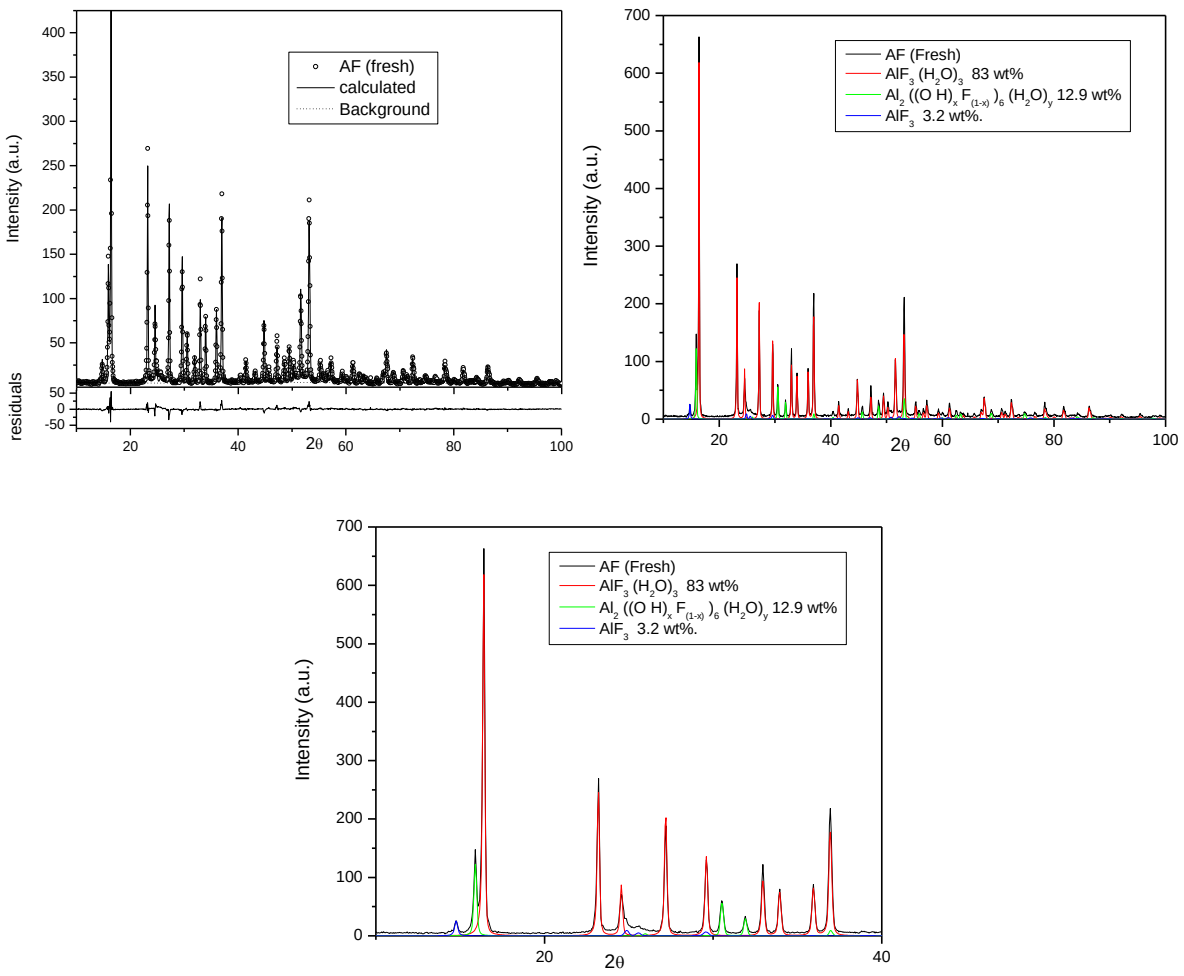

Figure 2.7. Rietveld analysis: XRD pattern of commercial AlF_3 $3H_2O$ (Fresh, black pattern) compared with three reported different AlF_3 phases (red, green and blue patterns)

The second most abundant component of AF_f, having the formula $Al_2[(F_{1-x}(OH)_x]_6(H_2O)_y$, was identified as a solid solution (SS) of AlF_3 and $Al(OH)_3$. This crystalline aluminum hydroxide fluoride SS showed a cubic pyrochlore structure cell with 16 formula units where aluminum atoms were centered in corner-shared AlF_xO_{6-x} octahedrons forming a network of channels. F and OH groups were statistically distributed at the corners of the octahedrons, while water molecules, present in the channels and on the surface of aluminum hydroxide fluorides, were hydrogen bonded with the AlF_xO_{6-x} network. Also, a minor amount of β-AlF_3 was present in the fresh AF solid.[70,71,72]

After calcination in air at 500 °C for 5 h, the resulting sample AF_c showed the XRD spectrum of pure α-AlF_3 (Figure 2.8)

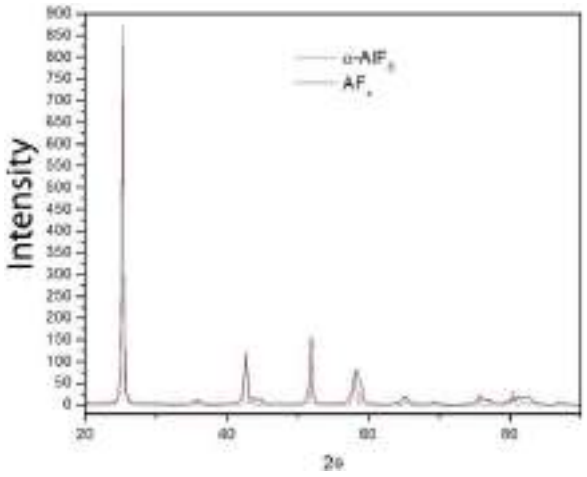

Figure 2.8. XRD pattern of calcined commercial AF in air at 500 °C for 5 h (black) compared with the reported α-AlF_3 pattern (red)

Water and hydroxyl group were completely absent. The corresponding diffraction lines almost perfectly matched the standard patterns PDF # 44-0231 and 01-080-1007, and the structure ICSD 68826. This outcome differed from literature data, reporting instead that β-AlF_3 was formed by the calcination of $AlF_3 \cdot 3H_2O$.[65] Such a discrepancy was not clearly rationalized, but a role was possibly played by the fact that the starting AF sample was a ternary mixture rather than a pure compound.

The structure of the used catalysts (AF_1 and AF_2) was remarkably affected by the nature of the reagents with which these systems came into contact. In particular, if NaCl was absent in the reactant glycerol (**Glyc 1-4**), the corresponding catalyst (AF_1) did not undergo any appreciable change of its composition (Figure 2.9).

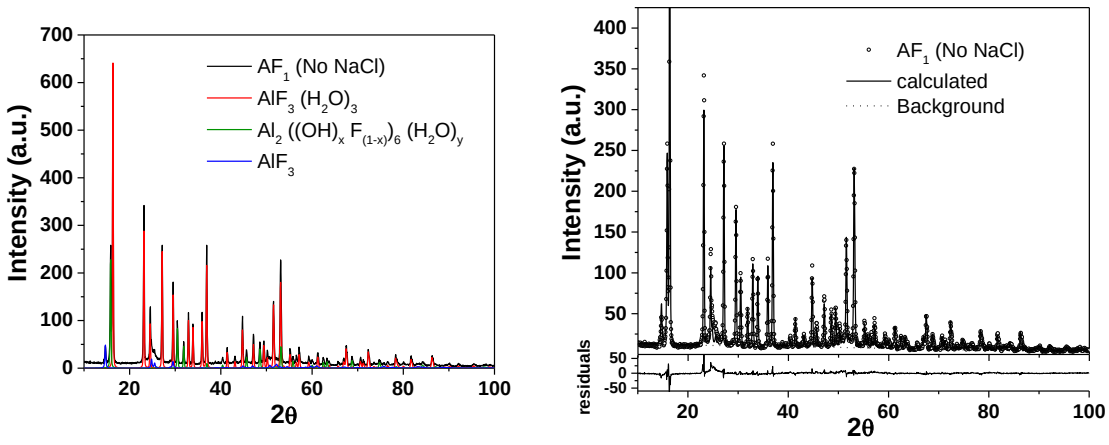

Figure 2.9. (**Left**) XRD patterns of AF_1 (black pattern) compared with three reported different AF phases (red, green and blue patterns); (**Right**) AF_1 and calculated XRD pattern. The residual between the patterns are shown at the bottom of the figure

The XRD pattern of AF_1 showed a composition similar to that of the fresh catalyst $AlF_3 \cdot 3H_2O$, SS and β-AlF_3 in the relative weight amount of 79%, 16%, and 5%, respectively. Conversely, if NaCl was present in the glycerol stream, a substantial structural modification of the catalyst (AF_2) took place (Figure 2.10).

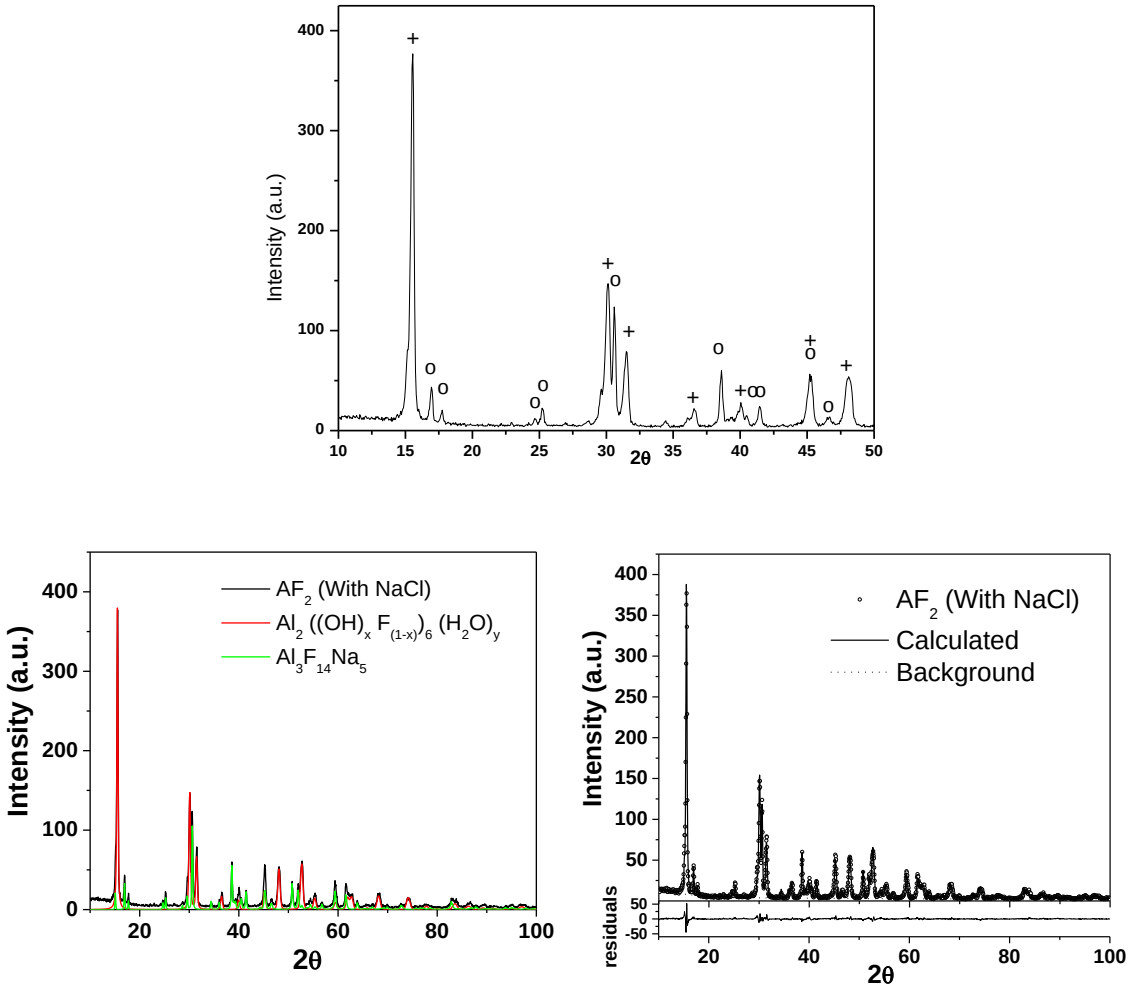

Figure 2.10. Top: Diffraction pattern of AF_2 sample: (**+**) $Al_2[(OH)_xF_{(1-x)}]_6(H_2O)_y$ COD 1000086 (63.4 wt%); (**o**) $Al_3F_{14}Na_5$ ICSD 26419 (36.6 wt%). **Bottom, left:** XRD patterns of AF_2 (black pattern) compared with two reported different AF phases (red and green patterns); **Bottom, right**: AF_2 and calculated XRD pattern. The residual between the patterns are shown at the bottom of the figure

After the acetalization of **Glyc5** and **Glyc6** with acetone, the XRD analyses proved that the residual AF_2 sample was a binary mixture composed of the above described SS and a new compound of formula $Na_5Al_3F_{14}$ identified (PDF # 30-1144) as a Chiolite phase (ChPh). These two components were in the relative weight amount of 63.4% and 36.6%, respectively. Of note, with respect to the original AF solid, both $AlF_3 \cdot 3H_2O$ and β-AlF_3 phases completely disappeared in AF_2.

2.2.4 Effects of T, p, and reaction mixtures recycling with AF

2.2.4.1 Reactions at nearly atmospheric pressure

The second step of the investigation was focused on further exploring the effect of reaction conditions on the performance of $AlF_3 \cdot 3H_2O$ for the CF-acetalization of glycerol. The model acetalization of pure glycerol (**Glyc1**) with acetone (Scheme 2.8), was considered with the aim of detecting operational limits of the catalyst. Initial tests were carried out to at the lowest possible pressure (~2 bar)[61] and at temperatures in the range of 45-60 °C below the boiling point of acetone. A screening of conditions indicated that experiments could be conveniently performed using a cylindrical steel reactor (V= 0.875 mL; L= 12 cm; Ø = 1/4 “) filled with powdered AF (1.5 g). Reagents were delivered as two separate streams to the reactor. Due to solubility limitations,[73] flow rates were set at 0.02 mL/min for glycerol, and 0.40 mL/min for acetone. This corresponded to a acetone:glycerol molar ratio (Q) of 20.[74] Since it was expected that a moderate conversion was reached under these conditions (cfr. results of Figure 2.5), the recycling of the liquid stream collected at the reactor exit was considered to increase the amount of products. In a typical experiment, reactants were flowed for 4-6 hours, during which the reaction mixture was sampled and analyzed by GC. The recovered colorless solution was conveyed from the outlet to the inlet of the CF-reactor and re-used as such, without any purification or water removal. Such an operation was repeated up to eight times. At each reaction temperature a fresh catalytic bed was used and the same bed was used for all the recycle experiments (passes). Glycerol conversion and product distribution were periodically monitored by GC and GC/MS.

The results are reported in Figure 2.11a-b. Figure 2.11a refers to the reaction run at 55 °C. The 3D-plot shows the trend of glycerol conversion with time during each pass of reactants through the CF-reactor (left axis), and after the first pass and the subsequent recycles (right axis). Figure 2.11b compares the combined effect of the recycle and the reaction temperature: each point of the four profiles represents an average (glycerol) conversion calculated as the mean of 3-to-6 values of GC-conversion measured during recycle tests carried out at 45, 50, 55, and 60 °C.[75]

The analysis of Figure 2.11 (55 °C) highlighted three major aspects: i) a moderate conversion of only 22% was achieved after the first pass. This perfectly matched the result of the acetalization of wet glycerol **Glyc3** carried out at the same temperature, but at a pressure of 10 bar (Figure 2.5a). Apparently, both the pressure and the presence of water

had limited, if any, effect on the reaction outcome at least until the reactant acetone was in the liquid state. ii) The conversion of glycerol improved from 22% up to 72% after the 1st and the 8th pass, respectively (right axis). In each test the conversion stabilized after 1-2 hours (left axis). The catalytic bed was therefore able to reach steady operating conditions in a relatively short time notwithstanding a spatial velocity (WHSV) as high as 13.7 h^{-1}. iii) Regardless of the conditions and the composition of the reactant mixture used (fresh or recycled), the overall selectivity was >99% towards the formation of isomeric acetals **2.1a** and **2.1a'**.

Figure 2.11b compares the conversion profiles achieved in the range of 45-60 °C. Not only the recycle of the reactant mixture, but also the reaction temperature favored the formation of acetals. A moderate rise of 10 °C, from 45 to 55 °C, enhanced the glycerol conversion by more than 20% (compare black, blue, and green curves). At 55°C, additional tests – not shown here – proved that the performance of the catalyst was not appreciably altered even after a time-on-stream of ~100 h. The acetalization however, was no longer improved above the boiling point of acetone (red profile at 60 °C). The increase of the temperature was plausibly offset by the partitioning of acetone in the gas phase, this hindering the contact between reagents.

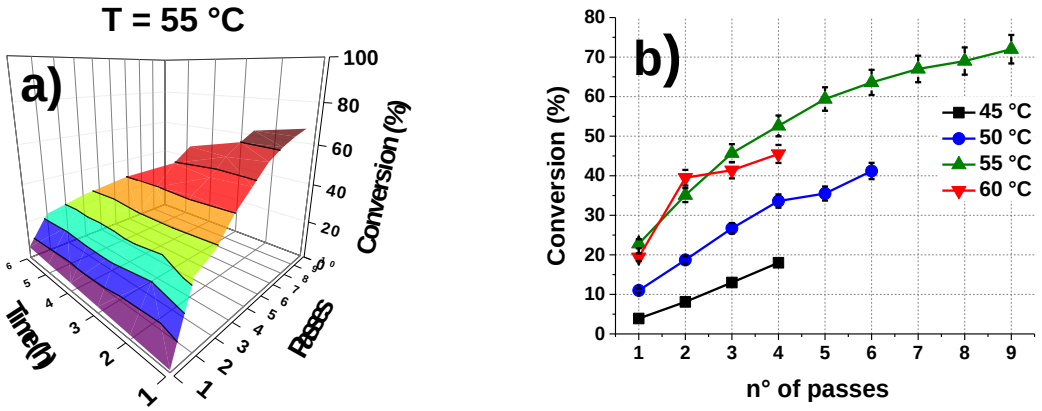

Figure 2.11. CF-acetalization of glycerol with acetone over commercial $AlF_3 \cdot 3H_2O$ as a catalyst. Tests were performed at ambient pressure. **a)** Profiles of glycerol conversion vs time (left axis) and number of passes (right axis), achieved at 55 °C; **b)** Mean values of glycerol conversion per each pass at 45, 50, 55, and 60 °C; **c)** **2.1a**/**2.1a'** isomer ratio determined by GC. Other conditions: molar ratio acetone:glycerol=20; total flow = 0.42 mL/min.

2.2.4.2 Reactions at moderate T and p with recycle.

The investigation was continued by performing the same acetalization reaction with recycling of the mixture at temperature and pressure of 80 and 100 °C, and 10, 25 and 50 bar, respectively. Like tests already described in Figure 2.5, the increase of pressure was considered to allow the process in the liquid phase even operating above the standard boiling point of acetone. In a typical experiment, a fresh mixture of acetone (0.40 mL/min) and glycerol (0.02 mL/min) in a 20:1 molar ratio, was allowed to flow for 3 hours over a catalytic bed of AF (1.5 g). Then, the solution recovered at the reactor outlet was recycled twice according to the above described procedure. Recycle runs were carried out for a total of 3 hours each. Results are reported in Figure 2.12 where the trend of glycerol conversion is indicated after the first pass and two subsequent recycles.

Experiments confirmed that: i) the combined effect of the temperature and the recycle could remarkably improve the reaction outcome. For example, at 80 °C and 10 bar, the conversion of glycerol increased progressively from 42 to 65 and 78% after the first, second and third pass, respectively (Figure 2.12a); while at the same pressure, a substantially quantitative reaction was reached at 100 °C after the third pass (conversion ~95%; Figure 2.12b). ii) Minor, if any, changes were achieved by enhancing the pressure up to 25 and 50 bar. This result was in analogy to those reported in Figure 2.4 and Figure 2.5: the acetalization process was insensitive to pressure, although necessary to operate under liquid conditions.

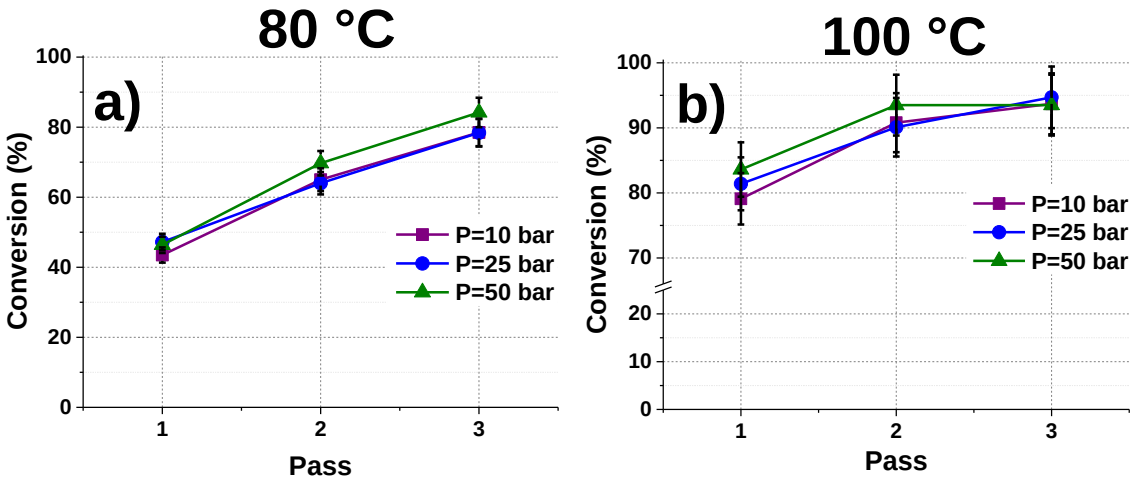

Figure 2.12. CF-acetalization of glycerol with acetone using commercial $AlF_3 \cdot 3H_2O$ as a catalyst. **a)** T = 80 °C; p=10, 25, and 50 bar. **b)** T = 100 °C; p=10, 25, and 50 bar. Other conditions: molar ratio acetone:glycerol=20; total flow = 0.42 mL/min.

Reactions of Figure 2.12 also proved that the selectivity towards acetalization was 100%, irrespective of the reaction conditions. These conditions however, had a dramatic influence on the ratio (W) of isomer products **2.1a** and **2.1a'**. The result can be visualized in Figure 2.13 that compare the W ratio and the conversion achieved by reactions carried out at 55 °C and ~2 bar, 80 °C and 10 bar, and 100 °C and 10 bar.

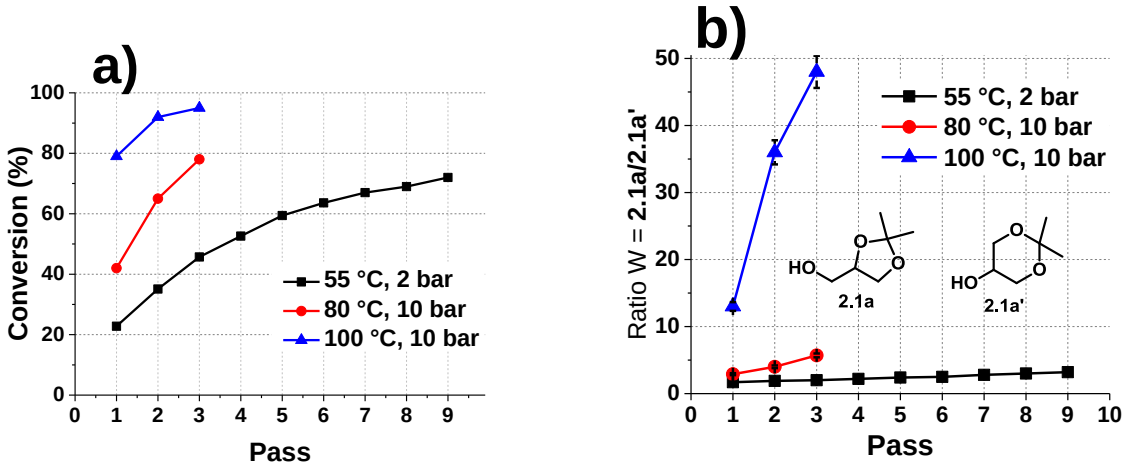

Figure 2.13. The CF-acetalization of glycerol with acetone carried out at: i) 55 °C, ~2 bar; ii) 80 °C, 10 bar; iii) 100 °C, 10 bar. **a)** The conversion of glycerol and the **b)** ratio of isomer **2.1a/2.1a'** are reported versus the number of passes through the CF-reactor. Other conditions: molar ratio (Q) acetone:glycerol=20; total flow rate=0.42 mL/min. Each dot is the average of values of GC-conversion and of the **2.1a/2.1a'** isomer ratio measured during 3-hours tests.

At 55 °C and ~ 2 bar, the increase of the glycerol conversion from 22 to 72% induced only a moderate change of the W ratio, from 1.7 to 3.2 (compare black profiles of Figure 2.13a and Figure 2.13b), with a non-negligible formation of the six-membered ring acetal **2.1a'** (up to 17% of 2,2-dimethyl-1,3-dioxan-5-ol). Of note, such a compound is achieved only by multistep sequences,[76,77,78] while its amount is usually less than 5% when straightforward acetalization or transacetalization reactions are used.[68,79,80,81]

At 10 bar however, the **2.1a/2.1a'** ratio almost doubled when the reaction was carried out at 80 °C (Figure 2.13 red profiles), while it dramatically increased at 100 °C. Under such conditions, the acetalization became quantitative and the 5-membered ring compound **2.1a** was achieved with a selectivity >97% with only trace amount (2%) of the isomer **2.1a'** (blue profiles).

The CF-procedure was suited not only to improve the reaction conversion by recycling the mixture, but also to tune the product distribution: the change of T and p plausibly modifies the thermodynamic *vs* kinetic control of the reaction at the level that either a

mixture of the isomer acetals **2.1a** and **2.1a'** or only the more stable product **2.1a** could be selectively obtained.[82]

2.2.4.3 The reaction with butanone

Three sets of tests were performed to examine the effects of T, p, also on the acetalization of glycerol (**Glyc1**) with 2-butanone. The first two were carried out at ~2 bar (55 and 75 °C) while a third one was done at 100 °C and 10 bar. Since the solubility of glycerol in 2-butanone was even lower than that in acetone, the reactant molar ratio (Q) was set to 60: this corresponded to relative flow rates of 0.01 mL/min for glycerol, and 0.74 mL/min for 2-butanone, respectively. Results are reported in Figure 2.14 which shows the (average) conversion of glycerol measured in the first pass and the subsequent recycles of the reactant mixture. Each test (pass) lasted 3 hours.

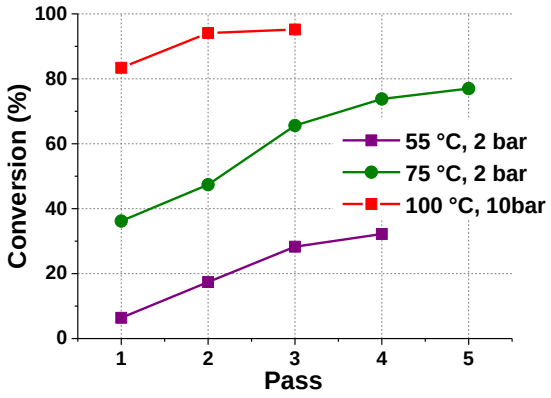

Figure 2.14. The conversion of glycerol in the CF-reaction with 2-butanone. Flow rates were 0.01 mL/min for glycerol and 0.74 mL/min for 2-butanone. A fresh catalytic bed of $AlF_3 \cdot 3H_2O$ (1.5 g) was used at any different temperature.

Like the acetalization with acetone, also the reaction of 2-butanone was remarkably affected by the temperature: at nearly ambient pressure, the glycerol conversion showed a ~30% increase from 55 to 75 °C (purple and green curves); however, as both T and p were raised to 100 °C and 10 bar, an almost quantitative reaction was reached after the first recycle of the reactant mixture (95%, 2nd pass, red profile).

The acetalization selectivity was always 100% towards isomeric acetals **2.3a** and **2.3a'**. Reaction conditions remarkably affected the relative proportions of such products, being the five-membered ring acetal **2.3a** always the most abundant compound. Figure 2.15 reports the ratio W_1=(**2.3a-*trans*+2.3a-*cis*)**/(Total of acetal products) for the investigated reactions.

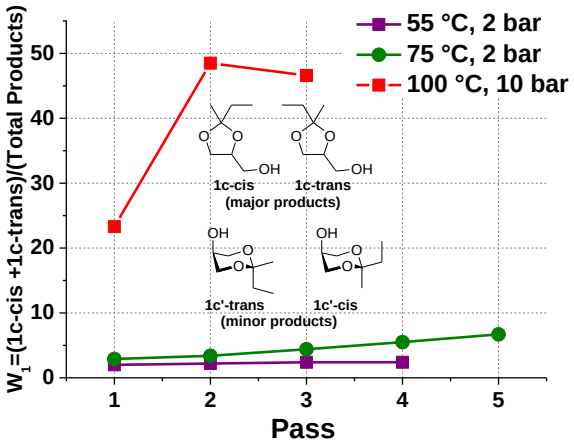

Figure 2.15. The ratio W_1=(**2.3a-*trans*+2.3a-*cis*)**/(Total of acetal products) observed in the CF-acetalization of glycerol with 2-butanone carried out at: i) 55 °C, ~ 2 bar; ii) 75 °C, ~ 2 bar; iii) 100 °C, 10 bar.

The behaviour was similar to that described for the acetalization of glycerol with acetone. At 55-75 °C and ~ 2 bar, the increase of glycerol conversion from 7 to 75% brought about a modest change of the W_1 ratio, from 2 to 7 (purple and green profiles). However, at 100 °C and 10 bar, the reaction became not only quantitative, but also extremely selective towards the more stable acetal **2.3a** (*cis+trans* isomers): the corresponding W_1 raised up to ~50 (red profiles). Also in this case, the variation of temperature and pressure could tune the distribution of conformer products.

2.3 Discussion

The here described investigation offers an approach for a rationale design of the catalytic acetalization of glycerol with commercial $AlF_3 \cdot 3H_2O$. To the best of our knowledge, such compound has never been previously reported as an acetalization catalyst. The study proves that the choice of the catalyst determines the outcome of the reaction depending on the grade of the reactant glycerol, while the implementation of the process in the CF mode allows to tune T, p, reactants flow rate and WHSV in order to improve the reaction productivity and to facilitate product isolation.

2.3.1 Acetalization catalysts

Experiments leave few doubts that the reaction of pure or wet glycerol is most efficiently catalyzed by A36 with respect to AF. As shown by the model acetalization of **Glyc3** with acetone, at 10 bar, AF requires temperatures as high as 100 °C to offer results

comparable to those achieved by using A36 at only 25 °C (Figure 2.4a and Figure 2.5a). This different catalytic performance is plausibly due to the effect of strong Brønsted acidity of the resin[83] compared to the weaker acidity of Lewis acid sites and hydroxyl groups on the hydrated aluminum fluoride (see also later on this section).[84,85]

Notwithstanding the thermodynamic limitation that water (as an acetalization by-product) may involve on the equilibrium of the reaction, the activity of both catalysts is only partly affected by the use of wet reagents: under conditions optimized for A36 and AF, steady and good conversions (>80%) are obtained for different types of glycerol containing amounts of water variable in a broad range, from 4 to 25 wt% (**Glyc3** and **Glyc4**: Figure 2.4a and Figure 2.5b). An explanation for this result is offered by the dynamic transfer of reagents and products in the continuous-flow mode that helps the desorption of water from the catalytic bed. In the case of AF, the hydrolytic stability of the catalyst is further proved by the very low leaching of both aluminum and fluoride. The concentration of F^- measured in acetal mixtures collected at the reactor outlet is <3 ppm (less than half the U.S. EPA level of 4.0 ppm allowed in drinking water[86,87] though, the comparatively higher release of fluoride ions with respect to Al (200 ppb) is plausibly due to some exchange with hydroxide groups at the catalyst surface.

Also, the addition of MeOH (22-30 wt%) to the reactant glycerol has negligible, if any, effects on the performance of both A36 and AF systems (compare **Glyc1** and **Glyc2**: Figures Figure 2.4a and Figure 2.5b).

The most intriguing aspect emerging from the comparison of the two catalysts is their different tolerance to the presence of NaCl in the reactant stream. In the reaction of crude-like glycerol (**Glyc5** and **Glyc6**) with acetone, stable conversion and productivity up to 78% and 5.6 h^{-1} are reached by using AF as a catalyst (Table 2.5), while A36 severely deactivates in few hours proving it unsuitable for the continuous process where a long catalyst lifetime is imperative (Figure 2.4b). The exchange of protons with sodium cations (Na^+) accounts for the progressive decrease of acidity of the organic resin and consequently, for its loss of activity over time. On the other hand, the reasons for the stability of AF to NaCl deserve a more in-depth consideration which may take the cue from the XRD analysis of Figure 2.6 and Figure 2.7. Diffractogram of fresh commercial AF proves that the compound is comprised of a mixture of $AlF_3 \cdot 3H_2O$, a solid solution (SS) of formula $Al_2[(F_{1-x}(OH)_x]_6(H_2O)_y$, and very minor amounts of β-AlF_3. Such a composition is fully preserved even after a prolonged use (up to 30 h) of AF as a catalyst for the reaction of pure or wet glycerol (**Glyc1-4**) with acetone

(Table 2.7: AF_1 sample). However, if reactants include NaCl as an additive, then AF undergoes a phase change: of its initial main components, the solid solution {SS: $Al_2[(F_{1-x}(OH)_x]_6(H_2O)_y$} remains unaltered, while $AlF_3{\cdot}3H_2O$ is progressively and quantitatively transformed into a chiolite ($Na_5Al_3F_{14}$, ChPh) phase during the CF-acetalization tests. This is clearly proved by XRD spectra of the AF_2 sample (Figure 2.10). Although, at the moment, no clear reasons explain why only $AlF_3{\cdot}3H_2O$ is sensitive to a structural modification, the fact that the AF_2 solid shows a constant catalytic performance for the conversion of crude-like glycerol **Glyc5-6** provides evidence that the SS component is the authentic active phase for the investigated reaction. This is further confirmed by the observation that the calcined AF_c compound (pure α-AlF_3 phase) is no longer an acetalization catalyst. The overall behavior is summarized in Scheme 2.11.

A hypothesis to explain the catalytic role of the SS phase is based on the general mechanism of formation of acetals which starts from the electrophilic activation of the reacting ketones. Accordingly, Scheme 2.12 shows a pictorial view of the possible interactions (a and b) between the catalyst surface and acetone as a model ketone. The Brønsted acidity associated to the OH groups of the SS phase offers the major contribution for the initiation of the acetalization reaction (path a, top). While, the lack of activity of anhydrous α-AlF_3 phase suggests a minor influence, if any, of Lewis acid sites (path b). Pure α-AlF_3 is inactive for the acetalization reaction (Scheme 2.11). This phase, either pure on in three hydrate form (α-$AlF_3{\cdot}3H_2O$), has been reported as a poor Lewis acid system.[88] In the second step of the reaction, water as a base restores the acidity of the catalyst, and at the same time, it also readily desorbs from the active surface due to the dynamic mass transfer operating in the CF reactor.

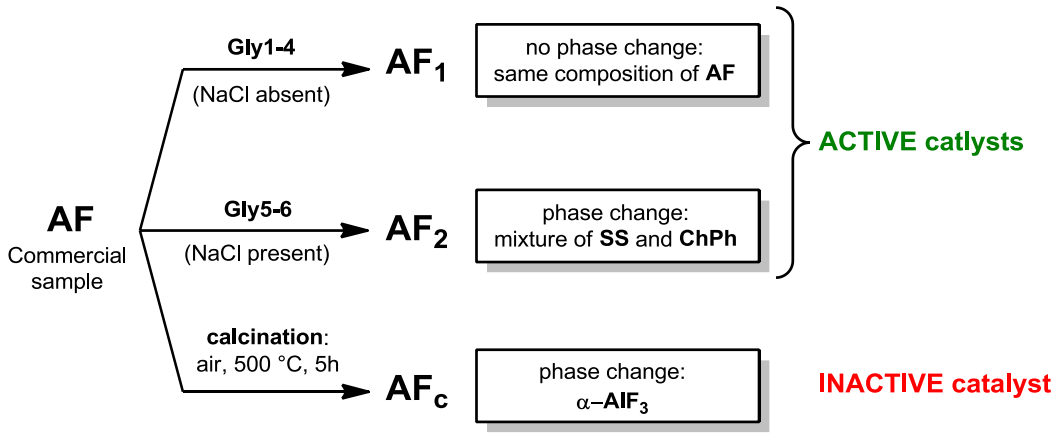

Scheme 2.11. The behavior of commercial AF sample in the acetalization with acetone. AF sample is composed by a mixture of $AlF_3 \cdot 3H_2O$, $Al_2[(F_{1-x}(OH)_x]_6(H_2O)_y$ (SS) and β-AlF_3 in the relative proportion of 83, 13 and 4% respectively. AF_2 is composed by a mixture of the SS and $Na_5Al_3F_{14}$ (chiolite phase, ChPh) in the relative proportion of 63.4 and 36.6 % respectively. AF_c is entirely composed by α-AlF_3.

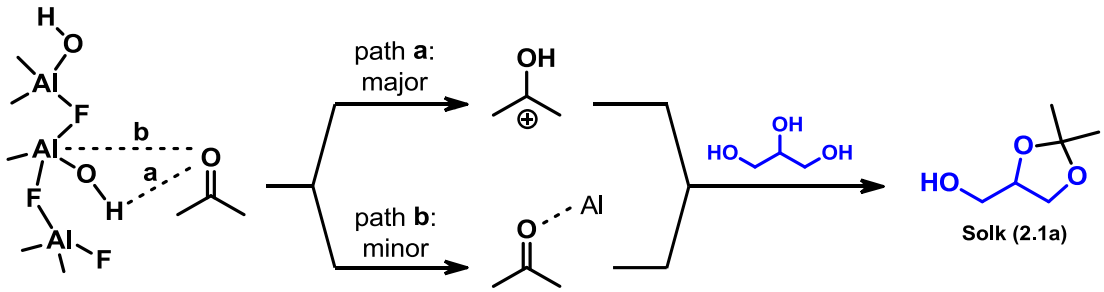

Scheme 2.12. Activation of ketones over Brønsted and Lewis acid sites of the catalytic phase (SS)

The equilibrium position therefore shifts to the right pushing the reaction forward. Unlike the Amberlyst resin, AF keeps on catalyzing the acetalization of crude-like glycerol (**Glyc5-6**) with unchanged conversion and selectivity over time since the (weak) acidity of the hydroxyl groups of the SS phase does not allow exchange reactions with NaCl. Also, a contribution might derive from surface F atoms (of the SS phase) which possibly offer an hydrophobic shell able to mitigate, if not hinder, the contact of the catalyst with Na cations in the reacting aq. solution.[89] Whatever the reason, the outcome highlights the potential and the possible synthetic (and economic as well) advantage of AF with respect to the Amberlyst system: since the isolation of acetal products (*e.g.* solketal) by distillation of final reaction mixtures is not only simpler but also cheaper than techniques required for the purification of off-grade glycerol,[3,90] it is by far more convenient to convert CG rather than refining the crude reagent and then proceeding with its upgrading.

It should also be noted that the performance of the active SS phase should be evaluated as such rather than in the commercial mixture with $AlF_3 \cdot 3H_2O$. Although this study is beyond

the scope of this paper, future investigations will be focused on the synthesis and applications of the pure SS compound through comparative tests with other acid acetalization catalysts.

2.3.2 The continuous-flow (CF) conditions

CF-conditions may significantly improve the reaction outcome through the optimization of T, p, and reactant flow rate/ratio. This is clear from results of: i) Figure 2.11 and Figure 2.12 which show, for example, how the acetalization of glycerol with acetone can be run at 10 bar well below the previously reported operating pressure (30-120 bar)[41,42,43,44,45] for the same reaction; ii) Table 2.5 and Table 2.6 which demonstrate how the reaction productivity (P) almost linearly grows by increasing WHSV from 2 to 6 h^{-1}. In this range, while the viscosity issue often limits the implementation of CF-processes using glycerol solutions (see introduction), nonetheless in our case clogging drawbacks of the reactor have never been experienced. Such an observation probably indicates that a further increase of the reactant flow rate can be applied in a large scale preparation to optimize P, thereby improving the overall performance of the procedure according to the requirement of process intensification. Finally, this also confirms the suitability of AF - even in its powdered commercial form - as a catalyst for the synthesis of GAs.

CF-conditions improve the reaction outcome through an easy implementation of recycle operations. This is clear from tests at 45-55 °C and ~2 bar where the recycle of reaction mixtures allows to increase the glycerol conversion up to an equilibrium value of 72% (Figure 2.11), and it is emphasized by the experiments at 80-100 °C and 10-50 bar where a substantially quantitative transformation can be achieved after only one recycle step (Figure 2.12).

2.3.3 2-Butanone

This study proves that the AF catalyst is active not only for the CF-acetalization of crude-like glycerol with acetone, but also with other carbonyl compounds, particularly 2-butanone. Although experimental conditions used for the two ketones are not strictly comparable (see Table 2.5 and Table 2.6), 2-butanone appears less reactive than acetone. This trend seems consistent with steric limitations on the kinetics: the more hindered the carbonyl group, the slower its reactions. An analogous behaviour has been described also in previous studies on the acetalization of glycerol with different aldehydes, where the process

was progressively disfavored by heavier substrates, from butanal to pentanal, hexanal, octanal and decanal.[91]

In the range of 55-100 °C, the acetalization of pure glycerol (**Glyc1**) with 2-butanone at nearly ambient pressure and at 10 bar shows that the combination of the CF-mode and recycle operations allow to improve the glycerol conversion up to a substantially quantitative value (Figure 2.14).

2.3.4 Isomer distribution

The reaction of glycerol with both aldehydes and ketones yields mixtures of five- and six-membered ring isomer acetals (C_5 and C_6 cyclic products, respectively), the proportion of which is affected by the experimental conditions. Although it is generally accepted that six-membered ring compounds are thermodynamically favoured over the corresponding five-membered isomers,[92,93] recent DFT theoretical calculations have demonstrated that an opposite trend holds for the ketals produced by the reaction of glycerol with acetone (Scheme 2.13: **2.1a** and **2.1a'**, respectively).[76,77,78] Due to repulsive interactions between methyl groups and hydrogen atoms in the axial positions of the cyclic C_6 product (2,2-dimethyl-1,3-dioxan-5-ol, **2.1a'**), this compound is 1.7 kcal mol^{-1} less stable than the C_5 isomer (2,2-dimethyl-1,3-dioxolan-4-yl) methanol: solketal **2.1a**). On the other hand, the greater reactivity of primary *vs* secondary hydroxyl groups of glycerol is expected to make the C_6-ring closing reaction faster than the C_5-one. The two isomers are also able to interconvert: previous studies have proven the occurrence of an acid-catalyzed equilibrium reaction for the mutual transformation of cyclic acetals of glycerol (Scheme 2.13).[33,94,95,96]

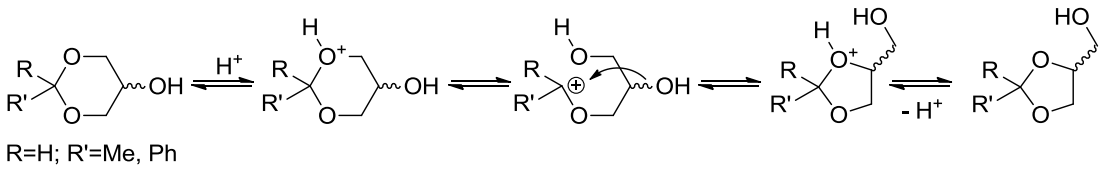

Scheme 2.13. Acid-catalyzed interconversion of C_5 and C_6 cyclic acetal isomers.

On this basis, an explanation may be offered for the isomer distribution observed in this work. Consider for example, the reaction of glycerol with acetone. At nearly atmospheric ambient pressure (2 bar) and 55 °C, the **2.1a**/**2.1a'** ratio varies from 1.7 to ~3 meaning that isomeric acetals are achieved in almost comparable amounts (Figure 2.13, black profile). This result can be accounted for by two aspects: i) as long as the per-pass conversion is

moderate (≤15%, Figure 2.11 and Figure 2.13), CF-conditions and low contact times favor a dynamic desorption of **2.1a** and **2.1b'** from the catalyst surface before further transformations occur; ii) the low reaction temperature disfavours the isomer interconversion of Scheme 2.13. It seems plausible that thermodynamic and kinetic products may coexist under such circumstances. However, as the temperature is increased, the formation of the thermodynamically preferred product **2.1a** increases as well (Figure 2.13: red profile at 80 °C and 10 bar), and at 100 °C **2.1a** becomes the almost exclusive derivative.

The outcome of the reaction of glycerol with 2-butanone is even more peculiar in view of the fact that both C_5/C_6 ring-closing reactions and *cis/trans* isomerism are possible. In this case, the preferred formation of cyclic C_5 compounds can be accounted for by the same line of reasoning as above, *i.e.* the greater thermodynamic stability of C_5 *vs* C_6 isomers. Results of Figure 2.15 support this conclusion. On the other hand, the occurrence of approximately equal amounts of C_5 isomers (**2.3a-cis** and **2.3a-trans**) indicates that the corresponding structures have comparable energies. This is in agreement with previous findings on the synthesis of such compounds via both acetalization and transacetalization processes catalysed by protic acids,[1,68,97] but it is opposite to results described for the reaction of glycerol with acetaldehyde and benzaldehyde where the cyclic C_5 trans-isomer products are favoured over the corresponding cis-ones.[33,94 ,95,96] The latter behaviour has been explained with intramolecular H-bonding.

The proportions of geometric isomers of cyclic C_6 acetals (**2.3a'-trans** and **2.3a'-cis** of Scheme 2.10) plausibly follow the same pattern described for C_5 products. However, the modest formation of such (C_6) compounds does not allow any detailed discussion.

2.4 **Conclusion**

Catalysts for the implementation of robust CF-methods for organic synthesis must be active, durable and versatile so as to accommodate reactant feeds with variable chemical compositions. In the specific case of the CF-acetalization of glycerol with ketones, this investigation proposes for the time the use of commercial $AlF_3 \cdot 3H_2O$ as a catalyst and compares its activity to that of Amberlyst 36 as an acidic resin. This study demonstrates that A36 and AF possess complementary activities and features. A36 is the most efficient system:

it is capable to operate under very mild conditions, but it is readily poisoned by even small amount of NaCl which is a common contaminant of CG. The second compound (AF) requires a higher operating temperature, but its performance is insensitive to the presence of inorganic salts, being thereby suitable for the conversion of different kinds of raw glycerol. Overall, the here reported approach shows that the design of a CF synthesis of GAs can be conveniently tailored according to the quality of the starting materials, by using either conventional acid organic resins or introducing new acetalization catalysts such as AF. Both catalysts, when used at optimized T, p, and flow rates (WHSV) afford stable activity in the long run, though AF may offer a more attractive standpoint for the straightforward valorization of CG. AF has been successfully operated for weeks with no loss of activity or selectivity: ICP-OES and ionic chromatographic analyses of liquid mixtures recovered at the reactor outlet confirm that the release of Al and F was <0.1wt% per working (40 hours) week.

This study provides XRD evidences that the activity of the investigated commercial sample of AF is reasonably due to the presence of a solid solution (SS) phase composed of an aluminum hydroxide fluoride $Al_2[F_{1-x}(OH)_x]_6(H_2O)_y$ in the relative amount of 13%. The catalytic performance is plausibly associated to the occurrence of surface hydroxyl groups able to confer Brønsted acidity to the catalyst. These acid sites trigger the acetalization reaction by an electrophilic activation of ketones, while the co-product water (as a base) assists the process by restoring the catalyst through a continuous proton exchange on its surface.

An extended analysis of the CF-acetalization of pure glycerol over AF has been carried out by investigating the effect of T, p, and the recycling of the reaction mixture recovered at the reactor exit. Under the best found conditions (100 °C and 10 bar), recycling operations allow to achieve substantially quantitative conversion and complete selectivity towards acetal products after a single recycle (two passes) of mixtures collected from the CF-reactor. Experimental conditions also allow to tune the relative amounts of five- and six-membered ring isomers. The higher the temperature, the higher the formation of the more thermodynamically stable C_5 acetals: in particular, the **2.1a/2.1a'** and **2.3a/2.3a'** isomer ratios may increase by a factor of ~25, from ~2 up to 48. Whenever geometric isomers are possible such as in the reaction of glycerol with 2-butanone, the *trans*- and *cis*-compounds are obtained in almost equal amounts, indicating structures of comparable energy.

2.5 Experimental

2.5.1 Materials

Glycerol, acetone, 2-butanone were ACS grade from Aldrich and were used as received. Aluminum fluoride trihydrate ($AlF_3 \cdot 3H_2O$, 97%), Amberlyst-36 and sand (50-70 mesh) were from Aldrich and used as received. Water was of milli-Q grade.

2.5.2 Analysis instruments

GC/MS (EI, 70 eV) analysis were run using a HP5-MS capillary column (L=30 m, Ø=0.32 mm, film=0.25 μm). The following conditions were used: carrier gas: He; flow rate: 1.2 mL/min; split ratio: 10:1; initial T: 50 °C (3 min), ramp rate: 15 °C/min; final T: 250 °C (3 min).

GC/FID analysis were run using an Elite-624 capillary column (L=30 m, Ø=0.32 mm, film=1.8 μm). The following conditions were used. Carrier gas: N_2; flow rate: 5.0 mL/min; split ratio: 1:1; initial T: 100 °C (0 min), ramp rate: 15 °C/min; final T: 220 °C (5 min). ICP-OES analysis were run using a Perkin Elmer Optima 5300DV.

Inductively coupled plasma optical emission spectrometry (ICP-OES) analyses were run on a Perkin Elmer Optima 5300 DV in axial direction at 394.401 nm.

Ion chromatography analyses were run on a Dionex LC20 (Chromatography enclosure) equipped with a Dionex GP40 gradient pump and a Dionex ECD ED40 (working at 100 mA). A Dionex AS14 was used as column with 1mM carbonate/3.5 mM bicarbonate as a mobile phase.

XRPD patterns were recorded at room temperature with a step size of 0.05° in the 5–100° range. The diffraction data were collected (10 s $step^{-1}$) using a Philips X'Pert system (PW3020 vertical goniometer and PW3710 MPD control unit) equipped with a focusing graphite monochromator on the diffracted beam and with a proportional counter (PW1711/90) with electronic pulse height discrimination. A 0.5° divergence slit was used, together with a receiving slit of 0.2 mm, an antiscatter slit of 0.5° and Ni-filtered Cu Kα radiation (30 mA, 40 kV).

^{1}HNMR were recorded at 300 MHz, ^{13}C spectra at 75 MHz and chemical shift were reported in δ values downfield from TMS; $CDCl_3$ was used as solvent.

2.5.3 CF apparatus

The apparatus used for the investigation was assembled in-house (Figure 2.16). Two twin HPLC pumps (P1 and P2) were used to deliver one or two liquid reactants (1 and 2) to two stainless steel tubular chambers both placed in the upright position. The first chamber (L=12 cm, Ø=1/4", 0.875 cm^3 inner volume) was filled with sand (2.3 g) and served as a static mixer, while the second one was the reactor containing the catalyst: AF or A36. Depending on the experiments, different reactor dimension were considered: (a) L=12 cm, Ø=1/4", inner volume=0.875 cm^3; and (b) L=12 cm, Ø=3/8", inner volume=3.5 cm^3. For the reactor a) the loading used were: AF=1.5 or 0.67 g; A36= 0.9 g. For the reactor b) the loading used was: AF=4.2 g. Both the static mixer and the reactor were placed in a gas chromatographic oven (GC oven) and heated at the desired temperature. A JASCO BP-2080 back pressure regulator (BPR), placed at the outlet of the reactor, was used to maintain the pressure constant over the whole system throughout the reaction (line B). When experiments were carried at ambient pressure the BPR was bypassed (line A).

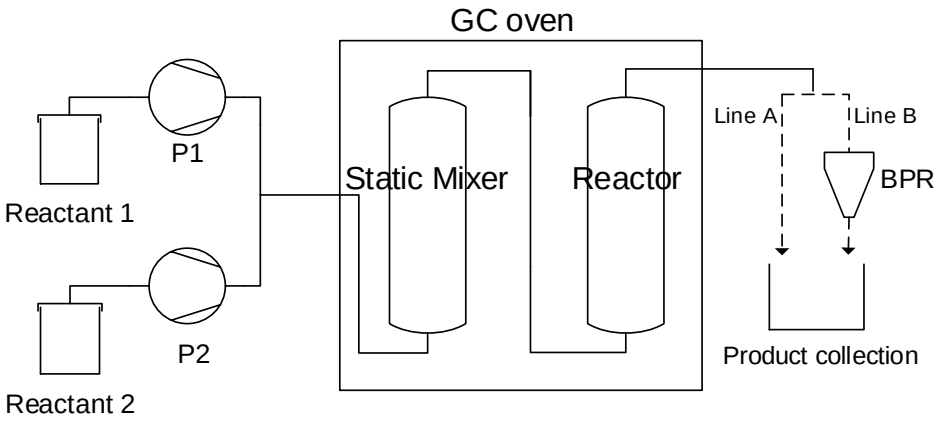

Figure 2.16. Experimental setup used for the continuous-flow acetalization of Gly with acetone and 2-butanone

2.5.4 General procedure for the CF acetalization of Glycerol

A typical CF acetalization reaction was carried out according to the following operations. Depending on the typology of the experiment, the procedure can be divided in two different procedures

2.5.4.1 Separate reactants and recycling of the mixture

First pass of reactants. Pumps P1 and P2 were set in a constant flow mode adjusting the flow rates in the range of 0.02-0.07 mL/min for glycerol, and 0.35-0.74 mL/min for the acetone, respectively. Then, reagents were delivered as two separate streams to the static mixer followed by the reactor. The BPR and the GC oven were set to the operating pressure and temperature (10-50 bar and 45-100 °C). For the experiments at atmospheric pressure, the BPR was simply bypassed (Line A). Under such conditions, the apparatus was preliminarily conditioned for 20 minutes. Afterwards, the reaction mixture was collected at time intervals of 60 min, for a minimum of 3 to a maximum of 6 samples, and analyzed by GC/FID and GC/MS.

Recycle of the reaction mixture. All the samples collected during the *first pass of reactants*, were mixed together achieving an homogeneous mixture. Without any further purification, the latter was conveyed to the reactor at a flow rate corresponding to the total flow rate used in the first pass by mean of pump 2. Other conditions, including temperature, pressure, conditioning, sampling, and GC-analysis were left unchanged with respect to the previous step. When indicated, such recycle procedure was repeated.

Change of reaction conditions: system cleaning and restart. Once an experiment first pass (or recycles) was complete, the GC oven and the BPR were set to 50 °C and atmospheric pressure, while a cleaning solution of acetone (50 mL at 0.5 mL/min) was delivered to the mixer and reactor. Afterwards, pumps were stopped and the GC oven was allowed to cool at RT. A new experiment could then start by changing the reaction conditions (T, P, and flow rates), or, when specified, by replacing also the catalytic bed with a fresh one. In the latter case, the previously used reactor was dried overnight in a stove, emptied, and refilled with a fresh charge of AF.

2.5.4.2 Homogeneous reactants mixture of glycerol blends

Six different types of glycerol (**Glyc1-**6) were considered. These were all prepared by mixing ACS-grade glycerol (**Glyc1**, 10 g) with different amounts of water (0.5 to 11 mL), MeOH (1.26 to 11.36 mL) and NaCl (0.5 g) in order to reach the compositions described in Table 2.3. Then, the CF-acetalization reactions were carried as below described

Reaction procedure. The homogeneous solution of **Glyc1-6** and the desired ketone (acetone or 2-butanone) in the molar ratio (Q =ketone:glycerol) variable from 4 to 60 was delivered by means of the HPLC pump 2 to the reactor. In these experiments, when a

homogeneous mixture was used, the static mixer wes removed from the apparatus. The reactor was previously filled with 0.9 g of A36 or with 0.67 g AF (4.2 g if the reactor type b) was used). Each reaction was run at a constant flow mode. The explored range of flow rates of the mixture was from 0.1 to 1.18 mL/min. The operating pressure and temperature were set and checked at the desired values (10-35 bar and 25-100 °C). The apparatus was preliminarily conditioned for 1h. Afterwards, the reaction mixture was sampled at time intervals of 60 min, for a minimum of 3 samples, and analyzed by GC/FID and GC/MS.

System cleaning and reuse of the reactor. Once the experiment was completed, if the catalytic bed was reused, the GC oven was set to 50 °C and pure acetone (50 mL at 0.5 mL/min) was delivered to the reactor. In the specific case when the reactants mixture contained sodium chloride (if **Glyc5** or **Glyc6** was used), Milli-Q water was delivered to the reactor (50 mL at 0.5 mL/min) prior to the acetone cleaning. Afterwards, the pump was stopped, the system was vented to the atmospheric pressure and the GC oven was allowed to cool at RT.

2.5.5 ICP-OES and ionic chromatographic analyses

In the presence of AF as a catalyst, the acetalization of **Glyc3** with acetone was carried out according to the above described procedure (100 °C, 10 bar: conditions of Figure 2.5b). Once the experiments were complete, the mixtures sampled were used for ICP and ion chromatography analysis.

2.5.5.1 ICP analysis

Sample. Prior the analysis, the sample was rotary evaporated (60 °C, 40 mbar, 1h). The oily residues was initially diluted with milli-Q water (20 mL) and then diluted again in a 1:3 v/v ratio.

Blank sample. A bank sample was prepared by flowing the reactants mixture through the CF-apparatus in the absence of the catalyst at the same operating conditions used for the sample (100 °C, 10 bar). The mixture collected was rotary evaporated (60 °C, 40 mbar, 1h) and the oily residues diluted with milli-Q water (20 mL).

Calibration curve. A calibration curve was obtained by using seven aqueous solutions containing 300, 200, 150, 100, 60, 40 and 20 ppb of Al. These solutions were all prepared by dilution of a 1000 mg/L standard solution of ionic Al in HNO_3. The linear fit was

automatically calculated by the ICP software resulting with interceptor = −151.8, slope = 21.70 and correlation coefficient = 0.996961. (see appendix A).

The analysis results are reported in Table 2.4. Each analysis was the average of 6 subsequent acquisitions.

2.5.5.2 Ion chromatography analysis

Sample. The sample was diluted with milli-Q water in a 1:5 v/v ratio.

Blank sample. A bank sample was prepared by flowing the reactants mixture through the CF-apparatus in the absence of the catalyst at the same operating conditions used for the sample (100 °C, 10 bar). The mixture collected was diluted with milli-Q water in a 1:5 v/v ratio.

Calibration curve. A calibration curve was obtained by using four aqueous solutions containing 0.5, 1, 3, 7 ppm of F^-. The linear fit was automatically calculated by the chromatograph control software (Chromeleon) resulting with slope = 0.131, interceptor forced to 0 and correlation coefficient = 0.999868. (see appendix A).

The analysis results are reported in Table 2.4. Each analysis was the average of 3 subsequent acquisitions.

2.5.6 Isolation and characterization of products.

(2,2-dimethyl-1,3-dioxolan-4-yl)methanol (Solketal, 2.1a)

The product was isolated from two reactions (A and B) starting from **Glyc1** and **Glyc5**.

The acetalization of **Gly1** with acetone (Q=40) carried out under the conditions of Figure 2.5b (100 °C and 10 bar; flow rate = 0.2 mL/min; AF = 0.67 g). The reaction was allowed to proceed for 15 h. The homogeneous mixture recovered at the reactor outlet was rotary evaporated (60 °C, 40 mbar, 1h) and distilled (70 °C, 40 mbar). The title product was obtained as a colorless mixture of isomers **2.1a** and **2.1a'** (ratio **2.1a**/**2.1a'**~50) in a 74% overall yield (5.8 g, purity 98% by GC/FID).

The acetalization of **Glyc5** with acetone (Q=4) was carried out under the conditions of Figure 2.5b (100 °C and 10 bar; flow rate = 0.34 mL/min; AF = 0.67 g). The reaction was allowed to proceed for 3 h. The homogeneous (pale green) mixture recovered at the reactor outlet was rotary evaporated (60 °C, 40 mbar, 1h), filtered to remove the solid residue of sodium chloride, and distilled (70 °C, 40 mbar). The title product was obtained as a colorless

mixture of isomers **2.1a** and **2.1a'** (ratio **2.1a**/**2.1a'**~50) in a 59% overall yield (11.5 g, purity 98% by GC/FID). The structure of the product was confirmed by ^{1}H NMR, ^{13}C NMR and GC/MS and by comparison to an authentic commercial sample of solketal. (see appendix A).

(2-Ethyl-2-methyl-1,3-dioxolan-4-yl)methanol (2.3a)

The product was isolated from the acetalization of **Gly1** with 2-butanone (Q=60) carried out under the conditions of entry 1 in Table 2.6 (100 °C and 10 bar; flow rate = 0.2 mL/min; AF = 0.67 g). The reaction was allowed to proceed for 24 h. The homogeneous mixture recovered at the reactor outlet was rotary evaporated (60 °C, 40 mbar, 1h) and distilled (79 °C, 40 mbar). The title product was obtained as a colorless mixture in a 68% overall yield (5.2 g, purity 96% by GC/FID). It was characterized by ^{1}H NMR, ^{13}C NMR and GC/MS. (see appendix A).

^{1}H NMR mostly shows multiplets due to a partial overlap of the signals of cis- and trans-isomers of **2.3a** present in approximately equal concentrations.

^{1}H NMR (300 MHz, $CDCl_3$) δ (ppm): 4.25 (m, 2H), 4.12 – 4.00 (m, 2H), 3.85 – 3.72 (m, 4H), 3.61 (m, 2H), 1.79 – 1.62 (m, 4H), 1.39 (s, 3H), 1.33 (s, 3H), 0.96 (m, 6H). 13C NMR (75 MHz, $CDCl_3$) δ (ppm): 111.91 , 111.61 , 76.93 , 76.25 , 66.23 , 66.19 , 63.46 , 63.28 , 32.90 , 31.99 , 24.54 , 23.45 , 8.86 , 8.57. GC/MS (relative intensity, 70eV) m/z: 145 (M^+, <1%), 131 (20), 117 (100), 115 (27), 86 (11), 73 (11), 61 (14), 57 (84), 55 (18), 43 (80).

2.6 Bibliography

[1] V. B. Vol'eva, I. S. Belostotskaya, A. V. Malkova, et al., New approach to the synthesis of 1,3-dioxolanes, *Russ. J. Org. Chem.*, **2012**, 48, 638-641.

[2] B. Burczyk, A. Piasecki and L. Weclas, Chemical structure and surface activity. 10. The effect of hydroxyl group configuration on the adsorption of 2-alkyl-4-(hydroxymethyl)-1,3-dioxolanes and 2-alkyl-5-hydroxy-1,3-dioxanes at the aqueous solution-air interface, *J. Phys. Chem.*, **1985**, 89, 1032-1035.

[3] A. E. Diaz-Alvarez, J. Francos, B. Lastra-Barreira, et al., Glycerol and derived solvents: new sustainable reaction media for organic synthesis, *Chem. Commun.*, **2011**, 47, 6208-6227.

[4] L. Moity, A. Benazzouz, V. Molinier, et al., Glycerol acetals and ketals as bio-based solvents: positioning in Hansen and COSMO-RS spaces, volatility and stability towards hydrolysis and autoxidation, *Green Chem.*, **2015**, 17, 1779-1792.

[5] V. R. Ruiz, A. Velty, L. L. Santos, et al., Gold catalysts and solid catalysts for biomass transformations: Valorization of glycerol and glycerol–water mixtures through formation of cyclic acetals, *J. Catal.*, **2010**, 271, 351-357.

[6] E. García, M. Laca, E. Pérez, et al., New Class of Acetal Derived from Glycerin as a Biodiesel Fuel Component, *Energy & Fuels*, **2008**, 22, 4274-4280.

[7] B. Delfort, I. Durand, A.Jaecker et al., Diesel fuel compositions with reduced particulate emission, containing glycerol acetal derivatives, FR2833607 (A1), **2003**.

[8] G. Hillion, B. Delfort and I. Durand, Method For Producing Biofuels, Transforming Triglycerides Into At Least Two Biofuel Families: Fatty Acid Monoesters And Ethers And/Or Soluble Glycerol Acetals, WO093015 (A1), **2005**.

[9] Collective of authors in *Proceedings of IAC-EIaT 2014,* Czech Institute of Academic Education, Prague, **2014**.

[10] The pour point of a liquid is the temperature at which it becomes semi solid and loses its flow characteristics

[11] N. Rahmat, A. Z. Abdullah and A. R. Mohamed, Recent progress on innovative and potential technologies for glycerol transformation into fuel additives: A critical review, *Renew. Sust. Energ. Rev.*, **2010**, 14, 987-1000.

[12] B. Delfort, I. Durand, A. Jaecker et al., Diesel fuel compositions that contain glycerol acetal carbonates, US0025417 (A1), **2004**.

[13] M. J. Climent, A. Corma and A. Velty, Synthesis of hyacinth, vanilla, and blossom orange fragrances: the benefit of using zeolites and delaminated zeolites as catalysts, *Appl. Catal., A*, **2004**, 263, 155-161.

[14] http://www.femaflavor.org/fema-gras%E2%84%A2-flavoring-substance-list FEMA-GRAS flavouring substance list (last access: 2016/08/17)

[15] http://www.lambiotte.com/ Innovative solvents, acetals (last access: 2016/08/17)

[16] A. Piasecki, Alkoxyalkyl-substituted glycerol acetals: New hydrophobic intermediates for surfactant synthesis, *J. Am. Oil Chem. Soc.*, **1992**, 69, 639-642.

[17] A. Piasecki, A. Sokołowski, B. Burczyk, et al., Synthesis and surface properties of chemodegradable anionic surfactants: Sodium (2-n-alkyl-1,3-dioxan-5-yl)sulfates, *J. Am. Oil Chem. Soc.*, **1997**, 74, 33-37.

[18] K. Holmberg in *Novel surfactants Preparation, application and biodegradability*, 2nd ed., Marcel Dekker, Gothenburg, **2003**.

[19] M. Selva, V. Benedet and M. Fabris, Selective catalytic etherification of glycerol formal and solketal with dialkyl carbonates and K2CO3, *Green Chem.*, **2012**, 14, 188-200.

[20] F. A. J. Meskens, Methods for the Preparation of Acetals from Alcohols or Oxiranes and Carbonyl Compounds, *Synthesis*, **1981**, 501-522.

[21] B. Karimi and B. Golshani, Iodine-Catalyzed, Efficient and Mild Procedure for Highly Chemoselective Acetalization of Carbonyl Compounds under Neutral Aprotic Conditions, *Synthesis*, **2002**, 784-788.

[22] H. R. Prakruthi, B. M. Chandrashekara, B. S. Jai Prakash, et al., Microwave rehydrated Mg–Al-LDH as base catalyst for the acetalization of glycerol, *Catal. Sci. Technol.*, **2015**, 5, 3667-3674.

[23] M. B. Smith and J. March in *March's Advanced Organic Chemistry, Reactions, Mechanisms, and Structure*, 6th ed., Wiley Interscience, **2007**.

[24] P. J. Kocienski in *Protecting Groups*, 3rd ed., Stuttgart, **2005**.

[25] A. F. B. Cameron, J. S. Hunt, J. F. Oughton, et al., Studies in the synthesis of cortisone. Part III. The degradation of the ergosterol side chain, *J. Chem. Soc*., **1953**, 3864-3869.

[26] N. Suriyaprapadilok and B. Kitiyanan, Synthesis of Solketal from Glycerol and Its Reaction with Benzyl Alcohol, *Energy Procedia*, **2011**, 9, 63-69.

[27] T. Coleman and A. Blankenship, Process for the Preparation of Glycerol Formal, US Pat., US20100094027(A1), **2010**.

[28] M. R. Capeletti, L. Balzano, G. de la Puente, et al., Synthesis of acetal (1,1-diethoxyethane) from ethanol and acetaldehyde over acidic catalysts, *Appl. Catal., A*, **2000**, 198, L1-L4.

[29] J. Deutsch, A. Martin and H. Lieske, Investigations on heterogeneously catalysed condensations of glycerol to cyclic acetals, *J. Catal.*, **2007**, 245, 428-435.

[30] M. Kaufhold ad M. El-Chahawi, Process for preparing acetaldehyde diethyl acetal, US5527969 (A), **1996**.

[31] G. S. Nair, E. Adrijanto, A. Alsalme, et al., Glycerol utilization: solvent-free acetalisation over niobia catalysts, *Catalysis Science & Technology*, **2012**, 2, 1173.

[32] H. Yamamoto and K. Ishihara in *Acid Catalysis in Modern Organic Synthesis*, Wiley-VCH, Weinheim, **2007**

[33] B. Wang, Y. Shen, J. Sun, et al., Conversion of platform chemical glycerol to cyclic acetals promoted by acidic ionic liquids, *RSC Advances*, **2014**, 4, 18917.

[34] C.-N. Fan, C.-H. Xu, C.-Q. Liu, et al., Catalytic acetalization of biomass glycerol with acetone over TiO2–SiO2 mixed oxides, *Reaction Kinetics, Mechanisms and Catalysis*, **2012**, 107, 189-202.

[35] M. S. Khayoon and B. H. Hameed, Solventless acetalization of glycerol with acetone to fuel oxygenates over Ni–Zr supported on mesoporous activated carbon catalyst, *Appl. Catal., A*, **2013**, 464-465, 191-199.

[36] H. Serafim, I. M. Fonseca, A. M. Ramos, et al., Valorization of glycerol into fuel additives over zeolites as catalysts, *Chem. Eng. J.*, **2011**, 178, 291-296.

[37] C. Gonzalez-Arellano, R. A. D. Arancon and R. Luque, Al-SBA-15 catalysed cross-esterification and acetalisation of biomass-derived platform chemicals, *Green Chem.*, **2014**, 16, 4985-4993.

[38] R. Pal, T. Sarkar and S. Khasnobis, Amberlyst-15 in organic synthesis, *Arkivoc*, **2012**, 570-609.

[39] http://www.sigmaaldrich.com/catalog/product/aldrich/436712?lang=it&region=IT&cm_sp=Insite-_-prodRecCold_xorders-_-prodRecCold2-1 Amberlyst® 36 (last access 2016/08/19)

[40] A. Behr, J. Eilting, K. Irawadi, et al., Improved utilisation of renewable resources: New important derivatives of glycerol, *Green Chem.*, **2008**, 10, 13-30.

[41] J. S. Clarkson, A. J. Walker and M. A. Wood, Continuous Reactor Technology for Ketal Formation: An Improved Synthesis of Solketal, *Org. Proc. Res. Dev.*, **2001**, 5, 630-635.

[42] M. R. Nanda, Z. Yuan, W. Qin, et al., A new continuous-flow process for catalytic conversion of glycerol to oxygenated fuel additive: Catalyst screening, *Appl. Energy*, **2014**, 123, 75-81.

[43] M. R. Nanda, Z. Yuan, W. Qin, et al., Catalytic conversion of glycerol to oxygenated fuel additive in a continuous flow reactor: Process optimization, *Fuel*, **2014**, 128, 113-119.

[44] J. C. Monbaliu, M. Winter, B. Chevalier, et al., Effective production of the biodiesel additive STBE by a continuous flow process, *Bioresour. Technol.*, **2011**, 102, 9304-9307.

[45] M. Shirani, H. S. Ghaziaskar and C. Xu, Optimization of glycerol ketalization to produce solketal as biodiesel additive in a continuous reactor with subcritical acetone using Purolite® PD206 as catalyst, *Fuel Process. Technol.*, **2014**, 124, 206-211.

[46] G. Eltanany, S. Rüdiger and E. Kemnitz, Supported high surface AlF3: a very strong solid Lewis acid for catalytic applications, *J. Mater. Chem.*, **2008**, 18, 2268.

[47] A. Tressaud in *Functionalized Inorganic Fluorides, Synthesis, Characterization and Properties of Nanostructured Solids*; John Wiley & Sons, **2010**.

[48] S. M. Coman, S. Wuttke, A. Vimont, et al., Catalytic Performance of Nanoscopic, Aluminium Trifluoride-Based Catalysts in the Synthesis of (all-rac)-α-Tocopherol, *Adv. Synth. Catal.*, **2008**, 350, 2517-2524.

[49] G. Busca in *Heterogeneous Catalytic Materials, Sold State Chemistry, Surface Chemistry, and Catalytic Behavior*, Elsevier, The Netherlands, **2014**.

[50] A. Corma and H. García, Lewis Acids: From Conventional Homogeneous to Green Homogeneous and Heterogeneous Catalysis, *Chem. Rev.*, **2003**, 103, 4307-4366.

[51] A. D. Harley and J. Puga, Aluminum trifluoride catalyst for production of diaryl carbonates, EP0516355 (A2), **1992**.

[52] http://www.sigmaaldrich.com/catalog/product/fluka/236098?lang=it&region=IT&cm_sp=Insite-_-prodRecCold_xviews-_-prodRecCold10-2 Aluminum fluoride trihydrate 97% (last access 2016/08/19)

[53] http://www.balcoindia.com/operation/pdf/aluminium-production-process.pdf Aluminium Production Technology (last access 2016/08/19)

[54] www.aluminiumtoday.com Aluminium Fluoride (AlF_3) - A market striving towards equilibrium March/April 2010 (last access 2016/08/19)

[55] S. Guidi, M. Noè, P. Riello, et al., Towards a Rational Design of a Continuous-Flow Method for the Acetalization of Crude Glycerol: Scope and Limitations of Commercial Amberlyst 36 and AlF3·3H2O as Model Catalysts, *Molecules*, **2016**, 21, 657.

[56] M. Selva, S. Guidi, A. Perosa et al., Continuous-flow alkene metathesis: the model reaction of 1-octene catalyzed by Re_2O_7/[gamma]-Al_2O_3 with supercritical CO_2 as a carrier, *Green Chem*.,**2012**, 14, 2727-2737.

[57] M. Selva, S. Guidi and M. Noè, Upgrading of glycerol acetals by thermal catalyst-free transesterification of dialkyl carbonates under continuous-flow conditions, *Green Chem*., **2015**, 17, 1008–1023.

[58] Y. Xiao, G. Xiao and A. Varma, A Universal Procedure for Crude Glycerol Purification from Different Feedstocks in Biodiesel Production: Experimental and Simulation Study, *Ind. Eng. Chem. Res.*, **2013**, 52, 14291-14296.

[59] S. Hu, X. Luo, C. Wan, et al., Characterization of Crude Glycerol from Biodiesel Plants, *J. Agric. Food. Chem.*, **2012**, 60, 5915-5921.

[60] J. C. Thompson and B. B. He, Characterization of crude glycerol from biodiesel production from multiple feedstocks, *Appl. Eng. Agric*, **2006**, 22, 261-265.

[61] When necessary, pumps were set at the lowest pressure (~2 bar) allowing the transfer of the reaction mixture through the catalytic bed. Reactants were forced to flow from bottom to top of the reactor to rule out any gravity-driven pathway.

[62] P. Harriott, Ideal Reactors, in *Chemical Reactor Design*, chap. 3, Marcel Dekker, Inc. New York, USA, **2003**.

[63] In the repeated tests carried out under the same conditions, values of conversion and amount of products (determined by GC analysis) differed by less than 5% from one reaction to another.

[64] G. Vicente, J. A. Melero, G. Morales, et al., Acetalisation of bio-glycerol with acetone to produce solketal over sulfonic mesostructured silicas, *Green Chem.*, **2010**, 12, 899.

[65] M. Estruga, F. Meng, L. Li, et al., Large-scale solution synthesis of α-AlF3·3H2O nanorods under low supersaturation conditions and their conversion to porous β-AlF3 nanorods, *J. Mater. Chem.*, **2012**, 22, 20991.

[66] Similar data (Al and F contents) were not gathered for the reaction of Glyc5 because of analytical interferences of Na+ and Cl- ions present in the reactant mixture.

[67] It should be noted that the assignment of structures of diastereoisomers **2.3a** and **2.3a'** was complicated by a partial overlap of signals in both NMR and GC/MS spectra: this drawback was already reported for the characterization of the same compounds and of other glycerol acetals.

[68] N. Fadnavis, R. Gowrisankar, G. Ramakrishna, et al., Highly Regioselective Preparation of 1,3-Dioxolane-4-methanol Derivatives from Glycerol Using Phosphomolybdic Acid, *Synthesis*, **2009**, 2009, 557-560.

[69] Rietveld refinement is a technique devised for use in the characterisation of crystalline materials. The height, width and position of these reflections can be used to determine many aspects of the material's structure such as the relative amounts.

[70] G. Scholz, S. Brehme, R. König, et al., Crystalline Aluminum Hydroxide Fluorides AlFx(OH)3−x·H2O: Structural Insights from 1H and 2H Solid State NMR and Vibrational Spectroscopy, *The Journal of Physical Chemistry C*, **2010**, 114, 10535-10543.

[71] P. J. Chupas, D. R. Corbin, V. N. M. Rao, et al., A Combined Solid-State NMR and Diffraction Study of the Structures and Acidity of Fluorinated Aluminas: Implications for Catalysis, *The Journal of Physical Chemistry B*, **2003**, 107, 8327-8336.

[72] P. E. Rosenberg, Stability relations of aluminum hydroxy-fluoride hydrate, a ralstonite-like mineral, in the system AlF_3–Al_2O_3–H_2O–HF, *Can. Mineral,* **2006**, 44, 125-134.

[73] T. S. a. D. Association, *glycerine: an overview*, 475 Park Avenue South, New York, **1990**.

[74] Flow rates of reactants were chosen in order to avoid additional co-solvents. Even with such an excess acetone, a homogeneous (Gly/acetone) solution was achieved only at T≥45 °C.

[75] In all CF-runs, measured values of GC-conversion were arithmetically averaged once the conversion itself was stable with time, usually after 1-2 h from the start of the process. Under such conditions, in each test, GC-values of conversion differed less than 3% from one to another.

[76] M. Majewski, D. M. Gleave and P. Nowak, 1,3-Dioxan-5-ones: synthesis, deprotonation, and reactions of their lithium enolates, *Can. J. Chem.*, **1995**, 73, 1616-1626.

[77] H. Watanabe, T. Watanabe, K. Mori, et al., Synthetic study on azadirachtin (part 2). Construction of the decalin moiety with full functionality on B-ring, *Tetrahedron Lett.*, **1997**, 38, 4429-4432.

[78] D. C. Forbes, D. G. Ene and M. P. Doyle, Stereoselective Synthesis of Substituted 5-Hydroxy-1,3-dioxanes, *Synthesis*, **1998**, 1998, 879-882.

[79] G. J. F. Chittenden, Some aspects of the reaction of glycerol with 2,2-dimethoxypropane, *Carbohyd. Res*., **1983**, *121*, 316–323

[80] D. Y. He, Z. J. Li, Z. J. Li, et al., Studies on Carbohydrates X. A New Method for the Preparation of Isopropylidene Saccharides, *Synth. Commun.*, **1992**, 22, 2653-2658.

[81] C. Crotti, E. Farnetti and N. Guidolin, Alternative intermediates for glycerol valorization: iridium-catalyzed formation of acetals and ketals, *Green Chem.*, **2010**, 12, 2225.

[82] L. P. Ozorio, R. Pianzolli, M. B. S. Mota, et al., Reactivity of glycerol/acetone ketal (solketal) and glycerol/formaldehyde acetals toward acid-catalyzed hydrolysis, *Journal of the Brazilian Chemical Society*, **2012**, 23, 931-937.

[83] R. Weingarten, G. A. Tompsett, W. C. Conner, et al., Design of solid acid catalysts for aqueous-phase dehydration of carbohydrates: The role of Lewis and Brønsted acid sites, *J. Catal.*, **2011**, 279, 174-182.

[84] A. Hess and E. Kemnitz, Characterization of Catalytically Active Sites on Aluminum Oxides, Hydroxyfluorides, and Fluorides in Correlation with Their Catalytic Behavior, *J. Catal.*, **1994**, 149, 449-457.

[85] L. c. Francke, E. Durand, A. Demourgues, et al., Synthesis and characterization of Al3+, Cr3+, Fe3+ and Ga3+ hydroxyfluorides: correlations between structural features, thermal stability and acidic properties, *J. Mater. Chem.*, **2003**, 13, 2330.

[86] A. L. Choi, G. Sun, Y. Zhang, et al., Developmental fluoride neurotoxicity: a systematic review and meta-analysis, *Environ. Health Perspect.*, **2012**, 120, 1362-1368.

[87] http://water.epa.gov/drink/contaminants/ National Primary Drinking Water Regulations, available online (last access: 2016/01/15).

[88] I. Murwani, K. Scheurell and E. Kemnitz, Liquid phase oxidation of ethylbenzene on pure and metal doped HS-AlF3, *Catal. Commun.*, **2008**, 10, 227-231.

[89] Y. Kuwahara, K. Maki, Y. Matsumura, et al., Hydrophobic Modification of a Mesoporous Silica Surface Using a Fluorine-Containing Silylation Agent and Its Application as an Advantageous Host Material for the TiO2 Photocatalyst, *The Journal of Physical Chemistry C*, **2009**, 113, 1552-1559.

[90] F. Yang, M. A. Hanna and R. Sun, Value-added uses for crude glycerol--a byproduct of biodiesel production, *Biotechnol Biofuels*, **2012**, 5, 1-10.

[91] I. Agirre, I. García, J. Requies, et al., Glycerol acetals, kinetic study of the reaction between glycerol and formaldehyde, *Biomass Bioenergy*, **2011**, 35, 3636-3642.

[92] P. H. Silva, V. L. Goncalves and C. J. Mota, Glycerol acetals as anti-freezing additives for biodiesel, *Bioresour. Technol.*, **2010**, 101, 6225-6229.

[93] S. Chandrasekhar, Product stability in kinetically-controlled organic reactions, *Chem. Soc. Rev.*, **1987**, 16, 313.

[94] G. Aksnes, P. Albriktsen and P. Juvvik, Studies of Cyclic Acetal and Ketal Isomers of Glycerol, *Acta Chem. Scand.*, **1965**, *19*, 920–930.

[95] C. Piantadosi, C. E. Anderson, E. A. Brecht, et al., The Preparation of Cyclic Glycerol Acetals by Transacetalation1, *J. Am. Chem. Soc.*, **1958**, 80, 6613-6617.

[96] J. S. Câmara, J. C. Marques, A. Alves, et al., Heterocyclic acetals in Madeira wines, *Analytical and Bioanalytical Chemistry*, **2003**, 375, 1221-1224.

[97] It should be noted that the assignment of structures of diastereoisomers **2.3a** and **2.3a'** was complicated by a partial overlap of signals in both NMR and GC/MS spectra: this drawback was already reported for the characterization of the same compounds and of other glycerol acetals

3 GLYCEROL: SYNTHESIS OF N-HETEROCYCLES

3.1 Introduction

3.1.1 Quinoline and its derivatives

Part of this Thesis work has been dedicated to the use of glycerol for the synthesis of N-heterocycles of which quinoline (Qui) was the most investigated one. Qui is a colorless, high-boiling, weak aromatic base (pK_a=9.5) whose major use as such is in the manufacture of nicotinic acid (NA). NA serves as an active agent for both the prevention of pellagra in humans,[1] and as a starting substrate for the synthesis of 8-hydroxyquinoline, this being a versatile chelating agent and a precursor to a range of pharmacologically active products.[2]

However, the Qui nucleus occurs in several natural compounds (cinchona alkaloids) and drugs including antimalarial, anti-bacterial, antifungal, anthelmintic, cardiotonic, anticonvulsant, anti-inflammatory, and analgesic products. Figure 3.1 shows a few model derivatives.[3]

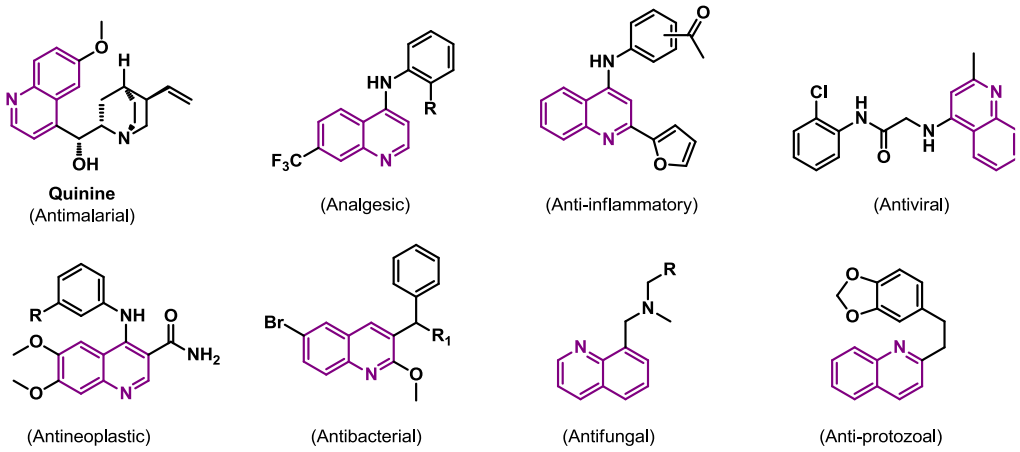

Figure 3.1. Examples of pharmaceutical active compounds including the quinoline ring system

Quinoline derivatives find also applications in the manufacturing of a wide range of dyes[4,5] and food colorants,[6] of which cyanine represents the oldest example. (Figure 3.2).

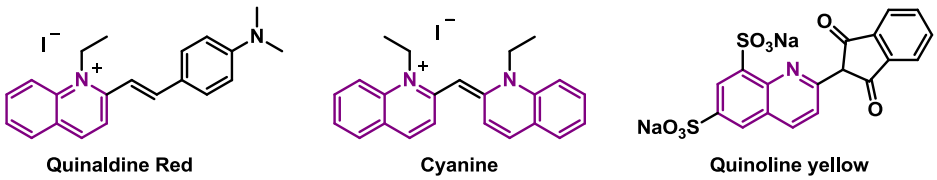

Figure 3.2. Example of quinoline dyes

Quinoline derivatives are also used as ligands in organometalic complexes for catalysts preparation and for various fluorescent applications.[7,8,9]

Notwithstanding its nontoxicity on oral absorption and inhalation by humans, Qui is reported as an environmental pollutant mostly associated with facilities processing oil shale or coal (the contaminant effect comes from the relatively high hydrosolubility of Qui that facilitates its transfer through different environmental compartments). In fact, one of the principal sources of commercial Qui is coal-tar from which the heterocyclic compound as such was first isolated in 1834. Also, crude oil, particularly the virgin diesel fraction, contains minor amounts of Qui and some of its derivatives. A hydrodenitrification process is usually carried out to remove such compound since they reduce the quality of the fuel.

Qui can be prepared in several different ways, including for example:[10] i) the distillation of cinchoninic acid with lime; ii) the reduction of ortho-aminocinnamic aldehyde;[11] iii) the high temperature reaction of allyl aniline over lead oxide; iv) the condensation of ortho-aminobenzaldehyde with acetaldehyde in the presence of aq. NaOH;[12] and v) the reaction of orthotoluidine with glyoxal.

However, the Qui core is most often synthesized from aniline by using well-known reactions, some of them dating back to more than two centuries ago. These are: i) the Combes and Conrad-Limpach synthesis in which aniline (or anilines) is set to react with β-diketones and β-ketoesters; ii) the Doebner or the Doebner-Miller reaction of aniline with aldehyde and pyruvic acid or α,β-unsaturated carbonyl compounds, respectively; v) the Gould-Jacobs reaction of aniline and ethyl ethoxymethylenemalonate, and vi) the Skraup synthesis in which aniline and glycerol produce Qui in the presence of nitrobenzene and sulfuric acid (Scheme 3.1).[13,14,15,16]

A number of procedures have also been devised to build up quinoline or quinoline-like structures through the so-called Camps, Friedländer, Knorr, Niementowski, Pfitzinger and Povarov syntheses. These methods are usually very effective, but they often require

specifically substituted anilines and corrosive and harmful reagents which generate large amounts of wastes.

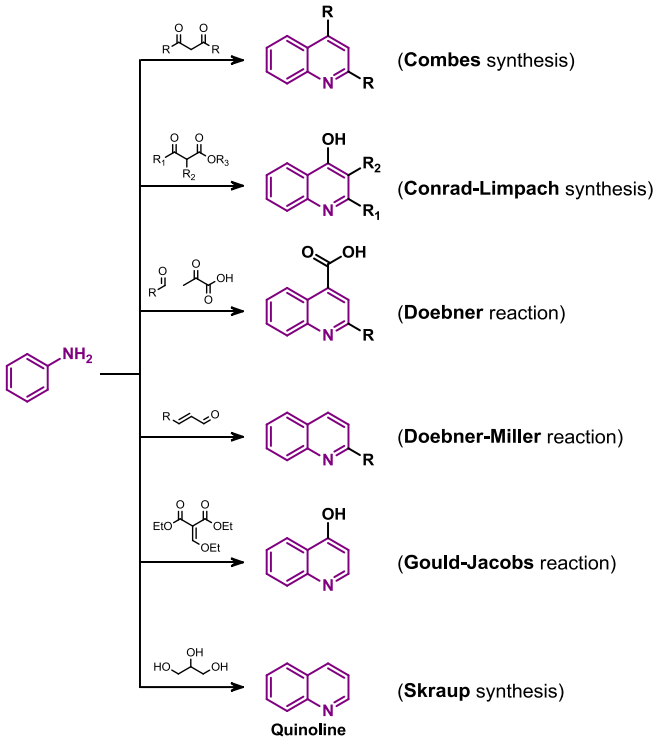

Scheme 3.1. Some of the most common synthesis of quinoline and its derivatives

With the double aim of inventing eco-friendly synthesis of Qui and innovative catalytic reactions of glycerol, part of this Thesis work has been focused on a modified Skraup synthesis.

3.1.1.1 The Skraup synthesis

The Skraup reaction brings the name of Zdenko Hans Skraup,[17] a Czech scientist who first discovered that Qui could be obtained by the condensation of glycerol and aniline in the presence of concentrated H_2SO_4 and an oxidizing agent. The latter compound was initially arsenic acid (As_2O_5), but this was later replaced by nitrobenzene which not only allowed a better control of the process, but it also acted as a solvent.

Although the mechanism of the Skraup condensation has not been yet completely clarified, there are good reasons to believe that the first step of the reaction is an acid-promoted dehydration of glycerol to form acrolein as an intermediate (Scheme 3.2).[18] Several works suggest that Brønsted acids allow the protonation of the secondary hydroxyl group of glycerol; then, the release of a water molecule produces a secondary carbocation

which rapidly loses a proton, thereby forming 3-hydroxypropanal. This compound is unstable and it further dehydrates into acrolein.[19]

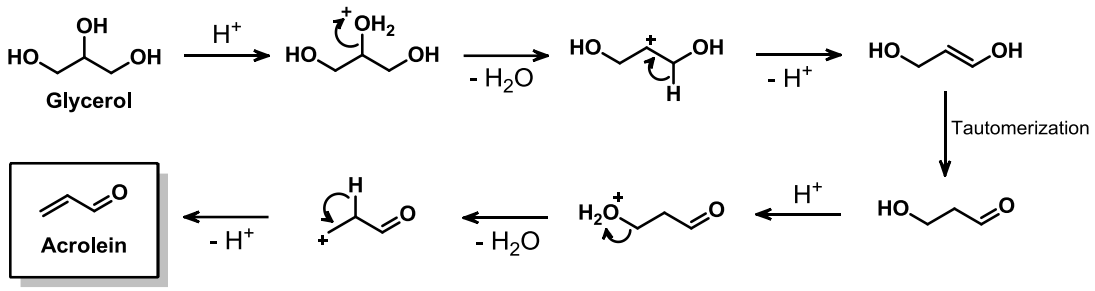

Scheme 3.2. Acid catalyzed dehydration of glycerol to acrolein

In the second step of the process, an acid catalyzed condensation of acrolein with aniline produces 1,2,3,4-tetrahydroquinolin-4-ol. The latter undergoes two subsequent reactions of dehydration and oxidation (the mechanism of which is rather unclear) ending up in the formation of Qui (Scheme 3.3).[16]

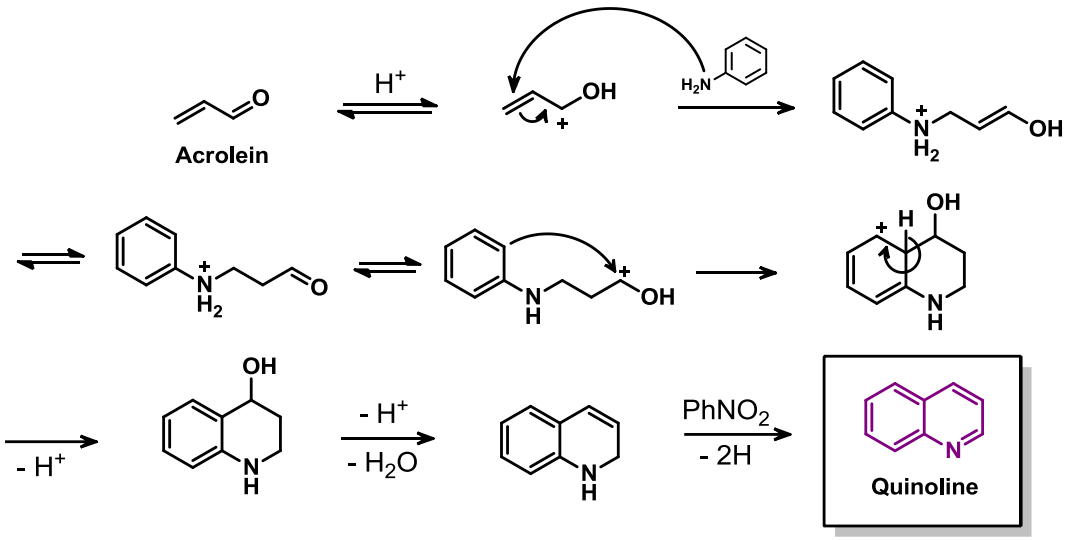

Scheme 3.3. A mechanism for the acid catalyzed condensation of acrolein with aniline in the Skraup reaction

Notwithstanding the catalytic role of the acid, the conventional Skraup condensation requires large amounts of concentrated H_2SO_4. Moreover, harsh operating conditions must be used including temperatures as high as 230 °C, which may result in mixtures of products with moderate yields of Qui.[16,20]

These aspects represent an obvious limitation to the exploitation and scale up of the process, especially for the implementation of the reaction under continuous-flow conditions where the acid corrosion of the plant can be a further serious issue. A completely different

approach must be considered starting from the choice of a strong acidic heterogeneous catalyst. This must be not only able to promote the two key steps of the Skraup reaction (Scheme 3.2 and Scheme 3.3), but it should also be cheap and chemically-mechanically stable in the CF-mode.

Based on these considerations, a literature survey has been carried out in this work to examine solid acids able to effectively catalyze at least the first of the two desired reactions, *i.e.* the dehydration of glycerol to acrolein (Scheme 3.2):[18,21] among the available systems including zeolites,[22,23] heteropolyacids,[19,24,25] and metal oxides[26,27] the attention was focused on niobium oxides,[28,29,30,31,32] particularly on niobium phosphate.

3.1.2 Niobium phosphate

Niobium exhibits formal oxidation states from +5 to -1, being +5 the most stable one. In this state, Niobium(V) oxide (niobic acid, Nb_2O_5) is a representative compound. It is a white, air-stable and water insoluble solid obtained as a precipitate with an indeterminate water content when water-soluble complexes of the metal are hydrolyzed or when a solution of niobate is acidified.[33] Hydrated niobic acid has a high acid strength (H_o from -5.6 to -8.2).[34] It possesses both Lewis acid sites and Brønsted acid sites on its surface,[35] whose relative amount (Lewis *vs* Brønsted sites) can be modified by thermal pretreatments of the solid. This surface acidity however, is greatly decreased if niobic acid is heated over 500-600 °C. At this temperature, a phase transformation of amorphous $Nb_2O_5{\cdot}nH_2O$ to T-T phase Nb_2O_5 occurs, as observed by DTA and XRD.[35,36]

Nb_2O_5 is known as an effective solid acid catalyst for reactions in which water molecules participate or are liberated:[37,38] remarkable examples include recently reported dehydration reactions of bio-based chemicals such as xylose,[39] fructose,[40] cellulose.[41] Though, it has been discovered that Niobium phosphate ($NbOPO_4$: NbP) obtained by the reaction of niobic acid or niobium(V) chloride with H_3PO_4, is even a more active and stable system than Nb_2O_5, because NbP is able to retain its surface acidity even when treated at high temperatures.[42,43,44,45] As was mentioned above, the known activity of NbP to catalyze the dehydration of glycerol to acrolein prompted us to consider the application of this solid acid for the continuous flow investigation of the Skraup synthesis.

3.2 Results

The CF investigation of the Skraup synthesis was carried out in the laboratories of the Clean Technologies Group at The University of Nottingham (UK). The experimental apparatus used was similar to that described in the previous chapter (see chapter 2). It was composed of two twin HPLC pumps for the separate delivery of liquid reactants, a static mixer, a reactor (**Ra**) and a BPR. The mixer and the reactor were wrapped in aluminum blocks heated by electric cartridges. All tests were carried out by filling up the reactor with Niobium phosphate ($NbOPO_4$: NbP, 1.2 g) as the catalyst. NbP was used as received without any prior treatment. An in-line GC/FID was placed between the reactor and the BPR, and used to automatically sample and analyze the reaction mixture. The latter was controlled by a MathLab software (further details in the experimental paragraph).

3.2.1 Choice of the solvent and starting materials

Catalytic tests with NbP were initially performed by using equimolar aqueous solutions (0.275 M) of both glycerol and aniline as the two reactants. It should be considered that while glycerol was completely miscible in water, the solubility of aniline was limited to a maximum of ~0.4 M.[46] However, water was chosen not only for its intrinsic eco-friendly character, but also for the good tolerance of niobium oxides to the aqueous medium.[40,47]

The Skraup reaction was investigated under a wide range of conditions by varying the temperature and the pressure from 200 to 300 °C and 1 to 100 bar. Though, at a complete conversion, a mixture of products (most of them were not identified) was observed in which the desired quinoline (**3.1a**) was achieved in a very moderate GC-yield, never exceeding 10%. It is well-known that aniline easily reacts with polar protic compounds such as light alcohols: accordingly, the poor selectivity observed in the Skraup CF-tests was ascribed to undesired side-reactions of aniline with the aqueous medium.

The rather unsatisfactory results of initial tests prompted us to consider the replacement of water with an organic apolar medium such as toluene. However, although toluene was completely inert toward aniline, it could not act as a solvent for glycerol. This apparent drawback was overcome by using cyclic acetals, particularly solketal as a synthon for glycerol. The investigation was then continued by exploring the CF reaction of solketal and aniline in the presence of NbP as a catalyst. Under acid conditions, it was plausible that

solketal underwent a rapid ring opening reaction (deacetalization) and therefore a Skraup reaction could eventually occur.

3.2.2 Effects of the temperature and the flow rate

Four sets of experiments were carried out isothermally at 225, 250 and 275 °C at 100 bar with a constant reagent ratio Q=1 (solketal/aniline). Two equimolar solutions of solketal and aniline in toluene (0.275 M) were separately delivered to the reactor at a flow rate of 0.1 mL/min each. CF-reactions were monitored for 24 hours. The results are reported in Figure 3.3 in which the profiles of aniline conversion and selectivity towards Qui are shown.

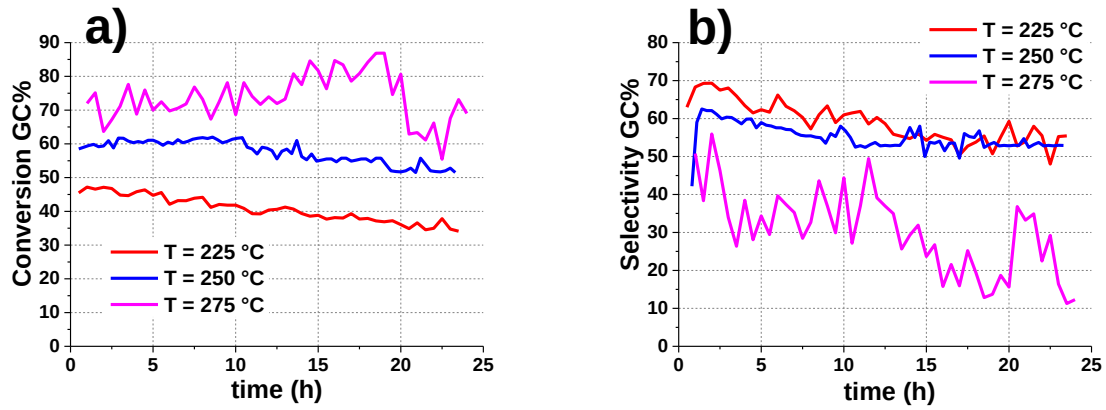

Figure 3.3. a) Aniline conversion and **b)** quinoline selectivity of three sets of experiments with the mixer and reactor heated at 225, 250 and 275 °C. Other conditions: flow rate = 0.1 mL/min for both solution of solketal and aniline in toluene (0.275M each); p = 100 bar; catalyst (NbP) loading = 1.2 g

The first significant observation was that the Skraup reaction took place since Qui was noticed as the major reaction product. This notwithstanding the use of solketal in place of glycerol (Scheme 3.4). Tests showed that an increase of the conversion from ~40% up to ~80% could be reached by progressively enhancing the temperature from 225 °C to 275 °C (Scheme 3.3a). The selectivity however, followed a different trend. It increased up to maximum value of 55-60% at 250 °C; afterwards, it dropped to 20-30% at 275 °C due to the onset of several side-reactions leading to unknown products. This trend was confirmed by two additional experiments (not shown here) carried at a lower and a higher temperature: in particular, at 200 and 300 °C, the reaction proceeded with a conversion of ~20 % and ~85%, and a Qui selectivity of ~8% and ~10%, respectively.

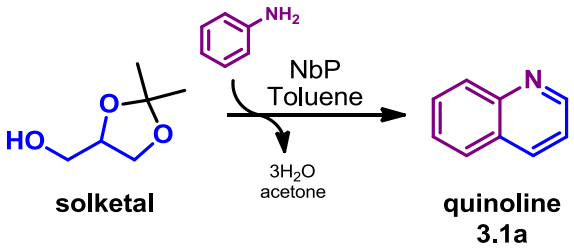

Scheme 3.4. Quinoline from the CF reaction of solketal and aniline over NbP

The best compromise in term of conversion and selectivity was clearly achieved at 250 °C. Under such conditions, being the other parameters unchanged, two further tests were run by either decreasing or increasing the reactants flow rate at 0.05 and 0.2 mL/min, respectively. Figure 3.4 a) and b) show the results. For a convenient comparison, Figure 3.4 also reports the profile achieved at a flow rate of 0.1 mL/min (black curve, same of Figure 3.3).

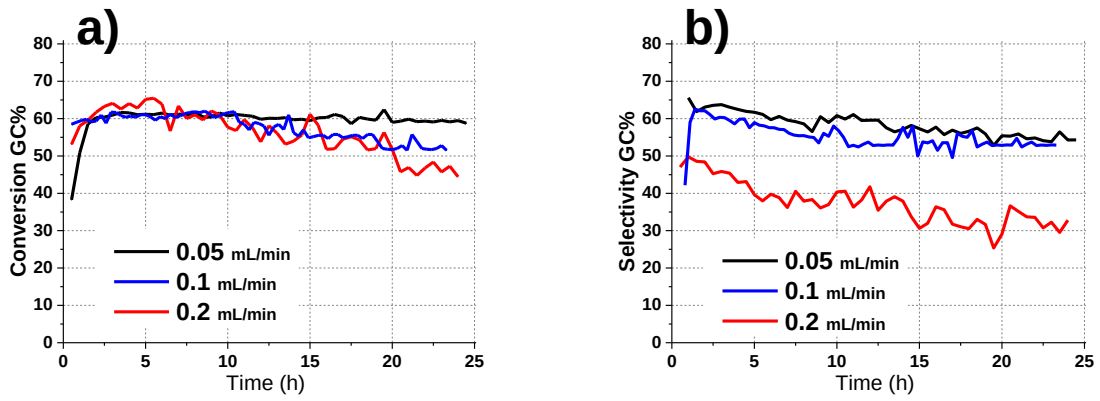

Figure 3.4. a) aniline conversion and **b)** quinoline selectivity of three sets of experiments with the mixer and reactor heated at 250 °C. Other conditions: flow rates were set at 0.05, 0.1 and 0.2 mL/min for both the solutions of solketal and aniline in toluene (0.275 M); p = 100 bar; catalyst (NbP) loading = 1.2 g

Tests proved that the flow rate had a minor effect, if any, on the conversion of aniline. This remained substantially steady at 55-60% for the first 10-15 h of reaction (Figure 3.4a). Then, if the experiments were prolonged, the higher flow rate (0.2 mL/min) brought about a decrease of the conversion to 45%: this was noticed starting from 20 hours on (red profile).

The selectivity towards Qui (~55%) was also not affected by the flow rate when this was set in the range of 0.05-0.1 mL/min; though, as for the conversion, the selectivity decreased (30-40 %) at 0.2 mL/min (Figure 3.4b).

Overall, results were consistent with the mechanism shown in Scheme 3.5. The acidity of the catalyst (NbP) plausibly promoted a first step of deprotection of the ketal by which

glycerol (and acetone) formed. Such a reaction was triggered by the amount of water present in the catalyst. Then, the dehydration of glycerol to acrolein occurred according to the mechanism known for niobium oxides.[21,26,28] Finally, the reaction of acrolein with aniline produced the desired Qui through the chemistry described for the Skraup reaction in Scheme 3.3.

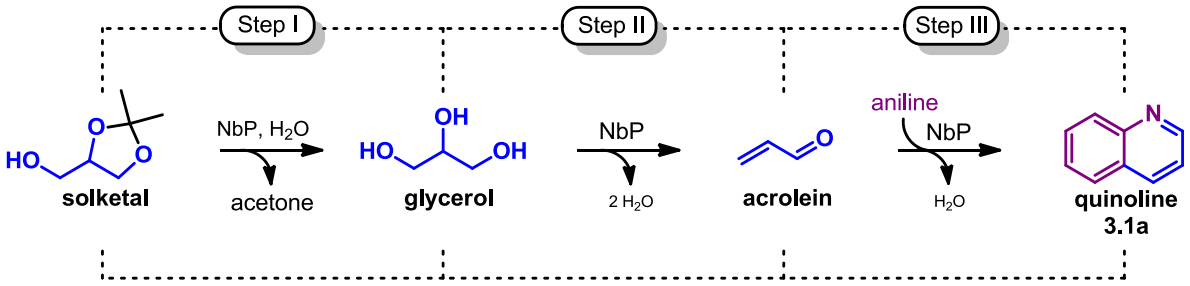

Scheme 3.5. The mechanism proposed for the continuous-flow synthesis of quinoline (**3.1a**) from aniline and solketal over niobium phosphate

The CF-tests of Figure 3.3 and Figure 3.4 also indicated the formation of several by-products. One of these, *i.e.* 3-methyl-1*H*-indole, was observed in a sizeable quantity (up to 25%, (Figure 3.5), while other derivatives did not exceed 3% amount each in all the final reaction mixtures.

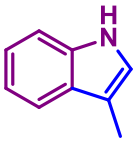

3-methyl-1*H*-indole
3.1b

Figure 3.5. Major by-product of the reaction of solketal and aniline over NbP

Acetone released by the hydrolysis of solketal (Scheme 3.5, step 1) was plausibly responsible for the presence of compound **3.1b**. Therefore, an additional test was run under the same conditions of Figure 3.3 (250 °C) by replacing the solution of solketal with a 0.275 M solution of acetone in toluene. The experiment showed the formation of two products (in a total amount <8 %), the structure of which was assigned after isolation and characterization by MS and NMR analyses (Scheme 3.6).

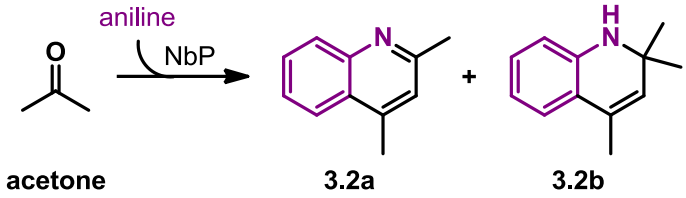

Scheme 3.6. Products observed from the CF reaction of acetone and aniline over NbP

None of these compounds corresponded to 3-methyl-1*H*-indole, thereby negating the hypothesis that such product (**3.1b**) derived from the reaction of acetone and aniline. Curiously, the same reaction (acetone+aniline) was reported to produce product **3.2b** over zeolite catalysts;[48] though, neither **3.2a** nor **3.2b** were observed (not even in traces) during the tests of Figure 3.3 and Figure 3.4 in the presence of NbP. Further considerations on the mechanism for the formation of 3-methyl-1*H*-indole are reported later on this chapter (see discussion section).

3.2.3 Effects of reagents concentration and pressure

Four sets of experiments were carried out under the above described conditions (250 °C, 100 bar, flow rate of 0.1 mL/min for both aniline and solketal solutions), but by varying the reagents concentration. In particular, from 0.275 to 0.55 M for aniline, and from 0.275 to 0.825 M for solketal. The results are reported in Figure 3.6 a) and b) which show the profiles of aniline conversion and selectivity towards Qui obtained in the different reactions.

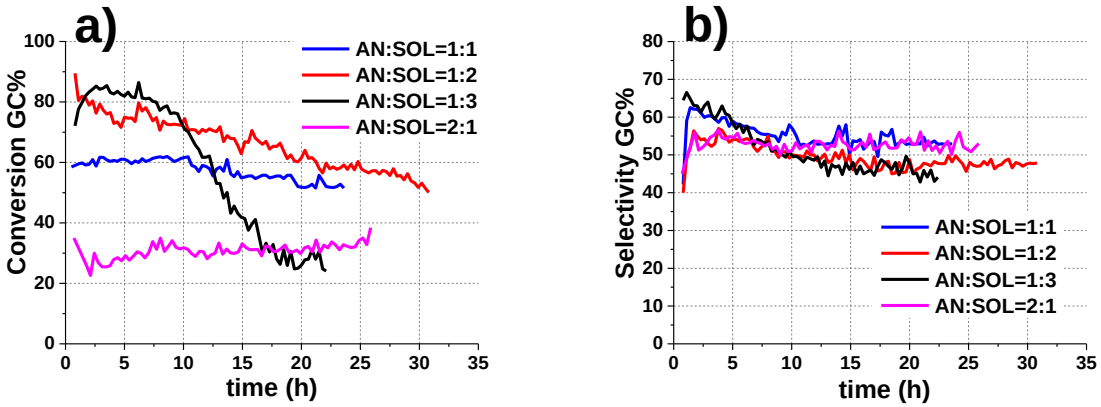

Figure 3.6. a) aniline conversion and **b)** quinoline selectivity of four sets of experiments carried out at 250 °C, 100 bar, and at a flow rate of 0.1 mL/min for both aniline and solketal solutions. Reagents concentration was: 0.275 M for aniline and Solketal (**blue**); 0.275 M for aniline and 0.55 M for Solketal (**red**); 0.275 M for aniline and 0.825 M for Solketal (**black**); 0.55 M for aniline and 0.275 M for Solketal (**pink**). The catalyst (NbP) loading was 1.2 g.

In the first ten hours of the reaction, the increase of the solketal concentration led to an enhancement of the conversion from ~60% to ~80% (Figure 3.6a: compare blue to red and black profiles). However, if the test was prolonged up to 24 hours, the higher the solketal excess (with respect to aniline), the faster the deactivation of the catalyst. This was particularly manifest when aniline and Solketal were used in a 1:3 molar ratio. After 17 h, the conversion dropped to ~25 % (Figure 3.6a: black profile). By contrast, the selectivity toward Qui remained substantially steady at ~50% regardless of the relative concentration of reagents (Figure 3.6b).

To investigate the effect of the pressure, additional tests were carried out at 250 °C by using aniline and solketal in a 1:3 molar ratio. Solutions of both reactants were delivered at a flow rate of 0.1 mL/min, while p was varied from ambient pressure to 50 bar. The results are reported in Figure 3.7 which show the profiles of aniline conversion and selectivity towards Qui obtained in the different reactions (the black profile is the same of Figure 3.6).

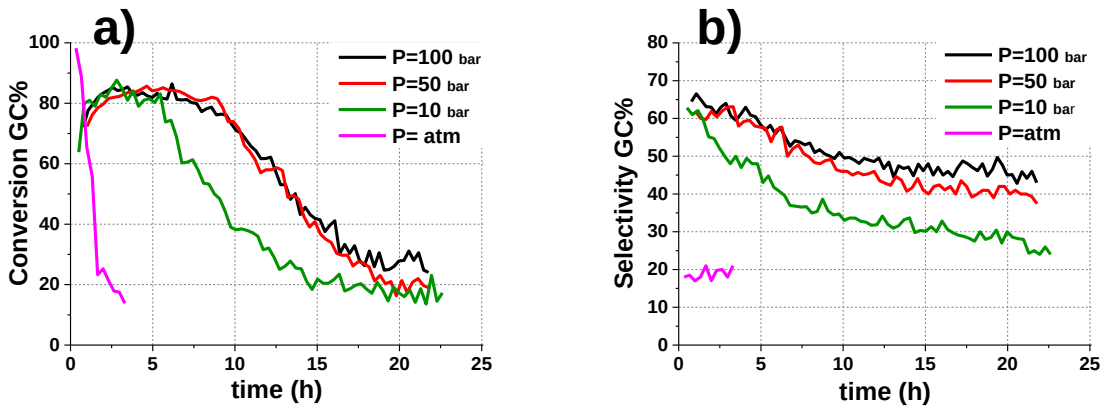

Figure 3.7. a) aniline conversion and **b)** quinoline selectivity of four sets of experiments at 250 °C. Solutions of solketal (0.825 M) and aniline (0.275 M) in toluene were both pumped at a flow rate of 0.1 mL/min. Pressure was set to ambient, and at 10, 50, and 100 bar, respectively. The catalyst (NbP) loading was 1.2 g.

In the range of 50-100 bar, the conversion profiles almost perfectly overlapped to each other. However, if the pressure was decreased, the conversion of aniline decreased as well. This effect was particularly pronounced for the test carried out at ambient pressure, where the conversion dropped below 20% after only 2.5 hours. Of note, providing that a pressure of at least 10 bar was applied, the conversion stabilized to ~20% after 20 hours of reaction (Figure 3.7 a). By contrast, a Qui selectivity of ~50% was achieved only if the operating pressure was ≥50 bar (black and red profiles); below this value, the selectivity rapidly dropped to less than 30% (green and pink profiles).

3.2.4 The scale-up of the reaction

The scale-up of the reaction was investigated by using a CF-system similar to that previously described with the only variation on the reactor setup. This reactor (**Rb**) was composed by three steel tubes (20 cm, Ø=1/4") connected in series to each other (see experimental section for further details). The total volumetric capacity was of ~4.5 mL and the total catalyst (NbP) loading 3.6 g. Experiments were run under the same condition of those in Figure 3.3 (250 °C, 100 bar) by using equimolar solutions of both reactants at flow rates of 0.1 and 0.3 mL/min. The results are shown in Figure 3.8 where the profiles of conversion of aniline and selectivity towards Qui are indicated. For a more convenient comparison, the Figure also reports the results of Figure 3.3 (blue profile).

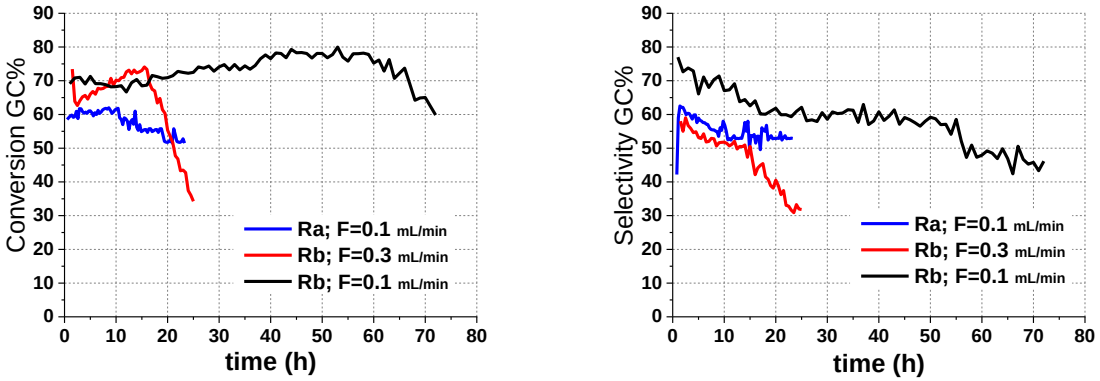

Figure 3.8. a) aniline conversion and **b)** quinoline selectivity at 250 and 100 bar. A 0.275 M solketal and 0.275M aniline solutions were used. Reactor **Rb** with NbP load = 3.6 g.

The use of a high capacity CF-reactor improved the reaction outcome if the operating flow rate was set to 0.1 mL/min: a conversion as high as 70-80% was steadily reached for 65 hours with only a moderate decrease to 60% after 72 h (black profile: Figure 3.8a). Under such conditions, the product distribution also took advantage: the Qui selectivity stabilized at ~60% for up to 50 hours with a progressive decrease to 45% after 72 h. (black profile: Figure 3.8b).

By contrast, poor results were gathered when the flow rate was set at 0.3 mL/min. The catalyst was rapidly deactivated at the level that both conversion and selectivity did not exceed 35% after only 25 hours (red profiles in Figure 3.8).

3.2.5 The scope of the reaction

The CF-protocol investigated for aniline was extended to two different primary aromatic amines including an electron rich- and a bifunctional- substrate such as 4-mehoxyaniline and 4,4'-methylenedianiline (MDA), respectively. The reactions were run under the same conditions of Figure 3.3. Due to the limited solubility of MDA in toluene, acetone (10% v/v) was added as a co-solvent. Scheme 3.7 shows the structure of major products.

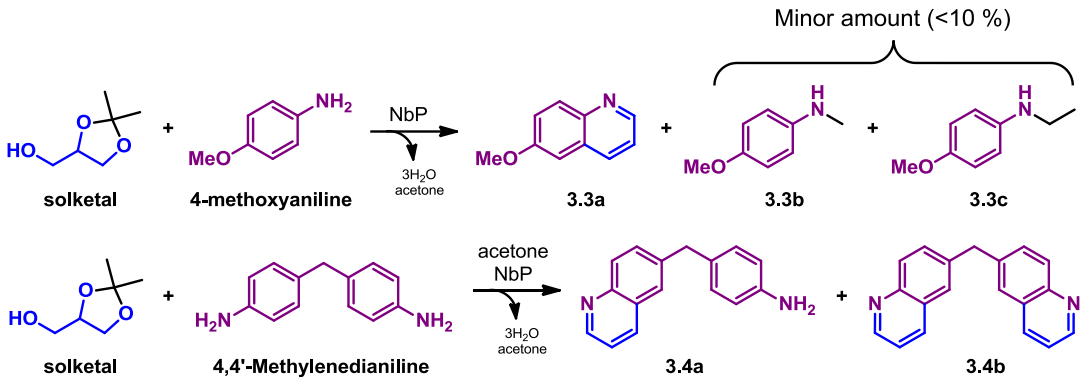

Scheme 3.7. Products observed from the CF reaction of 4-mehoxyaniline and 4,4'-methylenedianiline with solketal over NbP.

In both cases, the expected quinoline derivatives were the most abundant compounds. Although conditions were not optimized, once the CF-reaction of 4-methoxyaniline with solketal was allowed to proceed for 24 h, 6-methoxy quinoline **3.3a** was obtained in a GC-yield of 30%. Two main by-products were **3.3b** and **3.3c** in a total amount <15%. All these compounds were isolated and characterized by MS and NMR analyses (further details in the experimental section).

The reaction of MDA with glycerol was rather sluggish at 250 °C: after 2.5 h, a conversion of only 57% was reached. Therefore, being the other conditions unaltered, a higher temperature of 300 °C was used. This allowed to obtain both the mono- and di-substituted quinolines **3.4a** and **3.4b**, respectively. The corresponding GC-yields were 20 and 12 % after a CF-reaction carried out for 6 hours. The two products were never previously reported: they were isolated and characterized by MS and NMR analyses (further details in the experimental section). Also, a crystal of compound **3.4a** was obtained and the structure was confirmed by crystallographic analysis (Figure 3.9).

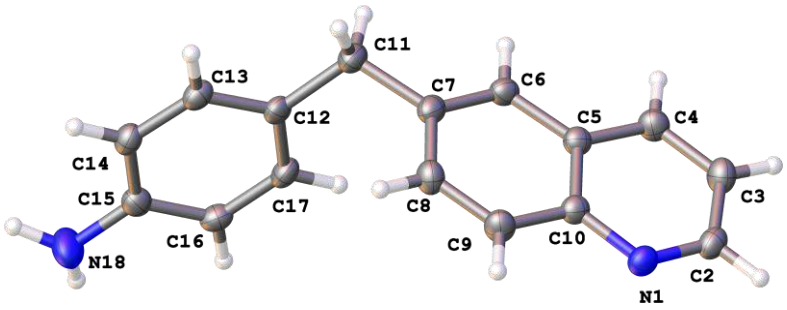

Figure 3.9. Crystallographic structure of compound **3.4a**

3.3 Discussion

The here described investigation offers a starting point for the development of an alternative route to the known Skraup reaction.[17] Particularly, the use of a heterogeneous acid catalyst such as NbP (in place of conc.d H_2SO_4) and CF conditions represent the most remarkable achievements of this study. By contrast, aspects that still require to be improved are the use of: i) toluene. Although this is considered an acceptable solvent,[49,50] it is not only an extra component (with respect to the conventional Skraup reaction), but it must be used in a relevant amount; ii) solketal as starting material in place of glycerol. Of course, the protocol would be more attractive through the straightforward use of glycerol, thereby avoiding protection (acetalization) reactions.

3.3.1 The reaction and the catalyst

Although the glycerol dehydration over niobium oxides is a known process,[28,29,32] the reaction between acrolein and aniline has never been reported in the presence of this type of catalysts. There are several examples of catalytic systems able to promote this reaction (Doebner-Miller, Scheme 3.1) such as HCl,[51,52] silver oxides[53] and even basic catalysts.[54] The literature however, offers very few cases of one-pot batch synthesis of quinoline compounds, able to start directly from glycerol and using catalysts different from sulphuric acid. One example is the microwave-assisted synthesis of Qui by the reaction of 1-(1-alkylsulfonic)-3-methylimidazolium chloride ionic liquid.[55] Also, some mixed oxides based on Al_2O_3 have been described to catalyze the synthesis of Qui from glycerol.[56]

To the best of our knowledge, only two CF procedures report the formation of Qui from the reaction of glycerol and aniline. However, in both processes, Qui is observed as a minor product. The first CF-method makes use of a Cu/Cr catalyst supported over Al_2O_3 and doped with alkali earth elements:[57] this system produces 3-methyl-1*H*-indole in a 65% yield, while

Qui is detected in low amounts from 0.7 to 10.6%. The second protocol is based on a microwave-assisted CF-reaction catalyzed by diluted H_2SO_4.[58] Under these conditions, notwithstanding the complex apparatus used, the maximum conversion of aniline and yield of Qui are 5.3 and 4%, respectively.

The present study demonstrates the feasibility of CF-protocol for a Skraup-like synthesis in which NbP and solketal (rather than glycerol) are used for the first time as a catalyst and a reagent. Under the best found conditions, the conversion of aniline and the selectivity towards Qui do not exceed 80% and 60%, respectively, which means that there might be still room for improvement. It should however be considered that the overall reaction occurs through three subsequent catalytic steps (Scheme 3.5). If one examines the critical step of dehydration of glycerol (step II), available data indicate that the reaction over NbP or mesoporous siliconiobium phosphate as catalysts proceeds with conversion and selectivity from 68 to 100% and from 70 to 75%, respectively.[29,30,32]. It is therefore predictable that once the dehydration of glycerol is coupled to the other two catalytic steps of Scheme 3.5, *i.e.* the ketal deprotection and the condensation of acrolein with aniline, the result can only bring about a further decrement of the overall yield.

Another issue of the CF-dehydration of glycerol to acrolein is the fast deactivation of the catalyst, this aspect being one of the major drawback of the process. The literature reports that the acid strength of the most selective catalysts for such a reaction is between $-8.2 \leq H_0 \leq -3.0$.[21,59] Those systems having very strong acid sites ($H_0 \leq -8.2$) which include also niobium oxides, may offer a low reaction selectivity (40-50%) due to the onset of side reactions of polymerization of acrolein and coke deposition processes.[60] A significant breakthrough for practical applications in this field would require to overcome this problem. Various approaches have been proposed to limit the deactivation of dehydration catalysts.[21] These include the suppression of the rate of coking by adding O_2 or H_2 to the feed flow[19,61,62,63] and the modification of the catalysts with promoters able to change the acid properties.[24] Such methods however, have not been altogether successful and clearly additional improvements are needed. In the particular case of the dehydration of glycerol catalyzed by NbP, a fast deactivation of the catalyst has been reported after 8-10 h of time on stream.[29] Compared to the results obtained in this work, the deactivation of NbP is manifest also from Figure 3.4a (red profile) and even a more pronounced effect is shown in Figure 3.6a (black profile). It should be noted how the extent of the phenomenon is closely related to the amount of solketal (and thus, of glycerol) used in the reaction. The more

solketal is delivered to the reactor, the more acrolein is formed and consequently, the larger the coke deposition over the catalyst active phase. However, it is also clear that the catalyst shows a relatively slow rate of deactivation since conversion and selectivity are rather stable up to 24 hours (or even 50 hours if a large catalyst loading is used; Figure 3.8). This behavior can be plausibly explained by the fact that, as soon as acrolein is formed *in situ*, it is consumed through the reaction with aniline (step III, Scheme 3.5). Accordingly, only a modest concentration of acrolein may be available for polymerization side-reactions or coke formation at the catalyst surface.

3.3.2 The formation of 3-methyl-1*H*-indole as a by-product

As mentioned above, one of the major side-products of the investigated reaction of solketal with aniline is 3-methyl-1*H*-indole. The formation of this derivative might be explained by the presence of both Brønsted and Lewis acid sites on the niobium phosphate catalyst.[33,64,65]

It has been reported that catalysts bearing both Brønsted and Lewis acid sites may promote two different dehydration pathways of glycerol: Brønsted sites are responsible for the conversion of glycerol to acrolein, while Lewis sites account for the formation of hydroxyacetone.[66,67,68] Scheme 3.8 shows a mechanism proposed for the occurrence of hydroxyacetone over La_2CuO_4 as a catalyst.[66]

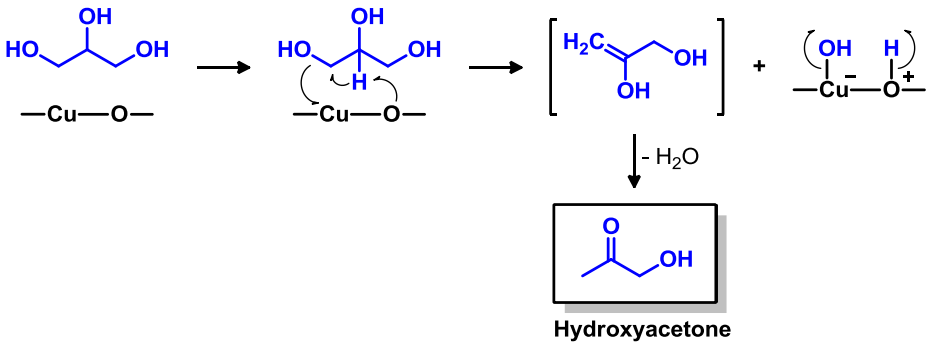

Scheme 3.8. Proposed mechanism for the formation of hydroxyacetone from glycerol over La_2CuO_4

A concerted reaction between copper (as a Lewis acid) and an oxygen ion allows the removal of water from a primary OH group of glycerol, yielding an unstable enol intermediate, which undergoes a rapid tautomerization to hydroxyacetone.

Once formed, hydroxyacetone may react with aniline to produce 3-methyl-1*H*-indole.[57] A hypothesis to describe this reaction has been proposed by Shi and co-workers who

investigated the reaction of glycerol and aniline over zeolites-supported Cu-based catalysts (Scheme 3.9).[69]

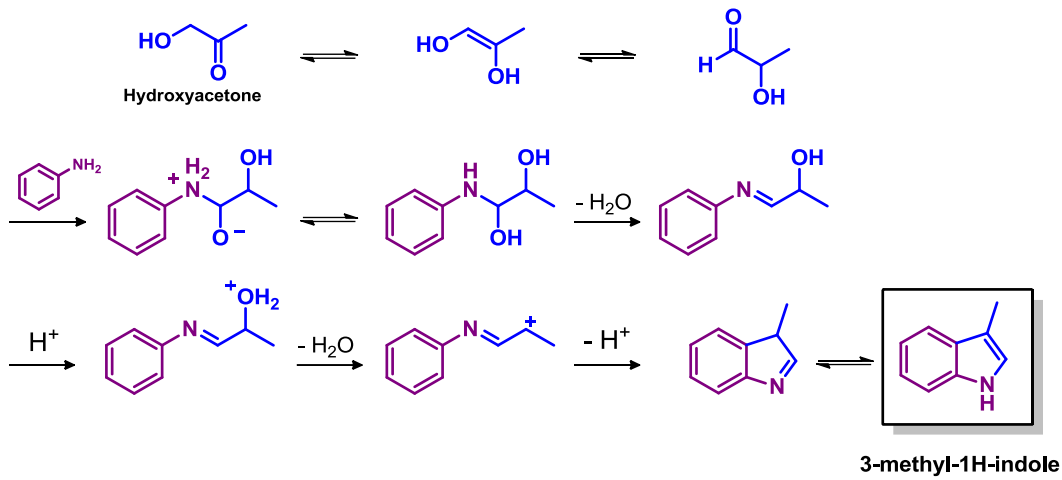

Scheme 3.9. The reaction of hydroxyacetone with aniline over zeolites-supported Cu-based catalysts

Once glycerol is converted to hydroxyacetone, the latter is transformed to 2-hydroxy-1-propanal via keto-enol tautomerism. The aldehyde undergoes a condensation with aniline to form a α-hydroxyimine intermediate. Then, the loss of a second molecule of water generates a secondary carbocation able to trigger a ring closing reaction which provides the final indol derivative. The presence of Cu-based weak acid sites is believed to favor the cleavage of C-O bonds during the subsequent dehydration processes.

Mechanisms similar to those depicted in Scheme 3.8 and Scheme 3.9 plausibly operate also on niobium phosphate in which Nb cations are the Lewis acid sites able to originate first hydroxyacetone and then, 3-methyl-1*H*-indole (Scheme 3.10, bottom). This preliminary hypothesis must be confirmed by further studies.

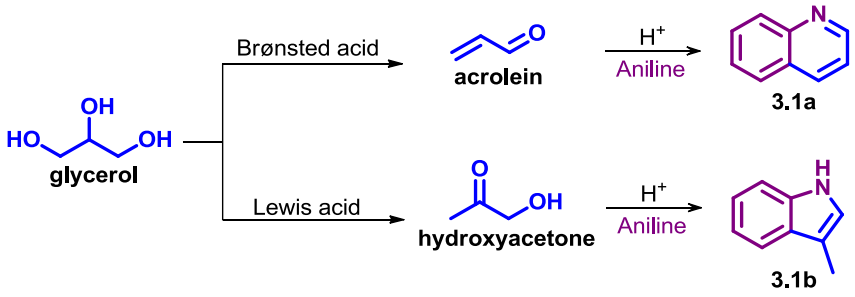

Scheme 3.10. Effect of the nature of the acid site on the reaction selectivity

3.3.3 Different anilines

NbP is an active catalyst not only for the Skraup-like condensation of solketal with aniline, but also for the reaction of other electron rich primary aromatic amines such as 4-methoxyaniline and 4,4'-methylenedianiline (MDA). Although the experimental conditions probably need a case-by-case optimization, the investigation proves the concept by demonstrating the general scope of the CF-procedure.

Particularly, the reaction of MDA is the more interesting case since it allows the access to a mono- and a bis-quinoline derivative (compounds **3.4a** and **3.4b**, respectively). It should be noted that the literature offers only one example of a reaction of MDA with glycerol catalyzed by concentrated H_2SO_4;[70] though, being concentrated sulfuric acid a far more reactive catalyst than NbP, only the bis-quinoline product **3.4b** has was achieved. By contrast, not only an unprecedented synthesis of compound **3.4a**, but also its crystallographic characterization have been demonstrated in this work. Compound **3.4b** was also isolated, but no crystals could be obtained.

3.4 Conclusions

The here described procedure represents one of the few examples of CF-synthesis of Qui, and, to the best of our knowledge, it is the only procedure which reports the use of a heterogeneous catalyst. Niobium phosphate (NbP) as solid acid has been investigated. Although the implementation of the reaction in aqueous solution would appear as the most convenient approach, catalytic tests have demonstrated that the combined used of a hydrocarbon (aprotic apolar) solvent such as toluene, and a protected form of glycerol such solketal as a starting reagent, offers a satisfactory practical solution to reach conversion and selectivity up to ~60%. If one considers that the overall process is comprised of 3 different catalytic steps, the overall performance of NbP is more than acceptable at this stage. Another interesting aspect is the outstanding on-stream life of the catalyst. With respect to the crucial step of dehydration of glycerol to acrolein, it is known that NbP is rapidly deactivated in few (8-10) hours due to coke deposition. However, in the investigated Skraup-like condensation, NbP may operate for up to 24 hours (or even 50 hours if a large catalyst loading is used) without any loss of its performance. It is reasonable that the co-reactant aniline limits the formation of acrolein (and coke) by trapping glycerol in the desired process of synthesis of Qui.

The proposed CF-protocol has proven suitable to other anilines such as 4-methoxy aniline and MDA, the latter (MDA) allowing the preparation of a never previously reported compound (**3.4a**).

3.5 **Experimental**

3.5.1 Materials

Acetone, aniline, cyclohexane, ethyl acetate, glycerol, methanol, 4-methoxyaniline, 4,4'-methylenedianiline (MDA), 1,2-Isopropylideneglycerol (Solketal), and toluene were ACS grade. They were all purchased from Aldrich and used as received without further purification. Water was of MilliQ grade. Carbon dioxide was obtained from BOC Gases (Food grade) and used as received. Sand was also from Aldrich and used as such. Niobium Phosphate ($NbOPO_4$, NbP) was supplied by Companhia Brasileira de Metalurgia e Mineração (CBMM) and used as received.

3.5.2 Analysis instruments

GC/FID analysis were run on a Shimadzu GC/FID-2014 spectrometer using an Restek Rtx-1 capillary column (L=30 m, Ø=0.32 mm, film=0.25 μm). The following conditions were used. Carrier gas: N_2; flow rate: 5.0 mL/min; split ratio: 1:10; initial T: 50 °C (3 min), ramp rate: 15 °C/min; final T: 240 °C (10 min).

^{1}H and ^{13}C NMR analyses were recorded on 300, 400 and 500 MHz Bruker units. Chemical shift were reported in δ values downfield from TMS and $CDCl_3$ was used as solvent.

Mass analysis were run on a Bruker MicroTOF with positive ionization mode.

X-ray analyses were collected at 120 K with a monochromatic wavelength of 1.54184.

3.5.3 CF apparatus

The apparatus used for the investigation was assembled in-house (Figure 3.10). Stainless steel pipes (Ø=1/16'') with appropriate Swagelok fittings were used to connect all the parts. Two Jasco PU-980 HPLC pumps (**P1** and **P2**) were used to deliver the reactant's solutions (**reactant 1:** glycerol or solketal, and **reactant 2:** aniline) to two stainless steel tubular chambers (20 cm, Ø=1/4", inner volume=1.46 cm^3) placed in the upright position.

The first (**Mixer**) was filled with sand and the second (**Reactor, Ra**) filled with NbP (1.2 g). Two aluminum blocks, both equipped with heating cartridges (controlled by Eurotherm 2616 heaters), were used to heat the **Mixer** and the **Reactor** at the desired temperature which was monitored by a Picologger. A temperature trip (Eurotherm 2122) was introduced in the system to prevent overheating. After the **Reactor**, the mixture was real-time analyzed by a GC/FID (**in-line GC/FID**). The pressure was controlled by a Jasco BP-1580-81 back pressure regulator (**BPR**). The system pressure was monitored by a pressure sensor placed before the **Mixer**. Pressure, temperature and pumps flow rates were all monitored and controlled by a Mathlab program. A **CO_2** cylynder was connect between the pumps and the **Mixer**.

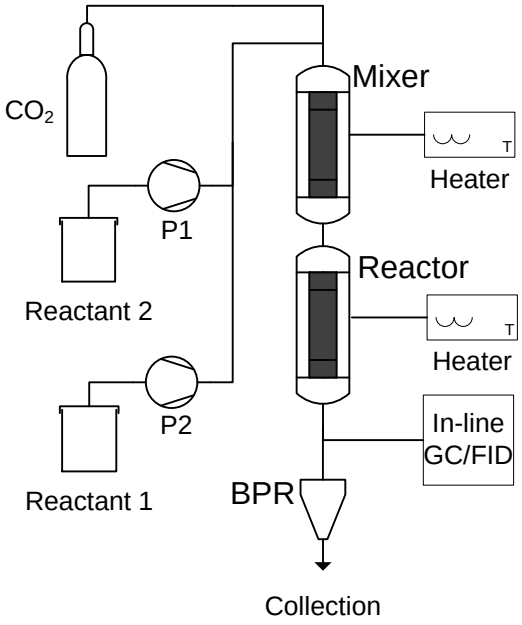

Figure 3.10. Experimental setup used for the CF anilines aromatization over NbP

The scale-up of the reaction was investigated by adopting a different configuration. The mixer and the reactor were replaced by a 4 in-line tubular chambers as shown in Figure 3.11. The first chamber was filled with sand (**Mixer**) and the 3 remaining tubes with 3.6 g (3 x 1.2 g) of NbP (**Reactor**, **Rb**). A single aluminum block, with four heating cartridges, was used to heat the multiple reactor.

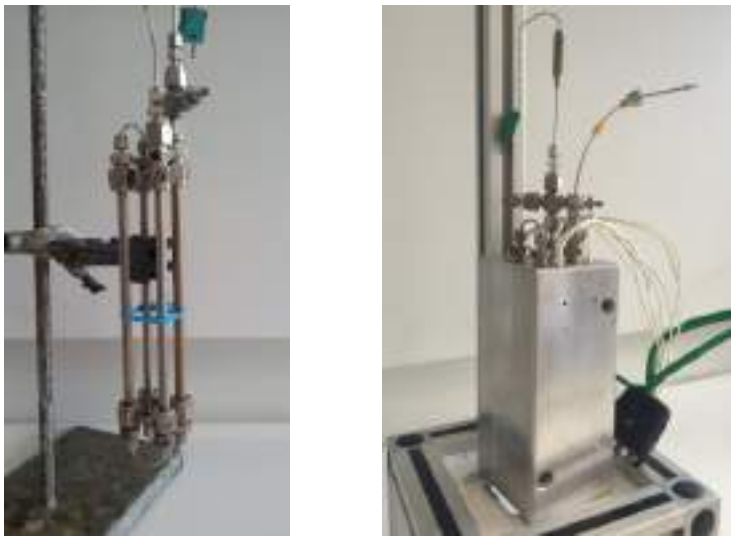

Figure 3.11. Scale-up mixer and reactor setup

3.5.4 General procedure for the CF-synthesis of N-heterocycles

Preliminary procedures. The substrates (aniline or solketal or glycerol or acetone) solutions were prepared by using toluene or water as solvent at these following concentration: 0.275, 0.550 and 0.825 M. The **Mixer** was filled with sand and the **Reactor** (**Ra**) with 1.2 g of NbP. Prior to the reaction, a leak detection was performed by filling the system with 100 bar of CO_2 and checking all the fitting with a liquid leak detector.

Reaction procedure. A preliminary conditioning of the apparatus was carried out by delivering the two reactants solutions to the system at flow rates in the range 0.05-0.2 mL/min for a minimum of 5 minutes. Afterwards, the **BPR** was set to the operating pressure (from atmospheric to 100 bar). When the pressure was stabilized, both the **Mixer** and the **Reactor** (**Ra**) were heated at the working temperature (225-300 °C). Then, the reaction mixture was analyzed by the in-line GC/FID at regular intervals (usually every 30 min) for 24-72 h.

System shutdown and cleaning. Once the experiment was complete, the aluminum blocks were set to cool down at r.t. while pure methanol (50 ml at 0.5 mL/min) was delivered to the system. Afterwards, CO_2 was pumped to flush the methanol away. The system was then vented to the atmospheric pressure and the reactor emptied.

3.5.5 Isolation and characterization of products

Quinoline (3.1a)

The reaction was carried out accordingly to the general procedure above described: two 0.275 M solutions of aniline and solketal in toluene, were allowed to react at 0.1 mL/min over 1.2 g of NbP at 250 °C and 100 bar for 1 hours (Figure 3.3). The mixture sampled out of the reactor was rotary evaporated (45 °C, 40 mbar, 30 min) and vacuumed in a schlenk line (r.t., 3h). The brown oily residue was purified by FCC (cyclohexane:ethylacetate 85:15 v/v) and charachterized by NMR and mass analyses.

^{1}H NMR (400 MHz, $CDCl_3$) δ 8.92 (dd, J = 4.2, 1.7 Hz, 1H), 8.19 – 8.09 (m, 2H), 7.85 – 7.80 (m, 1H), 7.72 (ddd, J = 8.5, 6.9, 1.5 Hz, 1H), 7.55 (ddd, J = 8.1, 6.9, 1.2 Hz, 1H), 7.40 (dd, J = 8.3, 4.2 Hz, 1H). ^{13}C NMR (100 MHz, $CDCl_3$) δ 150.53, 148.40, 136.22, 129.60, 129.58, 128.43, 127.92, 126.68, 121.21. Mass (Most Intense MS Peaks) *m/z*: 158.0968 (51.0), 144.0808 (31.0), 131.0683 (10.6), 130.0653 (100.0).

3-Methyl-1H-indole (3.1b)

The reaction was carried out accordingly to the general procedure above described: two 0.275 M solutions of aniline and solketal in toluene, were allowed to react at 0.1 mL/min over 1.2 g of NbP at 250 °C and 100 bar for 1 hours (Figure 3.3). The mixture sampled out of the reactor was rotary evaporated (45 °C, 40 mbar, 30 min) and vacuumed in a schlenk line (r.t., 3h). The oily residue was purified by FCC (cyclohexane:ethylacetate 80:20 v/v) and charachterized by NMR and mass analyses.

^{1}H NMR (500 MHz, $CDCl_3$) δ 7.59 (dd, J = 7.8, 1.1 Hz, 1H), 7.35 (dd, J = 8.0, 0.9 Hz, 1H), 7.19 (ddd, J = 8.2, 7.0, 1.3 Hz, 1H), 7.12 (ddd, J = 7.9, 7.0, 1.0 Hz, 1H), 6.97 (dd, J = 2.3, 1.2 Hz, 1H), 2.34 (d, J = 1.1 Hz, 3H). ^{13}C NMR (125 MHz, $CDCl_3$) δ 136.39, 128.41, 121.98, 121.68, 119.23, 118.95, 111.86, 111.06, 9.80. Mass (Most Intense MS Peaks) *m/z*: 289.1683 (10.2) 263.1535 (13.3), 190.1229 (12.3), 158.0967 (58), 146.0963 (24.7), 144.0809 (48.9), 131.0687 (11.0), 130.0654 (100.0).

6-Methoxyquinoline (3.3a)

The reaction was carried out accordingly to the general procedure above described: two 0.275 M solutions of aniline and solketal in toluene, were allowed to react at 0.1 mL/min over 1.2 g of NbP at 250 °C and 100 bar for 1 hours (Scheme 3.7). The mixture sampled out of the reactor was rotary evaporated (45 °C, 40 mbar, 30 min) and vacuumed in a schlenk line (r.t., 3h). The oily residue was purified by FCC with gradient solutions of cyclohexane:ethylacetate from 85:15 to 50:50 v/v) and charachterized by NMR and mass analyses.

^{1}H NMR (300 MHz, $CDCl_3$) δ 8.78 (dd, J = 4.3, 1.7 Hz, 1H), 8.12 – 8.07 (m, 1H), 8.07 – 8.02 (m, 1H), 7.43 – 7.36 (m, 2H), 7.09 (d, J = 2.8 Hz, 1H), 3.95 (s, 3H). ^{13}C NMR (75 MHz, $CDCl^3$) δ 157.95, 147.72, 144.15, 135.25, 130.68, 129.48, 122.63, 121.49, 105.24, 55.68. Mass (Most Intense MS Peaks) *m/z*: 161.0789 (11.2), 160.0766 (100.0).

4-Methoxy-N-methylaniline (3.3b)

The reaction was carried out accordingly to the general procedure above described: two 0.275 M solutions of aniline and solketal in toluene, were allowed to react at 0.1 mL/min over 1.2 g of NbP at 250 °C and 100 bar for 1 hours (Scheme 3.7). The mixture sampled out of the reactor was rotary evaporated (45 °C, 40 mbar, 30 min) and vacuumed in a schlenk line (r.t., 3h). The oily residue was purified by FCC with gradient solutions of cyclohexane:ethylacetate from 85:15 to 50:50 v/v) and charachterized by NMR and mass analyses.

^{1}H NMR (300 MHz, $CDCl_3$) δ 6.84 – 6.78 (m, 2H), 6.69 – 6.62 (m, 2H), 3.76 (s, 3H), 2.82 (s, 3H). ^{13}C NMR (75 MHz, $CDCl_3$) δ 152.7, 142.9, 115.1, 114.4, 55.98, 32.2. Mass (Most Intense MS Peaks) *m/z*: 301.1545 (25.2), 188.1068 (11.3), 160.0756 (18.3), 138.0919 (100.0), 123.0679 (20.5).

N-Ethyl-4-methoxyaniline (3.3c)

The reaction was carried out accordingly to the general procedure above described: two 0.275 M solutions of aniline and solketal in toluene, were allowed to react at 0.1 mL/min over 1.2 g of NbP at 250 °C and 100 bar for 1 hours (Scheme 3.7). The mixture sampled out of the reactor was rotary evaporated (45 °C, 40 mbar, 30 min) and vacuumed in a schlenk line (r.t., 3h). The oily residue was purified by FCC with gradient solutions of cyclohexane:ethylacetate from 85:15 to 50:50 v/v) and charachterized by NMR and mass analyses.

^{1}H NMR (300 MHz, $CDCl_3$) δ 6.82 – 6.75 (m, 2H), 6.62 – 6.55 (m, 2H), 3.75 (s, 3H), 3.11 (q, J = 7.1 Hz, 2H), 1.24 (t, J = 7.1 Hz, 3H). ^{13}C NMR (75 MHz, $CDCl_3$) δ 152.19, 142.91, 115.04, 114.25, 55.98, 39.60, 15.16. Mass (Most Intense MS Peaks) *m/z*: 323.1751 (11.4), 301.1554 (17.2), 153.1104 (10.), 152.1077 (100.0), 123.0680 (15.5).

4-(Quinolin-6-ylmethyl)aniline (3.4a)

The reaction was carried out accordingly to the general procedure above described: two 0.275 M solutions of aniline and solketal in toluene, were allowed to react at 0.1 mL/min

over 1.2 g of NbP at 250 °C and 100 bar for 1 hours (Scheme 3.7). The mixture sampled out of the reactor was rotary evaporated (45 °C, 40 mbar, 30 min) and vacuumed in a schlenk line (r.t., 3h). The oily residue was purified by FCC with gradient solutions of cyclohexane:ethylacetate from 80:20 to 30:70 v/v) and charachterized by NMR and mass analyses.

^{1}H NMR (400 MHz, $CDCl_3$) δ 8.85 (dd, J = 4.3, 1.7 Hz, 1H), 8.07 (dd, J = 8.3, 1.8, 1H), 8.01 (d, J = 9.2, 1H), 7.58 – 7.54 (m, 2H), 7.36 (dd, J = 8.3, 4.2 Hz, 1H), 7.02 (d, J = 8.3 Hz, 2H), 6.67 – 6.63 (m, 2H), 4.06 (s, 2H). ^{13}C NMR (100 MHz, $CDCl_3$) δ 149.9, 147.3, 144.9, 140.7, 135.9, 131.4, 130.6, 130.1, 129.5, 128.5, 126.6, 121.2, 115.5, 41.2. Mass (Most Intense MS Peaks) *m/z*: 236.1273 (18.8), 235.1245 (100.0).

di(Quinolin-6-yl)methane (3.4b)

The reaction was carried out accordingly to the general procedure above described: two 0.275 M solutions of aniline and solketal in toluene, were allowed to react at 0.1 mL/min over 1.2 g of NbP at 250 °C and 100 bar for 1 hours (Scheme 3.7). The mixture sampled out of the reactor was rotary evaporated (45 °C, 40 mbar, 30 min) and vacuumed in a schlenk line (r.t., 3h). The oily residue was purified by FCC with gradient solutions of cyclohexane:ethylacetate from 80:20 to 30:70 v/v) and charachterized by NMR and mass analyses.

^{1}H NMR (300 MHz, $CDCl_3$) δ 8.91 (dd, J = 4.3, 1.7 Hz, 2H), 8.09 (m, 4H), 7.70 – 7.57 (m, 4H), 7.41 (dd, J = 8.3, 4.2 Hz, 2H), 4.39 (s, 2H). ^{13}C NMR (100 MHz, $CDCl_3$) δ 150.1, 147.3, 138.9, 135.7, 131.2, 129.8, 128.4, 127.1, 121.3, 41.8. Mass (Most Intense MS Peaks) *m/z*: 277.1343 (24.0), 272.1270 (19.9), 271.1245 (100.0), 139.0734 (15.4).

2,4-Dimethylquinoline (3.2a).

The reaction was carried out accordingly to the general procedure above described: two 0.275 M solutions of aniline and acetone in toluene, were allowed to react at 0.1 mL/min over 1.2 g of NbP at 250 °C and 100 bar for 1 hours (Scheme 3.6). The mixture sampled out of the reactor was rotary evaporated (45 °C, 40 mbar, 30 min) and vacuumed in a schlenk line (r.t., 3h). The oily residue was purified by FCC (cyclohexane:ethylacetate 50:50 v/v) and charachterized by NMR and mass analyses.

^{1}H NMR (500 MHz, $CDCl_3$) δ 8.02 (d, J = 8.5, 1H), 7.95 (dd, J = 8.3, 1.4 Hz, 1H), 7.67 (ddd, J = 8.4, 6.8, 1.4 Hz, 1H), 7.50 (ddd, J = 8.2, 6.9, 1.3 Hz, 1H), 7.14 (d, J = 1.1 Hz, 1H), 2.70 (s, 3H), 2.67 (d, 3H). ^{13}C NMR (126 MHz, CDCl3) δ 158.80 , 147.84 , 144.32 , 129.28 , 129.24 , 126.70

, 125.55 , 123.72 , 122.86 , 25.38 , 18.74. Mass (Most Intense MS Peaks) *m/z*: 266.1900 (10.7), 172.1123 (53.1), 159.0992 (12.9), 158.0961 (100.0).

2,2,4-Trimethyl-1,2-dihydroquinoline (3.2b)

The reaction was carried out accordingly to the general procedure above described: two 0.275 M solutions of aniline and acetone in toluene, were allowed to react at 0.1 mL/min over 1.2 g of NbP at 250 °C and 100 bar for 1 hours (Scheme 3.6). The mixture sampled out of the reactor was rotary evaporated (45 °C, 40 mbar, 30 min) and vacuumed in a schlenk line (r.t., 3h). The oily residue was purified by FCC (cyclohexane:ethylacetate 50:50 v/v) and charachterized by NMR and mass analyses.

^{1}H NMR (500 MHz, $CDCl_3$) δ 7.07 (dd, J = 7.6, 1.5 Hz, 1H), 6.99 (td, J = 7.6, 1.5 Hz, 1H), 6.67 (td, J = 7.5, 1.3 Hz, 1H), 6.53 – 6.49 (d, 1H), 5.32 (d, J = 1.5 Hz, 1H), 1.99 (d, J = 1.4 Hz, 3H), 1.30 (s, 6H). ^{13}C NMR (125 MHz, $CDCl_3$) δ 142.63 , 128.75 , 128.53 , 128.49 , 123.78 , 122.06 , 117.89 , 113.58 , 52.17 , 30.82 , 18.71. Mass (Most Intense MS Peaks) *m/z*: 278.1801 (15.0), 214.1602 (16.7), 175.1316 (13.6), 174.1287 (100.0), 172.1126 (12.3), 158.0962 (15.9).

3.6 **Bibliography**

[1] http://www.webmd.com/drugs/2/drug-6142/nicotinic-acid-oral/details Nicotinic Acid - Uses (last access: 2016/09/04)

[2] Y. n. Song, H. Xu, W. Chen, et al., 8-Hydroxyquinoline: a privileged structure with a broad-ranging pharmacological potential, *Med. Chem. Commun.*, **2015**, 6, 61-74.

[3] A. Marella, O. P. Tanwar, R. Saha, et al., Quinoline: A versatile heterocyclic, *Saudi Pharm J*, **2013**, 21, 1-12.

[4] I. Pyszka and Z. Kucybała, Quinolineimidazopyridinium derivatives as visible-light photoinitiators of free radical polymerization, *Polymer*, **2007**, 48, 959-965.

[5] http://www.lumiprobe.com/tech/cyanine-dyes Cyanine dyes (last access: 2016/09/04)

[6] http://www.food.gov.uk/science/additives/enumberlist Current EU approved additives and their E Numbers (last access: 2016/09/04)

[7] A. B. Pradhan, S. K. Mandal, S. Banerjee, et al., A highly selective fluorescent sensor for zinc ion based on quinoline platform with potential applications for cell imaging studies, *Polyhedron*, **2015**, 94, 75-82.

[8] B. Machura, M. Wolff, E. Benoist, et al., Oxorhenium(V) complexes of quinoline and isoquinoline carboxylic acids--synthesis, structural characterization and catalytic application in epoxidation reactions, *Dalton Trans*, **2013**, 42, 8827-8837.

[9] D. Sarkar, A. Pramanik, S. Jana, et al., Quinoline based reversible fluorescent 'turn-on' chemosensor for the selective detection of Zn2+: Application in living cell imaging and as INHIBIT logic gate, *Sensors and Actuators B: Chemical*, **2015**, 209, 138-146.

[10] https://www.studylight.org/encyclopedias/bri/view.cgi?n=27200 Encyclopedia Britannica – Quinoline (last access: 2016/09/04)

[11] A. Baeyer and V. Drewsen, Einwirkung von Orthonitrobenzaldehyd auf Aldehyd, *Berichte der deutschen chemischen Gesellschaft*, **1883**, 16, 2205-2208.

[12] P. Friedlaender, Ueber o-Amidobenzaldehyd, *Berichte der deutschen chemischen Gesellschaft*, **1882**, 15, 2572-2575.

[13] R. H. Manske, The Chemistry of Quinolines, *Chem. Rev*, **1942**, 30, 113-144.

[14] https://en.wikipedia.org/wiki/Quinoline Quinoline (last access: 2016/09/04)

[15] S. M. Prajapati, K. D. Patel, R. H. Vekariya, et al., Recent advances in the synthesis of quinolines: a review, *RSC Advances*, **2014**, 4, 24463.

[16] Z. Wang, Skraup Reaction in *Comprehensive Organic Name Reactions and Reagents*, John Wiley & Sons, Inc., **2010**.

[17] Z. H. Skraup, Eine Synthese des Chinolins, *Monatsh. Chem.*, **1880**, 1, 316-318.

[18] A. Talebian-Kiakalaieh, N. A. S. Amin and H. Hezaveh, Glycerol for renewable acrolein production by catalytic dehydration, *Renew. Sust. Energ. Rev.*, **2014**, 40, 28-59.

[19] A. Alhanash, E. F. Kozhevnikova and I. V. Kozhevnikov, Gas-phase dehydration of glycerol to acrolein catalysed by caesium heteropoly salt, *Appl. Catal., A*, **2010**, 378, 11-18.

[20] G. Jones, Synthesis of the Quinoline Ring System in *Quinolines*, Wiley, New York, **1977**.

[21] B. Katryniok, S. Paul, V. Bellière-Baca, et al., Glycerol dehydration to acrolein in the context of new uses of glycerol, *Green Chem.*, **2010**, 12, 2079.

[22] C.-J. Jia, Y. Liu, W. Schmidt, et al., Small-sized HZSM-5 zeolite as highly active catalyst for gas phase dehydration of glycerol to acrolein, *J. Catal.*, **2010**, 269, 71-79.

[23] K. Pathak, K. M. Reddy, N. N. Bakhshi, et al., Catalytic conversion of glycerol to value added liquid products, *Appl. Catal., A*, **2010**, 372, 224-238.

[24] B. Katryniok, S. Paul, M. Capron, et al., A long-life catalyst for glycerol dehydration to acrolein, *Green Chem.*, **2010**, 12, 1922.

[25] E. Tsukuda, S. Sato, R. Takahashi, et al., Production of acrolein from glycerol over silica-supported heteropoly acids, *Catal. Commun.*, **2007**, 8, 1349-1353.

[26] P. Lauriol-Garbay, J. M. M. Millet, S. Loridant, et al., New efficient and long-life catalyst for gas-phase glycerol dehydration to acrolein, *J. Catal.*, **2011**, 280, 68-76.

[27] L.-Z. Tao, S.-H. Chai, Y. Zuo, et al., Sustainable production of acrolein: Acidic binary metal oxide catalysts for gas-phase dehydration of glycerol, *Catal. Today*, **2010**, 158, 310-316.

[28] N. R. Shiju, D. R. Brown, K. Wilson, et al., Glycerol Valorization: Dehydration to Acrolein Over Silica-Supported Niobia Catalysts, *Top. Catal.*, **2010**, 53, 1217-1223.

[29] Y. Choi, D. S. Park, H. J. Yun, et al., Mesoporous siliconiobium phosphate as a pure Bronsted acid catalyst with excellent performance for the dehydration of glycerol to acrolein, *ChemSusChem*, **2012**, 5, 2460-2468.

[30] L. C. A. Oliveira, M. F. Portilho, A. C. Silva, et al., Modified niobia as a bifunctional catalyst for simultaneous dehydration and oxidation of glycerol, *Applied Catalysis B: Environmental*, **2012**, 117-118, 29-35.

[31] G. S. Foo, D. Wei, D. S. Sholl, et al., Role of Lewis and Brønsted Acid Sites in the Dehydration of Glycerol over Niobia, *ACS Catalysis*, **2014**, 4, 3180-3192.

[32] Y. Y. Lee, K. A. Lee, N. C. Park, et al., The effect of PO4 to Nb2O5 catalyst on the dehydration of glycerol, *Catal. Today*, **2014**, 232, 114-118.

[33] I. Nowak and M. Ziolek, Niobium Compounds: Preparation, characterization, and Application in Heterogeneous Catalysis, *Chem. Rev.*, **1999**, 99, 3603-3624.

[34] The Hammett acidity function (H_0) is a measure of acidity used for very concentrated solutions of strong acids, including superacids. It is the best-known acidity function used to extend the measure of Brønsted–Lowry acidity beyond the dilute aqueous solutions for which the pH scale is useful.

[35] I. Tokio, O. Kazuharu and T. Kozo, Acidic and Catalytic Properties of Niobium Pentaoxide, *Bull. Chem. Soc. Jpn.*, **1983**, 56, 2927-2931.

[36] M. L. A. Robinson, Dielectric properties of Nb_3O_7Cl crystals, *J. Phys. Chem. Solids*, **1968**, 29, 2064-2065.

[37] M. Moraes, W. d. S. F. Pinto, W. A. Gonzalez, et al., Benzylation of toluene and anisole by benzyl alcohol catalyzed by niobic acid: influence of pretreatment temperature in the catalytic activity of niobic acid, *Appl. Catal., A*, **1996**, 138, L7-L12.

[38] M. Ziolek, Niobium-containing catalysts—the state of the art, *Catal. Today*, **2003**, 78, 47-64.

[39] M. J. C. Molina, M. L. Granados, A. Gervasini, et al., Exploitment of niobium oxide effective acidity for xylose dehydration to furfural, *Catal. Today*, **2015**, 254, 90-98.

[40] Y. Zhang, J. Wang, J. Ren, et al., Mesoporous niobium phosphate: an excellent solid acid for the dehydration of fructose to 5-hydroxymethylfurfural in water, *Catalysis Science & Technology*, **2012**, 2, 2485.

[41] J. Xi, Y. Zhang, D. Ding, et al., Catalytic production of isosorbide from cellulose over mesoporous niobium phosphate-based heterogeneous catalysts via a sequential process, *Appl. Catal., A*, **2014**, 469, 108-115.

[42] O. Susumu, K. Masao, I. Tokio, et al., The Effect of Phosphoric Acid Treatment on the Catalytic Property of Niobic Acid, *Bull. Chem. Soc. Jpn.*, **1987**, 60, 37-41.

[43] A. Florentino, P. Cartraud, P. Magnoux, et al., Textural, acidic and catalytic properties of niobium phosphate and of niobium oxide, *Appl. Catal., A*, **1992**, 89, 143-153.

[44] W. Weng, M. Davies, G. Whiting, et al., Niobium phosphates as new highly selective catalysts for the oxidative dehydrogenation of ethane, *Phys. Chem. Chem. Phys.*, **2011**, 13, 17395-17404.

[45] S. Okazaki and N. Wada, Surface properties and catalytic activities of amorphous niobium phosphate and a comparison with those of H3PO4-treated niobium oxide, *Catal. Today*, **1993**, 16, 349-359.

[46] J. C. Smith and R. E. Drexel, Solubility Data for the System Aniline–Toluene–Water, *Industrial & Engineering Chemistry*, **1945**, 37, 601-602.

[47] K. Nakajima, Y. Baba, R. Noma, et al., Nb2O5.nH2O as a heterogeneous catalyst with water-tolerant Lewis acid sites, *J. Am. Chem. Soc.*, **2011**, 133, 4224-4227.

[48] A. Hegedüs, Z. Hell, T. Vargadi, et al., A new, simple synthesis of 1,2-dihydroquinolines via cyclocondensation using zeolite catalyst, *Catal. Lett.*, **2007**, 117, 99-101.

[49] K. Alfonsi, J. Colberg, P. J. Dunn, et al., Green chemistry tools to influence a medicinal chemistry and research chemistry based organisation, *Green Chem.*, **2008**, 10, 31-36.

[50] https://www.acs.org/content/dam/acsorg/greenchemistry/industriainnovation/roundtable/solvent-selection-guide.pdf Collaboration to Deliver a Solvent Selection Guide for the Pharmaceutical Industry (last access: 2016/09/10)

[51] G. A. Ramann and B. J. Cowen, Quinoline synthesis by improved Skraup–Doebner–Von Miller reactions utilizing acrolein diethyl acetal, *Tetrahedron Lett.*, **2015**, 56, 6436-6439.

[52] X.-G. Li, X. Cheng and Q.-L. Zhou, A convenient synthesis of 2-alkyl-8-quinoline carboxylic acids, *Synth. Commun.*, **2002**, 32, 2477-2481.

[53] X. Zhang and X. Xu, Silver-catalyzed oxidative coupling of aniline and ene carbonyl/acetylenic carbonyl compounds: an efficient route for the synthesis of quinolines, *Chemistry, an Asian journal*, **2014**, 9, 3089-3093.

[54] J. Horn, S. P. Marsden, A. Nelson, et al., Convergent, Regiospecific Synthesis of Quinolines from o-Aminophenylboronates, *Org. Lett.*, **2008**, 10, 4117-4120.

[55] A. S. Amarasekara and M. A. Hasan, 1-(1-Alkylsulfonic)-3-methylimidazolium chloride Brönsted acidic ionic liquid catalyzed Skraup synthesis of quinolines under microwave heating, *Tetrahedron Lett.*, **2014**, 55, 3319-3321.

[56] B. M. Reddy and I. Ganesh, Vapour phase synthesis of quinoline from aniline and glycerol over mixed oxide catalysts, *J. Mol. Catal. A: Chem.*, **2000**, 151, 289-293.

[57] Y. Chen, C. Xu, C. Liu, et al., Synthesis of 3-Methylindole from Glycerol Cyclization with Aniline over CuCr/Al2O3Catalysts Modified by Alkali Earth Oxides, *Heteroat. Chem*, **2013**, 24, 263-270.

[58] H. Saggadi, I. Polaert, D. Luart, et al., Microwaves under pressure for the continuous production of quinoline from glycerol, *Catal. Today*, **2015**, 255, 66-74.

[59] B. Katryniok, S. Paul, M. Capron, et al., Towards the sustainable production of acrolein by glycerol dehydration, *ChemSusChem*, **2009**, 2, 719-730.

[60] A. Corma, G. Huber, L. Sauvanaud, et al., Biomass to chemicals: Catalytic conversion of glycerol/water mixtures into acrolein, reaction network, *J. Catal.*, **2008**, 257, 163-171.

[61] A. Ulgen and W. Hoelderich, Conversion of Glycerol to Acrolein in the Presence of WO_3/ZrO_2 Catalysts, *Catal. Lett.*, **2009**, 131, 122-128.

[62] F. Wang, J.-L. Dubois and W. Ueda, Catalytic dehydration of glycerol over vanadium phosphate oxides in the presence of molecular oxygen, *J. Catal.*, **2009**, 268, 260-267.

[63] F. Wang, J. Xu, J. L. Dubois, et al., Catalytic oxidative dehydration of glycerol over a catalyst with iron oxide domains embedded in an iron orthovanadate phase, *ChemSusChem*, **2010**, 3, 1383-1389.

[64] P. Carniti, A. Gervasini, F. Bossola, et al., Cooperative action of Brønsted and Lewis acid sites of niobium phosphate catalysts for cellobiose conversion in water, *Applied Catalysis B: Environmental*, **2016**, 193, 93-102.

[65] M. Delacruz, J. Dasilva and E. Lachter, Catalytic activity of niobium phosphate in the Friedel–Crafts reaction of anisole with alcohols, *Catal. Today*, **2006**, 118, 379-384.

[66] M. Velasquez, A. Santamaria and C. Batiot-Dupeyrat, Selective conversion of glycerol to hydroxyacetone in gas phase over La2CuO4 catalyst, *Applied Catalysis B: Environmental*, **2014**, 160-161, 606-613.

[67] S. Sato, D. Sakai, F. Sato, et al., Vapor-phase Dehydration of Glycerol into Hydroxyacetone over Silver Catalyst, *Chem. Lett.*, **2012**, 41, 965-966.

[68] C.-W. Chiu, M. A. Dasari, G. J. Suppes, et al., Dehydration of glycerol to acetol via catalytic reactive distillation, *AlChE J.*, **2006**, 52, 3543-3548.

[69] Y. Cui, X. Zhou, Q. Sun, et al., Vapor-phase synthesis of 3-methylindole from glycerol and aniline over zeolites-supported Cu-based catalysts, *J. Mol. Catal. A: Chem.*, **2013**, 378, 238-245.

[70] W. Boreohe and G. A. Klenlta, Chinolin- and Indolderlvate from 4.4'-Diamido-diphenylmethan, *Chem. Ber.*, **1910**, 43, 2336.

4 CATALYST-FREE TRANSESTERIFICATION

4.1 Introduction

The upgrade of biomass-derived glycerol generally encompasses two classes of reactions: a) oxidations or reductions to prepare mostly three-carbon atom derivatives, and b) conversion of glycerol into higher homologues. [1,2,3]

Only to cite a few examples, class a) often includes metal (Pd, Pt, Bi and Au)-catalysed oxidation[4,5,6] and hydrogenation/hydrogenolysis processes,[7,8,9] as well as fermentative pathways to produce 1,2- and 1,3-PDO (1,x-propanediol), dihydroxyacetone, glyceric and tartronic acids, biosurfactants and other organic acids.[10,11] While, class b) is mainly oriented to the chemical conversion of glycerol into: i) esters (especially di-, and tri-acetylglycerols) and ethers for pharmaceutics, cosmetics, fuel and food additives, and polymers,[1,12,13,14] ii) epichlorohydrin for epoxyresins, iii) glycerol carbonate and acetals for polymer, surfactant and solvent/anti-freezing applications.[15,16,17] This massive activity also fuels another area of investigation dealing with the upgrading of major glycerol derivatives. In this Thesis work, the attention has been focused on the reactivity of glycerol and its most common acetal derivatives (see chapter 2, Figure 2.1) with organic carbonates.

4.1.1 The transesterification reaction

Transesterification is one of the classic organic reactions that have enjoyed numerous applications in laboratory practice as well as in the synthesis of a variety of intermediates in the pharmaceutical, cosmetic, fragrance, fuel and polymers industry.[18] Transesterification reactions are catalyzed under acid, basic or even neutral conditions.[19] An excellent review by Otera *et al.*, has detailed many applications of the most popular catalytic systems.[20] These include both acids such as sulfuric, sulfonic, phosphoric, and hydrochloric, and bases such as metal -alkoxides, -acetates, -oxides, and -carbonates. It should be noted that transesterification reactions are often carried out over solid (heterogeneous) catalysts to improve work-up, recycle, and purification of products, especially for large scale preparations. Heterogeneous systems include supported metal oxides and binary oxide mixtures: for example, MoO_3/SiO_2 and sol-gel MoO_3/TiO_2 have found applications in the polycarbonate chemistry for the preparation of diphenyl oxalate

monomer (DPO, Scheme 4.1),[21,22] while TiO_2/SiO_2 and similar binary combinations have been used in the transesterification of β-ketoesters[23] and in the synthesis of unsymmetrical carbonates $R_1OC(O)OR_2$.[24]

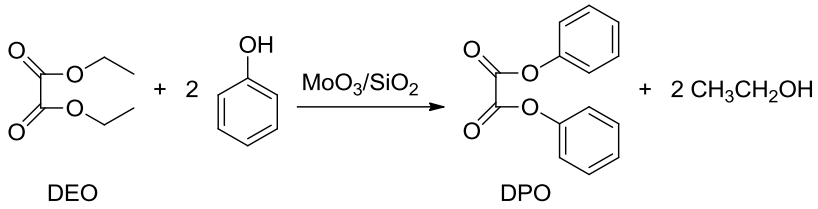

Scheme 4.1. Transesterification of diethyl oxalate (DEO) with phenol catalyzed by MoO_3/SiO_2.

Superacid solids have been described as transesterification catalysts: a remarkable case is the recently patented synthesis of sucrose-6-ester – a food sweetener – by a process carried out over a mixture of sulfated oxides of various metals.[25] Acidic ion exchange resins should also be mentioned in this context. The performance of such system has been proven in an elegant investigation by Van de Steene *et al.* on the model transesterification of ethyl acetate with methanol.[26]

The production of biodiesel blends is another sector in which the catalytic transesterification is extensively used. In particular, heterogeneous catalysts including calcium, manganese and zinc oxides as such or mixed, are widely used to convert natural triglycerides into FAMEs or FAEEs (Fatty Acid Methyl- or Ethyl Esters) with methanol or ethanol, respectively.[27] The most common system is CaO which is obtained by calcination of readily available and cheap resources including waste products such as shells and even livestock bones.[28,29,30,31] However, traditional catalysts such as alkali bases or alkaline methoxides are still encountered even for novel syntheses of biofuels: an example is biodiesel achieved by the transesterification of oils with dimethyl carbonate (DMC) in the presence of KOH (Scheme 4.2).[32,33]

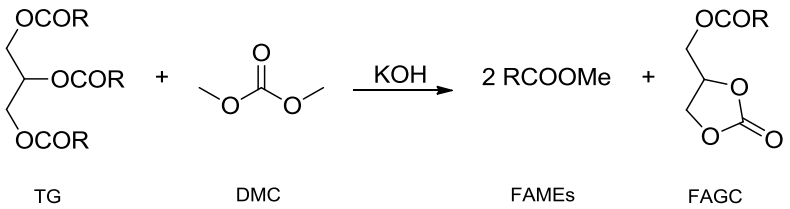

Scheme 4.2. Transesterification of a triglyceride with DMC for biodiesel production using KOH as base catalyst.

The reaction allows to obtain FAMEs and fatty acid glycerol carbonate monoesters (FAGCs), without the concurrent formation of glycerol, often a highly undesirable by-product.

The transesterification reaction can also be promoted by enzymes. A major driver for the choice of enzymes is their high efficiency that allows to operate under very mild conditions and with a variety of raw materials. However, since these advantages are partly offset by their cost and relatively short life, the implementation of biocatalytic processes makes sense preferably for the preparation of high added-value chemicals. This holds true also for esterification and transesterification reactions for which the literature often claims the use of lipase as a biocatalyst. To cite a few examples: i) Tudorache *et al.* reported the lipase-mediated reaction of glycerol with DMC for the synthesis of glycerol carbonate under solvent-free conditions. A 60% yield was achieved along with an effective recycle of the catalyst;[34] ii) the formation of six-membered cyclic carbonates as monomers for polyurethanes and polycarbonates, was achieved by a high yielding (85%) transesterification of dialkyl carbonates (DAlCs) with trimethylolpropane carried out in the presence of lipase at 80 °C;[35] in a very recent review on the bioconversion of oils, lipase was mentioned as the most suitable enzyme for an innovative and green production of biodiesel.[36]

In addition to the above described catalysts, amines and organometallic derivatives should also be cited in the field of homogeneous catalytic systems for transesterification reactions. Remarkable cases are those of triethylamine and Fe–Zn double-metal cyanide complexes:[37,38] among other applications, these compounds successfully catalyzed the reaction of DMC with both polyols (glycerol) and other OCs to achieve the expected transesterification products with total conversion and selectivity.

4.1.2 Dialkyl carbonates (DAlCs)

Over the last two decades, DAlCs have gained attention as *green* reagents. Starting from DMC, the simplest term of this class of compounds, DAlCs are among the most promising candidates for the replacement of conventional noxious solvents and fuel additives as well as for the development of innovative intermediates in the pharma, lubricant and polymer industries (Figure 4.1).[39,40]

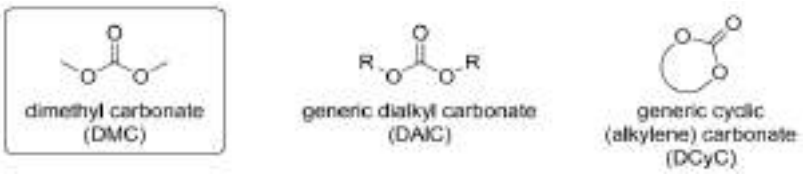

Figure 4.1. DMC and examples of generic alkyl carbonates

The interest for these compounds comes from multiple aspects, which include: i) safety and toxicological properties; ii) synthesis and chemical reactivity, and iii) physical and solvent characteristics. A good model example is DMC which is a non-toxic derivative, and it is merely classified as a flammable liquid.[41] (Table 4.1)

Table 4.1. Toxicological data of DMC

Toxicity	LD50 (g/kg)
Oral (rat)	13.0
Intraperitoneal (rat)	1.6
Oral (mouse)	6.0
Intraperitoneal (mouse)	0.8
Dermal (rabbit)	5.0

Other carbonates used in this work are diethyl carbonate (DEC), dibenzyl carbonate (DBnC) and propylene carbonate (PC). The toxicological profiles of these compounds are neither as good nor complete as that of DMC. For example, although DEC is still classified as a nontoxic liquid, it is not only a flammable, but also an irritating substance, while DBnC (low melting solid) is harmful by contact to skin and ingestion.[42,43] Nonetheless, these products can be considered far safer and greener than many conventional dangerous reagents including phosgene, dialkyl halides, and dialkyl sulfates that are used for similar reactions and synthetic scopes.

Dimethyl carbonate. The success of DMC as a green reagent is mostly due to the combination of its nontoxicity and its versatile reactivity, being DMC able to exhibit a double nature as a methylating and a carboxymethylating agent.

Both methylation and a carboxymethylation reactions are conventionally carried out by using methyl iodide or dimethyl sulphate in the first case, and phosgene in the second one. These procedures however, pose several drawbacks which make them undesirable from several points of view: i) the (methylating and carbonylating) reactants, particularly phosgene, are highly toxic and corrosive compounds; ii) stoichiometric amounts of bases

are always required to neutralize acidic by-products formed during the reactions. Therefore, the production of contaminated salts to be disposed of, cannot be ruled out; iii) organic solvents are necessary to ensure not only homogeneity, but also an accurate heat-control since reactions are highly exothermic processes.[44]

DMC can be efficiently used to overcome most of these issues. As mentioned above, since DMC bears two electrophilic sites, *i.e.* the carbonyl and the alkyl carbons, it may display a dual reactivity.[45] Scheme 4.3 exemplifies the reaction between a generic dialkyl carbonate and nucleophile (NuH) in the presence of a base catalyst (B).

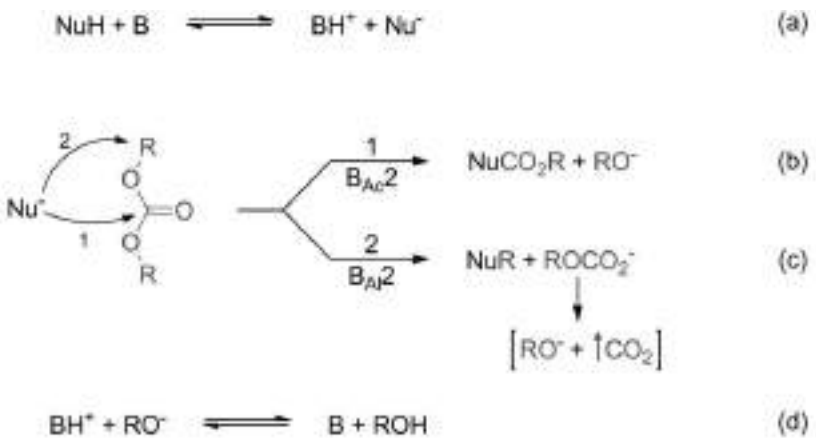

Scheme 4.3. Dual reactivity of DAlCs

Once the reaction of NuH with the base takes place, an activated (anionic) nucleophile (Nu^-) is obtained (Eq. a). This species is able to attack both the carbonyl and the alkyl positions of the carbonate (Eqn. b and c: paths 1 and 2, respectively), leading to the transesterification ($NuCO_2R$) and/or the alkylation (NuR) derivative. The reactions conditions, particularly the temperature and the nature of the catalyst, may effectively tune the product distribution by steering the process to the selective formation of only one of two possible products (this will be further clarified later in this chapter). The alkylation reaction produces an alkylcarbonate anion ($ROCO_2^-$) which due to its instability, rapidly decomposes to CO_2 and an alkoxide RO^-. The latter is finally neutralised by the protonated base BH^+ to form the corresponding alcohol and the initial base that is regenerated as a catalyst.

On other hand, the nontoxicity of DMC is a result of the recent evolution of the methods for its synthesis on an industrial scale. Before the 80's, the preparation of DMC was based on a reaction involving a lethal chemical: the phosgenation (Cl_2CO) of methanol

(Scheme 4.4, top). Since then, the processes for the production of DMC have progressively improved in terms of environmental impact, safety and economics.

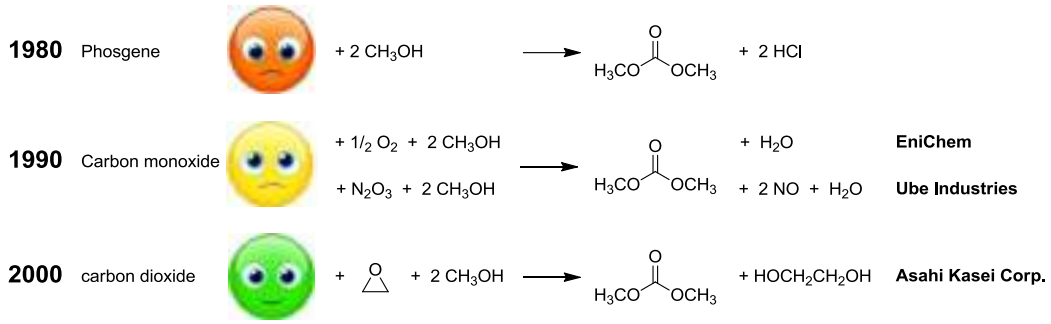

Scheme 4.4. Top: phosgenation of methanol; **middle**: EniChem and Ube Processes; **bottom**: Asahi Process for the production of DMC.

Thus, by the early 90's, two main phosgene-free large-capacity processes were operative, both based on the incorporation of carbon monoxide (CO) and methanol by transition metal catalysis: one developed by EniChem[46] and the other by Ube Industries.[47] The EniChem process involved the oxidative carbonylation of methanol, *i.e.* the reaction of methanol with carbon monoxide and oxygen catalyzed by cuprous chloride, while the Ube process was based on oxidative carbonylation of methanol via methyl nitrite using NO_x as oxidant instead of oxygen and a palladium catalyst (Scheme 4.4, middle). Although both these routes were highly safer than that starting from phosgene, they still continued to use poisonous carbon monoxide and methyl nitrite as raw materials, and potentially corrosive chlorine-based catalysts.

Carbon dioxide is the natural green alternative carbonyl source to these undesirable feedstocks (in particular to CO), though its thermodynamic stability poses severe challenges. This potential limitation was overcome by Asahi Kasei Corp. that recently industrialized a catalytic polycarbonate production process based on the use of CO_2 for the synthesis of DMC as an intermediate for the preparation of diphenyl carbonate monomer. The overall manufacture starts with the organo-catalytic insertion of CO_2 into ethylene oxide to give ethylene carbonate. Then, the second step involves the transesterification of ethylene carbonate with methanol and is carried out in a continuous distillation reactor loaded with quaternary ammonium strongly basic anion exchange resin and in the presence of alkali hydroxides. This reaction yields pure dimethylcarbonate (DMC) and it is one of the major breakthrough of Asahi-Kasei process (Scheme 4.4, bottom). The third and final step is the transesterification of DMC with phenol by catalytic reactive distillation in

the presence of a homogeneous Ti, Bu-Sn, or Pb catalysts. A high purity diphenyl carbonate is so achived.[48]

It should be noted how the catalytic transesterification is a crucial reaction not only for the preparation of DMC, but also for the synthesis of higher organic carbonate homologues (Scheme 4.5).[49]

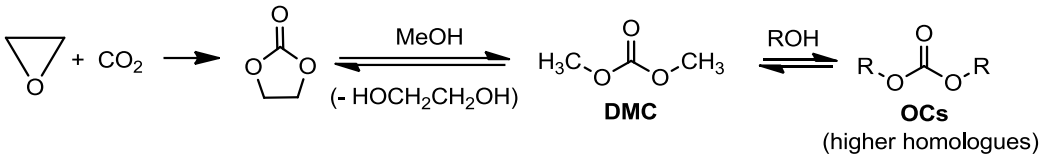

Scheme 4.5. The transesterification in the synthesis of OCs.

Moreover, the synthesis of DMC by transesterification of ethylene carbonate with methanol does not necessarily require transition metal catalysis as did the EniChem and Ube processes. Instead, it can be effectively catalyzed by a combination of supported basic ammonium resins and homogeneous alkaline bases.[48] This demonstrates that there is a large potential for the development of new transition metal-free catalytic systems for the transesterification reaction both towards the synthesis of OCs as well as in view of their further transformations.

Many dialkyl- and alkylene- carbonates including DMC, DEC, and propylene carbonate have another important characteristic that makes them desirable while designing a green reaction or process: they are good solvents able to solubilize most of the common organic compounds and, even though at relatively high temperatures, some inorganic bases such as alkaline carbonates (M_2CO_3: M=Na, K).[45] For this reason, DAlCs may often serve with a double function acting both as solvents and a reagents. The absence of additional components (solvents or co-solvents) greatly improves the safety and facilitates the final work-up of the mixture since the (reactant/solvent) carbonates have usually lower boiling point than the products, and they can simply be removed by distillation and recycled. Moreover, inorganic base catalysts can also be filtered off at room temperature, and re-used virtually indefinitely (Scheme 4.3).

4.2 Catalyst-free transesterification of DAlCs with glycerol acetals

Glycerol acetals (GAs), particularly glycerol formal (GlyF) and Solketal, have been widely described in Chapter 2. Among their attractive properties as renewables and safe

derivatives, these compounds possess a short OH-capped tether (hydroxymethylene group) which allows a synthetic access to a number of other functionalities.[50,51,52] These features have been a great stimulus to explore in this Thesis work, innovative protocols for the conversion of glycerol acetals into high added-value derivatives. Our research group recently succeeded in the reaction of glycerol formal and solketal with different DAlCs (dimethyl, diethyl-, and dibenzyl-carbonate): under batch conditions (≥200 °C), it was demonstrated that a highly selective (up to 99%) and high-yielding (80-99%) O-alkylation reaction of acetals occurred at T≥ 200 °C and in the presence of K_2CO_3 as a catalyst.[53] Scheme 4.6 illustrates the model reaction with DMC.

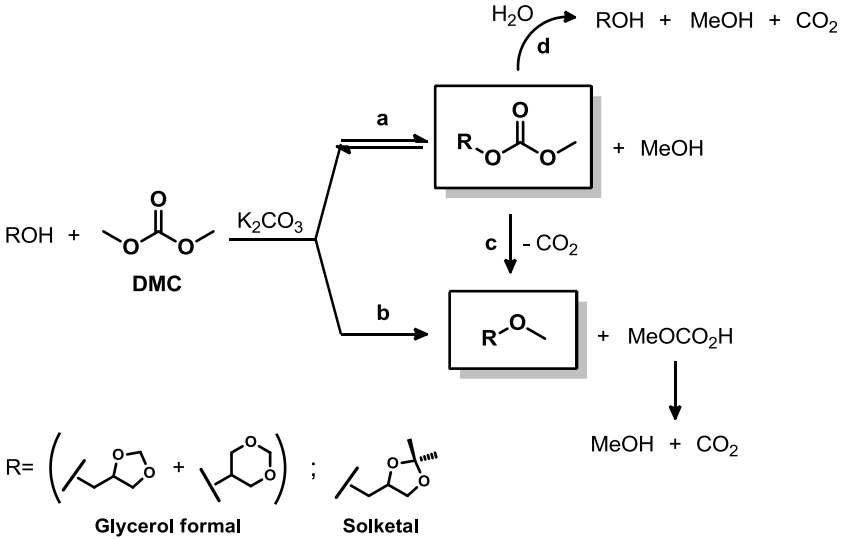

Scheme 4.6. The mechanism for the methylation of GlyF and Solketal with DMC

The overall transformation could be explained by a combined sequence of alkylation, carboxyalkylation, decarboxylation and hydrolysis processes. Both methyl and carboxymethyl derivatives of acetals were initially formed (ROMe and $ROCO_2Me$, respectively; paths a and b. Compare Scheme 4.3). However, as the methylation proceeded, the reversible transesterification backtracked: $ROCO_2Me$ gradually decreased to zero, while ROMe became the final product. The disappearance of the carboxymethyl product was further assisted by competitive decarboxylation and hydrolysis reactions [paths (c) and (d)],[54] that also took place for DMC [paths (e)-(f)]. Hydrolysis reactions were plausibly due to traces of water adsorbed by the highly hygroscopic K_2CO_3.[55]

Besides the synthetic value, the procedure also exemplified a genuine green model since it coupled innocuous renewables (GAs) to non-toxic alkylating agents such as DAlCs in a catalytic reaction.

In a continuation of this investigation, the same reaction was explored with a different objective: the selective mono-transesterification of DAlCs with glycerol acetals (Scheme 4.7).

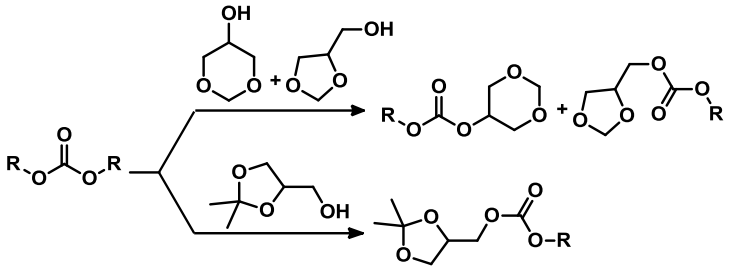

Scheme 4.7. Selective mono-transesterification of DAlCs with glycerol acetals

No previous studies were available in the literature for such a transformation. Among the possibilities to envisage a synthetic protocol, organocatalysis offered an attractive perspective as recently reported by us.[56,57,58] However, other preliminary results of our group suggested that the mono-transesterification reaction could take place also under catalyst-free batch conditions providing that a reasonably high temperature (≥ 200 °C) were used.[53] Of the two (organocatalysis and catalyst-free) options, the second one was more promising since in the absence of catalysts, operating conditions and product separation procedures could be simplified; moreover, an easier implementation of large scale productions could be devised. These aspects have inspired the work discussed above in this section, which demonstrates that the catalyst-free transesterification of DAlCs with glycerol acetals can be optimized under continuous-flow conditions.

The results of this study have been the object of a publication on the RSC journal *Green Chemistry*, which is described in the following paragraphs, from 4.2.1 to 4.2.4.[59]

4.2.1 Results

The catalyst-free reaction of DMC with glycerol formal was chosen as a model process to begin the investigation. Conditions for the initial tests, in particular the temperature and the reactant molar ratio, were selected according to our preliminary results obtained for batch reactions.[53]

The experimental apparatus used for the investigation was similar to that described in previous works of our research group,[60] and in Chapters 2 and 3 of this Thesis. It was composed of a HPLC pump for the delivery of liquid reactants, a thermostated oven, a static

mixer, a reactor and a back pressure regulator. A detailed description of the overall system is given in the experimental paragraph.

4.2.1.1 Effects of the pressure and the temperature.

Four sets of experiments were carried out isothermally at 225, 250, 275, and 300 °C, respectively, using a constant DMC:GlyF molar ratio (Q) of 20 (the excess DMC served both as reagent and a carrier/solvent). In each experiment, a mixture of DMC (48.6 mL) and GlyF (2.5 mL) was fed to the reactor at a combined volumetric flow rate of 0.05 mL/min. The pressure was stepwise increased from ambient up to 100 bar: typical increments were of 5-10 bar. At any given pressure, the reaction was allowed to proceed for 90 min. Periodic GC/MS analyses of the mixture, collected at the reactor outlet, showed that both the conversion and the product distribution remained steady after a time interval of 60-80 min. On condition that a threshold pressure in the range of 20-50 bar was exceeded, an unprecedented result was obtained: not only the desired process occurred, but also the formation of the mono-transesterification product took place with a very high selectivity, over 95% (Scheme 4.8).

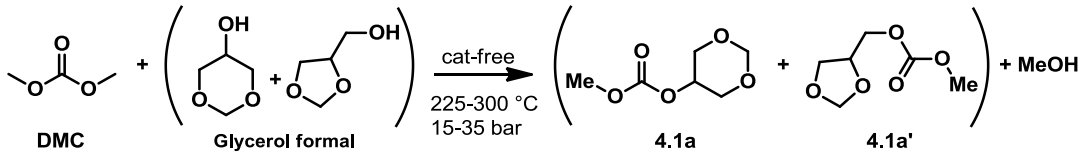

Scheme 4.8. The catalyst-free selective transesterification of DMC with glycerol formal

In particular, two isomeric carbonates **4.1a** and **4.1a'** [1,3-dioxan-5-yl methyl carbonate and (1,3-dioxolan-4-yl)methyl methyl carbonate, respectively] were obtained in the same (3:2) relative ratio of the starting glycerol formal acetals. The structures of **4.1a** and **4.1a'** were assigned by GC/MS and NMR analyses. Other by-products (total ≤5%) derived from the double transesterification of DMC with GlyF.

Figure 4.2 report the trend of reaction conversion and selectivity observed as a function of the pressure at each of the investigated temperatures.

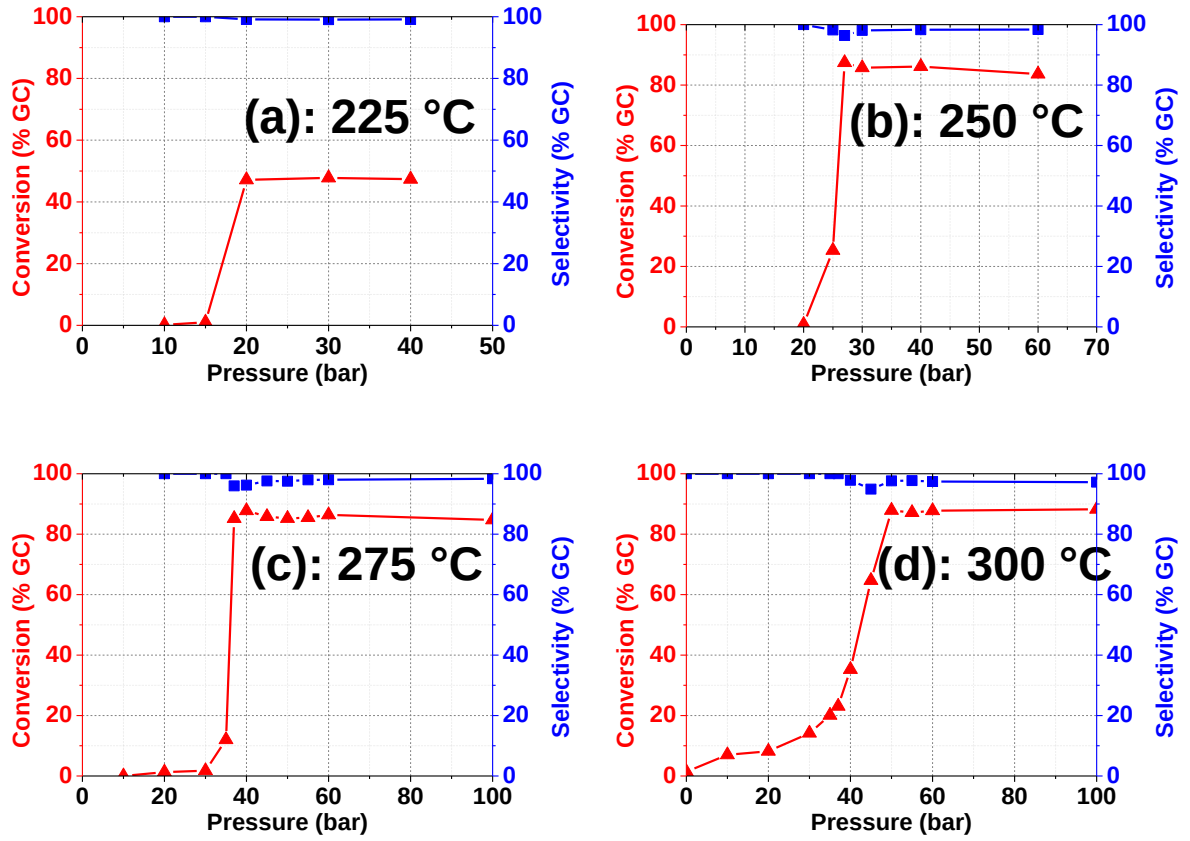

Figure 4.2. Effects of temperature and pressure on the non-catalytic (thermal) transesterification of DMC with GlyF. Four isothermal profiles are shown at: i) molar ratio Q=DMC:GlyF=20; ii) flow rate=0.05 mL/min; iii) sampling time (at any pressure)=1.5 hours

In no case did the reaction take place at ambient pressure. However, very small pressure increments could dramatically affect the process. For example, at the lowest investigated temperature (225 °C), a significant enhancement of the conversion from 2 to 48% was achieved between 15 and 20 bar (Figure 4.2a). No further improvements of the reaction outcome were appreciated at higher pressures. An analogous behavior was observed as the temperature was increased. Though, an even more remarkable effect was manifest. At 250 °C, the conversion of GlyF sharply boosted up from 1% to 85%, once the applied pressure went from 20 to 27 bar, and then it remained steady throughout the range of 30-60 bar (Figure 4.2b). The same held true at 275 °C, where a steep rise of the conversion (up to 87%) was observed between 30 and 37 bar (Figure 4.2c). A slightly different trend occurred at 300 °C. The reaction profile followed a gentler sloped sigmoidal curve that reached a stable value of 85-87% only at 50 bar (Figure 4.2d).

The comparison of Figure 4.2b-d indicated that an equilibrium conversion of ~85% could be achieved at 250-300 °C. However, as the temperature was increased, the pressure

necessary for the reaction to proceed must be progressively augmented from 27, to 37, and to 50 bar, respectively. At 225 °C, although a lower equilibrium conversion was achieved (48%), a lower operating pressure was required (20 bar).

An additional test was devised also under batch conditions. A solution (40 mL) of GlyF and DMC in a 1:20 molar ratio was charged in glass reactor placed inside a stainless steel autoclave (inner volume 150 mL). Attention was paid to avoid any contact of reagents with inner walls of the autoclave. The overall system was heated at 200 °C for 24 hours. GC/MS analyses of the final reaction mixture showed that the conversion was 84% with a mono-transesterification selectivity of 93% (the only by-product was from the double transesterification of DMC with GlyF). This result definitely proved the thermal nature of the reaction. Since the process occurred in a glass liner, any contribution of catalysis by metal components of stainless steel was ruled out.

4.2.1.2 Recycle of the mixture, reproducibility, mass balance, and productivity.

CF-processes are particularly suited to perform recycling operations aimed at improving the reaction outcome and the final productivity. Accordingly, based on previous results of Figure 4.2, two sets (A and B) of experiments were carried out to optimize the conversion of the investigated mono-transesterification. Conditions were those of Figure 4.2c. In set A, a continuous reaction of DMC and GlyF (in a 20:1 molar ratio, 0.05 mL/min) was allowed to proceed at 275 °C, 60 bar for 18 hours. Samples of the mixture at the reactor outlet were analyzed at time intervals (by GC/MS, every 1.5 hours). The colourless clear solution (54 mL) recovered at the end of the test was distilled to remove the MeOH/DMC azeotrope (70:30 v/v, 2.5 mL; bp=62-65 °C) formed during the reaction,[61,62] and the initial volume was restored by addition of fresh DMC. The solution was then recycled by feeding it to the CF-reactor where another reaction was allowed to occur under the above described conditions (275 °C, 60 bar, 0.05 mL/min). Also in this case, the composition of the mixture at the reactor outlet was periodically monitored by GC/MS.

In set B, two subsequent CF-reactions of DMC and GlyF were performed using the same procedure of set A, except for the fact that no fresh DMC was added between the first and the second reaction. The results are reported in Figure 4.3 where the conversion of GlyF and the mono-transesterification selectivity are reported for the two sequential sets of experiments.

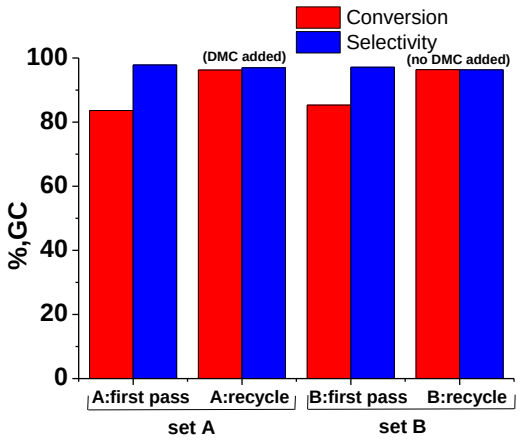

Figure 4.3. Recycling tests carried out at 275 °C and 60 bar. Initial runs (fresh) of both sets A and B were performed by using a mixture DMC/GLyF in a 20:1 molar ratio. The volumetric rate (F) was always 0.05 mL/min. Values of conversions and selectivities were those after 1.5 hours

Three major aspects emerged: i) an equilibrium position was readily achieved in all cases. GC/MS analyses showed that mixtures recovered at the reactor outlet preserved the same composition throughout the experiment, from 1 to 18 hours. On average, before the recycle, mixtures were composed of unreacted acetal (12-13%), transesterification product (mixture of isomers **4.1a** and **4.1a'**, 84-86%), and minor by-products (≤ 2-3%) (Figure 4.3: bars 1-2 and 5-6, respectively); while, recycled mixtures (after the second pass through the CF-reactor) contained less than 5% of GlyF and by-products, the remainder being the desired compound (**4.1a** and **4.1a'**) (bars 3-4 and 7-8, respectively). This proved that the recycle could improve the conversion of GlyF from ~85% up to a substantially quantitative value (95-97%, second pass), without any appreciable alteration of the selectivity that remained constant at 96-98%; ii) the addition of fresh DMC before the recycle did not affect the reaction outcome (compare A and B recycle, bars 3-4 and 7-8). This suggested that the overall process could be further intensified by decreasing the volume of DMC; iii) the comparison of Figure 4.2c and Figure 4.3 as well as the consistent composition of reaction mixtures sampled and analyzed during long-running tests (up to 18 hours) indicated that a robust procedure with highly reproducible results was achieved. This was substantiated also by the validation of the reaction mass balance: after the recycle tests, the transesterification product was isolated in a 92% yield (total of **4.1a** and **4.1a'**). Isomeric carbonates **4.1a** and **4.1a'** were obtained in the same (3:2) relative ratio of the starting acetals. Worthy of note was the extremely easy separation procedure that took place through a one-step distillation of the final mixtures (54 mL) without additional purifications or need for extra solvents.

To further explore the potential of the investigated procedure, the effect of the DMC amount was analyzed. The protocol of Figure 4.2 was changed by decreasing the volume of DMC: in particular, three CF-reactions were performed using reactant molar ratios Q (DMC:GlyF) of 20, 10 and 5. Experiments were carried out at 250 °C since this temperature offered the best compromise between good conversions and convenient, not too high, pressures (20-40 bars; Figure 4.2b). In each test, the combined flow rate was set to 0.05 mL/min and the pressure was gradually increased from ambient up to 50 bar.

Results are reported in Figure 4.4 which details the trend of the conversion of GlyF with the increase of the pressure at the different Q ratios used.

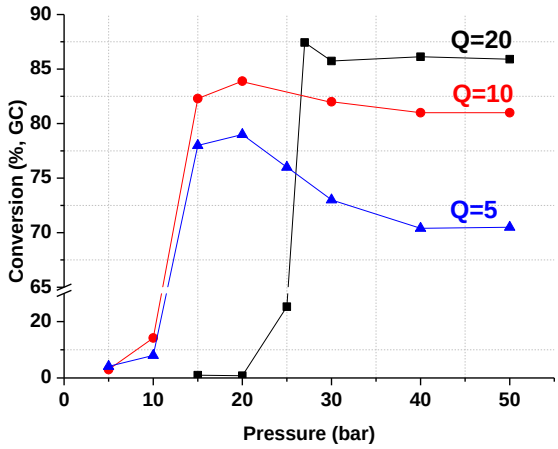

Figure 4.4. The conversion GlyF at different pressures and DMC:GlyF (Q) molar ratios. T=250 °C, volumetric rate F=0.05 mL/min. Values were determined after 1.5 hours

As Q was decreased from 20 to 10, the shape of reaction profiles was similar, but two differences were manifest: i) the onset of the reaction took place in the proximity of 15 bar (Q=10) and 25 bar (Q=20); ii) a slight drop of the equilibrium conversion, from ~85 to ~80%, was observed (black and red curves). The last aspect was far more evident when the Q ratio was further reduced to 5. The maximum allowed conversion declined from ~77% at 15-20 bar, to level off at a value of 70% at higher pressures (≥40 bar, blue profiles).

Also the reaction selectivity (not shown in the Figure) towards the product **4.1a** and **4.1a'** slightly decreased from 96-98% at Q=10-20, to 88-93% at Q=5, respectively. The lower DMC:GlyF ratio favored the double transesterification of DMC with GlyF. The reaction was most conveniently carried out by using a DMC excess of 10 molar equivs. with respect to GlyF. This allowed to operate at a moderate pressure (≤30 bar) with only a minor drop of the equilibrium conversion.

Under such conditions, a recycling experiment was carried out analogously to that described in Figure 4.3. A continuous reaction of DMC and GlyF (Q=10; F=0.05 mL/min) was allowed to proceed at 250 °C and 30 bar, for 18 hours. Then, the solution (54 mL) recovered at the reactor outlet was distilled to remove the MeOH/DMC azeotrope, and recycled for a second pass through the CF-reactor. The results confirmed those of Figure 4.3. The recycle of the mixture enhanced the GlyF conversion from 81 to 94% with no alteration of the mono-transesterification selectivity (≥ 96%). A final distillation gave isomers **4.1a/4.1a'** in a substantially quantitative yield (purity ≥98%, by GC). The relative ratio **4.1a/4.1a'** (3:2) corresponded to that of the starting acetals.

Additional tests were carried out to evaluate and possibly optimize the system productivity (P) as well. This was calculated by the mass of desired product obtained per time unit (mg/min of the isomer mixture **4.1a** and **4.1a'**. In the CF-mode, a DMC/GlyF mixture (Q=10) was set to react at 250 °C and 30 bar, by progressively increasing the total volumetric flow rate (F) from 0.05 mL/min to 0.6 mL/min. Typical increments were of 0.05-0.1 mL/min. At any chosen F rate, the same volume (10 mL) of the reaction mixture was used: the corresponding reaction times were variable from 17 to 180 min.[63] The solutions collected from the reactor were analyzed by GC/MS to determine both the conversion of GlyF and the product distribution. Results are reported in Figure 4.5.

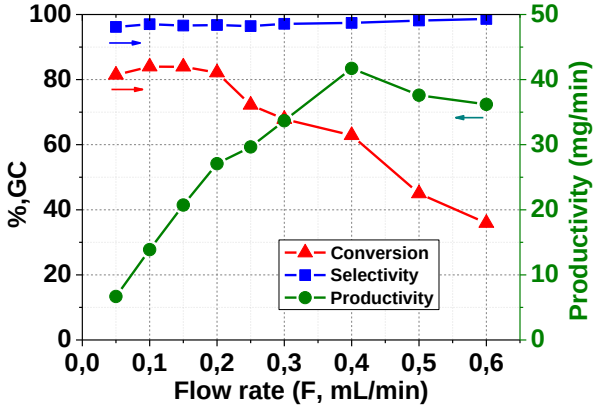

Figure 4.5. The effect of the flow rate (F) on conversion (red), selectivity (blue), and productivity (green) of the transesterification of DMC with GlyF. Conditions: 250 °C, 30 bar, Q=10

A 4-fold increase of the flow rate from 0.05 to 0.2 mL/min had no effects on the conversion that remained substantially constant at 80-83%. The progress of the reaction was apparently disfavored by further increments of F. The conversion dropped from ~80 to 35% as the residence time (τ) was gradually reduced from 300 to 100 sec (red profile, in

the range of 0.2-0.6 mL/min). Notwithstanding this, the mono-transesterification selectivity always remained very high (>95%), and even most importantly, the reaction productivity (P) showed an almost linear increase from 7 mg/min up to a maximum of 42 mg/min when F was changed from 0.05 to 0.4 mL/min (green profile). P then slightly decreased to 35 mg/min at higher flow rates (≥0.5 mL/min). Compared to the limited capacity of the used CF-reactor (1 mL), this result not only highlighted an excellent performance of the reaction, but also opened a perspective for larger scale applications and further process intensification.

Overall, the study described by Figure 4.2-Figure 4.5 proved the feasibility of the model catalyst-free thermal transesterification of DMC with GlyF, and offered a strategy to optimize the process under CF-conditions. To continue exploring its potential, the investigation was then focused on the scope and limitations of the synthesis by using other DAlCs and glycerol-derived acetals.

4.2.1.3 Different carbonates: the reaction of diethyl carbonate with glycerol formal.

Diethyl carbonate (DEC), the simplest linear C_5-homologue of DMC, was initially used. CF-reactions of DEC with GlyF were carried out based on the results, the method, and the apparatus above described for DMC. A mixture of DEC and GlyF (in a 10:1 molar ratio, respectively) was continuously fed through a CF-reactor thermostated at a temperature comprised between 250 and 300 °C. The flow rate was 0.05 mL/min. In analogy to experiments of Figure 4.2 and Figure 4.4, the pressure was gradually increased from ambient up to 100 bar. Conversion and product distribution were determined by GC/MS analyses of the mixtures that were periodically sampled at the reactor outlet.[64] Three isothermal reaction profiles were obtained at 250, 275, and 300 °C. In all cases, a highly selective (>95%) mono-transesterification reaction occurred providing that an operating pressure above 20 bar was applied (Scheme 4.9).

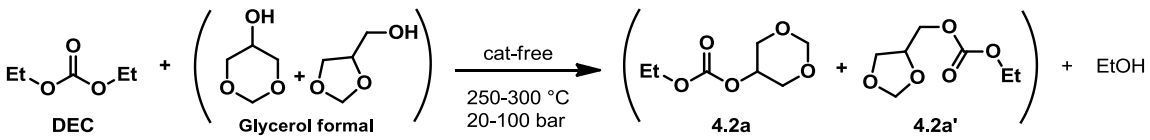

Scheme 4.9. The catalyst-free mono-transesterification of DEC with glycerol formal

As for DMC, this result was never previously reported under catalyst-free conditions, particularly in the CF-mode. The structures of isomeric carbonates **4.2a** and **4.2a'** [1,3-

dioxan-5-yl ethyl carbonate and (1,3-dioxolan-4-yl)methyl ethyl carbonate, respectively] were assigned by GC/MS and NMR analyses. The relative ratio **4.2a/4.2a'** was the same (3:2) observed for starting acetals. Other by-products (total ≤5%) derived from the double transesterification of DEC with GlyF. Figure 4.6 shows the trend of the reaction conversion as a function of pressure, at each of the investigated temperatures.

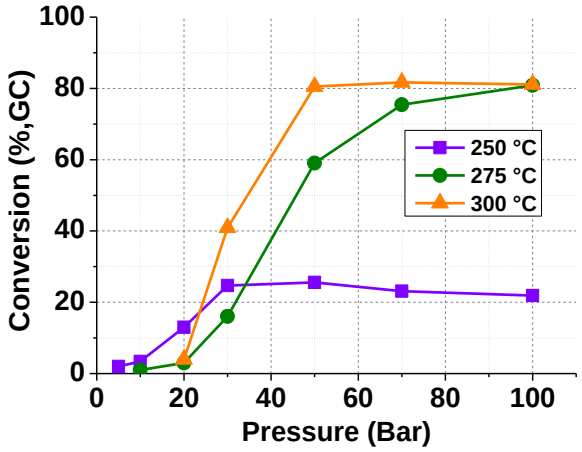

Figure 4.6. Effects of temperature and pressure on the non-catalytic transesterification of DEC with GlyF. Three isothermal profiles are shown at 250, 275, and 300 °C in the range of 10-100 bar. Other conditions: i) molar ratio Q=DEC:GlyF=10; ii) F=0.05 mL/min; iii) sampling time (at any pressure)=1.5 hours. In all cases the selectivity was greater than 95%

Isothermal profiles of the transesterification of DEC with GlyF showed both analogies and differences with respect to the corresponding reaction of DMC (Figure 4.2). Analogies were: i) the reaction did not take place at ambient pressure, but only over 20 bar, and ii) an equilibrium conversion (up to 80%) was reached with increasing pressure (green and orange curves). Differences included: i) conversion profiles did not show steep abrupt changes, but followed sigmoid-like curves extended over relatively large pressure intervals from 20 up to 50 bar (compare violet, orange, and green profiles); ii) a higher temperature was required for the reaction. For example, at 250 °C, (equilibrium) conversions of GlyF were 85% and 23% in the transesterification of DMC and DEC, respectively (Figure 4.2c and Figure 4.6); iii) less evident temperature/pressure relations were observed. At 250-275 °C, the behavior paralleled that of DMC: as the temperature increased, the pressure interval for the onset of the reaction should also increase. However, at 300 °C, the threshold pressure (25-30 bar) for the transesterification process was similar, if not lower, to that at 275 °C.

The results of Figure 4.6 allowed to conclude that DEC was less reactive than DMC and the formation of products **4.2a/4.2a'** could be conveniently carried out at 300 °C and 50 bar. Under such conditions, an additional test was carried out to evaluate the reaction productivity. The same procedure described for DMC (Figure 4.5) was used: a DEC/GlyF mixture (Q=10, 10 mL) was set to react in the CF-mode by progressively increasing the total volumetric flow rate from 0.05 mL/min to 1 mL/min. The corresponding reaction times were variable from 10 to 180 min.[63] The conversion and the product distribution of mixtures collected at the reactor outlet were determined by GC/MS. Results are reported in Figure 4.7.

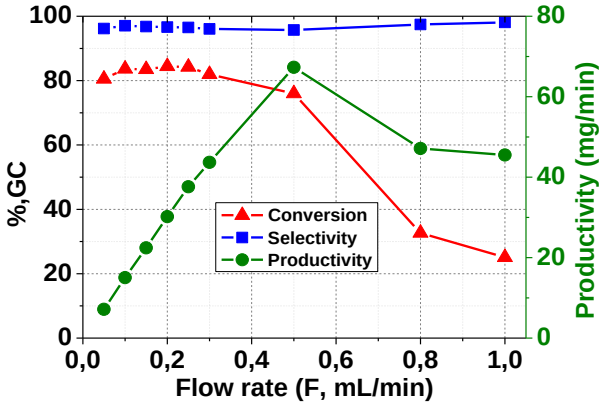

Figure 4.7. The effect of Flow rate on conversion (red), selectivity (blue), and productivity (green) of the transesterification of DEC with GlyF. Conditions: 300 °C, 50 bar, Q=10

The productivity was linearly enhanced from 8 to 68 mg/min of **4.2a/4.2a'** when F was increased by a factor of 10 from 0.05 to 0.5 mL/min. A drop to 48 mg/min was then observed at greater flow rates. With respect to DMC, the higher reaction temperature (300 *vs* 250 °C: Figure 4.7 and Figure 4.5, respectively) was the plausible reason for the better productivity achieved with DEC. The result confirmed that not only the CF-transesterification of DEC with GlyF was practicable under catalyst-free conditions, but also a robust and reproducible procedure was used.

Products **4.2a** and **4.2a'** were isolated by distillation of the mixture (total volume 54 mL) recovered after a reaction carried out for 18 hours at 300 °C and 50 bar. However, the separation was tricky: due to the close boiling points of the unconverted GlyF (~15%) and the products, the yield of compounds **4.2a** and **4.2a'** (total of the isomer mixture) did not exceed 73% (further details are in the experimental section).

4.2.1.4 Different carbonates: the reaction of PC and DBnC with GlyF.

Liquid propylene carbonate (PC, bp=242 °C) was a good model compound to investigate the behavior of alkylene carbonates in the reaction with GlyF. CF-conditions used for this study were based on the results described for DEC (Figure 4.6). A mixture of PC and GlyF (in a 10:1 molar ratio, respectively; F=0.05 mL/min) was set to react in the CF-mode at a temperature of 250, 275 and 300 °C under a constant pressure of 50 bar. No changes of the operating pressure were considered. GC/MS analyses of solutions recovered at the reactor outlet proved that a highly selective (>95%) mono-transesterification reaction occurred with the formation of four isomeric products (**4.3a** and **4.3a'**, and **4.4a** and **4.4a'**), whose relative ratios **4.3a**/**4.3a'** and **4.4a**/**4.4a'** corresponded to that of the starting acetals (3:2). (Scheme 4.10).

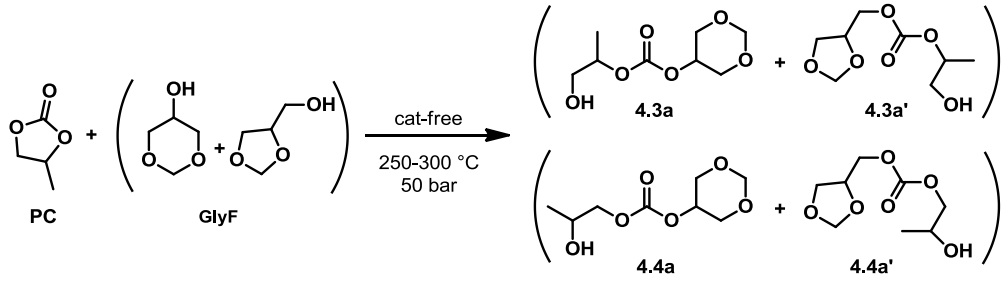

Scheme 4.10. The catalyst-free mono-transesterification of PC with GlyF

The structures of such carbonates were assigned by GC/MS analyses. Due to the complexity of the reaction mixtures, the NMR characterization was not practicable.[65] Experiments showed that the rise of the temperature from 250 to 275 and 300 °C brought about a corresponding increase of the conversion of GlyF from 7 to 23 and 53%, respectively. These results were not further optimized, nor the isolation of products was accomplished: any attempt to separate (by distillation) unreacted GlyF and excess PC from derivatives **4.3** and **4.4** was not successful because of the close boiling points of the involved compounds. However, tests for the CF-transesterification of PC with GlyF were repeated under the same conditions of Scheme 4.10 and with the additional validation of GC-analyses by an external standard (*n*-tetradecane). Results were in very good agreement to those of previous experiments. Calibrated conversions of 7, 27, and 48% were achieved at 250, 275 and 300 °C, respectively. The overall study proved the concept, thereby confirming that PC could be used for the investigated CF-protocol, though it was less active than DEC, and even less than DMC.

Dibenzyl carbonate (DBnC) was finally considered for the transesterification with GlyF. DBnC is a low melting solid (mp: 34 °C) which, upon heating, forms a highly viscous liquid (bp:180-190 °C/2 mmHg). A solvent/carrier was therefore necessary to perform CF-reactions. Two different solvents such as acetone and 1,2-dimethoxyethane (DME) were considered for their physicochemical properties (particularly, low-mid boiling points and polarity),[66,67] and acceptable toxicological profiles.[68] A preliminary screening was carried out using a solution of GlyF, DBnC and the solvent in a 1:5:12 molar ratio, respectively. This mixture was set to react in the CF-mode at 250 °C and 50 bar, at a flow rate of 0.05 mL/min. Experiments demonstrated that after 1.5 hours, the mono-transesterification reaction of DBnC with GlyF was achieved with excellent selectivity (>98%) (Scheme 4.11 and Figure 4.8).

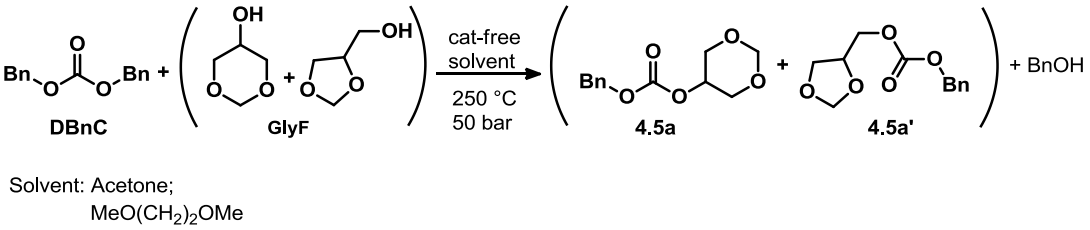

Scheme 4.11. The catalyst-free mono-transesterification of dibenzyl carbonate with GlyF

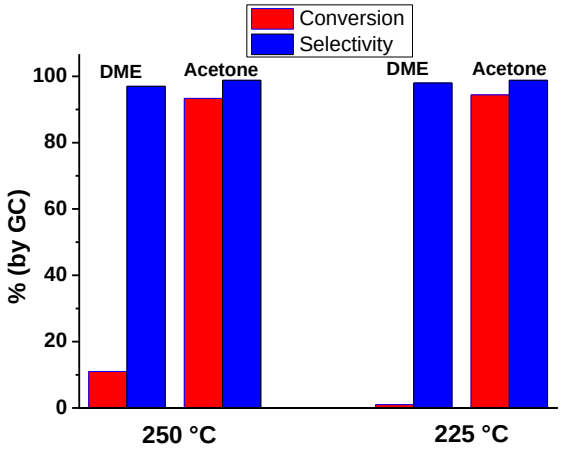

Figure 4.8. The transesterification of DBnC with GlyF. Effect of the solvent and temperature on conversion and selectivity. Conditions: 50 bar, molar ratio GlyF:DBnC:solvent=1:5:12; F=0.05 mL/min, 1.5 hours; left (first four bars): 250 °C; right: (second four bars): 225 °C

The solvent greatly affected the equilibrium conversion of GlyF that improved from 11% in the presence of DME to 94% in acetone (Figure 4.8: red bars on left). The result was substantiated by two other tests carried out under the same conditions (50 bar, molar ratio GlyF:DBnC:solvent=1:5:12; F=0.05 mL/min, 1.5 hours), but at a lower temperature of

225 °C. No reaction took place in DME, while an almost quantitative mono-transesterification was observed in acetone (Figure 4.8: red bars on right). Of note, the outcome of such a reaction was even better than that in DMC (compare Figure 4.2a). At 225 °C, the acetone-mediated process was allowed to proceed up to 4 hours. The volume (~12 mL) collected at the reactor outlet proved a substantially quantitative recovery of the reaction mixture. The GC/MS analysis of this solution confirmed that GlyF was converted into the corresponding carbonates **4.5a** and **4.5a'** with negligible amounts (1%) of double transesterification by-products. At the same time, also a partial decarboxylation of DBnC to dibenzyl ether [$(PhCH_2)_2O$, DBE] was noted in accordance to our previous results on the high-temperature behavior of DAlCs.[54,55] In line with these findings, DBnC was less thermally stable than other DAlCs such as DMC and DEC.

Products **4.5a** and **4.5a'** were new compounds. They were obtained in the same (3:2) relative ratio of starting acetals. Of the different techniques attempted for their isolation, FCC on silica gel (eluent: petroleum ether (PE)/diethyl ether (Et_2O), 1:1 *v/v*) was successful to separate even the single isomers in a highly pure form (>95%, by GC). Full structural details of compounds **4.5a** and **4.5a'** were achieved by NMR characterization study (see experimental section).

Figure 4.8 also indicated that in the range of 225-250 °C, the temperature had a minor effect on both the conversion and the selectivity. Although this suggested that there was room for improvement, the optimization of such reaction was not attempted. Overall, the reaction of DBnC not only confirmed that the CF-protocol was feasible for higher carbonates, but it offered new perspectives on benefits of the use of light solvents of low-to-mid polarity.

4.2.1.5 Different acetals: the reaction of DMC and DEC with solketal.

Solketal was used as a different acetal to further explore the thermal CF-transesterification of both DMC and DEC. Reaction conditions were those of previous experiments. A mixture of solketal and the chosen dialkyl carbonate (in a 1:20 molar ratio, respectively) was set to react in the CF-mode at different temperatures of 250 and 275 °C and at a total flow rate of 0.05 mL/min. Tests demonstrated that under a pressure ≥ 30 bar, highly selective (>98%) mono-transesterifications could be achieved also with solketal (Scheme 4.12).

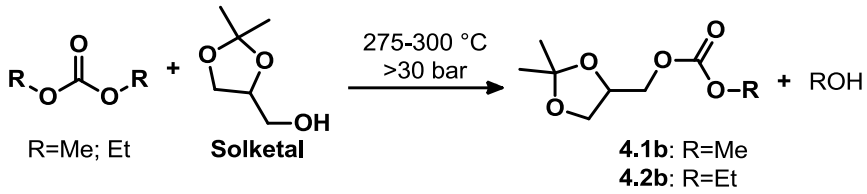

Scheme 4.12. The catalyst-free mono-transesterification of DMC and DEC with solketal

In the case of DMC, the reaction was monitored by changing the operating pressure from ambient up to 100 bar. Periodic GC/MS analyses of mixtures collected at the reactor outlet showed that both the conversion of solketal and the selectivity were steady after a sampling time of 60 min (at any given pressure). Figure 4.9 reports the results.

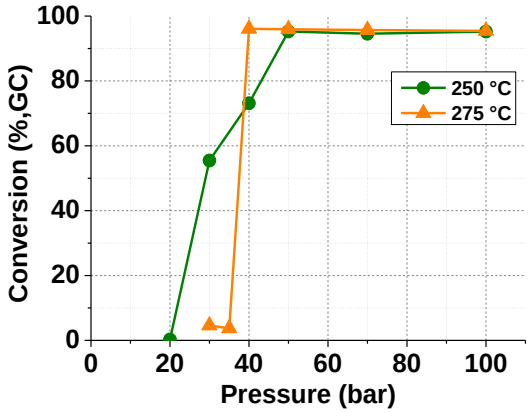

Figure 4.9. Effects of temperature and pressure on the non-catalytic transesterification of DMC with solketal. Isothermal profiles at 250 and 275 °C were obtained under the following conditions: i) molar ratio Q=DMC:solketal=20:1; ii) flow rate=0.05 mL/min; iii) sampling time (at any pressure)=1 hours

The behavior was similar to that observed for the reaction of DMC with GlyF (compare Figure 4.2b and c). This was especially true at 275 °C where an increment of the pressure from 35 to 40 bar allowed a steep enhancement of the conversion from 4 to 96%, respectively (orange curve). A broader profile was observed at 250 °C. Although the onset of the reaction was at 30 bar, the process was almost quantitative only at 50 bar (green curve). The two trends indicated that the lower the temperature, the lower the pressure at which the reaction initiated. Of note, the equilibrium conversion of solketal (>95%) was higher than that achieved for GlyF (~85%) in the same transesterification of DMC.

The reaction carried out at 275 °C was allowed to proceed for 18 hours. Then, the mixture collected at the reactor outlet (54 mL) was vacuum distilled. An almost

quantitative recovery of crude product **4.1b** (5.1 g; purity 96% by GC) was achieved. The structure of such a compound was assigned by GC/MS and NMR spectra.

In the case of DEC, two CF-experiments were carried out at 275 °C under a constant pressure of 30 and 50 bar. The conversion of solketal was 70 and 72%, respectively. This indicated that an equilibrium position was plausibly reached, though at a lower conversion than that achieved with DMC (>95%, Figure 4.9). As for the transesterifications with GlyF, reactions of solketal confirmed that DEC was less active than DMC.

The vacuum distillation of the mixtures (54 mL) recovered after these experiments, allowed to isolate the crude product **4.2b** in a 73% yield (3.2 g; purity 98% by GC), whose structure was assigned by GC/MS and NMR spectra.

4.2.2 Discussion

4.2.2.1 The non-catalytic nature of the reaction.

The present study provides evidence that the investigated CF-transesterification of DAlCs with GAs is triggered by a combined effect of temperature and pressure. Isothermal reaction profiles at T≥ 250 °C, show that the conversion of acetals can be tuned and improved by increasing the operating pressure over a threshold value in the range of 20-50 bar. Then, as expected for reversible processes, the transesterification reaches an equilibrium position with excellent conversions (85-95%) that remain steady for higher pressures (70-100 bar).

This is a general outcome that although with some variations, is observed when both different carbonates react with the same acetal (Figure 4.2 and Figure 4.6), and alternatively, when different acetals react with the same carbonate (Figure 4.2 and Figure 4.9).

The behavior of CF-reactions and the results of batch experiments on the transesterification of DMC with GlyF offer a convincing support for the occurrence of thermal (non-catalytic) processes. Such (thermal) transesterifications are not new reactions, but literature examples are almost exclusively referred to the production of biodiesel. Among the first reported cases in 1998, an investigation proposed a kinetic model for batch reactions of soybean oil with methanol performed at 220-235 °C and 55-60 bar.[69] Thereafter, different fundamental and applied studies demonstrated that the non-catalytic transesterification of vegetable oils conveniently proceeded under both batch and

CF modes in the presence of supercritical light alcohols (sc- methanol and ethanol).[70,71,72,73,74,75] Reaction kinetics took great advantage of the supercritical state. According to some Authors, this was possibly due to a decrease of the dielectric constant of sc-alcohols which favored the oil-in-alcohol miscibility and the formation of a single reacting phase.[70,76] Other benefits were further emphasized by the absence of any catalysts which allowed easy and cheap separation of products (FAME and FAEE).

In the synthesis of biodiesel, also the potential of supercritical DMC (sc-DMC: T_c=284 °C; P_c=48 bar; ρ_c=3.97 g/mL)[77] was explored for batch transesterifications of rapeseed and Jathropha oils.[78,79] These studies showed that at 350 °C and 20 MPa, yields on FAME obtained in sc-DMC were substantially equivalent to those in sc-MeOH. However, in sc-DMC, the nature (thermal, catalytic or both) of the reaction was unclear since the process originated also sizable amounts of citramalic acid that was suspected to act as a catalyst.[80]

4.2.2.2 The reaction of GlyF and DMC.

Notwithstanding the conceptual similarity, the thermal transformations investigated in this work differ from those cited in the case of biodiesel productions, for the important fact that both GlyF, solketal and carbonate products (**4.1a-4.5a**/**4.1a'-4.5a'** and **4.1b-4.2b**) form perfectly homogeneous solutions with DAlCs. Miscibility is therefore not an issue. However, since thermal processes may have substantial activation barriers, they require high reaction temperatures.[81] The relative vapor tension of reactants becomes a crucial factor. Consider, for example, the model case of the CF-transesterification of DMC (bp=90 °C) with GlyF (bp=192-193 °C) (Figure 4.2 and Figure 4.4). At T ≥ 200 °C and ambient pressure, reactants are in the vapor state even though dynamic flow conditions may allow some mixing of gases. As the pressure is increased, the vaporization is more difficult: the high boiling GlyF becomes mostly liquid, while the more volatile DMC initiates to partition between the gas and the GlyF liquid phases. The contact of the reactants starts to be effective as is highlighted by all further increments of the pressure, to the point that intimate interactions between GlyF and DMC allow the reaction to take place. In particular, the sigmoidal-like curves of Figure 4.2 indicate that transesterification starts once the optimal pressure (and the density of the reacting mixture) is reached, which corresponds to an abrupt improvement of the conversion. A hypothesis for this behavior stands on the occurrence of near-critical or supercritical solutions able to favor the contact of reactants and the process kinetics. Although a detailed investigation of this

aspect has not been considered, it should be noted that: (i) in Figure 4.2, p and T (225–300 °C, 20–50 bar) are not far from the supercritical state of DMC which shows a density four times higher than its liquid state.[79] The presence of GlyF in the reacting solutions may possibly alter the supercritical parameters with respect to pure sc-DMC. However, minor changes are expected due to the large excess (up to 20 molar equiv.) of the carbonate; (ii) conversion profiles are consistent with the effect of the temperature and of the DMC:GlyF molar ratio (Q). In Figure 4.2, the increase of the temperature plausibly reduces the density of the reacting mixtures so that a higher pressure is necessary to trigger the process. Figure 4.4, the decrease of the Q ratio originates solutions richer in the denser and less volatile component (under ambient conditions, densities of GlyF and DMC are 1.20 and 1.07 g mL^{-1}, respectively). This favors the contact between reagents and lowers the pressure interval at which the onset of the reaction is achieved; (iii) in general, conversion profiles parallel the isothermal trend of density with pressure displayed by several mixtures and pure compounds during the transition to their supercritical states.

Whether (or not) a sc-state is reached, if the pressure is high enough to maintain the (majority of) reacting mixture as a condensed phase, the contact of DMC and GAs is effective for a productive reaction; while, if the pressure drops below a threshold value, reactants (firstly DMC) rapidly vaporizes as soon as they reached the reactor. The residence time in the reactor is therefore dramatically reduced and so is the conversion. A different approach to consider these aspects, has been devised through a modified Wagner equation (Ambrose 1986) which was used to predict the liquid-vapor pressure profile of pure DMC up to its supercritical state.[82] Wagner invented an elaborate statistical method to develop an equation able to describe the vapor pressure behavior of N_2 and Ar. The modified equation represent the vapor pressure behavior of most substances over the entire liquid range.

$$\text{Ln } P_{vpr} = (a\tau + b\tau^{1.5} + c\tau^{2.5} + d\tau^{5})/T_r \qquad \text{(Eq. 1)}$$

where P_{vpr} is the reduced vapor pressure, Tr is the reduced temperature, and τ is 1-Tr. The values a, b, c and d for pure DMC are -8.24279, 3.25566, -4.2825 and -2.1194 respectively. Figure 4.10 reports the prediction profile.

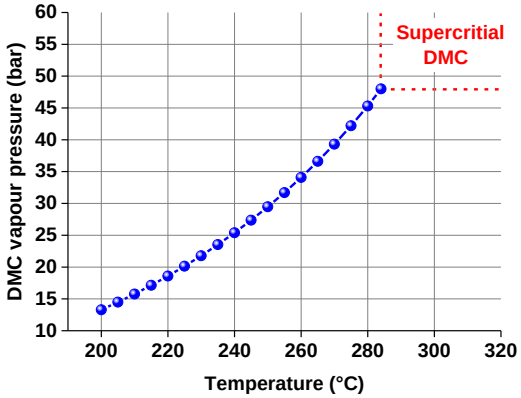

Figure 4.10. Liquid-vapor pressure prediction of pure DMC calculated with the Antoine equation

Notwithstanding the reactant mixture composition was obviously different from pure DMC, the abrupt change of conversion observed at 10, 27 and 38 bar (225, 250 and 275 °C) in the profiles of Figure 4.2 well suited the theoretical curve of Figure 4.10, thereby indicating that thermal reactions plausibly occurs on condition that condensed (liquid) DMC is present in the reactor.

4.2.2.3 Recycle and productivity.

The reversible nature of the transesterification offers an explanation for results of Figure 4.3 and Figure 4.4. In the model case of the reaction of DMC with GlyF, the success of the recycling procedure proves that the transesterification equilibrium may be shifted to the right by increasing the residence time of the reactant mixture in the CF-reactor. This helps to improve the conversion from 85 to 95% (Figure 4.3). On the other hand, the excess of the dialkyl carbonate also exerts a control on the reaction equilibrium. If the Q molar ratio (DMC:GlyF) is decreased, the reduced availability of DMC not only disfavors the conversion, but also the reaction selectivity, and the onset of a double transesterification process is observed (Figure 4.4).

As far as the productivity of both the reactions of DMC and DEC with GlyF, the optimization of the reactant flow rate allows quite satisfactory results, especially if one considers the limited capacity (1 mL) of the CF-reactor used in our study (Figure 4.5 and Figure 4.7). An issue however, may concern the overall convenience of the procedure in terms of energy consumption and safety. In a perspective of a larger scale application, it should be noted that technologies for the integrated heat and energy recovery of modern chemical plants often allow a very cheap access to high temperature (over 200 °C) and

mid-to-low pressure (40-50 bar) conditions. Detailed analyses of these aspects are available in the literature. Consider, for example, sc-transesterification reactions of oils. Although conditions for such processes may be rather severe (270-400 °C and 10-65 MPa), a recent simulation of a biodiesel production carried out for the reaction of natural triglycerides with methanol at 400 °C and 200 bar, has proved that the total energy consumption and the output PEI (potential environmental impact) per mass of product of a plant capacity of 10.000 tons/year, are even lower than that of a conventional base-catalyzed transesterification process.[83] Similar conclusions have been reported by other comparative studies on energy requirements of sc- and catalytic-reactions.[84,85]

4.2.2.4 Different carbonates and GAs.

Isothermal trends of conversion *vs* pressure show a sigmoidal shape also for the transesterification of DEC with GlyF (Figure 4.6). However, with respect to DMC, not only conversion profiles display smoother increases, but also the reaction is more energy demanding. both higher temperatures and pressures are necessary (275-300 °C and 30-70 bar). Among the factors that may account for such a difference, one of the most relevant is the intrinsic lower reactivity of DEC compared to DMC. This behavior, plausibly due to steric reasons, has been confirmed by a number of catalytic processes which include transesterifications and decarboxylations,[53,54,55] etherifications,[56,57,58] and alkylations.[86,87] A very recent study has further substantiated such trend also for thermal reactions: higher activation energies have been measured for transesterifications of vegetable oils carried out in supercritical DEC with respect to analogous transformations in sc-DMC.[88] In analogy to the above discussion, another contribution to results of Figure 4.6 is possibly given by the phase change of the reactants mixture (DEC in particular). This aspect however, can be hardly analyzed because of the lack of thermodynamic data; experiments in Fig. 4.6 take place under conditions very close to the supercritical state of DEC (Tc = 302 °C; Pc = 3.4 MPa),[88] but any information on the density of sc-DEC is unknown, nor a predicted vapour pressure profile for DEC could not be obtained from the Wagner equation for this organic carbonate.

The relative reactivity of the two GlyF isomers should also be considered. Irrespective of the dialkyl carbonate (and of temperature and pressure) used, isomeric products **4.1a** and **4.1a'** and **4.2a** and **4.2a'** are always obtained in the same relative ratio (3:2) of the starting acetals. Unlike our previous findings on base-catalyzed alkylations of

GlyF with DMC,[53] thermal (non-catalytic) conditions level off the relative transesterification rate of 5- and 6-membered ring acetals with both DMC and DEC. This holds true for higher carbonates. At present, no clear explanations can be offered for this behavior.

PC is considerably less reactive than DEC. At 300 °C and 50 bar, the conversion of PC does not exceed 53% (Scheme 4.10). Also in this case, steric reasons may be invoked to account for the result. A support from the literature comes for example, from studies on the synthesis of DMC via the transesterification of cyclic carbonates with methanol. These investigations have demonstrated that slower reactions as well as poorer (even three times lower) equilibrium yields are achieved when the bulkier PC is used instead of EC.[89,90,91] Notwithstanding the moderate reactivity, other properties of PC (mostly the boiling point and the viscosity) make this compound a preferred choice over other cyclic carbonates.

The CF-transesterification of DBnC with GlyF takes place in the presence of acetone as a solvent/carrier. Although this does not allow a direct comparison with the reactivity of other carbonates, the study of DBnC-mediated reactions provides two pieces of evidence: i) the nature of additional solvents may critically affect the thermal process; ii) a non-toxic, cheap, moderately polar and aprotic solvent such as acetone is not only compatible with the CF-setup, but remarkably, it allows quantitative transformations under less demanding conditions with respect to DMC (Figure 4.8, right). These aspects open a window on the potential of eco-friendly solvents for fundamental investigations and innovative preparative protocols in the arena of transesterifications.

To sum up, one should note that further studies are necessary to optimize and implement the CF-reactions of both PC and DBnC with GlyF, especially to improve the conversion and the product separation. The results however, offer a convincing proof-of-concept on the extension of thermal transesterification processes to higher homologues of linear and alkylene carbonates.

A comment should be finally made on the comparison between the two investigated acetals. Both the reactions of GlyF and solketal confirm the lower reactivity of DEC with respect to DMC. However, solketal may offer better results than GlyF. This is well exemplified by the transesterification of DMC carried out at 275 °C and 40 bar. Under these conditions, the equilibrium conversions were 85% for GlyF and 96% for solketal (Figure

4.2c and Figure 4.9). Such a difference can be hardly explained, though the higher density of GlyF (1.21 g/mL) with respect to solketal (1.07 g/mL) might play a role.

4.2.3 Conclusions

This investigation proposes the first reported procedure for the CF thermal mono-transesterification of DAlCs with GlyF and solketal. The method not only offers a clean synthetic route for the reaction, but also identifies a strategy (potentially valuable for large scale preparations and transferable to intensified process equipment) for the selective upgrading of GAs to the corresponding carbonates.

Besides the synthetic scope, the reaction exemplifies a genuine green archetype since it couples innocuous reactants of renewable origin (GAs) to non-toxic compounds such as DAlCs.

The process is triggered by a combined effect of temperature and pressure. Based on the predicted phase behavior of DMC, under isothermal conditions (250-275 °C), the increase of the pressure in the range of 20-38 bar, probably induces a phase transition of the carbonate from gaseous to liquid favoring the contact/mixing of the reactants at the point that the conversion of acetals can be improved up to 95%. On the other hand, the product distribution is tuned by the reactant molar ratio. A 10-molar excess of the dialkyl carbonate conveniently shifts to the right the equilibrium to reach a mono-transesterification selectivity as high as 98%.

Both the recycling operations and the productivity take advantage of CF-conditions. The first (recycle) can be simply implemented through the reuse of mixtures collected from the CF-reactor, without additional purification steps; the second (productivity) can be optimized up to ~70 mg/min according to the design and the capacity of the CF-apparatus. Moreover, the absence of any catalysts allows to run reactions virtually indefinitely with easy and cheap separation of products.

Two further aspects should be commented: i) the investigation carried out so far discloses the potential of a catalyst-free CF-method for the transesterification of a family of linear and alkylene DAlCs with GAs. Though, a case-by-case optimization is necessary and future studies will be required for a practical implementation of the reactions of heavier carbonates (propylene- and dibenzyl-carbonate) by the use of additional solvents; ii) one could be concerned about the energy consumption due to the demanding conditions for

non-catalytic transesterification processes. This problem may be considerably mitigated by modern technologies for heat and energy recovery. Recent examples of such engineering solutions (rather beyond the scope of this Thesis) have been reported for the case of supercritical transesterification of oils. These prove that sc-processes may be even economically advantageous over conventional base-catalyzed transesterification methods

4.2.4 Experimental

4.2.4.1 Materials

Glycerol formal (GlyF), solketal, acetone, 1,2-dimethoxyethane (DME), *n*-tetradecane, dimethyl carbonate (DMC), diethyl carbonate (DEC), propylene carbonate (PC), benzyl alcohol, ethyl acetate (EA), ethyl ether (Et_2O), petroleum ether (PE) and dichloromethane ($CHCl_2$) were ACS grade. They were all from Aldrich and were used as received. Dibenzyl carbonate (DBnC) was prepared via the transesterification of benzyl alcohol with DMC by using a method recently reported by us.[58]

4.2.4.2 Analysis instruments

GC/MS (EI, 70 eV) analyses were run using a HP5-MS capillary column (L=30 m, Ø=0.32 mm, film=0.25 μm). The following conditions were used. Carrier gas: He; flow rate: 1.2 mL/min; split ratio: 1:10; initial T= 50 °C (3 min), ramp rate: 7 °C/min; final T: 250 °C (5 min).

NMR analyses were recorded at a 400 MHz Varian unit. Chemical shift were reported in δ values downfield from TMS; $CDCl_3$ was used as the solvent.

4.2.4.3 CF apparatus

The apparatus used for the investigation was assembled in-house according to the chart of Figure 4.11. A Shimazdu LC-10AS HPLC pump were used to deliver liquid reactants to a stainless steel empty spiral-shaped reactor (1/16" Inner diameter, L=1.6 m, 1.0 mL inner volume). The reactor was placed in a GC oven, equipped with additional thermocouples for temperature control, by which the desired reaction temperature was reached. The outlet of the reactor was connected to a back pressure regulator (JASCO BP-2080) to set and control the operating pressure throughout the process.

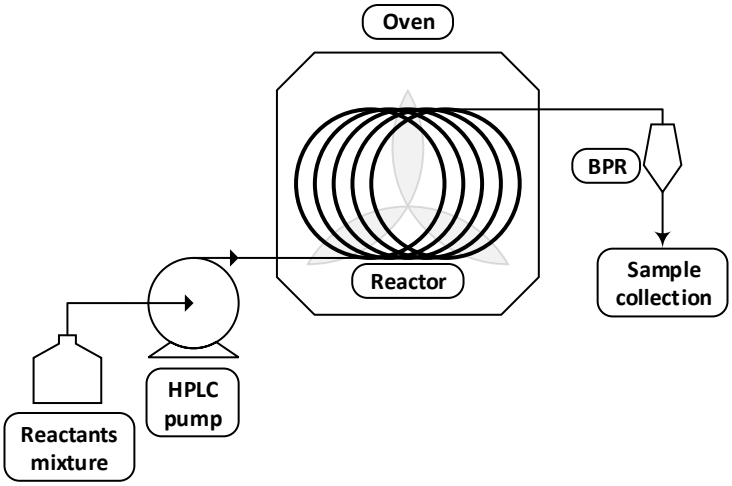

Figure 4.11. Schematic diagram for the in-house built continuous-flow apparatus

4.2.4.4 CF catalyst-free transesterification of DAlCs with GAs

General procedure. In a typical CF non-catalytic transesterification reaction, the following operations were performed. At ambient temperature and pressure, a preliminary conditioning of the apparatus was carried out by delivering 5 mL of the mixture of reactants (molar ratio dialkyl carbonate:glycerol acetal was set to 20, 10, and 5) to the CF-reactor. Afterwards, the BPR was set to the operating pressure (10-100 bar) and the flow rate of the mixture was adjusted to the desired value (0.05-1.00 mL/min). The reactor was then heated at a temperature comprised between 225 and 300 °C. At any given temperature and pressure, the reaction mixture was collected out of the BPR at time intervals of approximately 90 min. Samples were analyzed by GC/MS. Once the experiment was complete, the oven was set to 100 °C and the pumping of reagents was stopped. The overall apparatus was then cleaned by a flow of acetone (50 mL at 0.5 m/mL). The reactor was allowed to cool at rt and the pressure was gradually decreased to the ambient value.

Reaction of GlyF with DMC.

Three solutions of the reactants (51 mL each) were prepared by adjusting the DMC:GlyF molar ratio at 20, 10, and 5. They were obtained by dissolving the same amount of GlyF (3 g, 28.8 mmol) in 48.6, 24.3, and 12.1 mL of DMC. The corresponding molar concentrations were 0.56, 1.08, and 1.97M.

Effect of the pressure and the temperature (Figure 4.2). According to the above described general procedure, a 0.56 M solution of GlyF in DMC (51 mL; DMC:GlyF molar ratio=20) was sent to the CF reactor at a constant volumetric flow rate of 0.05 mL/min. Four isothermal tests were performed by heating the reactor at 225, 250, 275, and 300 °C.

In each test, the pressure was stepwise increased from ambient up to 100 bar. Typical increments were of 5-10 bar. At any given pressure, the reaction was allowed to proceed for 90 min to achieve steady conditions. Then, samples of the mixture were collected at the reactor outlet and analyzed by GC/MS.

Recycling tests (Figure 4.3). According to the above described general procedure, two sets (A and B) of experiments were carried out. In the set A (Figure 4.3, left), a 0.56 M solution of GlyF in DMC (molar ratio DMC:GlyF=20) was delivered to the CF-reactor at a flow rate of 0.05 mL/min. Temperature and pressure were kept constant at 275 °C and 60 bar, respectively. The reaction was allowed to proceed for 18 hours. The mixture collected at the reactor outlet (54 mL) was then analyzed by GC/MS and subjected to a partial distillation at ambient pressure. A total of 5 mL were distilled: they were composed of a MeOH/DMC azeotrope (2.5 mL, 70:30 v/v, bp=62-65 °C) and pure DMC (2.5 mL, bp= 90 °C). The residual solution (49 mL) was added with fresh DMC (5 mL) to restore the initial volume. This mixture was recycled. Under the above described conditions (0.05 mL/min, 275 °C and 60 bar), the mixture was allowed to flow once again through the reactor for 18 hours. Samples were collected at the reactor outlet every 90 min and analyzed by GC/MS. In the set B (Figure 4.3, right), two subsequent reactions were performed using the same procedure of set A except for the fact that no fresh DMC was added after the distillation carried out between the first and the second reaction.

A third recycling test was also run using a 1.08 M solution of GlyF in DMC (molar ratio DMC:GlyF=10). This mixture was set to react at 250 °C and 30 bar for 18 hours. Then, the solution recovered at the reactor outlet (54 mL) was topped by distillation and recycled using the same procedure described for the above described set A.

Effect of DMC:(1a-1a') molar ratio (Figure 4.4). The available solutions of reactants (51 mL each) of GlyF in DMC (0.56 M, 1.08 M, and 1.97 M, respectively; see above) were used in three separate tests. According to the above described general procedure, each mixture was set to react at a constant temperature of 250 °C. The flow rate was 0.05 mL/min. The operating pressure was gradually increased from ambient up to 100 bar, with typical increments of 5-10 bar. At any given pressure, the reaction was allowed to proceed for 90 min to ensure steady conditions. Then, samples of the mixture were collected at the reactor outlet and analyzed by GC/MS.

Effect of the flow rate and estimation of productivity (Figure 4.5). According to the above described general procedure, a 1.08 M solution of GlyF in DMC (molar ratio DMC:GlyF=10) was set to react at 250 °C and 30 bar. The initial flow rate (0.05 mL/min) was stepwise increased up to 0.6 mL/min. Typical increments were of 0.1 mL/min. At any given flow rate, the same volume (10 mL) of the reactants' mixture was delivered to the CF reactor in order to achieve steady conditions with an homogeneous composition of the stream recovered out of the BPR. Samples collected at the end of each test were analyzed by GC/MS. Data of conversion and selectivity were used to evaluate the reaction productivity.

Reaction of GlyF with different carbonates.

In the case of DEC and PC, solutions of the reactants (51 mL each) were prepared to achieve a molar ratio dialkyl carbonate:GlyF=10. They were obtained by dissolving 4.1 g of GlyF (39.4 mmol) in 47.7 mL of DEC and 5.7 g of GlyF (54.6 mmol) in 46.3 mL of PC. The corresponding molar concentrations were 0.77 (DEC) and 1.07 (PC).

DEC (Figure 4.6 and Figure 4.7). According to the above described general procedure, a 0.77 M solution of GlyF in DEC was sent to the CF-reactor at a constant volumetric flow rate of 0.05 mL/min. Three isothermal tests were performed by heating the reactor at 250, 275, and 300 °C. In each test, the pressure was stepwise increased from ambient up to 100 bar. Typical increments were of 5-10 bar. At any given pressure, the reaction was allowed to proceed for 90 min to ensure steady conditions. Then, samples of the mixture were collected at the reactor outlet and analyzed by GC/MS.

Another experiment based on the transesterification of DEC with GlyF was carried out to investigate the effect of the flow rate and evaluate the reaction productivity (Figure 4.7). The test was performed in analogy to that described for DMC (Figure 4.5). A 0.77 M solution of GlyF in DEC was set to react at 300 °C and 50 bar. The initial flow rate (0.05 mL/min) was stepwise increased up to 1 mL/min. Typical increments were of 0.1 mL/min. At any given flow rate, the same volume (10 mL) of the reactants' mixture was delivered to the CF-reactor in order to achieve steady conditions with an homogeneous composition of the stream recovered out of the BPR. Samples collected at the end of each test were analyzed by GC/MS. Data of conversion and selectivity were used to evaluate the reaction productivity.

PC. CF-transesterifications of PC with GlyF were carried out through the same procedure described for DEC. A 1.07 M solution of GlyF in PC was used. The conversion of GlyF was evaluated by a calibration method using *n*-tetradecane (C_{14}) as an external standard (further details are described in Appendix A).

DBnC (Figure 4.8). CF-transesterifications of DBnC (low melting point solid, mp: 34 °C), with GlyF were investigated in the presence of DME and acetone as solvents/carriers. Two mixtures of GlyF, DBnC and the solvent in a 1:5:12 molar ratio, respectively, were prepared. They were obtained by dissolving GlyF (0.69 g, 6.61 mmol) and DBnC (8 g, 33.0 mmol) in DME (8.2 mL) or acetone (5.8 mL). According to the above described general procedure, both the solutions were set to react at 225 and 250 °C, under a constant pressure of 50 bar. The flow rate was 0.05 mL/min. Each reaction was allowed to proceed for 90 min. Then, samples of the mixture were collected at the reactor outlet and analyzed by GC/MS.

Reaction of solketal with different carbonates.

Two solutions of the reactants (51 mL each) were prepared to achieve a molar ratio dialkyl carbonate:solketal=20. They were obtained by dissolving 3.72 g of solketal (28.15 mmol) in 47.4 mL of DMC and 2.64 g of solketal (19.98 mmol) in 48.4 mL of DEC, respectively. The corresponding molar concentrations were 0.55 (DMC) and 0.39 (DEC).

DMC (Figure 4.9). The study on the effect of the pressure and temperature on the thermal transesterification of DMC with solketal was carried out in analogy to that described for the same reaction of GlyF (Figure 4.2). According to the above described general procedure, a 0.55 M solution of solketal in DMC was set to react at 250 and 275 °C. The volumetric flow rate was 0.05 mL/min. In each test, the pressure was stepwise increased from ambient up to 100 bar, with increments of 5-10 bar. At any given pressure, the reaction was allowed to proceed for 90 min to achieve steady conditions. Then, samples of the mixture were collected at the reactor outlet and analyzed by GC/MS.

DEC. The transesterification of DEC with solketal was performed by a procedure similar to that used for DMC (Figure 4.9). A 0.39 M solution of solketal in DEC was set to react at 275 °C. The flow rate was 0.05 mL/min. Two reactions were allowed to proceed for 90 min under a pressure of 30 and 50 bar. Then, mixtures collected at the reactor outlet were analyzed by GC/MS.

4.2.4.5 Isolation and characterization of products

1,3-Dioxan-5-yl methyl carbonate (4.1a) and (1,3-dioxolan-4-yl)methyl methyl carbonate (4.1a'). A CF-reaction was carried out under the conditions of Figure 4.2b (0.56 M solution of GlyF in DMC; 250 °C, 40 bar, 18 hours; F=0.05 mL/min). The mixture (54 mL) collected at the reactor outlet was topped at atmospheric pressure to remove the co-product methanol (as a 70:30 MeOH:DMC azeotrope, bp=62-65 °C). The residual solution (49 mL) was subjected to a second CF-transesterification at 250 °C and 40 bar. A GlyF conversion of 94% was achieved. The final reaction mixture was concentrated by rotary evaporation (50 °C, 40 mbar) and distilled (94 °C, 40 mbar). Title products were obtained as a liquid colorless mixture of isomers in a 92% yield (4.5 g, purity 96% by GC/MS). They were characterized by ^{1}H NMR, ^{13}C NMR and GC/MS (see Appendix A). The ratio **4.1a**:**4.1a'** was approximately the same of the starting isomers of GlyF.

^{1}H NMR ($CDCl_3$, 400 MHz) δ (ppm): 5.04 (s, 1H), 4.89 (m, 2H), 4.81 (d, *J* = 6.2 Hz, 1H), 4.59 (m, 1H), 4.30 (qnt, 1H), 4.25 – 4.13 (m, 2H), 4.07 – 3.92 (m, 5H), 3.80 (s, 3H), 3.79 (s, 3H), 3.73 (dd, *J* = 8.5, 5.4 Hz, 1H). ^{13}C NMR ($CDCl_3$, 100 MHz) δ (ppm): 155.5, 155.1, 95.4, 93.5, 72.8, 68.8, 68.1, 67.2, 66.6, 54.9. Signals in the ^{13}C spectrum of **4.1a**/**4.1a'** were all singlets. GC/MS (relative intensity, 70eV) *m/z*: **4.1a** 162 (M^+, <1%), 161 ($[M-H]^+$, 6), 132 (10), 102 (100), 86 (63), 59 (38), 58 (60), 57 (30), 55 (15), 45 (44), 44 (12), 43 (42); **4.1a'** 162 (M^+, <1%), 161 ($[M-H]^+$, 8), 103 (32), 86 (61), 77 (25), 73 (100), 59 (38), 58 (23), 57 (40), 45 (92), 44 (35), 43 (23).

(2,2-Dimethyl-1,3-dioxolan-4-yl)methyl methyl carbonate (4.1b). A CF-reaction was carried out under the conditions of Figure 4.9 (0.55 M solution of solketal in DMC; 275 °C, 40 bar, 18 hours; F=0.05 mL/min). The final conversion was 95%. The mixture collected at the reactor outlet (54 mL) was concentrated by rotary evaporation (50 °C, 40 mbar) and distilled (99 °C, 40 mbar). Title product was obtained as a colorless liquid in a 93% yield (5.3 g, purity 95% by GC/MS). Compound **4.1b** was characterized by ^{1}H NMR, ^{13}C NMR and GC/MS (see Appendix A).

^{1}H NMR ($CDCl_3$, 400MHz) δ (ppm): 4.38 – 4.29 (m, 1H), 4.19 – 4.15 (m, 2H), 4.08 (dd, *J* = 8.6, 6.4 Hz, 1H), 3.81 – 3.75 (m, 4H), 1.43 (s, 3H), 1.36 (s, 3H). ^{13}C NMR ($CDCl_3$, 100MHz) δ (ppm): 155.5, 109.8, 73.2, 67.9, 66.2, 54.9, 26.6, 25.2. Signals in the ^{13}C spectrum of **4.1b** were all singlets. GC/MS (relative intensity, 70eV) *m/z*: 190 (M^+, <1%), 175 (50), 101 (17), 73 (10), 72 (11), 71 (19), 59 (31), 57 (14), 43 (100), 42 (12), 41 (19).

1,3-Dioxan-5-yl ethyl carbonate (4.2a) and (1,3-dioxolan-4-yl)methyl ethyl carbonate (4.2a'). A CF-reaction was carried out under the conditions of Figure 4.6 (0.77 M solution of GlyF in DEC; 300 °C, 50 bar, 18 hours; F = 0.05 mL/min). The final conversion was 81%. The mixture collected at the reactor outlet (54 mL) was concentrated by rotary evaporation (65 °C, 40 mbar) and distilled (116 °C, 40 mbar). Due to the close boiling points of the unconverted GlyF (~20%) and the products, the distillation was tricky. Title products were obtained as a liquid colorless mixture of isomers in a 73 % yield (5.27 g, purity 98% by GC/MS). They were characterized by ^{1}H NMR, ^{13}C NMR and GC/MS (see Appendix A). The ratio **4.2a**/**4.2a'** was approximately the same of the starting isomers of GlyF.

^{1}H NMR ($CDCl_3$, 400MHz) δ (ppm): 5.0 (s, 1H), 4.9 – 4.9 (m, 2H), 4.8 (d, J = 6.2 Hz, 1H), 4.6 (m, 1H), 4.3 (qnt, 1H), 4.3 – 4.1 (m, 6H), 4.1 – 3.9 (m, 5H), 3.7 (dd, J = 8.5, 5.4 Hz, 1H), 1.3 (dt, J = 7.1, 3.3 Hz, 6H). ^{13}C NMR ($CDCl_3$, 100MHz) δ (ppm): 154.7, 154.3, 95.2, 93.3, 72.7, 68.4, 68.0, 66.8, 66.4, 64.1, 14.0, 13.9. Signals in the ^{13}C spectrum of **4.2a**/**4.2a'** were all singlets. GC/MS (relative intensity, 70eV) *m/z*: **4.2a** 176 (M^+,<1%), 175 ([M-H]$^+$, 1), 116 (14), 86 (34), 57 (28), 55 (12), 45 (32), 44 (100), 43 (31); **4.2a'** 176 (M^+, <1%), 175 ([M-H]$^+$, 2), 91 (10), 89 (11), 86 (38), 73 (57), 58 (21), 57 (42), 45 (100), 44 (42), 43 (29).

(2,2-Dimethyl-1,3-dioxolan-4-yl)methyl ethyl carbonate (4.2b). A 0.39 M solution of solketal in DEC was set to react in the CF-mode at 275°C and 50 bar, for 18 hours (F = 0.05 mL/min). The final conversion was 72%. The mixture collected at the reactor outlet (54 mL) was concentrated by rotary evaporation (65 °C, 40 mbar) and distilled (102 °C, 40 mbar). The title product was obtained as a liquid colorless in a 76% yield (3.28 g, purity 98% by GC/MS). Compound **4.2b** was characterized by ^{1}H NMR, ^{13}C NMR and GC/MS (see Appendix A).

^{1}H NMR ($CDCl_3$, 400MHz) δ (ppm): 4.33 (m, 1H), 4.24 – 4.13 (m, 4H), 4.08 (dd, *J* = 8.5, 6.4 Hz, 1H), 3.78 (dd, *J* = 8.5, 5.8 Hz, 1H), 1.42 (s, 3H), 1.35 (s, 3H), 1.30 (t, *J* = 7.1 Hz, 3H). ^{13}C NMR ($CDCl_3$, 100MHz) δ (ppm): 154.7, 109.6, 73.1, 67.5, 66.0, 64.0, 26.4, 25.1, 14.0. Signals in the ^{13}C spectrum of **4.2b** were all singlets. GC/MS (relative intensity, 70eV) *m/z*: 204 (M^+,<1%), 189 (39), 161 (31), 101 (27), 72 (12), 61 (10), 59 (18), 57 (25), 43 (100), 42 (10).

Benzyl 1,3-dioxan-5-yl carbonate (4.5a) (1,3-dioxolan-4-yl)methyl benzyl carbonate (4.5a'). A mixture of GlyF:DBnC:acetone in a 1:5:12 molar ratio, respectively,

was allowed to react for 4 hours at 250 °C and 50 bar (F=0.05 mL/min). The final conversion of GlyF was 94%. The reaction mixture was concentrated by rotary evaporation (50 °C, 40 mbar), but the title product could not be isolated by further distillation under vacuum. The oily residue (2 g, after rotary evaporation) was subjected to flash column chromatography (FCC) over silica gel, by using a petroleum ether (PE)/diethyl ether (Et_2O) 1:1 *v/v* solution (column L=8 cm, Ø=2.5 cm) as the eluent. Under such conditions, isomers **4.5a** and **4.5a'** were both isolated in a pure form (98% by GC/MS): the first product (**4.5a**) was a colorless liquid, while the second compound (**4.5a'**) slowly crystallized on standing. They were characterized by GC/MS, ^{1}H NMR and ^{13}C NMR (2D-NMR spectra were also available for compound **4.5a'**; see Appendix A).

^{1}H NMR ($CDCl_3$, 400MHz) δ (ppm): **4.5a** 7.5 – 7.3 (m, 5H), 5.2 (s, 1H), 4.9 (d, *J* = 6.2 Hz, 1H), 4.8 (d, *J* = 6.3 Hz, 1H), 4.7 – 4.6 (m, 1H), 4.0 (dd, *J* = 12.1, 2.8 Hz, 1H), 4.0 (dd, *J* = 12.1, 4.3 Hz, 1H); **4.5a'** 7.5 – 7.3 (m, 5H), 5.2 (s, 2H), 5.0 (s, 1H), 4.9 (s, 1H), 4.3 (m, 1H), 4.3 – 4.2 (m, 2H), 4.0 (dd, *J* = 8.5, 6.7 Hz, 1H), 3.7 (dd, *J* = 8.5, 5.4 Hz, 1H). ^{13}C NMR ($CDCl_3$, 100MHz) δ (ppm): **4.5a** 154.3, 140.8, 134.7, 128.4, 128.2, 93.4, 69.8, 68.8, 68.0; **4.5a'** 155.0, 135.1, 128.7,128.7, 128.5, 95.6, 73.0, 70.0, 67.4, 66.8. Signals in the ^{13}C spectrum of **4.5a** and **4.5a'** were all singlets. GC/MS (relative intensity, 70eV) *m/z*: **4.5a** 238 (M^+, 1%), 107 (15), 92 (10), 91(100), 77 (10), 65 (17), 57(10); **4.5a'** 238 (M^+, <1%), 147(17), 107(17), 92 (18), 91(100), 79 (10), 77 (15), 73 (11), 65 (19), 57 (15), 45 (24).

1,3-dioxan-5-yl (1-hydroxypropan-2-yl) carbonate (4.3a), (1,3-dioxolan-4-yl)methyl (1-hydroxypropan-2-yl) carbonate (4.3a'), 1,3-dioxan-5-yl (2-hydroxypropyl) carbonate (4.4a) and (1,3-dioxolan-4-yl)methyl (2-hydroxypropyl) carbonate (4.4a'). A 1.07 M solution of GlyF in propylene carbonate was set to react for 4 hours at 300 °C and 50 bar (F=0.05 mL/min). The final conversion of GlyF was 48%. The reaction mixture was concentrated by rotary evaporation (50 °C, 40 mbar), but the title product could not be isolated by further distillation under vacuum. Also, any attempt to purify and separate compounds **4.3-4.4** by FCC was not successful. The oily residue was analyzed by GC/MS. Structure of products **4.3-4.4** were assigned by comparison of their MS spectra to those of starting acetals (GlyF) (see Appendix A).

GC/MS (relative intensity, 70eV) m/z: **4.3a** 206 (M+, <1%), 131 (45), 102 (18), 87 (41), 85 (44), 71 (11), 59 (84), 58 (38), 57 (65), 55 (11), 45 (100), 44 (68), 43 (56), 42 (11), 41 (38), 39 (17); **4.3a'** 206 (M+, <1%), 131 (46), 87 (52), 85 (69), 73 (19), 71 (12), 59 (87), 58 (18), 57 (100), 45 (86), 44 (31), 43 (56), 42 (12), 41 (38), 39 (22); **4.4a** 206 (M+, <1%),

131 (27), 87 (50), 85 (39), 73 (12), 59 (71), 58 (70), 57 (77), 45 (100), 44 (30), 43 (54), 42 (13), 41 (29), 39 (18); **4.4a'** 206 (M+, <1%), 117 (12), 88 (15), 87 (24), 75 (13), 73 (27), 72 (10), 71 (10), 59 (59), 58 (19), 57 (45), 45 (100), 44 (25), 43 39), 42 (10), 41 (21), 39 (12).

4.3 Catalyst-free transesterification of DMC with 1,*n* diols and glycerol

The above described results of the CF-transesterification of DAlCs with GAs have stimulated a further investigation on the potential of such thermal (catalyst-free) protocol for the upgrading of several model 1,*n*-diols including ethylene glycol (EG, **4.7**), 1,2-propanediol (PG, **4.6**), 1,3-propanediol (1,3-PD, **4.8**), 1,3-butanediol (1,3-BD, **4.9**), and 1,4-butanediol (1,4-BD, **4.10**)], and even most remarkably, of glycerol (**4.11**) (Figure 4.12).

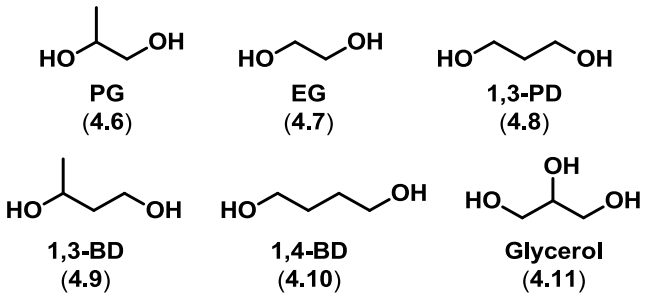

Figure 4.12. 1,*n*-diols and glycerol used for the thermal transesterification of DMC

To the best of our knowledge, no previous studies have been ever reported on this subject. Before investigating the process under CF-conditions, some explorative tests were carried out also under batch conditions in a steel autoclave. The screening of these reactions not only proved the feasibility of the process, but it demonstrated that: i) regardless of batch or CF-conditions, 1,2-diols were converted into the corresponding five-membered ring carbonates [ethylene carbonate (EC) and propylene carbonate (PC)] with a very high selectivity (up to 95%); ii) glycerol yielded glycerol carbonate (GlyC) in the CF-mode (250 °C and 50 bar), while either GlyC or its transesterification derivative [methyl (2-oxo-1,3-dioxolan-4-yl) methyl carbonate] could be selectively obtained under batch conditions (88% and 82%, respectively at 180 °C); iii) due to the moderate stability of six-membered ring carbonates, 1,3- and 1,4-BD always formed mixtures of the corresponding cyclic and linear (mono- and di-) transesterification derivatives.

The results of this study have been the object of a publication on the ACS journal *ACS Sustainable Chemistry and Engineering* which, for the part developed within this Thesis work, is described in the following paragraphs.[92]

4.3.1 Results and Discussion

Reactions were carried out under both batch and CF-conditions. Due to the relatively high temperatures used (120-220 °C), batch reactions were carried out in a stainless-steel

90-mL autoclave, while CF-experiments were performed by using an apparatus similar to that described for the catalyst-free transesterification of DAlCs with GAs, with a CF-reactor in the form of 1/16" steel tube of a capacity of 1.7 mL. Further details are in the experimental section.

4.3.1.1 Batch reactions of 1,2-diols with DMC

An initial investigation was carried out on the reaction of DMC with both EG (**4.6**) and PG (**4.7**).

Mixtures of DMC and the chosen diol were prepared in different molar ratios (Q=DMC:diol) Q = 2.5, 5, 10, and 20, and they were set to react for 5 h, in an autoclave, at 120, 150, 180, and 220 °C. All tests were repeated at least twice to check for reproducibility.[93] The screening definitely proved the feasibility of the thermal reaction: under the best found conditions (150 °C and Q=5), the diol conversion and selectivity towards the corresponding cyclic carbonate (**4.6a** and **4.7a**) were ~100% and 87-95%, respectively (Scheme 4.13). Particularly, the highest selectivity (95%) was achieved for PC. Minor by-products were mono- and di-transesterified derivatives **4.6b** and **4.7b**, **4.6b'**, and **4.6c** and **4.7c**.[57] The structure of all products was assigned by GC/MS analyses and by comparison to commercial samples.

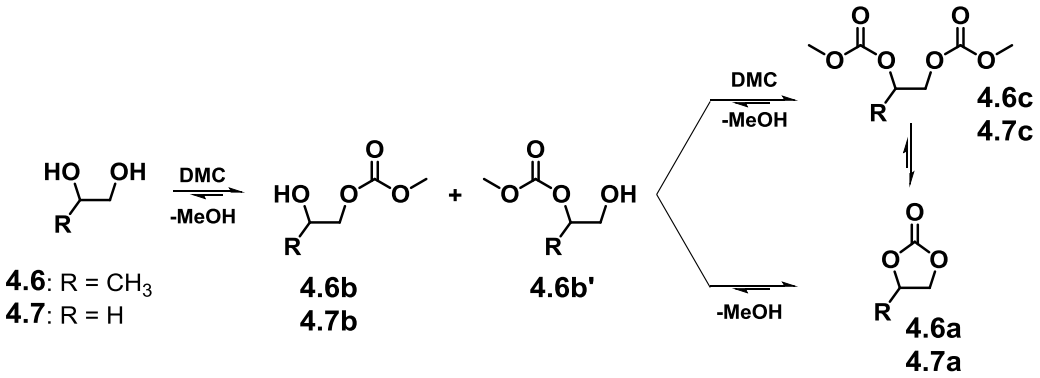

Scheme 4.13. Products observed in the batch catalyst-free reaction of 1,2-diols with DMC

The results are reported in Figure 4.13a) and b) which show the profiles of conversion and selectivity for cyclic carbonates (**4.6a** and **4.7a**) as a function of the Q (DMC:diol) molar ratio, for reactions carried out at 150 °C.

The transesterification of DMC with PG showed that at Q=2.5, the conversion and the selectivity did not exceed 78% and 67%, respectively (Figure 4.13a): the formation of sizeable amounts (33%) of unidentified by-products was noticed. The increase of the Q

ratio to 5 brought about a remarkable improvement of the reaction outcome: not only the process became quantitative, but propylene carbonate was the almost exclusive product. Then, neither the use of a higher DMC excess (Q>5) nor the increase of the temperature above 150 °C produced appreciable variations of the conversion or the products distribution.

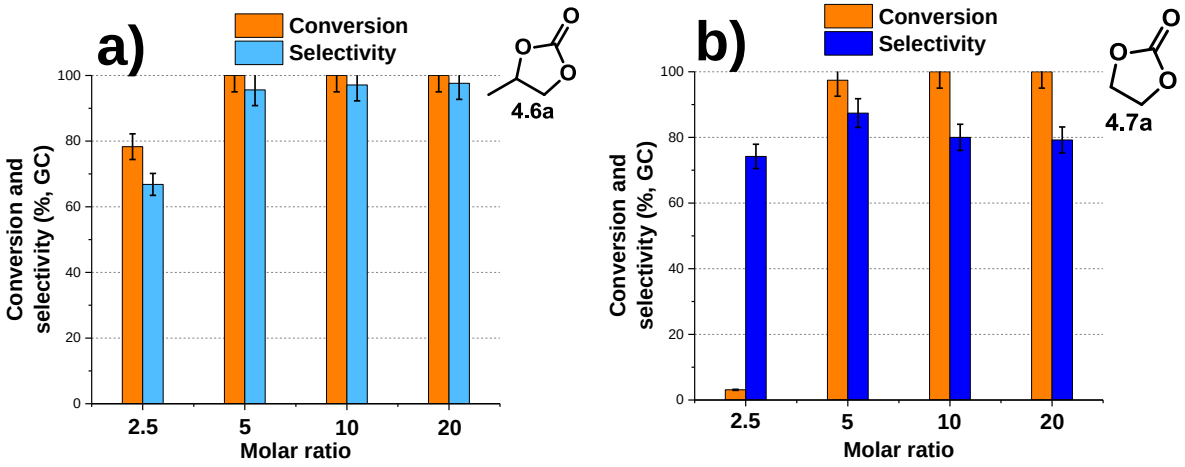

Figure 4.13. a) and **b)** Reaction of PG and EG with DMC, respectively. The conversion of diols and the selectivity toward alkylene carbonates **4.6a** and **4.7a** are shown as a function of Q (DMC:diol) molar ratio. Other conditions: 150 °C, 5 h.

To rule out any metal catalysis by the reactor and therefore to prove the authentic catalyst-free nature of the process, a test was run at 150 °C by loading the reactants mixture (DMC and PG in a Q ratio of 5) in a glass reactor placed inside the autoclave. The result was identical to that described in Figure 4.13a (Conversion: 100%; **4.6a**>95%).

EG proved remarkably less reactive than PG. This was manifest when a Q ratio as low as 2.5 was used. The conversion of PC and EC were 78% and 2%, respectively [cfr. Figure 4.13 a) and b)]. However, also for EG, a more than satisfactory result was achieved by using a moderate DMC excess (Q≥5), which allowed to reach a complete conversion and a selectivity towards EC (**4.7a**), though not as good as that for **4.6a**, of 87%.

Of note, no reaction took place at 120 °C with both PG and EG.

The results of batch thermal tests were then compared to those obtained in a previous study of our group, on the organocatalytic transesterification of DMC with PG and EG.[57] This analysis indicated that, although the catalytic method was less energy intensive (reactions took place at T≥90 °C) than the thermal one, the two procedures offered comparable selectivities at complete conversion, and proved the same reactivity trend for

the investigated 1,2-diols, in particular the easier formation of PC (**4.6a**) with respect to EC (**4.7a**). In this respect, different Authors have proposed that the presence of alkyl substituents in the carbon chain of the diol may facilitate intramolecular transesterification reactions with the formation of small carbonate rings.[94,95] These observations are often described within the many variations proposed for the so called "gem-disubstituent effect": the concept – originally formulated by Thorpe and Ingold[96] – has been reviewed in 2005 by Jung and Piizzi,[97] that offered an analysis of fascinating early and recent theories based on the mutual repulsion of substituents (valency deviation), and the effect of reactive rotamers.

4.3.1.2 CF-reactions of 1,2- and 1,n-diols with DMC

The thermal transesterification of DMC with PG was explored as a model reaction in the CF-mode. For initial tests, a solution of DMC and PG in a 5:1 molar ratio was used. Four isobaric experiments were run at 50 bar, while the temperature was progressively increased from 150 to 180, 220, and 240 °C. Then, five isothermal reactions were carried out at 240 °C, by decreasing the pressure from 40 to 20, 15, 10, 5 bar, and finally, to ambient. In all case, the reactant solution was delivered at 0.1 mL/min. Figure 4.14 reports the reaction conversion as a function of both the pressure and the temperature. In all cases, the selectivity (not reported in Figure 4.14) towards propylene carbonate (**4.6a**) was always >94%.

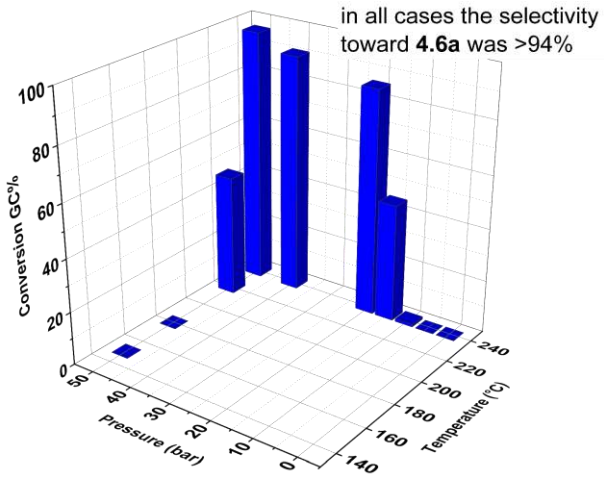

Figure 4.14. CF-reaction of PG with DMC. Conversion of PG in function of temperature and Pressure. Other conditions: DMC:PG molar ratio, Q=5; flow rate: 0.1 mL/min. In repeated tests, values of conversion differed by less than 5% from one reaction to another

At 50 bar, the reaction was triggered at 220 °C and went to completion at 240 °C (Figure 4.14: left to right), *i.e.* at a quite higher temperature than that required for batch experiments (150 °C). However, given the reactor volume (1.7 mL) and the operating flow rate were (0.1 mL/min), the corresponding residence time (τ) was of only ~15 min (compared to 5 hours of batch reactions). An energy input was therefore necessary to impart sufficiently fast kinetics to the CF-reaction. Different Authors have reported that OH groups of both alcohols and phenols could deprotonate through autoprotolysis at high temperatures (250-380 °C) in the absence of any catalyst (Scheme 4.14).[98,99,100,101]

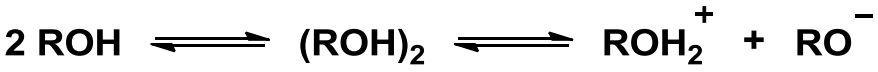

Scheme 4.14. Autoprotolysis of an alcohol occurring at high temperatures

If so, in the reaction of Figure 4.14, the alcohol might play a double role as a reactant and an acid catalyst for the process.

Even more interesting was the trend of conversion in function of the pressure. At 240 °C, no reaction occurred below 15 bar, while a sharp increase of the substrate conversion (from 1–2 to ~85%) was noted for small increments of the pressure in the range of 15–20 bar. At higher pressures, only an additional 10% improvement of the conversion (up to 95%) was observed.

This peculiar behavior matched our previous results on thermal reactions of GAs, thereby confirming the key role played on these transformations by phase transitions. If the pressure was high enough to maintain the (majority of) reacting mixture as a condensed phase, the contact of DMC and PG was effective for a productive reaction. However, if the pressure dropped below a threshold value, reactants rapidly vaporized as soon as they reached the reactor. Notwithstanding that the reactant mixture composition was obviously different from pure DMC (5:1 compared to 20:1 of Figure 4.2), the abrupt change of conversion observed at 15–20 bar well suited the theoretical profile of Figure 4.10.

Overall, if compared to the limited capacity (~1.7 mL) of used CF-reactor, CF-experiments allowed a satisfactory productivity up to 22 mg/min of **4.6a**. Once the thermal regime was reached, the CF-system could operate virtually indefinitely under the desired autogenous pressure; the latter had to be monitored and controlled, but no highly expensive compression/decompression cycles were involved. The high reaction

temperature apparently implied an energetic issue which however, could be efficiently mitigated by integrating the thermal reaction in a waste heat recovery system. Particularly, modern biorefinery units are developing elegant sustainable designs for heat recovery or exchange within heat sinks and the usage of excess heat as part of the cogeneration plants.[102]

The CF-reactions of DMC with EG (**4.7**), 1,3-propandiol (**4.8**), 1,3-butanediol (**4.9**) and 1,4-butanediol (**4.10**) were then explored Case by case, the reactants mixture was prepared by using the minimum amount of DMC able to ensure the formation of a homogeneous solution. All experiments were carried out at 50 bar. Although reactions were far from being optimized, Scheme 4.15 (and Scheme 4.13) shows the structure of the observed products, while Table 4.2 summarizes the best preliminary results achieved in terms of conversion and selectivity towards each of the obtained derivative.

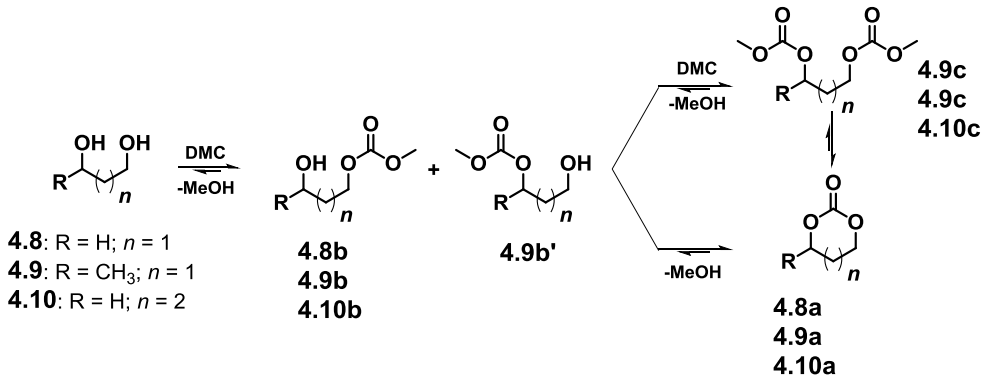

Scheme 4.15. Products observed in the catalyst-free CF-reaction of 1,2- and 1,n-diols with DMC

Table 4.2. The reaction of DMC with diols **4.7**, **4.8**, **4.9** and **4.10**

Entry	Diol	DMC:diol Molar ratio[a]	T (°C)	Conversion[b] (%)	Reaction products Selectivity[c] (%)		
1	**4.7**	14	240	99.5	**4.7a** (82)	**4.7b** (7)	**4.7c** (11)
2	**4.8**	19	260	75.0	**4.8a** (14)	**4.8b** (53)	**4.8c** (22)
3	**4.9**	6	240	94.0	**4.9a** (17)	**4.9b**+**4.9b'** (39)	**4.9c** (32)
4	**4.10**	19	280	99.5		**4.10b** (18)	**4.10c** (82)

[a] The DMC:diol molar ratio was adjusted case-by-case to obtain a homogeneous mixture.

[b] Reaction conversion was determined by GC.

[c] Selectivity towards each product was determined by GC. The structure of products **4.7a**, **4.8c**, **4.9c**, and **4.10c** was assigned by comparison with previously prepared authentic compounds;[57] products **4.9a**, **4.8b**, and (**4.9b**+**4.9b'**) were isolated and their structure was assigned by NMR and MS characterization (see experimental); the structure of products **4.8a**, **4.7b**, **4.7c** and **4.10b** was assigned from their GC/MS spectra. The reaction of diols **4.8** and **4.9** also produced unidentified by products (8% and 12% of total products, respectively).

As did PG, also EG yielded the corresponding cyclic carbonate with a high selectivity (**4.7a**:82%, entry 1); while, both 1,3- and 1,4-diols favored the formation of linear products derived from mono- or di- transesterification reactions (**4.8b**, **4.9b+4b.9', 4.10b** and **4.8c-4.10c,** respectively; entries 2-4). The situation was particularly evident for 1,4-butanediol (**4.10c**:82%). This reflected the general trend that favors 5-exo-dig over 6-exo-dig ring closure (C_5- and C_6-, respectively):[103] specifically, for OCs, the greater thermodynamic stability of C_5- with respect to C_6-cyclic derivatives was reported in many cases.[104,105] An analogue behavior was observed for the catalytic transesterification of DMC with 1,*n*-diols, where for $n \geq 3$, di-carbonate derivatives were by far the preferred products.[57] However, thermal CF-reactions of Table 4.2 allowed to isolate and characterize mono-transesterification compounds [**4.8b** and isomers (**4.9b**+**4.9b'**)] as well as the less common C_6-carbonate **4.9a**.[106]

4.3.1.3 The thermal (cat.-free) reaction of glycerol with DMC

Foreword: batch conditions. The batch thermal reaction of glycerol and DMC was investigated as a part of master Thesis program carried out in our research group.[107] Some of the major results are briefly summarized in the introductory section (foreword) of the present paragraph. These results help to describe the subsequent phase of the investigation related to the study of the same reaction under CF-conditions.

At T≥180 °C, not only the batch reaction of DMC with glycerol (**4.11**) took place in the absence of any catalyst, but the products distribution could be tuned by controlling both the time and the reactants molar ratio (Q=DMC:glycerol). At the best found conditions, two major products could be selectively achieved:

i) if the reaction was run for 1 hour at a Q ratio of 20, glycerol was almost quantitatively converted (94%), and glycerol carbonate (**4.11a**) was observed with a selectivity as high as 86%. The thermal reaction proceeded at a rate of ~0.53 mol L^{-1} h^{-1} (with respect to glycerol). Among the most effective catalytic procedures recently reported for the transesterification of DMC with glycerol, it was claimed that in the presence of Ca–La mixed-oxide catalysts, the reaction took place at 90 °C, but the overall rate (0.14 mol L^{-1} h^{-1}) was three times lower than that of the thermal transesterification.[108] Moreover, in the same work, the selectivity towards **4.11a** did not exceed 85%.

ii) if the reaction was run for 5 hours at a Q ratio of 60, multiple transesterification processes occurred resulting in the highly selective formation of methyl [(2-oxo-1,3-

dioxolan-4-yl)methyl] carbonate (compound **4.11b**). This compound was isolated in a 78% yield.

In both cases i) and ii), the DMC excess was completely recovered by distillation and recycled.

Scheme 4.16 summarizes the most plausible reaction pathways accounting for the products observed during the reaction.

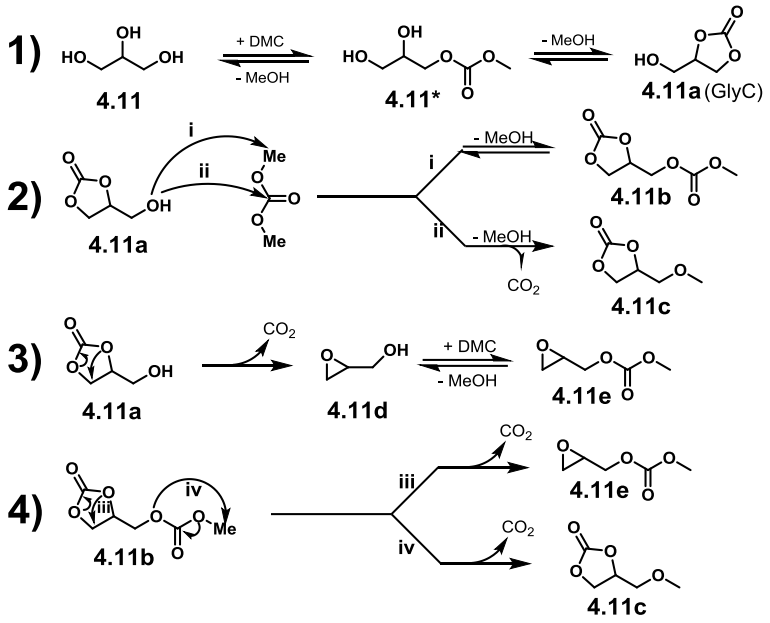

Scheme 4.16. The reaction of glycerol with DMC: major products and pathways for their formation

The process likely involved the double transesterification of glycerol to produce 2,3-dihydroxy propyl methyl carbonate (**4.11***) followed by the (more stable) five-membered ring product glycerol carbonate **4.11a** (Eq. 1). These equilibrium reactions were affected by the reactants molar ratio (Q). Results (not shown here)[92] indicated that the higher the relative amount of DMC (Q≥40), the larger the extent of a further (third) transesterification yielding carbonate **4.11b** (Eq. 2, path ii). A direct methylation of **4.11a** also occurred to produce compound **4.11c** (Eq. 2, path i). This compound however, was observed only in trace amounts consistently with the higher activation barrier of methylations with respect to transesterification reactions promoted by DMC.[45,53] Finally, glycidol (**4.11d**) and its methyl carbonate derivative [**4.11e**: methyl (oxiran-2-ylmethyl) carbonate] plausibly derived from decarboxylation processes of carbonates: these reactions have been previously described by us and by others (Eqn. 3 and 4).[109,110]

Besides being effective for the synthesis of either compound **4.11a** or its derivative **4.11b**, the study of the batch thermal reaction of DMC and glycerol also highlighted a

simple expedient to further control the outcome of the process. In fact, the regulation of the heating rate and the thermal inertia of the reactor (autoclave) could be an issue since the reaction could sometimes run out of control yielding products of multiple transesterification and undesired unidentified derivatives. It was noticed that at 180 °C operating under an additional pressure of CO_2 (20-to-50 bar), the reaction rate was decreased, but the selectivity towards **4.11a** was improved to 88% at a conversion of 94%. After 5 hours, glycerol carbonate (**4.11a**) was isolated in a 84% yield. By contrast, if CO_2 was substituted with an equal pressure of He, Ar, or N_2, respectively, the amount of glycerol carbonate was at best, ~35% at complete conversion. In this respect, CO_2 might also decrease, if not prevent, the occurrence of the above described decarboxylation reactions. A similar result has been described also in the catalytic liquid phase oxidation of *p*-xylene carried out in CO_2-expanded solvents.[111] However, it was not only the mere action of the operating pressure, but also the nature of the added gas, played a crucial role. For sure, the direct carboxylation of glycerol with CO_2 did not occur under the explored conditions. This transformation not only requires high T and p (180 °C and 50 bar), but also highly active catalysts (CeO_2) and powerful dehydrating co-reagents.[112] Other factors should therefore be considered. For example: i) at 180 °C, in the range 10-50 bar, the density of CO_2 varies between 0.015 and 0.06 g/mL, similar to Ar, but, on average, twice as high as N_2 and 10-fold higher than He;[113] ii) at 25 °C, the Henry constants for CO_2, Ar, N_2 and He in a model polar liquid such as methanol are 601, 10330, 17310 and 85500 Pa m^3 mol^{-1}, meaning that CO_2 is from 17- to 143-fold less soluble than other considered gases;[114] iii) at 25 °C and 70 bar, the viscosity for CO_2, Ar, N_2 and He are of 54.2, 24.1, 19,1 and 19.6 μPa·s^{-1}.[115,116] Not to mention the clustering effects that may operate in the proximity of the supercritical state (sc) of CO_2 (Figure 6: at P_{CO2} = 50 bar; see note 28).[117]

Further considerations are discussed in the above mentioned paper recently published by our group.[92]

4.3.1.4 CF-reaction of glycerol with DMC

Based on the study of the batch thermal reaction of glycerol and DMC, the work of this Thesis was focused at implementing the same reaction under CF-conditions. A first remarkable issue for the development of a CF-protocol was the complete lack of miscibility of the reactants at rt. Irrespective of their relative amounts and flow rates, when glycerol and DMC were delivered separately to the CF reactor, undesired side-reactions could not

be avoided: in particular, processes producing both glycidol (**4.11d**) and its transesterification derivative **4.11e**. These products rapidly formed polymeric-like materials[118] which eventually clogged the reactor. Table 4.3 shows some of the most representative results obtained under CF-investigation at different T and p.

Table 4.3. CF reaction of DMC with glycerol in function of pressure, temperature and molar ratio. $F_{glycerol}$=0.01 mL; F_{DMC}=0.06 mL/min

Entry	p (bar)	DMC:glycerol Molar ratio	T (°C)	Conversion[a] (%)	Selectivity (%)[a]		
					4.11a	4.11d	Others[c]
1	1	5	250	4	30	70	0
2	5	5	250	99	2	85	13
3		5	275	99	1	84	15
4	50	5	250	99	55	20	25
5	100	5	250	99	60	15	25

[a] The conversion of glycerol and the selectivity towards products 411.a, 4.11d, and "others" were determined by GC, after 2 hours.

[b] Total of other products including **4.11b**, **4.11c** and **4.11e**

At T≥250 °C, the reaction did not substantially occur at ambient pressure (entry 1), but the conversion of glycerol was quantitative in all experiments carried out at p≥ 5 bar. The operating pressure not only affected the conversion, but even more remarkably, the products distribution.

At 5 bar, the analysis of the mixture collected at the reactor outlet after 2 hours, proved the formation of glycidol as a major product (up to 85%: entries 2 and 3). Beside the decarboxylation of glycerol carbonate (Eq. 3 of Scheme 4.16), another reasonable pathway for the formation of glycidol was the direct 1,2-elimination of water from glycerol (Scheme 4.17).[119] The latter reaction could be facilitated by the high temperature and the modest DMC excess used for CF-reactions with respect to the above described batch processes (see previous paragraph).

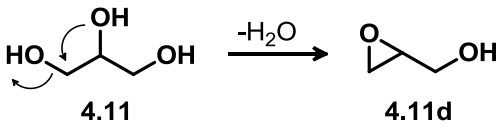

Scheme 4.17. The formation of glycidol via the direct 1,2-elimination of water from glycerol

However, CF-tests must be stopped soon after the formation of glycidol because of the clogging of the apparatus. This was due to the deposition of a highly viscous molasses-

like liquid inside the reactor. Figure 4.15 shows some pictures of the material recovered. If the vial containing the compound was turned upside down, more than 7 mins were required for a drop of the liquid to exit.

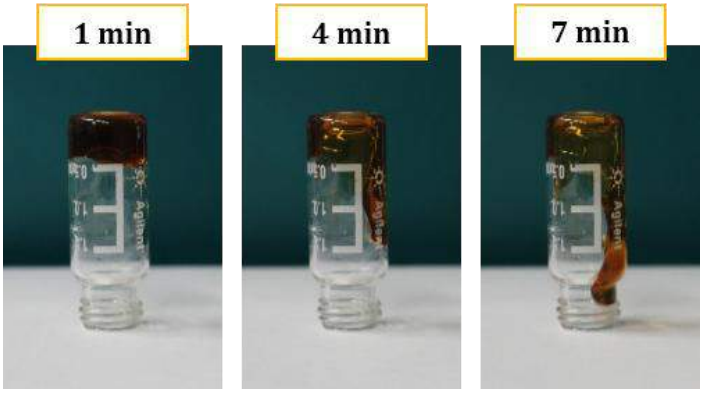

Figure 4.15. Molasses-like liquid recovered in the CF-reaction of DMC and glycerol at 5 bar after 2 hours

The high temperature used for CF-experiments and the reactivity of glycidol (**4.11d**) which formed as an initial product, plausibly triggered side-polymerization reactions responsible for the formation of the observed molasses-like product. Although the determination of the structure of this organic deposit was beyond the scope of the work, both ^{1}H and ^{13}C NMR spectra of such a compound (labelled as *glycidol polymer*) were acquired and compared to those of a commercially available standard of diglycerol. Results are reported in Figure 4.16.

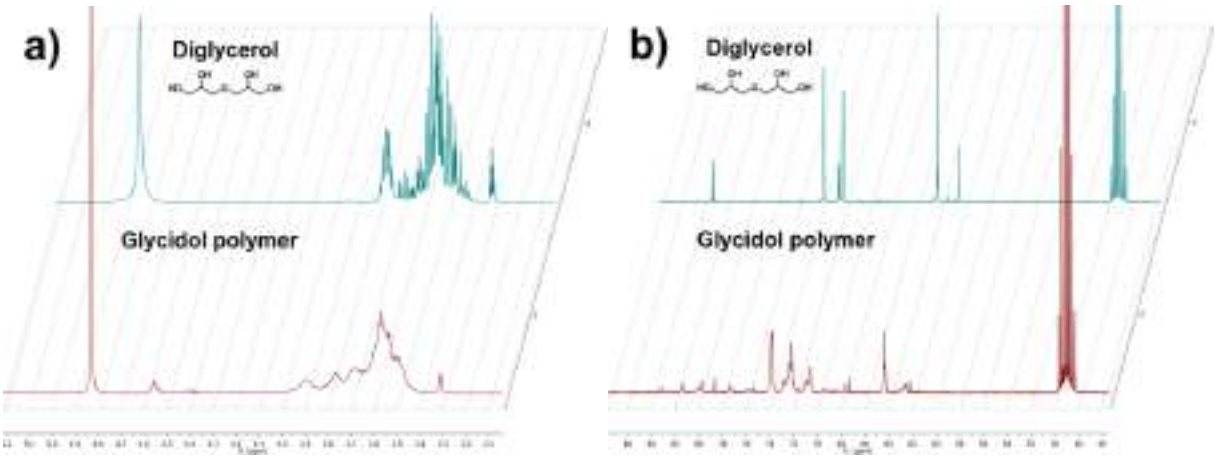

Figure 4.16. a) ^{1}H NMR and **b)** ^{13}C NMR of diglycerol and the molasses-like liquid (*glycerol polymer*) recorded in CD_3OD

A sort of diglycerol fingerprint could be recognized in both ^{1}H and ^{13}C NMR spectra, thereby suggesting that the organic deposit isolated after the CF-experiments was a polymer (or a polymeric mixture) constituted by a glycerol backbone. Moreover, the

deposit exhibited an excellent solubility in water comparable to that of all glycerol-derived oligomers and polymers.[120]

A significantly different distribution of products was noticed when the CF-reaction of glycerol with DMC was performed at a high working pressure of 50 and 100 bar, respectively. In this case, glycerol carbonate (**4.11a**) was the main product although the corresponding selectivity never exceeded 60% (Table 4.3, entry 4 and 5). The high pressure plausibly limited the extent of the decarboxylation of glycerol carbonate (Eq. 3: Scheme 4.16) and the subsequent formation of glycidol to a maximum 20% amount. Results however, were still not satisfactory. The use of a co-solvent was considered to implement additional CF-reactions in which a homogeneous solution of reactants was delivered to the reactor. Among the several solvents tested, methanol offered the best option.

Screening experiments were carried out by varying T, p, and the DMC:MeOH molar ratio in the range of 230-250 °C and ambient to 50 bar (Table 4.4). The best results were achieved at 50 bar and 230-250 °C, by feeding the CF-reactor at 0.1 mL/min with a mixture of DMC, methanol, and glycerol in a 10:6:1 molar ratio (**Q**), respectively (entries 1-3: Table 4.4). For an easier visualization, these data are also displayed by Figure 4.17.

Table 4.4. Screening experiments for the CF reaction of DMC with glycerol using MeOH as a co-solvent.

Entry	Molar ratio[a]		P	T	Conversion[b]	Selectivity (%)		
	DMC	MeOH	(bar)	(°C)	(%)	4.11a	4.11d	others[c]
1	10	6	50	230	79	91	3	6
2				240	83	88	4	8
3				250	95	83	3	14
4			1	250	0	---	---	---
5			5	250	99	---	83	17
6			20	250	99	2	65	33
7		10	50	250	97	65	16	19
8		20		250	96	38	43	19
9	20	7.3	50	220	24	97	---	3
10				230	73	93	3	4
11				240	98	78	3	19

[a] DMC and MeOH molar ratio respect to glycerol. The MeOH amount was adjusted case-by-case to obtain a homogeneous mixture**.** The total flow rate of the mixture (DMC+MeOH+glycerol) was 0.1 mL/min

[b] The conversion of glycerol and the selectivity towards products **411.a**, **4.11d**, and "others" were determined by GC, after 2 hours.

[c] Total of other products including **4.11b**, **4.11c** and **4.11e**

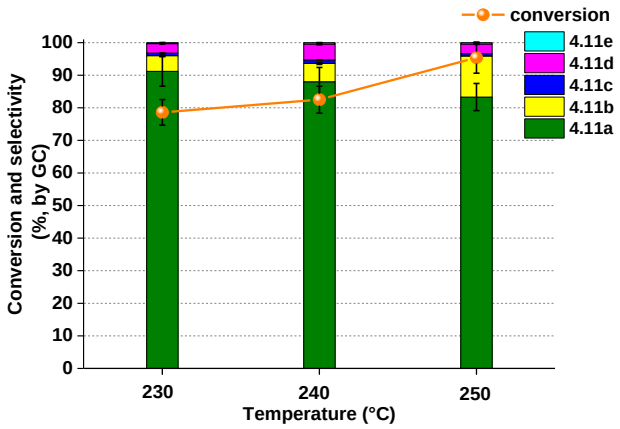

Figure 4.17. Conversion and selectivity of the CF-reaction of glycerol and DMC as a function of the temperature. Other conditions: DMC, methanol, and glycerol in a 10:6:1 molar ratio (**Q**), respectively; 50 bar; total flow rate: 0.1 mL/min.

As observed for the transesterification of diols (Figure 4.13 and Figure 4.14), the moderate residence time (τ~15 min) implied the need of a higher T for the CF-reaction of glycerol with DMC with respect to the batch-process (Figure 4.17). GlyC (**4.11a**) was the most abundant product: under the explored conditions, the conversion of glycerol and the selectivity towards compound **4.11a** were of 78% and 91% at 230 °C, and of 95% and 83%

at 250 °C. Moreover, the CF-system could operate virtually indefinitely since not only catalysts had not to be recovered/activated or disposed of, but the by-product glycidol was detected in trace amount, meaning that no substantial risk of side-polymerization reaction and clogging of the system. This also simplified the work-up of reaction mixtures. A complete recycle of the excess DMC was possible with isolated yields of glycerol carbonate in the range of 70-80%.[121] It should be noted here that of the many catalytic methods recently reviewed for the transesterification of DAlCs with glycerol,[17,122] most of them were not suitable for CF-applications because conventional bases (even solid compounds) used as catalysts were partially soluble in glycerol and/or DMC. To the best of our knowledge, the only reported CF-method using hydrotalcite-based catalysts was able to operate at 130 °C, but it required a highly noxious solvent such as DMSO and the best found selectivity for **4.11a** was 77% at complete conversion.[123] This value was comparable, if not lower, to that of the present CF-thermal reaction. Not to mention the impact of both upstream and downstream operations. The manufacture, activation and recycle (when possible) of heterogeneous catalysts needed energetically expensive calcination steps.[124]

On a final note, thermal CF-tests confirmed the role of the partitioning of reactants between liquid and vapor phases. At 250 °C, no reaction took place at ambient pressure, while, at only 5 bar, a quantitative process was observed and a fascinating shift of selectivity was observed: the decarboxylation of glycerol gave glycidol as the major product (**4.11d**:~83%) and only traces of GlyC were detected. The synthetic potential of this reaction was however, limited by the further polymerization of **4.11d**. This result will be the object of future investigations.

4.3.2 Experimental

4.3.2.1 Materials

1,2,3-trihydroxypropane (glycerol, **4.11**), 1,2-dihydroxypropane (propylene glycol, PG (**4.6**)), 1,2-ethanediol (ethylene glycol, EG (**4.7**)), 1,3-Dihydroxypropane (**4.8**), 1,3-Butanediol (**4.9**), 1,4-butanediol (**4.10**), diglycerol, dimethyl carbonate (DMC), methanol (MeOH), ethyl acetate (EA), cyclohexane (Cy), diethyl ether (EE) and dichloromethane (DCM) were ACS grade from Aldrich and were used as received. CO_2, N_2, He, Ar were research grade from SIAD and used as received.

4.3.2.2 Analysis instruments

GC/FID analysis were run using a Perkin Elmer Elite-624 capillary column (L=30 m, Ø=0.32 mm, film thickness=1.8 μm). The following conditions were used. Carrier gas: N_2; flow rate: 5.0 mL min^{-1}; split ratio: 1:1; initial T: 50 °C (3 min), ramp rate: 8 °C min^{-1}; final T: 220 °C (10 min).

GC/MS (EI, 70 eV) analysis were run using a Grace AT-624 capillary column (L=30 m, Ø=0.32 mm, film thickness=1.8 μm). The following conditions were used. Carrier gas: He; flow rate: 1.2 mL min^{-1}; split ratio: 10:1; initial T: 50 °C (3 min), ramp rate: 15 °C min^{-1}; final T: 220 °C (3 min).

^1H NMR were recorded at 400 MHz, ^{13}C spectra at 100 MHz and chemical shift were reported in δ values downfield from TMS; $CDCl_3$ was used as solvent

4.3.2.3 The autoclave

The batch autoclave used for the investigation was crafted by the Unviversità Ca' Foscari workshop and in-house assembled (Figure 4.18).

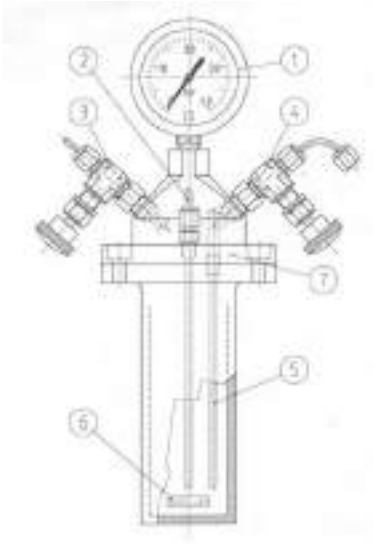

Figure 4.18. Representative scheme of the 200 mL stainless steel autoclave used in the investigation

It was composed by 1) a Pressure gauge; 2) Thermocouple housing (closed stainless steel tube); 3) Exhaust tap; 4) Inlet/sampling tap; 5) Inlet/sampling tube; 6) Stirring bar; 7) Flange, to be closed with 6 bolts (Teflon® or aluminum o-ring within the fitting).

4.3.2.4 CF apparatus.

The apparatus used for the investigation was in-house assembled (Figure 4.19). A HPLC Pump (Shimazdu LC-10AS) was used to send the reactants mixture (substrate and DMC) to an empty stainless steel tubular reactor (L=2.65 m, Ø=1/16", inner volume~1.7 mL). The reactor was heated at the desired temperature by placing it in a GC oven (HP 5890 GC). At the outlet of the oven, the reacting mixture was allowed to cool to ~60 °C by flowing through an additional segment of an empty capillary stainless steel tube (L=0.5 m, Ø=1/16") which was further cooled by a fan. The mixture then entered a manual Swagelok KPB1N0G412 back pressure regulator (BPR) equipped with an electronic pressure sensor. Because of the dead inner volume of the BPR (~8-10 mL), a long time of ~5 h was required for the reaction mixture to reach an equilibrium composition at the outlet of the BPR. The problem was overcome by placing a Rheodyne valve (7725i) with a 100 μL loop between the reactor and the BPR. The valve greatly facilitated the sampling of the reaction mixture and the monitoring of the reaction course.

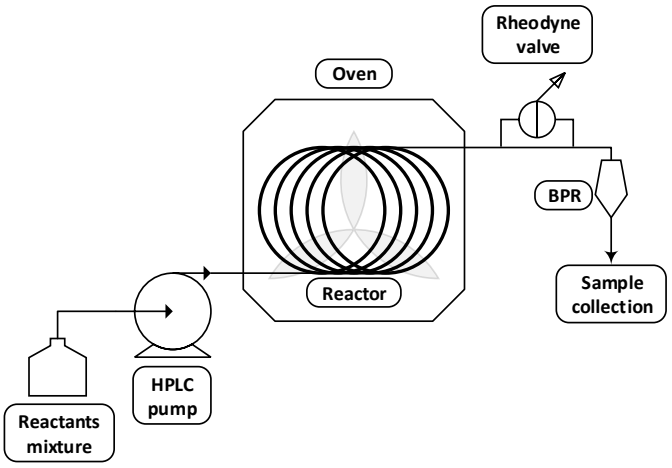

Figure 4.19. Schematic diagram for the in-house built continuous-flow apparatus

4.3.2.5 *CF catalyst-free transesterification of DMC with diols and glycerol*

Batch reactions: general procedure. A 200-mL stainless steel autoclave was charged with a mixture of a diol **4.6-4.8** (each substrate: 500 mg) and DMC. The reactants molar ratio (Q=DMC:substrate) was varied from 2 up to 80. The autoclave was degassed via three vacuum-nitrogen cycles, and then electrically heated at the desired temperature (120-220 °C). The reaction was allowed to proceed from 0.5 to 24 h during which the reacting mixture was kept under magnetic stirring. The autogeneous pressure was in the range of 2-

20 bar. At the end of each run, the autoclave was rapidly cooled at r.t. (in a water bath), and vented. The final mixture was analyzed by GC/FID and GC/MS.

Continuous-flow reactions: general procedure. A mixture of a diol (**4.6-4.10**) and DMC was prepared by varying the reactants molar ratio (Q) from 1.1 to 19. The reactants solution (10 mL) was initially used to prime the CF-apparatus at rt. Then, the solution was delivered to the CF-reactor (an empty capillary steel tube: 2.65 m x 1/16") at a flow rate of 0.1 mL/min, while the operating temperature and pressure were set at the desired values (from ambient to 50 bar, and 150 to 280 °C) by a back-pressure regulator and a thermostated oven. Once an amount of the reacting mixture (~8.5 mL) equal to 5 times the inner volume of the reactor was allowed to flow, samples were taken up (by a Rheodyne valve) at regular intervals of 30 min and analyzed by GC/FID and GC/MS. Once the experiment was complete, the reactor was cooled to 60 °C, washed with methanol (100 mL at 0.5 mL/min), and finally, vented at ambient pressure.

The same procedure was used also for the reaction of glycerol with one difference: due to the poor mutual miscibility of reactants, a mixture of glycerol, DMC, and methanol in 1:10:6 molar ratio, respectively, was used. Methanol (as a co-solvent) allowed the formation of a clear homogeneous solution.

4.3.2.6 Isolation and characterization of products

1,3-dioxan-2-one (4.8a). With reference to the experiment in Table 4.2 (entry 2), the reaction mixture was collected after the first sample for 1.5 h and concentrated by rotary evaporation (60 °C, 40 mbar). The oily residue was purified by FCC with EE:DCM=3:2 v/v. All the fractions of the title product (**4.8a**) also contained **4.8b** in a not negligible amount. The mixture was characterized by ^{1}H NMR, ^{13}C NMR. Comparing the mixture NMR spectra with the NMR of pure **4.8b,** it is possible to deduce the structure of **4.8a**. (see appendix A).

^{1}H NMR (400 MHz, $CDCl_3$) δ: 4.24 (td, J = 6.2, 2.3 Hz, 4H), 2.05 (quint, J = 6.2 Hz, 2H). ^{13}C NMR (100 MHz, $CDCl_3$) δ: 155.06, 64.43, 28.20.

3-hydroxypropyl methyl carbonate (4.8b). With reference to the experiment in Table 4.2 (entry 2), the reaction mixture was collected after the first sample for 1.5 h and concentrated by rotary evaporation (60 °C, 40 mbar). The oily residue was purified by FCC with EE:DCM=3:2 v/v. Title product was obtained in a small amount and characterized by ^{1}H NMR, ^{13}C NMR, HMQC, HMBC and GC/MS. (see appendix A).

^{1}H NMR (400 MHz, $CDCl_3$) δ: 4.30 (t, J = 6.2 Hz, 2H), 3.79 (s, 3H), 3.74 (t, J = 6.0 Hz, 2H), 1.92 (m, 2H). ^{13}C NMR (100 MHz, $CDCl_3$) δ: 156.21, 65.18, 59.18, 54.97, 31.82. GC/MS (relative intensity, 70eV) *m/z*: 134 (M^+, ≤1); 104.00 (22); 77.00 (100); 59.00 (31); 58.00 (20); 57.00 (30); 45.00 (19); 41.10 (10).

4-methyl-1,3-dioxan-2-one (4.9a). With reference to the experiment in Table 4.2 (entry 3), the reaction mixture was collected after the first sample for 1.5 h and concentrated by rotary evaporation (60 °C, 40 mbar). The oily residue was purified by FCC with EE:DCM=1:4 v/v. Title product was obtained in a small amount and characterized by ^{1}H NMR, ^{13}C NMR, HMQC, HMBC and GC/MS. (see appendix A).

^{1}H NMR (400 MHz, $CDCl_3$) δ: 4.61 (m, 1H), 4.47 – 4.34 (m, 2H), 2.12 – 1.86 (m, 2H), 1.44 (d, J = 6.3 Hz, 3H). ^{13}C NMR (100 MHz, $CDCl_3$) δ: 149.07, 75.83, 66.99, 28.81, 21.26. GC/MS (relative intensity, 70eV) *m/z*: 116.00 (M+, 3); 44 (25); 43 (100); 42 (78); 41 (35); 39 (16).

3-hydroxybutyl methyl carbonate + 4-hydroxybutan-2-yl methyl carbonate (4.9b+4.9b'). With reference to the experiment in Table 4.2 (entry 3), the reaction mixture was collected after the first sample for 1.5 h and concentrated by rotary evaporation (60 °C, 40 mbar). The oily residue was purified by FCC with EE:DCM=1:4 v/v. Title products were obtained as a mixture in a small amount and characterized by ^{1}H NMR, ^{13}C NMR. (see appendix A).

^{1}H NMR (400 MHz, $CDCl_3$): Characteristic signals are the doublets of the methyl groups δ=1.35-1.2 and the two singlets of the methyl groups at almost the same δ = 3.78. ^{13}C NMR (100 MHz, $CDCl_3$) δ: 156.17, 156.04, 72.80, 65.48, 64.86, 58.90, 54.96, 54.87, 39.03, 38.08, 23.72, 20.47.

4-(hydroxymethyl)-1,3-dioxolan-2-one (glycerol carbonate, 4.11a). With reference to the experiment in Figure 4.17 (240 °C), the reaction mixture was collected for 1 hour, concentrated by rotary evaporation (60 °C, 40 mbar) and the oily residue purified by FCC with EA:Cy=2:1 v/v. Title product was obtained in 78% yield (purity 98% by GC/FID). The product appeared as a colorless liquid and was characterized by GC/MS and the structure confirmed by comparison to a commercial sample. (see appendix A).

GC/MS (relative intensity, 70eV) *m/z*: 118 (M+, ≤1); 88 (38); 87 (40); 86 (15); 45 (9); 44 (100); 43 (94).

Methyl ((2-oxo-1,3-dioxolan-4-yl)methyl) carbonate (4.11b). With reference to the experiment in Figure 4.17 (250 °C), the reaction mixture was collected for 1 hour, concentrated by rotary evaporation (60 °C, 40 mbar) and the oily residue purified by FCC with EA:Cy=2:1 v/v. Title product was obtained in small amount, characterized by ^{1}H NMR, ^{13}C NMR and GC/MS and compared to the analyses reported in the Master thesis.[107] (see appendix A).

^{1}H NMR (400 MHz, $CDCl_3$) δ: 4.93 (m, 1H), 4.65 – 4.40 (t, 2H), 4.39 – 4.27 (m, 2H), 3.83 (s, 3H). ^{13}C NMR (100 MHz, $CDCl_3$) δ: 155.31, 154.24, 73.51, 66.15, 65.90, 55.61. GC/MS (relative intensity, 70eV) *m/z*: 176 (M^+, ≤1); 100 (61); 90 (71); 87 (24); 86 (9); 77 (67); 59 (100); 58 (34); 57 (16); 56 (20); 55 (8); 45 (71); 44 (9); 43 (82); 42 (15).

4-(methoxymethyl)-1,3-dioxolan-2-one (4.11c). With reference to the experiment in Figure 4.17 (250 °C), the reaction mixture was collected for 1 hour, concentrated by rotary evaporation (60 °C, 40 mbar) and the oily residue purified by FCC with EA:Cy=2:1 v/v. Title product was obtained in a small amount, characterized by ^{1}H NMR, ^{13}C NMR and GC/MS and compared to the analyses reported in the Master thesis.[107] (see appendix A).

^{1}H NMR (400 MHz, $CDCl_3$) δ: 4.80 (m, 1H), 4.53 – 4.31 (m, 2H), 3.61 (m, 2H), 3.43 (s, 3H). ^{13}C NMR (100 MHz, $CDCl_3$) δ: 154.98, 75.05, 71.62, 66.32, 59.81. GC/MS (relative intensity, 70eV) *m/z*: 132 (M^+, ≤1); 45 (100); 43 (8).

Methyl (oxiran-2-ylmethyl) carbonate (4.11e). With reference to the experiment in Figure 4.17 (250 °C), the reaction mixture was collected for 1 hour, concentrated by rotary evaporation (60 °C, 40 mbar) and the oily residue purified by FCC with EA:Cy=2:1 v/v. Title product was obtained in small amount, characterized by ^{1}H NMR, ^{13}C NMR and GC/MS. and compared to the analyses reported in the Master thesis.[107] (see appendix A).

^{1}H NMR (400 MHz, $CDCl_3$) δ: 4.40 (dd, J = 12.1, 3.3 Hz, 1H), 4.05 (dd, J = 12.0, 6.1 Hz, 1H), 3.83 (s, 3H), 3.27 – 3.21 (m, 1H), 2.85 (dd, J = 4.9, 4.1 Hz, 1H), 2.67 (dd, J = 4.9, 2.6 Hz, 1H). ^{13}C NMR (100 MHz, $CDCl_3$) δ: 155.69, 68.39, 55.19, 49.18, 44.71. GC/MS (relative intensity, 70eV) *m/z*: 132 (M^+, ≤1); 77 (16); 73 (20); 59 (100); 58 (67); 57 (23); 56 (26); 55 (8); 45 (89); 44 (7); 43 (62); 42 (12).

4.4 Bibliography

[1] M. Pagliaro and M. Rossi, in *The Future of Glycerol*, 2nd Ed. Royal Society of Chemistry, **2010**

[2] C. O. Tuck, E. Pérez, I. T. Horváth, et al., Valorization of Biomass: Deriving More Value from Waste, *Science*, **2012**, 337, 695-699.

[3] D. T. Johnson and K. A. Taconi, The glycerin glut: Options for the value-added conversion of crude glycerol resulting from biodiesel production, *Environ. Prog.*, **2007**, 26, 338-348.

[4] B. Katryniok, H. Kimura, E. Skrzyńska, et al., Selective catalytic oxidation of glycerol: perspectives for high value chemicals, *Green Chem.*, **2011**, 13, 1960.

[5] J. C. Beltrán-Prieto, K. Kolomazník and J. Pecha, A Review of Catalytic Systems for Glycerol Oxidation: Alternatives for Waste Valorization, *Aust. J. Chem.*, **2013**, 66, 511-521.

[6] S.-S. Liu, K.-Q. Sun and B.-Q. Xu, Specific Selectivity of Au-Catalyzed Oxidation of Glycerol and Other C3-Polyols in Water without the Presence of a Base, *ACS Catalysis*, **2014**, 4, 2226-2230.

[7] A. Perosa and P. Tundo, Selective Hydrogenolysis of Glycerol with Raney Nickel†, *Ind. Eng. Chem. Res.*, **2005**, 44, 8535-8537.

[8] M. Akiyama, S. Sato, R. Takahashi, et al., Dehydration–hydrogenation of glycerol into 1,2-propanediol at ambient hydrogen pressure, *Appl. Catal., A*, **2009**, 371, 60-66.

[9] I. Gandarias, P. L. Arias, S. G. Fernández, et al., Hydrogenolysis through catalytic transfer hydrogenation: Glycerol conversion to 1,2-propanediol, *Catal. Today*, **2012**, 195, 22-31.

[10] P. F. F. Amaral, T. F. Ferreira, G. C. Fontes, et al., Glycerol valorization: New biotechnological routes, *Food and Bioproducts Processing*, **2009**, 87, 179-186.

[11] R. W. Nicol, K. Marchand and W. D. Lubitz, Bioconversion of crude glycerol by fungi, *Appl. Microbiol. Biotechnol.*, **2012**, 93, 1865-1875.

[12] G. Morales, M. Paniagua, J. A. Melero, et al., Sulfonic Acid-Functionalized Catalysts for the Valorization of Glycerol via Transesterification with Methyl Acetate, *Ind. Eng. Chem. Res.*, **2011**, 50, 5898-5906.

[13] A. Sunder, R. Hanselmann, H. Frey, et al., Controlled Synthesis of Hyperbranched Polyglycerols by Ring-Opening Multibranching Polymerization, *Macromolecules*, **1999**, 32, 4240-4246.

[14] N. Rahmat, A. Z. Abdullah and A. R. Mohamed, Recent progress on innovative and potential technologies for glycerol transformation into fuel additives: A critical review, *Renew. Sust. Energ. Rev.*, **2010**, 14, 987-1000.

[15] I. Agirre, M. B. Güemez, A. Ugarte, et al., Glycerol acetals as diesel additives: Kinetic study of the reaction between glycerol and acetaldehyde, *Fuel Process. Technol.*, **2013**, 116, 182-188.

[16] L. Li, T. I. Koranyi, B. F. Sels, et al., Highly-efficient conversion of glycerol to solketal over heterogeneous Lewis acid catalysts, *Green Chem.*, **2012**, 14, 1611-1619.

[17] C. Len and R. Luque, Continuous flow transformations of glycerol to valuable products: an overview, *Sustain. chem. process.*, **2014**, 2, 1.

[18] W. Riemenschneider and H. Bolt in *Esters, Organic*. Wiley-VCH Verlag GmbH & Co. KGaA, **2000**.

[19] M. B. Smith and J. March in *Addition to Carbon–Hetero Multiple Bonds*. John Wiley & Sons, Inc., **2006**.

[20] J. Otera, Transesterification, *Chem. Rev.*, **1993**, 93, 1449-1470.

[21] A. V. Biradar, S. B. Umbarkar and M. K. Dongare, Transesterification of diethyl oxalate with phenol using MoO3/SiO2 catalyst, *Appl. Catal., A*, **2005**, 285, 190-195.

[22] T. Kotbagi, D. L. Nguyen, C. Lancelot, et al., Transesterification of Diethyl Oxalate with Phenol over Sol–Gel MoO3/TiO2 Catalysts, *ChemSusChem*, **2012**, 5, 1467-1473.

[23] D. Srinivas, R. Srivastava and P. Ratnasamy, Transesterifications over titanosilicate molecular sieves, *Catal. Today*, **2004**, 96, 127-133.

[24] D. Yanmin, C. Xingquan, Z. Chunxiang, et al., Synthesis of methyl propyl carbonate via gas-phase transesterification over TiO2/Al2O3, *J. Mol. Catal. A: Chem.*, **2010**, 331, 125-129.

[25] D.L. Ho and W. Zhenghao, Process For The Preparation Of Sucrose-6-Ester By Esterification In The Presence Of Solid Superacid Catalyst. US2008103295, **2008**.

[26] E. Van de Steene, J. De Clercq and J. W. Thybaut, Ion-exchange resin catalyzed transesterification of ethyl acetate with methanol: Gel versus macroporous resins, *Chem. Eng. J.*, **2014**, 242, 170-179.

[27] S. Limmanee, T. Naree, K. Bunyakiat, et al., Mixed oxides of Ca, Mg and Zn as heterogeneous base catalysts for the synthesis of palm kernel oil methyl esters, *Chem. Eng. J.*, **2013**, 225, 616-624.

[28] J. Boro, D. Deka and A. J. Thakur, A review on solid oxide derived from waste shells as catalyst for biodiesel production, *Renew. Sust. Energ. Rev.*, **2012**, 16, 904-910.

[29] W. Suryaputra, I. Winata, N. Indraswati, et al., Waste capiz (Amusium cristatum) shell as a new heterogeneous catalyst for biodiesel production, *Renewable Energy*, **2013**, 50, 795-799.

[30] S. M. Smith, C. Oopathum, V. Weeramongkhonlert, et al., Transesterification of soybean oil using bovine bone waste as new catalyst, *Bioresour. Technol.*, **2013**, 143, 686-690.

[31] R. Rezaei, M. Mohadesi and G. R. Moradi, Optimization of biodiesel production using waste mussel shell catalyst, *Fuel*, **2013**, 109, 534-541.

[32] T. Kai, G. L. Mak, S. Wada, et al., Production of biodiesel fuel from canola oil with dimethyl carbonate using an active sodium methoxide catalyst prepared by crystallization, *Bioresour. Technol.*, **2014**, 163, 360-363.

[33] L. Zhang, B. Sheng, Z. Xin, et al., Kinetics of transesterification of palm oil and dimethyl carbonate for biodiesel production at the catalysis of heterogeneous base catalyst, *Bioresour. Technol.*, **2010**, 101, 8144-8150.

[34] M. Tudorache, L. Protesescu, S. Coman, et al., Efficient bio-conversion of glycerol to glycerol carbonate catalyzed by lipase extracted from Aspergillus niger, *Green Chem.*, **2012**, 14, 478.

[35] S.-H. Pyo, P. Persson, S. Lundmark, et al., Solvent-free lipase-mediated synthesis of six-membered cyclic carbonates from trimethylolpropane and dialkyl carbonates, *Green Chem.*, **2011**, 13, 976.

[36] A. Guldhe, B. Singh, T. Mutanda, et al., Advances in synthesis of biodiesel via enzyme catalysis: Novel and sustainable approaches, *Renew. Sust. Energ. Rev.*, **2015**, 41, 1447-1464.

[37] J. R. Ochoa-Gomez, O. Gomez-Jimenez-Aberasturi, C. Ramirez-Lopez, et al., Synthesis of glycerol 1,2-carbonate by transesterification of glycerol with dimethyl carbonate using triethylamine as a facile separable homogeneous catalyst, *Green Chem.*, **2012**, 14, 3368-3376.

[38] R. Srivastava, D. Srinivas and P. Ratnasamy, Fe–Zn double-metal cyanide complexes as novel, solid transesterification catalysts, *J. Catal.*, **2006**, 241, 34-44.

[39] B. A. V. Santos, V. M. T. M. Silva, J. M. Loureiro, et al., Review for the Direct Synthesis of Dimethyl Carbonate, *ChemBioEng Reviews*, **2014**, 1, 214-229.

[40] C. Martín, G. Fiorani and A. W. Kleij, Recent Advances in the Catalytic Preparation of Cyclic Organic Carbonates, *ACS Catalysis*, **2015**, 5, 1353-1370.

[41] http://datasheets.scbt.com/sc-239770.pdf Dimethyl carbonate - hazards identification (last access: 2016/09/18)

[42] http://www.sigmaaldrich.com/catalog/product/aldrich/517135?lang=it&region=IT see Diethyl carbonate Safety Data Sheet (last access: 2016/09/26)

[43] http://www.sigmaaldrich.com/catalog/product/aldrich/477907?lang=it&region=IT see Dibenzyl carbonate Safety Data Sheet (last access: 2016/09/26)

[44] P. T. Anastas and M. M. Kirchhoff, Origins, Current Status, and Future Challenges of Green Chemistry, *Acc. Chem. Res.*, **2002**, 35, 686-694.

[45] P. Tundo and M. Selva, The Chemistry of Dimethyl Carbonate, *Acc. Chem. Res.*, **2002**, 35, 706-716.

[46] U. Romano, R. Tesel, M. M. Mauri, et al., Synthesis of Dimethyl Carbonate from Methanol, Carbon Monoxide, and Oxygen Catalyzed by Copper Compounds, *Industrial & Engineering Chemistry Product Research and Development*, **1980**, 19, 396-403.

[47] K. Nishihira, S. Yoshida and S. Tanaka, Process for purifying dimethyl carbonate, US 5292917, **1994**.

[48] S. Fukuoka, I. Fukawa, M. Tojo, et al., A Novel Non-Phosgene Process for Polycarbonate Production from CO2: Green and Sustainable Chemistry in Practice, *Catalysis Surveys from Asia*, **2010**, 14, 146-163.

[49] B. Schäffner, F. Schäffner, S. P. Verevkin, et al., Organic Carbonates as Solvents in Synthesis and Catalysis, *Chem. Rev.*, **2010**, 110, 4554-4581.

[50] A. Behr, J. Eilting, K. Irawadi, et al., Improved utilisation of renewable resources: New important derivatives of glycerol, *Green Chem.*, **2008**, 10, 13-30.

[51] A. E. Diaz-Alvarez, J. Francos, B. Lastra-Barreira, et al., Glycerol and derived solvents: new sustainable reaction media for organic synthesis, *Chem. Commun.*, **2011**, 47, 6208-6227.

[52] http://www.lambiotte.com/ Innovative solvents, acetals (last access: 2016/08/17)

[53] M. Selva, V. Benedet and M. Fabris, Selective catalytic etherification of glycerol formal and solketal with dialkyl carbonates and K2CO3, *Green Chem.*, **2012**, 14, 188-200.

[54] M. Selva, M. Fabris and A. Perosa, Decarboxylation of dialkyl carbonates to dialkyl ethers over alkali metal-exchanged faujasites, *Green Chem.*, **2011**, 13, 863-872.

[55] J. S. Moya, E. Criado and S. De Aza, The K2O·Al2O3-Al2O3 system, *Journal of Materials Science*, **1982**, 17, 2213-2217.

[56] M. Selva, M. Noe, A. Perosa, et al., Carbonate, acetate and phenolate phosphonium salts as catalysts in transesterification reactions for the synthesis of non-symmetric dialkyl carbonates, *Org. Biomol. Chem.*, **2012**, 10, 6569-6578.

[57] M. Selva, A. Caretto, M. Noe, et al., Carbonate phosphonium salts as catalysts for the transesterification of dialkyl carbonates with diols. The competition between cyclic carbonates and linear dicarbonate products, *Org. Biomol. Chem.*, **2014**, 12, 4143-4155.

[58] G. Fiorani and M. Selva, Synthesis of dibenzyl carbonate: towards a sustainable catalytic approach, *RSC Advances*, **2014**, 4, 1929-1937.

[59] M. Selva, S. Guidi and M. Noè, Upgrading of glycerol acetals by thermal catalyst-free transesterification of dialkyl carbonates under continuous-flow conditions, *Green Chem.*, **2015**, 17, 1008-1023.

[60] M. Selva, S. Guidi, A. Perosa et al., Continuous-flow alkene metathesis: the model reaction of 1-octene catalyzed by Re_2O_7/[gamma]-Al_2O_3 with supercritical CO_2 as a carrier, *Green Chem.*,**2012**, 14, 2727-2737.

[61] D. Delledonne, F. Rivetti and U. Romano, Developments in the production and application of dimethylcarbonate, *Appl. Catal., A*, **2001**, 221, 241-251.

[62] M. Fuming, L. Guangxing, N. Jin, et al., A novel catalyst for transesterification of dimethyl carbonate with phenol to diphenyl carbonate: samarium trifluoromethanesulfonate, *J. Mol. Catal. A: Chem.*, **2002**, 184, 465-468.

[63] The chosen volume (10 mL) of reactants mixture was equal to ten times that of the reactor. Under such conditions, the stream spilled from the CF-reactor showed a constant composition with time.

[64] As for DMC, no variations of the conversion and the product distribution of the reactant mixtures were appreciated after the initial 60-80 min of reaction.

[65] NMR analyses were recorded at 400 MHz. Under such conditions, mixtures deriving from the reaction of PC and GlyF showed a plethora of overlapped NMR resonances due to the presence of 4 diasteromers and 8 enantiomers with very similar structures. This made doubtful and unreliable any interpretation of NMR spectra.

[66] M. Mohsen-Nia, H. Amiri and B. Jazi, Dielectric Constants of Water, Methanol, Ethanol, Butanol and Acetone: Measurement and Computational Study, *J. Solution Chem.*, **2010**, 39, 701-708.

[67] J.-F. Côté, D. Brouillette, J. Desnoyers, et al., Dielectric constants of acetonitrile, γ-butyrolactone, propylene carbonate, and 1,2-dimethoxyethane as a function of pressure and temperature, *J. Solution Chem.*, **1996**, 25, 1163-1173.

[68] See MSDS on www.sigmaaldrich.com.

[69] M. Diasakou, A. Louloudi and N. Papayannakos, Kinetics of the non-catalytic transesterification of soybean oil, *Fuel*, **1998**, 77, 1297-1302.

[70] S. Saka and D. Kusdiana, Biodiesel fuel from rapeseed oil as prepared in supercritical methanol, *Fuel*, **2001**, 80, 225-231.

[71] A. Demirbaş, Biodiesel from vegetable oils via transesterification in supercritical methanol, *Energy Convers. Manage.*, **2002**, 43, 2349-2356.

[72] K. Bunyakiat, S. Makmee, R. Sawangkeaw, et al., Continuous Production of Biodiesel via Transesterification from Vegetable Oils in Supercritical Methanol, *Energy & Fuels*, **2006**, 20, 812-817.

[73] M. N. Varma and G. Madras, Synthesis of Biodiesel from Castor Oil and Linseed Oil in Supercritical Fluids, *Ind. Eng. Chem. Res.*, **2006**, 46, 1-6.

[74] S. A. Pasias, N. K. Barakos and N. G. Papayannakos, Catalytic Effect of Free Fatty Acids on Cotton Seed Oil Thermal Transesterification, *Ind. Eng. Chem. Res.*, **2009**, 48, 4266-4273.

[75] Y.-T. Tsai, H.-m. Lin and M.-J. Lee, Biodiesel production with continuous supercritical process: Non-catalytic transesterification and esterification with or without carbon dioxide, *Bioresour. Technol.*, **2013**, 145, 362-369.

[76] K. T. Tan and K. T. Lee, A review on supercritical fluids (SCF) technology in sustainable biodiesel production: Potential and challenges, *Renew. Sust. Energ. Rev.*, **2011**, 15, 2452-2456.

[77] W. V. Steele, R. D. Chirico, S. E. Knipmeyer, et al., Thermodynamic Properties and Ideal-Gas Enthalpies of Formation for Dicyclohexyl Sulfide, Diethylenetriamine, Di-n-octyl Sulfide, Dimethyl Carbonate, Piperazine, Hexachloroprop-1-ene, Tetrakis(dimethylamino)ethylene, N,N'-Bis-(2-hydroxyethyl)ethylenediamine, and 1,2,4-Triazolo[1,5-a]pyrimidine, *Journal of Chemical & Engineering Data*, **1997**, 42, 1037-1052.

[78] Z. Ilham and S. Saka, Dimethyl carbonate as potential reactant in non-catalytic biodiesel production by supercritical method, *Bioresour. Technol.*, **2009**, 100, 1793-1796.

[79] Z. Ilham and S. Saka, Two-step supercritical dimethyl carbonate method for biodiesel production from Jatropha curcas oil, *Bioresour. Technol.*, **2010**, 101, 2735-2740.

[80] The transesterification of oils in sc-DMC gives glycerol carbonate as a co-product. Citramalic acid is plausibly originated by the reaction of GlyC and DMC in the presence of water and free fatty acids in the feedstock (crude oils).

[81] K. N. Houk, R. W. Gandour, R. W. Strozier, et al., Barriers to thermally allowed reactions and the elusiveness of neutral homoaromaticity, *J. Am. Chem. Soc.*, **1979**, 101, 6797-6802.

[82] E. Poling, J. M. Prausnitz and J. P. O'Connell, Vapor pressures and enthalpies of vaporization of pure fluids in *The Properties of Gases and Liquids,* 5th Ed., McGraw-Hill, **2004**.

[83] V. F. Marulanda, Biodiesel production by supercritical methanol transesterification: process simulation and potential environmental impact assessment, *Journal of Cleaner Production*, **2012**, 33, 109-116.

[84] S. Glisic and D. Skala, The problems in design and detailed analyses of energy consumption for biodiesel synthesis at supercritical conditions, *The Journal of Supercritical Fluids*, **2009**, 49, 293-301.

[85] J. M. N. van Kasteren and A. P. Nisworo, A process model to estimate the cost of industrial scale biodiesel production from waste cooking oil by supercritical transesterification, *Res. Cons. Recycling*, **2007**, 50, 442-458.

[86] A. Perosa, M. Selva, P. Tundo, et al., Alkyl Methyl Carbonates as Methylating Agents. The O-Methylation of Phenols, *Synlett*, **2000**, 2000, 272-274.

[87] M. Selva, A. Perosa and M. Fabris, Sequential coupling of the transesterification of cyclic carbonates with the selective N-methylation of anilines catalysed by faujasites, *Green Chem.*, **2008**, 10, 1068-1077.

[88] V. Rathore, S. Tyagi, B. Newalkar, et al., Glycerin-Free Synthesis of Jatropha and Pongamia Biodiesel in Supercritical Dimethyl and Diethyl Carbonate, *Ind. Eng. Chem. Res.*, **2014**, 53, 10525-10533.

[89] B. M. Bhanage, S.-i. Fujita, Y. Ikushima, et al., Synthesis of dimethyl carbonate and glycols from carbon dioxide, epoxides, and methanol using heterogeneous basic metal oxide catalysts with high activity and selectivity, *Appl. Catal., A*, **2001**, 219, 259-266.

[90] C. Murugan, H. C. Bajaj and R. V. Jasra, Transesterification of Propylene Carbonate by Methanol Using KF/Al2O3 as an Efficient Base Catalyst, *Catal. Lett.*, **2010**, 137, 224-231.

[91] A. Pyrlik, W. F. Hoelderich, K. Müller, et al., Dimethyl carbonate via transesterification of propylene carbonate with methanol over ion exchange resins, *Applied Catalysis B: Environmental*, **2012**, 125, 486-491.

[92] S. Guidi, R. Calmanti, M. Noè, et al., Thermal (Catalyst-Free) Transesterification of Diols and Glycerol with Dimethyl Carbonate: A Flexible Reaction for Batch and Continuous-Flow Applications, *ACS Sustainable Chem. Eng.*, **2016**, DOI: 10.1021/acssuschemeng.6b01633.

[93] In the repeated tests carried out under the same conditions, values of conversion and amount of products (determined by GC/MS) differed by less than 5% from one reaction to another

[94] J. Matsuo, K. Aoki, F. Sanda, et al., Substituent Effect on the Anionic Equilibrium Polymerization of Six-Membered Cyclic Carbonates, *Macromolecules*, **1998**, 31, 4432-4438.

[95] S. Sarel, L. A. Pohoryles and R. Ben-Shoshan, Organic Carbonates. IV.1a,b,c Factors Affecting Formation of Homologous Cyclic Carbonates, *The Journal of Organic Chemistry*, **1959**, 24, 1873-1878.

[96] R. M. Beesley, C. K. Ingold and J. F. Thorpe, CXIX.-The formation and stability of spiro-compounds. Part I. spiro-Compounds from cyclohexane, *Journal of the Chemical Society, Transactions*, **1915**, 107, 1080-1106.

[97] M. E. Jung and G. Piizzi, gem-Disubstituent Effect: Theoretical Basis and Synthetic Applications, *Chem. Rev.*, **2005**, 105, 1735-1766.

[98] D. Kusdiana and S. Saka, Effects of water on biodiesel fuel production by supercritical methanol treatment, *Bioresour. Technol.*, **2004**, 91, 289-295.

[99] Y. Takebayashi, H. Hotta, A. Shono, et al., Noncatalytic Ortho-Selective Methylation of Phenol in Supercritical Methanol: the Mechanism and Acid/Base Effect, *Ind. Eng. Chem. Res.*, **2008**, 47, 704-709.

[100] I. Vieitez, C. da Silva, I. Alckmin, et al., Continuous catalyst-free methanolysis and ethanolysis of soybean oil under supercritical alcohol/water mixtures, *Renewable Energy*, **2010**, 35, 1976-1981.

[101] Y. Horikawa, Y. Uchino and T. Sako, Alkylation and Acetal Formation Using Supercritical Alcohol without Catalyst, *Chem. Lett.*, **2003**, 32, 232-233.

[102] R. T. L. Ng, D. H. S. Tay and D. K. S. Ng, Simultaneous Process Synthesis, Heat and Power Integration in a Sustainable Integrated Biorefinery, *Energy & Fuels*, **2012**, 26, 7316-7330.

[103] H. C. Brown, J. H. Brewster and H. Shechter, An Interpretation of the Chemical Behavior of Five- and Six-membered Ring Compounds1, *J. Am. Chem. Soc.*, **1954**, 76, 467-474.

[104] H. Tomita, F. Sanda and T. Endo, Reactivity comparison of five- and six-membered cyclic carbonates with amines: Basic evaluation for synthesis of poly(hydroxyurethane), *J. Polym. Sci., Part A: Polym. Chem.*, **2001**, 39, 162-168.

[105] H. R. Kricheldorf and J. Jenssen, Polylactones. 16. Cationic Polymerization of Trimethylene Carbonate and Other Cyclic Carbonates, *Journal of Macromolecular Science: Part A - Chemistry*, **1989**, 26, 631-644.

[106] S.-H. Pyo and R. Hatti-Kaul, Chlorine-Free Synthesis of Organic Alkyl Carbonates and Five- and Six-Membered Cyclic Carbonates, *Adv. Synth. Catal.*, **2016**, 358, 834-839.

[107] R. Calmanti. Master Thesis "New pathways for transformations of glycerol and its derivatives to higher value-added chemicals", Università Ca' Foscari Venezia, AY 2016

[108] P. Kumar, P. With, V. C. Srivastava, et al., Glycerol Carbonate Synthesis by Hierarchically Structured Catalysts: Catalytic Activity and Characterization, *Ind. Eng. Chem. Res.*, **2015**, 54, 12543-12552.

[109] C. L. Bolívar-Diaz, V. Calvino-Casilda, F. Rubio-Marcos, et al., New concepts for process intensification in the conversion of glycerol carbonate to glycidol, *Applied Catalysis B: Environmental*, **2013**, 129, 575-579.

[110] J. S. Choi, F. S. H. Simanjuntaka, J. Y. Oh, et al., Ionic-liquid-catalyzed decarboxylation of glycerol carbonate to glycidol, *J. Catal.*, **2013**, 297, 248-255.

[111] X. Zuo, F. Niu, K. Snavely, et al., Liquid phase oxidation of p-xylene to terephthalic acid at medium-high temperatures: multiple benefits of CO2-expanded liquids, *Green Chem.*, **2010**, 12, 260.

[112] M. Honda, M. Tamura, K. Nakao, et al., Direct Cyclic Carbonate Synthesis from CO2and Diol over Carboxylation/Hydration Cascade Catalyst of CeO2with 2-Cyanopyridine, *ACS Catalysis*, **2014**, 4, 1893-1896.

[113] http://webbook.nist.gov/chemistry/ Chemistry webbook (last access: 2016/09/22)

[114] P. Luehring and A. Schumpe, Gas solubilities (hydrogen, helium, nitrogen, carbon monoxide, oxygen, argon, carbon dioxide) in organic liquids at 293.2 K, *Journal of Chemical & Engineering Data*, **1989**, 34, 250-252.

[115] P. S. van der Gulik, Viscosity of carbon dioxide in the liquid phase, *Physica A: Statistical Mechanics and its Applications*, **1997**, 238, 81-112.

[116] C. Evers, H. W. Lösch and W. Wagner, An Absolute Viscometer-Densimeter and Measurements of the Viscosity of Nitrogen, Methane, Helium, Neon, Argon, and Krypton over a Wide Range of Density and Temperature, *Int. J. Thermophys.*, **2002**, 23, 1411-1439.

[117] P. G. Jessop and W. Leitner in *Chemical Synthesis using Supercritical Fluids*, Wiley-VCH, **1999**.

[118] S. R. Sandler and F. R. Berg, Room temperature polymerization of glycidol, *Journal of Polymer Science Part A-1: Polymer Chemistry*, **1966**, 4, 1253-1259.

[119] T. Laino, C. Tuma, A. Curioni, et al., A Revisited Picture of the Mechanism of Glycerol Dehydration, *The Journal of Physical Chemistry A*, **2011**, 115, 3592-3595.

[120] A. Martin and M. Richter, Oligomerization of glycerol – a critical review, *Eur. J. Lipid Sci. Technol.*, **2011**, 113, 100-117.

[121] The recycle was even facilitated by the highly different boiling points between DMC and the MeOH/DMC azeotrope (90 °C and 62–65 °C, respectively), and the heavy GlyC (354 °C). The same held true also for the separation of DMC from higher cyclic homologues including EC and PC, and carbonate derivatives of diols **4.8**, **4.9**, and **4.10** (Table 4.2).

[122] W. K. Teng, G. C. Ngoh, R. Yusoff, et al., A review on the performance of glycerol carbonate production via catalytic transesterification: Effects of influencing parameters, *Energy Convers. Manage.*, **2014**, 88, 484-497.

[123] M. G. Álvarez, M. Plíšková, A. M. Segarra, et al., Synthesis of glycerol carbonates by transesterification of glycerol in a continuous system using supported hydrotalcites as catalysts, *Applied Catalysis B: Environmental*, **2012**, 113-114, 212-220.

[124] J. R. Ochoa-Gómez, O. Gómez-Jiménez-Aberasturi, C. Ramírez-López, et al., A Brief Review on Industrial Alternatives for the Manufacturing of Glycerol Carbonate, a Green Chemical, *Org. Proc. Res. Dev.*, **2012**, 16, 389-399.

5 CONCLUDING REMARKS

In this Thesis work, a systematic application of continuous-flow (CF) procedures has been investigated for the chemical upgrading of important bio-based platform molecules including glycerol and its derivatives. Apart from the reactivity of the different substrates, the implementation of such techniques shows intrinsic difficulties associated with physical properties such as the high viscosity, the high boiling points and the poor miscibility (especially for glycerol) in the common organic solvents, of the involved reactants. Last, but not least, glycerol and its derivatives may act as solvents for several inorganic compounds, thereby limiting the choice of solid catalysts to be used under CF-conditions.

In the first part of the project, the CF-acetalization of glycerol has been explored by comparing the performance of a conventional acid catalyst such as Amberlyst 36 to that of commercial $AlF_3 \cdot 3H_2O$. The latter has never been previously reported for the investigated reaction and it has been selected not only for its acid properties, but also for economic reasons and its chemical/mechanical stability. The most salient result of this study is the ability of the AF catalyst to promote an effective acetalization of a crude-like glycerol, meaning glycerol contaminated by the most common impurities deriving from the biodiesel manufacturing. These include water, methanol, and NaCl. Since the isolation of acetal products by distillation of final reaction mixtures is not only simpler, but also cheaper than common techniques required for the purification of off-grade glycerol, it is by far more convenient to convert crude glycerol (to acetals) rather than refining the crude reagent and then proceeding with its upgrading. By contrast, Amberlyst 36, though far more active than AF for the conversion of pure glycerol, is rapidly deactivated by the presence of even traces of inorganic salts. The characterization of commercial $AlF_3 \cdot 3H_2O$ has proven that the active phase for the acetalization process is likely a solid solution (SS) composed of $Al_2[(F_{1-x}(OH)_x]6(H_2O)_y$. This finding opens an attractive perspective for future studies aimed at exploring the synthesis and applications of the pure SS compound as a catalyst for both acetalization reactions and other model acid-promoted processes. Furthermore, real batches of crude glycerol, instead of crude-like ones, could be taken into consideration as more real representative samples.

The second part of the Thesis project has been carried out at the University of Nottingham, UK. This investigation has allowed to implement one of the few examples of a CF-synthesis of quinoline starting from the reaction of solketal as a bio-based platform chemical belonging to glycerol derivatives, with primary aromatic amines in the presence of niobium phosphate (NbP) as a solid catalyst. The study proposes a modification of the known Skraup synthesis not only for the fact that a glycerol acetal (rather than glycerol) was chosen as a reactant, but also for the unprecedented use of NbP as a solid catalyst in place of the conventional liquid H_2SO_4. Although the procedure is limited to conversion and selectivity not exceeding 60% and 80%, respectively, the explored CF-arrangement allow to avoid harsh conditions necessary to run the Skraup synthesis in the batch mode. The inedited catalytic activity displayed by NbP for this reaction, has been confirmed using different anilines. In particular, the reaction of solketal with 4,4'-methylenedianiline has given a new compound whose crystallographic structure has been determined. Due to lack of time, no attempts to restore the activity of the spent catalyst were made. It could be interesting to investigate thermal treatments able to restore the catalyst activity. In addition to this, the both Lewis and Bronsted nature of the Niobium phosphate could be exploited. In particular, if it could possible to treat the solid in order to obtain a complete Lewis or Bronsted acid, the reaction could be controlled forming selectively the quinoline or the indole derivative.

The last part has been focused on the study of the CF-reactivity of glycerol and glycerol acetals (GAs) with dialkyl carbonates (DAlCs). The reactions of GAs were previously investigated by our research group under batch conditions in the presence of base catalysts. The first attractive aspect emerging from the experiments carried out during this Thesis work, is that, providing a certain temperature and pressure, the mono-transesterification of DAlCs with GAs takes place under catalyst-free conditions operating in the CF-mode. The reaction affording the desired products, with almost complete conversion and selectivity. The absence of a catalyst allows to avoid several issues dealing with not only the cost of the catalytic system (which may have a limited incidence), but rather the problems of deactivation and reactivation procedures, as well as the leaching phenomena and the drop of the performance with time. This last aspect being a critical drawback especially for CF-procedures. The success of the thermal reactions between DAlCs and GAs has prompted us to investigate the same process by using also 1,*n*-diols and eventually glycerol, as the most attractive natural derived "*triol*". Parallel investigations of

catalyst-free reactions have been carried out under both batch and CF-conditions. 1,*n*-diols, particularly 1,2-diols, allow the selective synthesis of the corresponding cyclic carbonate derivatives. While, the most intriguing result comes from the reaction of glycerol whose selectivity can be switched by varying the conditions: in the batch mode, by changing the reaction time and the reactants molar ratio, either glycerol carbonate or its transesterification derivative, *i.e.* methyl [(2-oxo-1,3-dioxolan-4-yl)methyl] carbonate can be obtained with selectively 85% and 88%, respectively. In the flow-mode, by varying the operating pressure, glycerol carbonate or glycidol can be produced with high selectivity. The captivating aspect of this study is the catalyst-free nature of the protocol: once reaction parameters (p, T, flow rate) are set, the process can be run virtually indefinitely without alteration of the product distribution and with very simple downstreaming operations for the purification of products and the recover/recycle of excess (unconverted) reactants. The thermal transesterification of DAlCs should not be restricted only to substrates such as glycerol or its derivatives. For instance catechol carbonate, used as an intermediate for syntheses of a variety of chemicals, may be synthesized from catechol and DMC trough a thermal CF process.

Acknowledgments

I would like to express my special appreciation and thanks to my advisor Professors Maurizio Selva and Alvise Perosa for encouraging my research and for allowing me to grow as a research scientist. I would also like to thank Dr. William Lewis for his support for the crystallographic analyses, Dr. Ke Jie for his help for the phase behaviour predictions, Prof. Pietro Riello for the XRD analyses and Jing Jin for her important contribution to the thesis work.

6 APPENDIX A

6.1 Glycerol acetalization (chapter 2)

6.1.1 ICP analysis

ICP-OES analyses were carried out to evaluate the leaching of Al from the catalytic bed of $AlF_3 \cdot 3H_2O$ (AF). Analyses were run on a Perkin Elmer Optima 5300DV in axial direction at 394.401 nm. A calibration curve was obtained by using seven aqueous solutions containing 300, 200, 150, 100, 60, 40 and 20 ppb of Al. These solutions were all prepared by dilution of a 1000 mg/L standard solution of ionic Al in HNO_3. The linear fit was automatically calculated by the ICP software resulting with interceptor=-151.8, slope=21.70 and correlation coefficient=0.996961.

A total of three samples were considered for Al-analyses. They were obtained according to the procedure described in the experimental section. The first two samples (A and B) derived from the reaction of glycerol with acetone catalyzed by $AlF_3 \cdot 3H_2O$: they were expected to contain the same amount of Al. While, the third one was prepared by flowing the reactants glycerol (**Glyc1**) and acetone through the CF-apparatus in the absence of the catalyst (Blank).

Before any measure, each sample was first diluted with milli-Q water (20 mL). A and B were then diluted again in a 1:3 v/v ratio. **Table A1** reports the results. Each analysis was the average of 6 subsequent acquisitions.

Table A1. ICP-OES analyses of the Al content

Entry	Sample	Aluminium content (μg/L)
1	**A**	214.0
2	**B**	188.1
3	**Blank**	137.4

6.1.2 Ion chromatography analysis

Ion chromatography analyses were carried out to evaluate the leaching of F^- from the catalytic bed of $AlF_3 \cdot 3H_2O$ used in this investigation. Analyses were run on a Dionex LC20 (Chromatography enclosure) equipped with a Dionex GP40 gradient pump and a Dionex ECD ED40 (working at 100 mA). A Dionex AS14 was used as column with 1mM carbonate/3.5 mM bicarbonate as a mobile phase. A calibration curve was obtained by using four aqueous solutions containing 0.5, 1, 3, 7 ppm of F^-.The linear fit was automatically calculated by the chromatograph control software (Chromeleon) resulting with slope=0.131, interceptor forced to 0 and correlation coefficient=0.999868.

A total of two samples were considered for F^- analyses. They were obtained according to the procedure described in the experimental section. The first sample (A) was derived from the reaction of glycerol (**Glyc1**) with acetone catalyzed by $AlF_3 \cdot 3H_2O$ while, the second one was prepared by flowing the reactants in the absence of the catalyst (blank).

Before any measure, each sample was first diluted with milli-Q water in a 1:5 v/v ratio. **Table A2** reports the results. Each analysis was the average of 4 subsequent acquisitions.

Table A2. Ion chromatography analyses of the F^- content

Entry	Sample	F- content (mg/L)
1	**A**	2.808
2	**Blank**	0.274

6.1.3 NMR and mass analyses

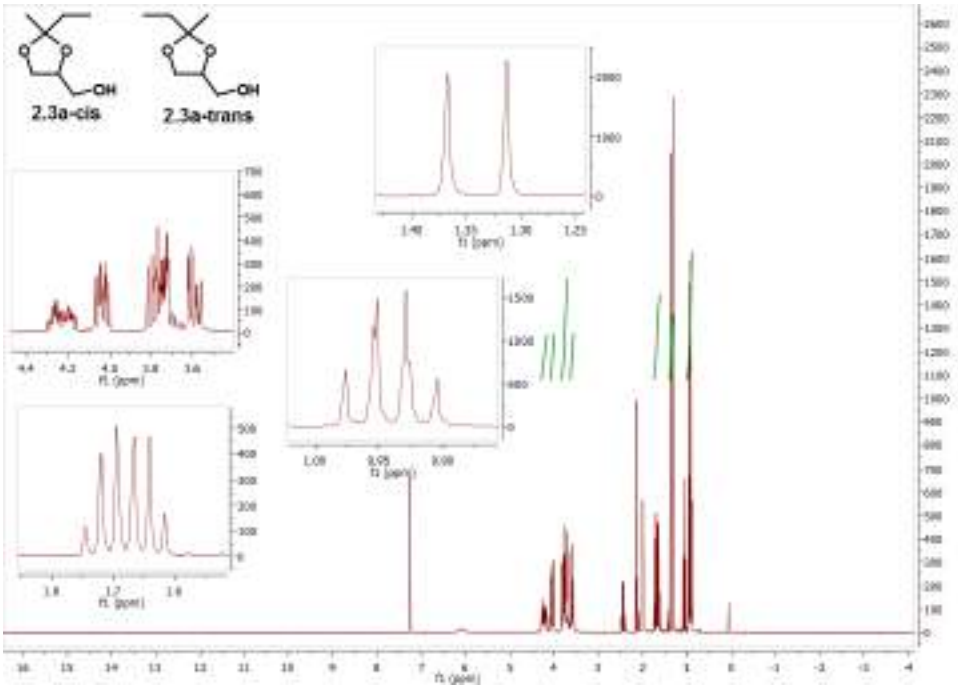

Figure A1. ^{1}H NMR spectra of **2.3a**

^{1}H NMR (300 MHz, $CDCl_3$) δ (ppm): 4.25 (m, 2H), 4.12 – 4.00 (m, 2H), 3.85 – 3.72 (m, 4H), 3.61 (m, 2H), 1.79 – 1.62 (m, 4H), 1.39 (s, 3H), 1.33 (s, 3H), 0.96 (m, 6H).

The spectrum also showed traces of 2-butanone which corresponded to the following signals: ^{1}H NMR (300 MHz, $CDCl_3$) δ (ppm): 2.47 (q, *J* = 7.3 Hz, 2H), 2.15 (s, 3H), 1.07 (t, *J* = 7.3 Hz, 3H).

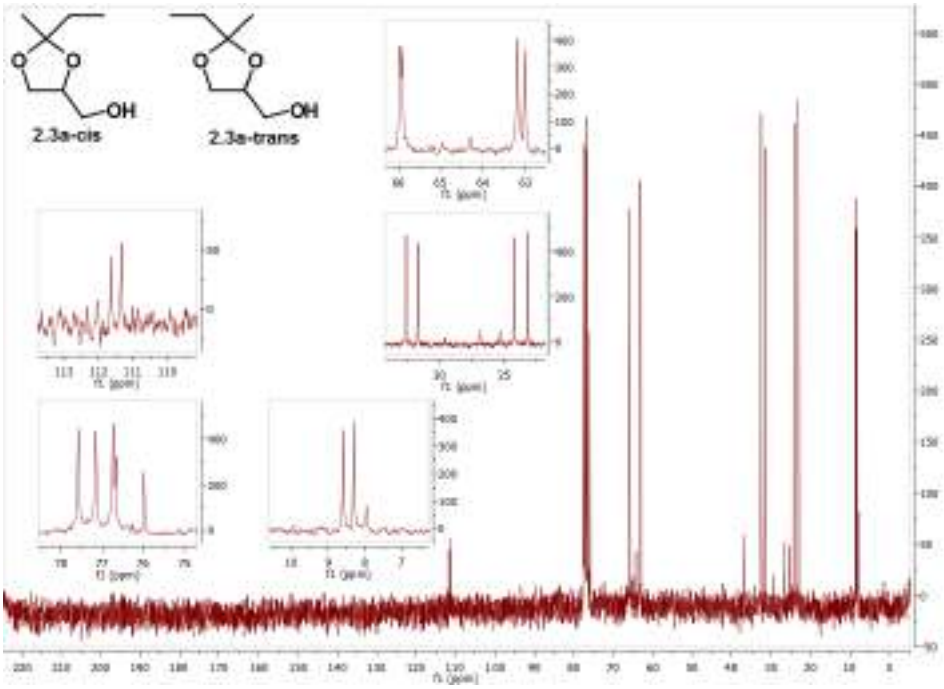

Figure A2. ^{13}C NMR spectra of **2.3a**

^{13}C NMR (75 MHz, $CDCl_3$) δ (ppm): 111.91, 111.61, 76.93, 76.25, 66.23, 66.19, 63.46, 63.28, 32.90, 31.99, 24.54, 23.45, 8.86, 8.57.

The spectrum also showed traces of 2-butanone which corresponded to the following signals: ^{13}C NMR (75 MHz, $CDCl_3$) δ (ppm): 37.00, 29.59, 7.96.

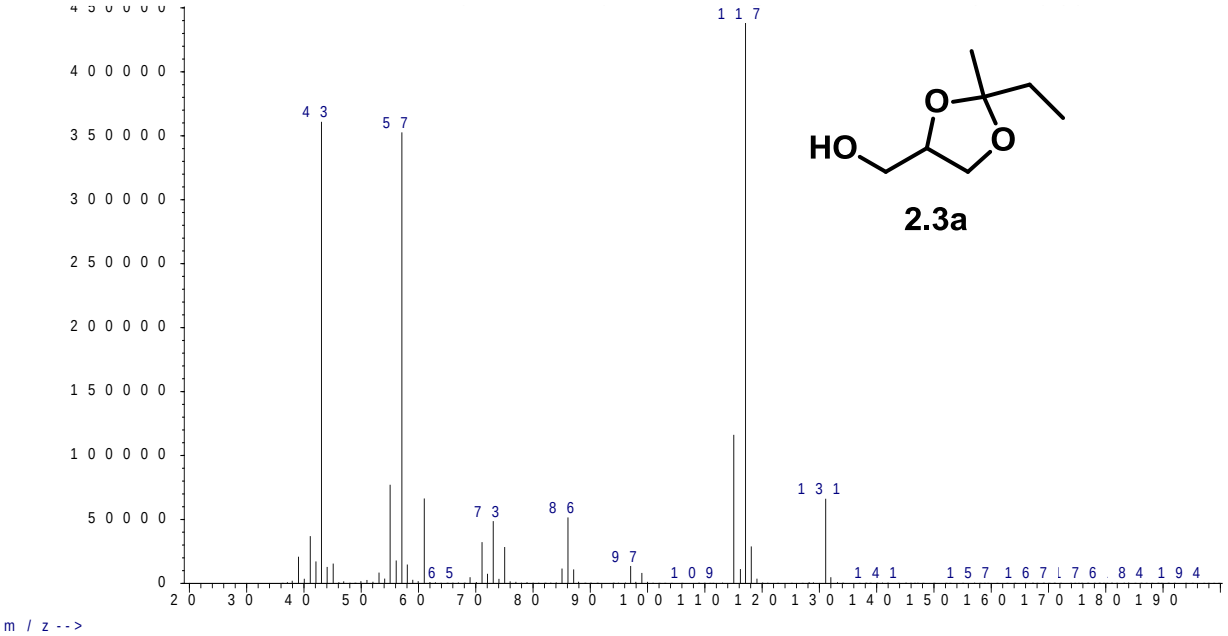

Figure A3. MS spectra of **2.3a**

GC/MS (relative intensity, 70eV) m/z: 146 (M^+, <1%), 131 (20), 117 (100), 115 (27), 86 (11), 73 (11), 61 (14), 57 (84), 55 (18), 43 (80).

Figure A4 and Figure A5 report the MS spectra consistent with the structure of the cyclic six-membered ring acetals **2.3a'**. However, it is not possible to establish which isomer corresponds to which MS spectrum

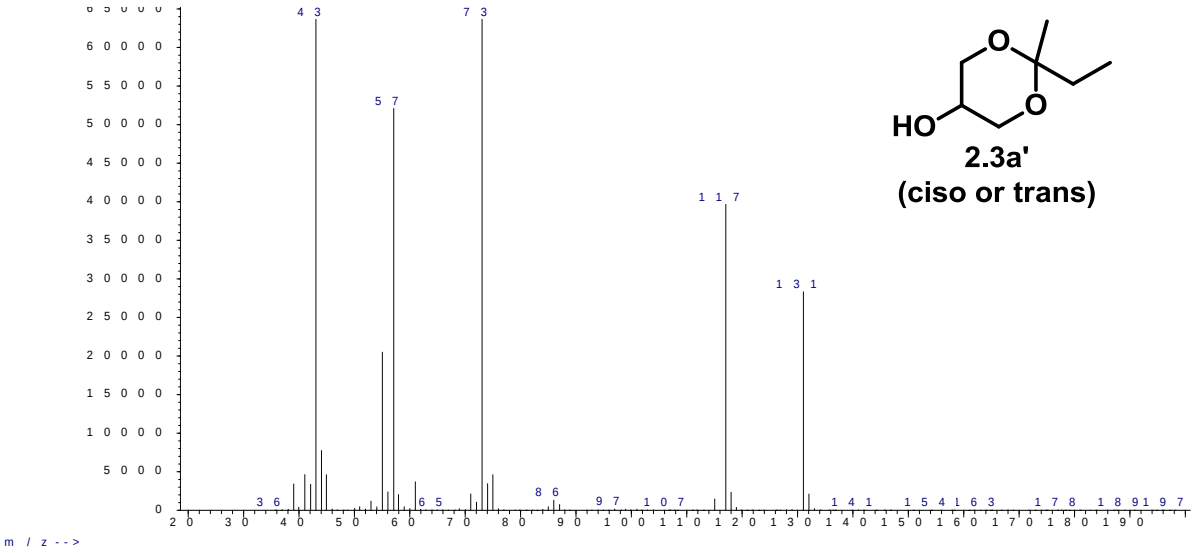

Figure A4. MS spectra of **2.3a'** (cis or trans)

GC/MS (relative intensity, 70eV) m/z: 146 (M^+, <1%), 131 (43), 117 (61), 73 (99), 57 (80), 55 (31), 44 (12), 43 (100).

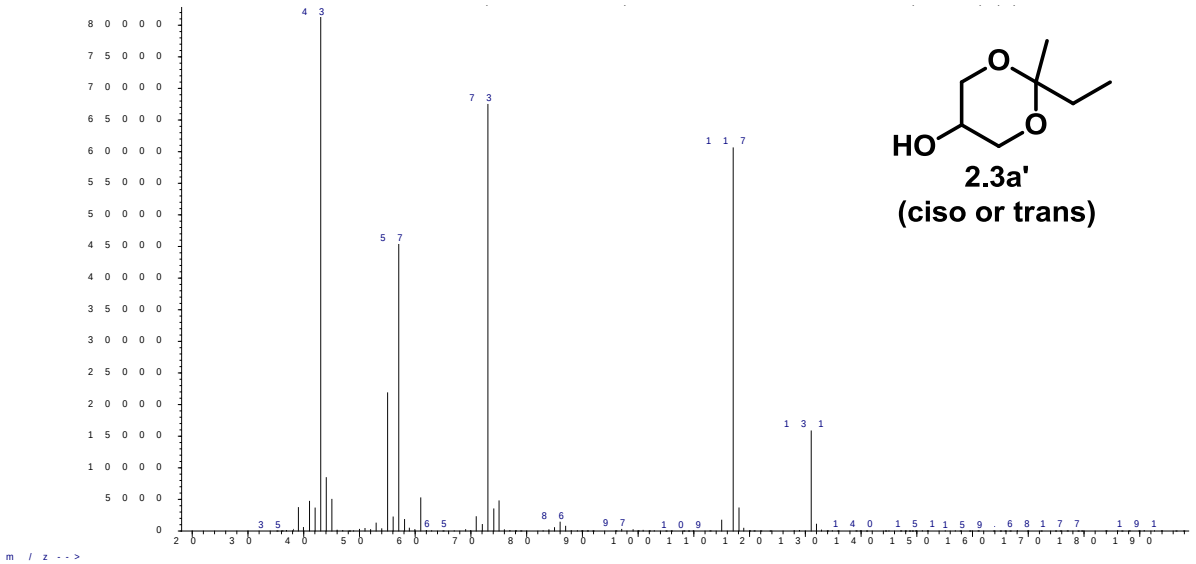

Figure A5. MS spectra of **2.3a'** (cis or trans)

GC/MS (relative intensity, 70eV) m/z: 146 (M^+, <1%), 131 (22), 117 (82), 73 (85), 57 (56), 55 (27), 44 (10), 43 (100).

6.2 Glycerol for the synthesis of N-heterocycles (chapter 3)

6.2.1 NMR and mass analyses

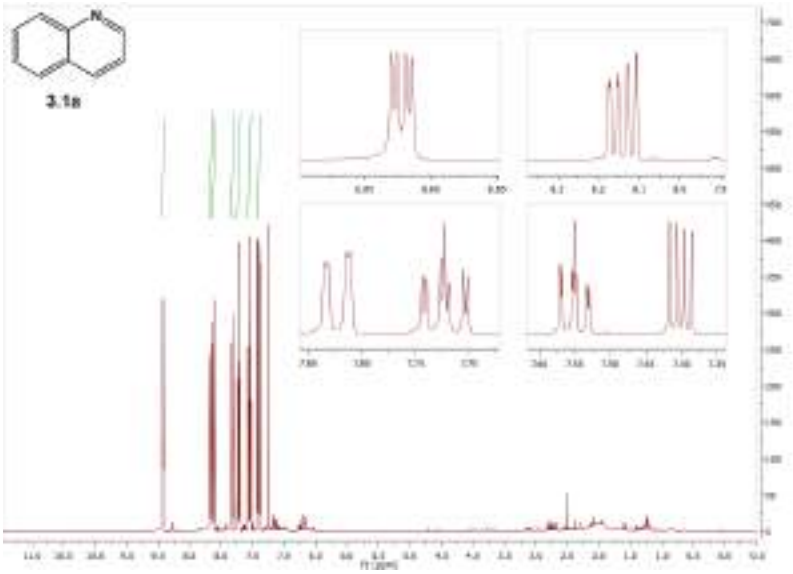

Figure A6. ^{1}H NMR spectra of **3.1a**

^{1}H NMR (400 MHz, $CDCl_3$) δ 8.92 (dd, J = 4.2, 1.7 Hz, 1H), 8.16 (m, 1H), 8.12 (m, 1H), 7.85-7.80 (m, 1H), 7.72 (ddd, J = 8.5, 6.9, 1.5 Hz, 1H), 7.55 (ddd, J = 8.1, 6.9, 1.2 Hz, 1H), 7.40 (dd, J = 8.3, 4.2 Hz, 1H).

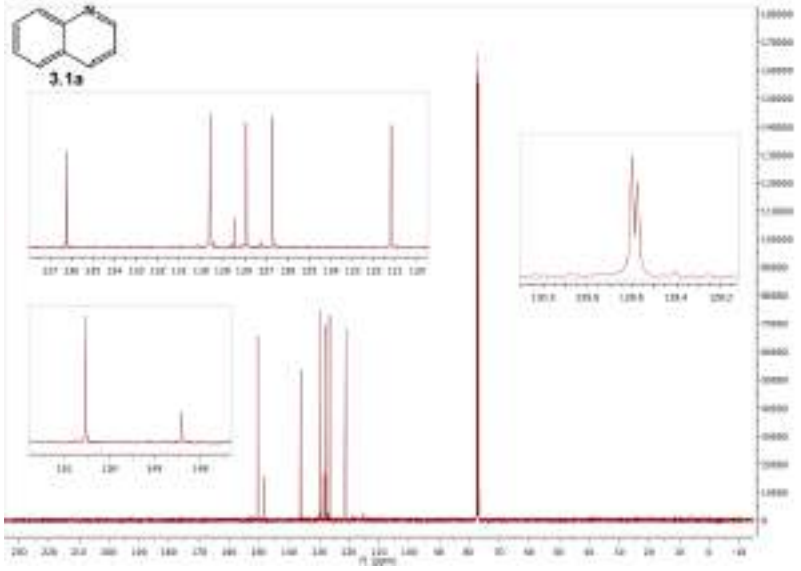

Figure A7. ^{13}C NMR spectra of **3.1a**

^{13}C NMR (100 MHz, $CDCl_3$) δ 150.53, 148.40, 136.22, 129.60, 129.58, 128.43, 127.92, 126.68, 121.21.

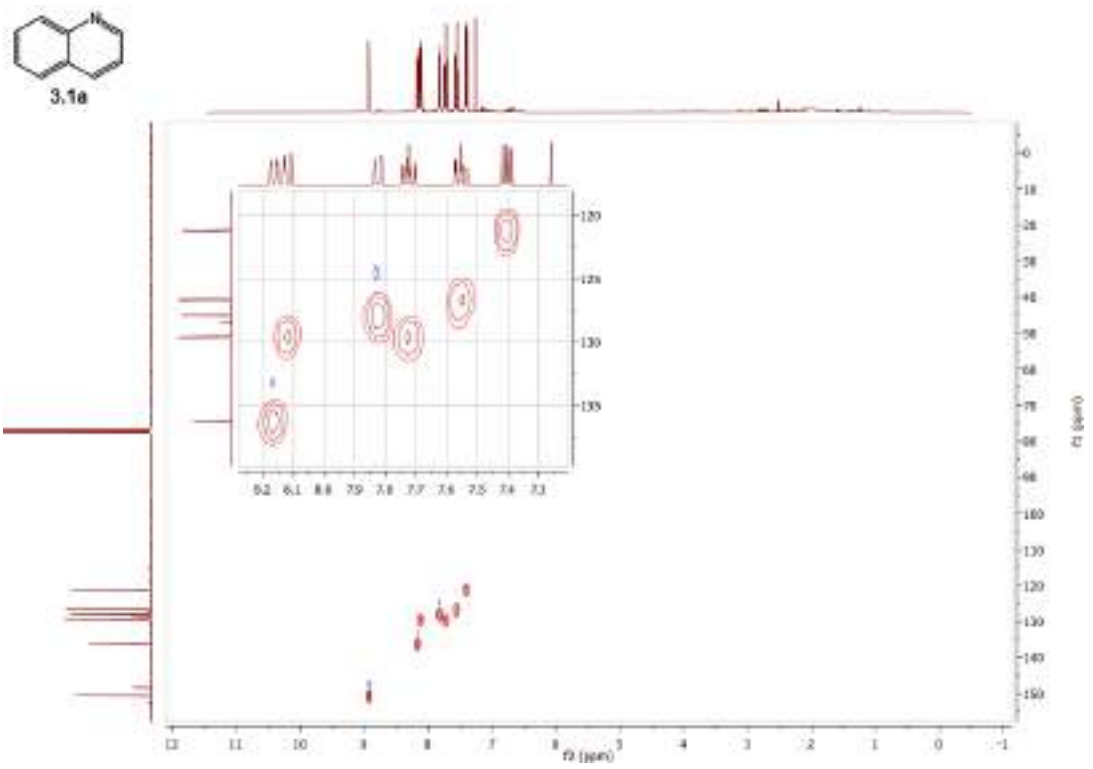

Figure A8. HMQC spectra of **3.1a**

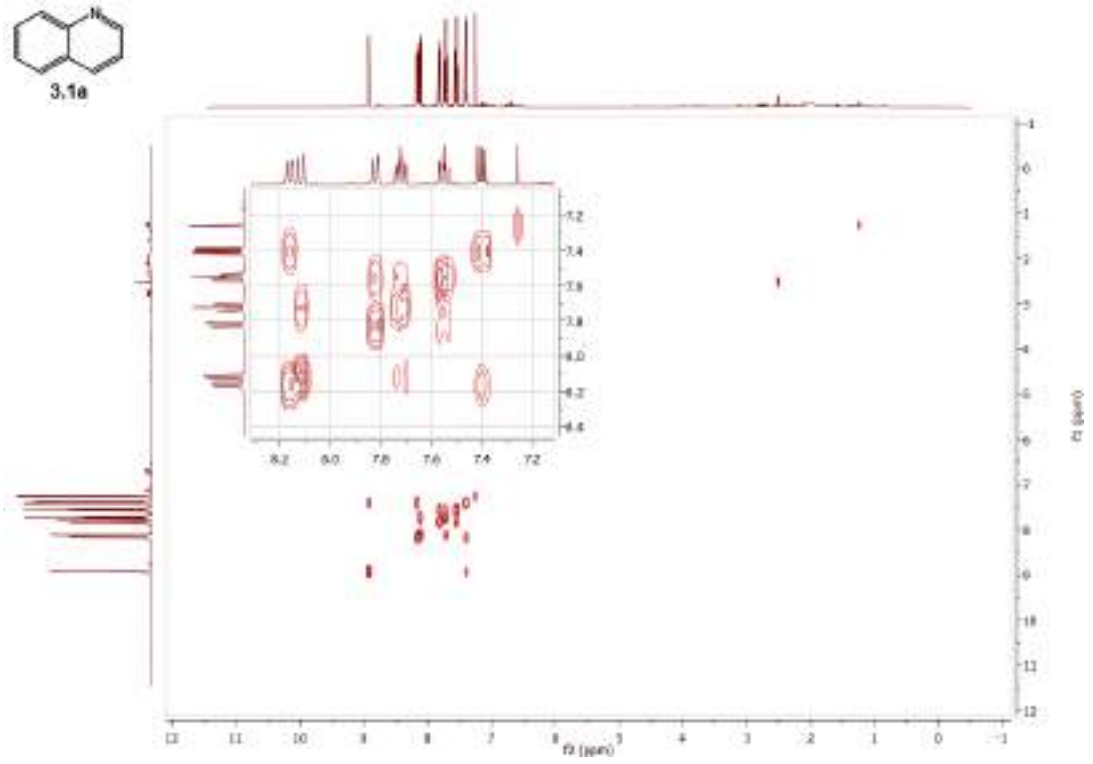

Figure A9. COSY spectra of **3.1a**

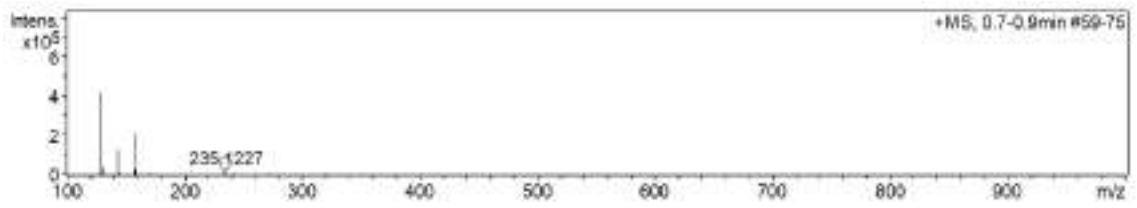

Figure A10. Mass spectra of **3.1a**

Mass (Most Intense MS Peaks) *m/z*: 158.0968 (51.0), 144.0808 (31.0), 131.0683 (10.6), 130.0653 (100.0).

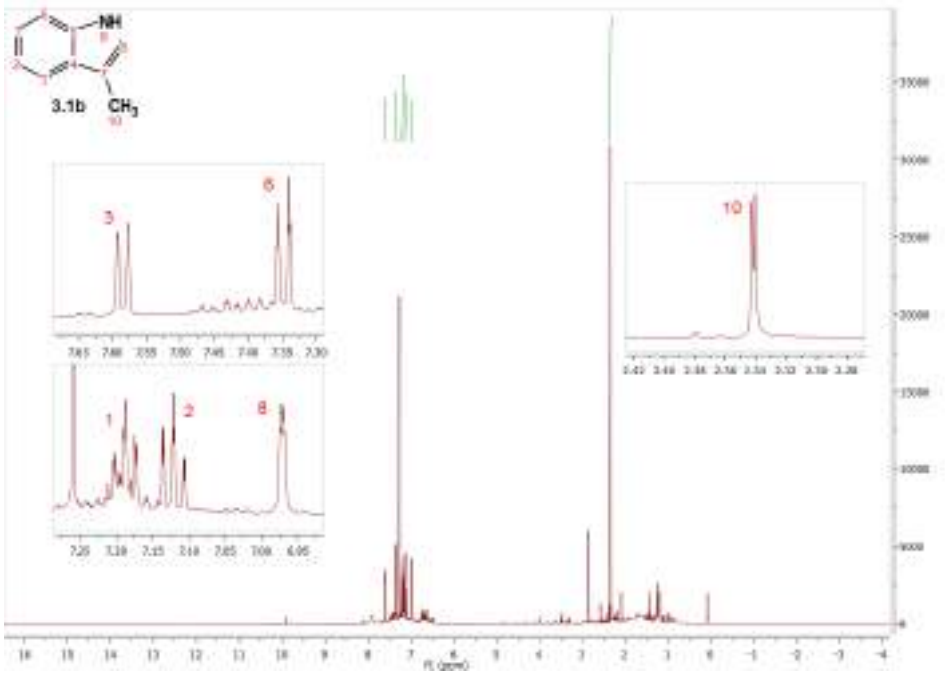

Figure A11.[1]H NMR spectra of **3.1b**

^{1}H NMR (500 MHz, $CDCl_3$) δ 7.59 (dd, J = 7.8, 1.1 Hz, 1H), 7.35 (dd, J = 8.0, 0.9 Hz, 1H), 7.19 (ddd, J = 8.2, 7.0, 1.3 Hz, 1H), 7.12 (ddd, J = 7.9, 7.0, 1.0 Hz, 1H), 6.97 (dd, J = 2.3, 1.2 Hz, 1H), 2.34 (d, J = 1.1 Hz, 3H).

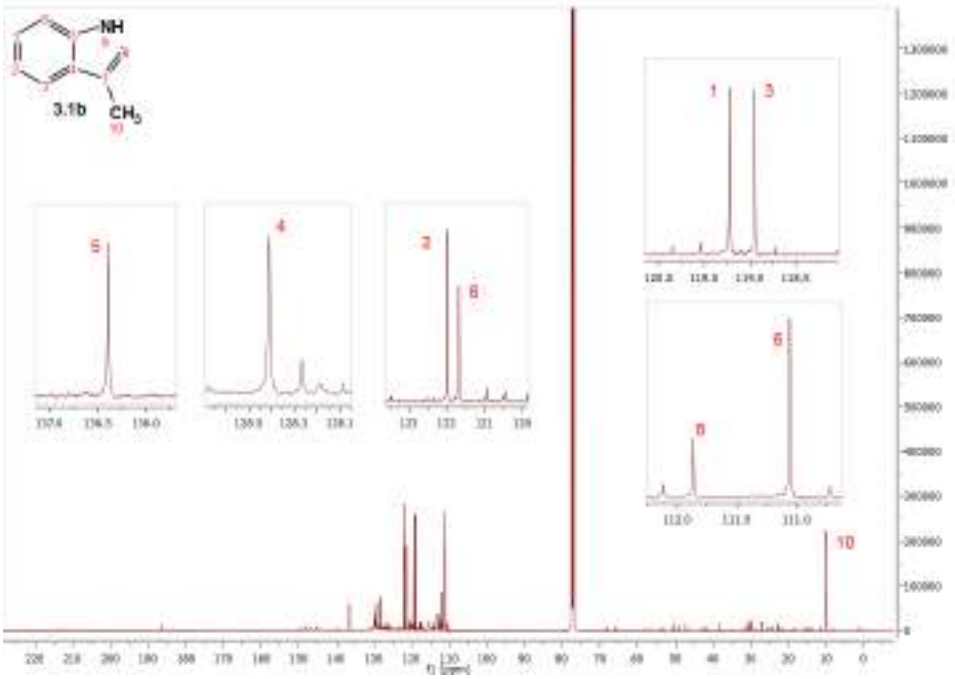

Figure A12. [13]C NMR spectra of **3.1b**

^{13}C NMR (125 MHz, $CDCl_3$) δ 136.39, 128.41, 121.98, 121.68, 119.23, 118.95, 111.86, 111.06, 9.80.

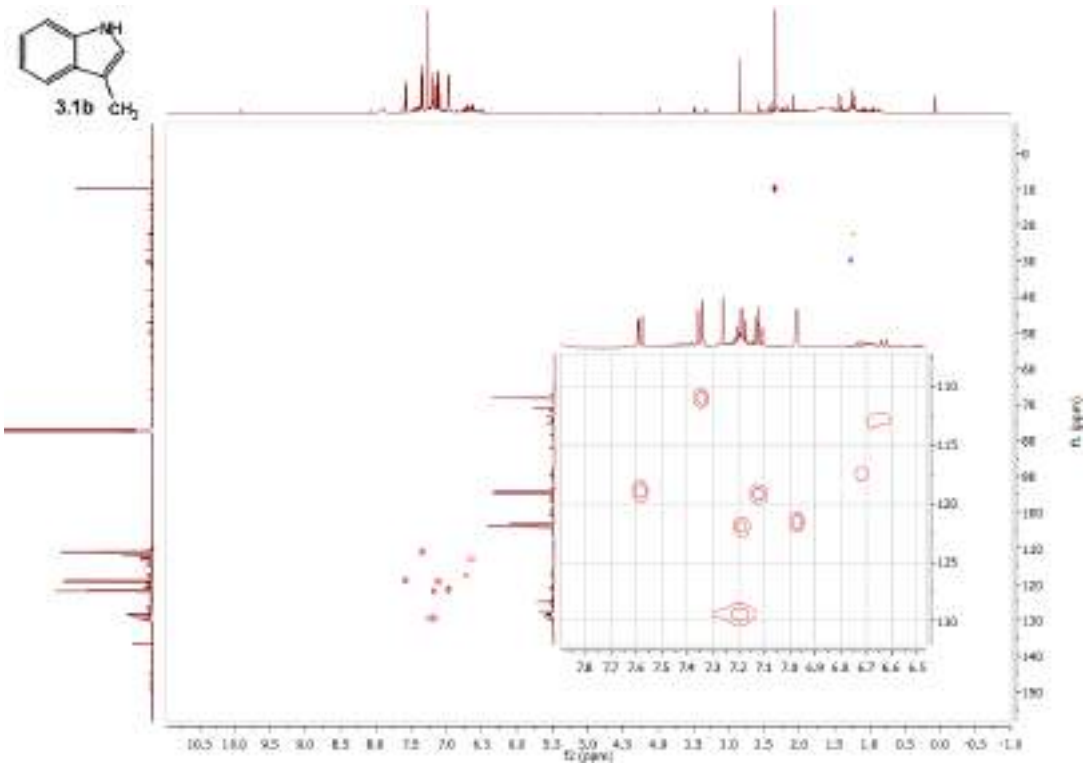

Figure A13. HMQC spectra of **3.1b**

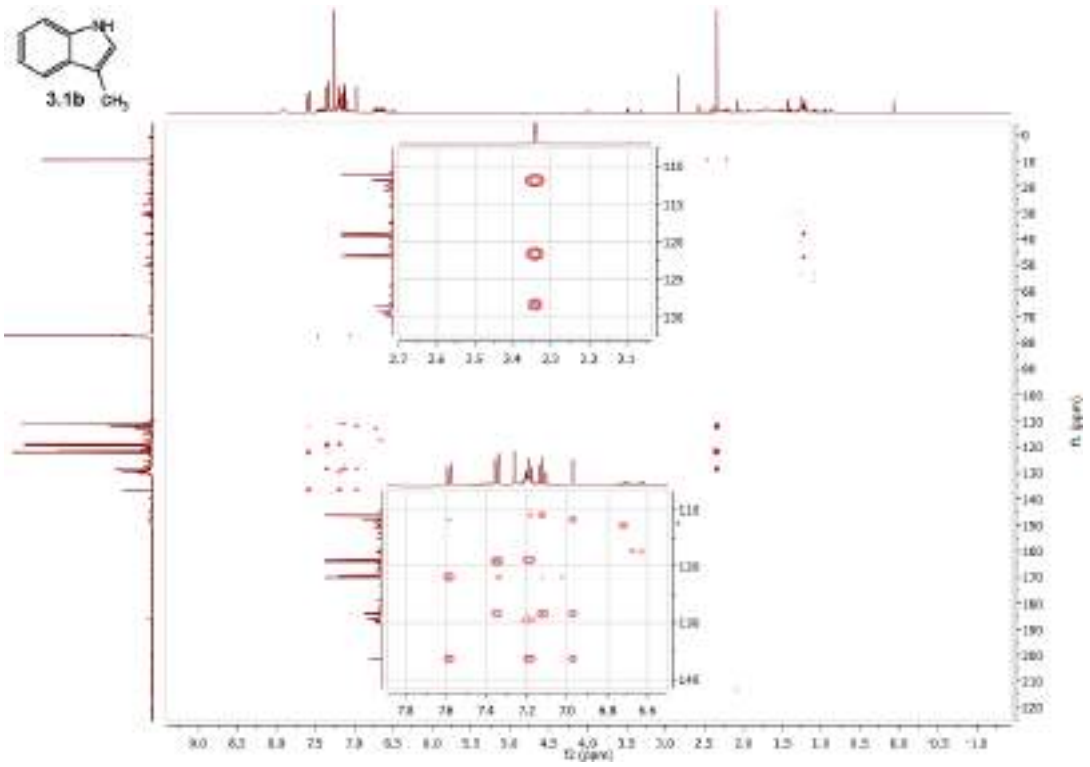

Figure A14. HMBC spectra of **3.1b**

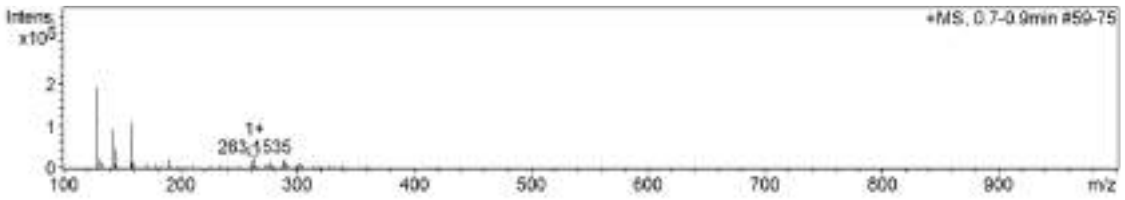

Figure A15. Mass spectra of **3.1b**

Mass (Most Intense MS Peaks) *m/z*: 289.1683 (10.2) 263.1535 (13.3), 190.1229 (12.3), 158.0967 (58), 146.0963 (24.7), 144.0809 (48.9), 131.0687 (11.0), 130.0654 (100.0).

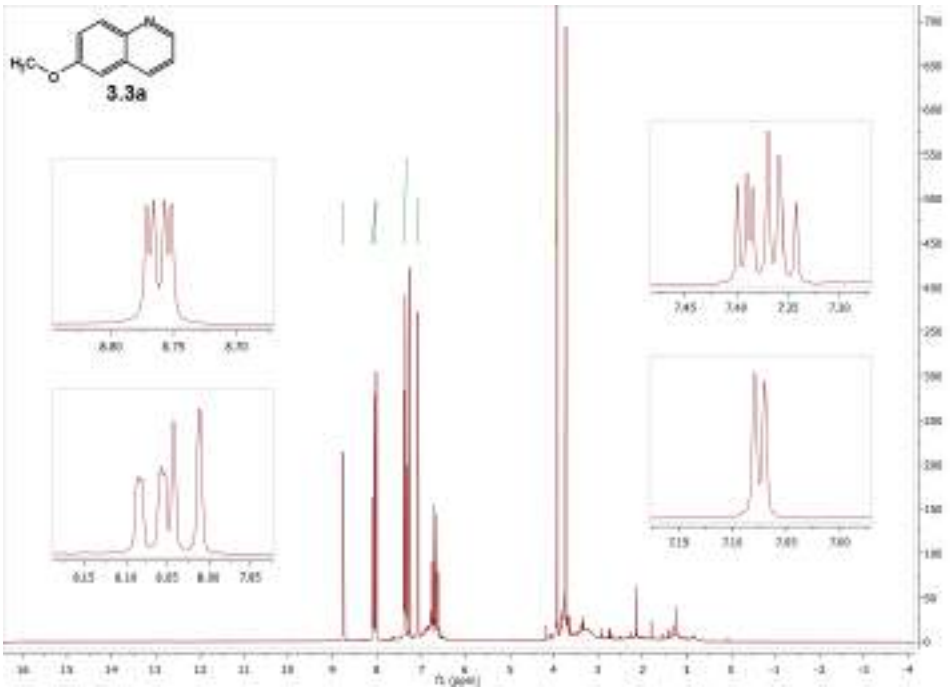

Figure A16. ^{1}H NMR spectra of **3.3a**

^{1}H NMR (300 MHz, $CDCl_3$) δ 8.78 (dd, J = 4.3, 1.7 Hz, 1H), 8.12 – 8.07 (m, 1H), 8.07 – 8.02 (m, 1H), 7.43 – 7.36 (m, 2H), 7.09 (d, J = 2.8 Hz, 1H), 3.95 (s, 3H).

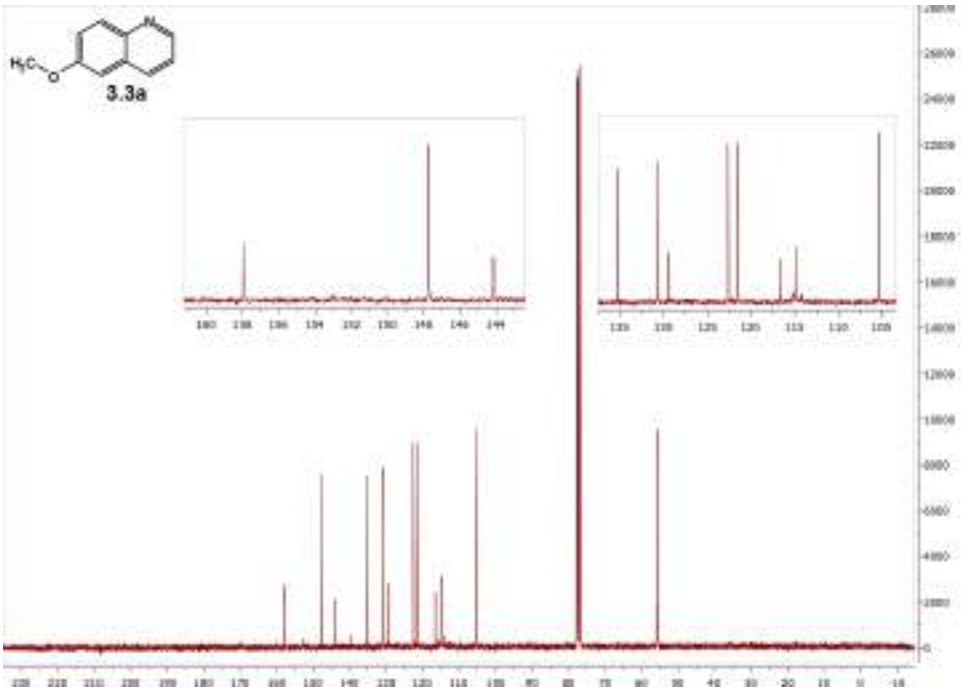

Figure A17. ^{13}C NMR spectra of **3.3a**

^{13}C NMR (75 MHz, $CDCl_3$) δ 157.95, 147.72, 144.15, 135.25, 130.68, 129.48, 122.63, 121.49, 105.24, 55.68.

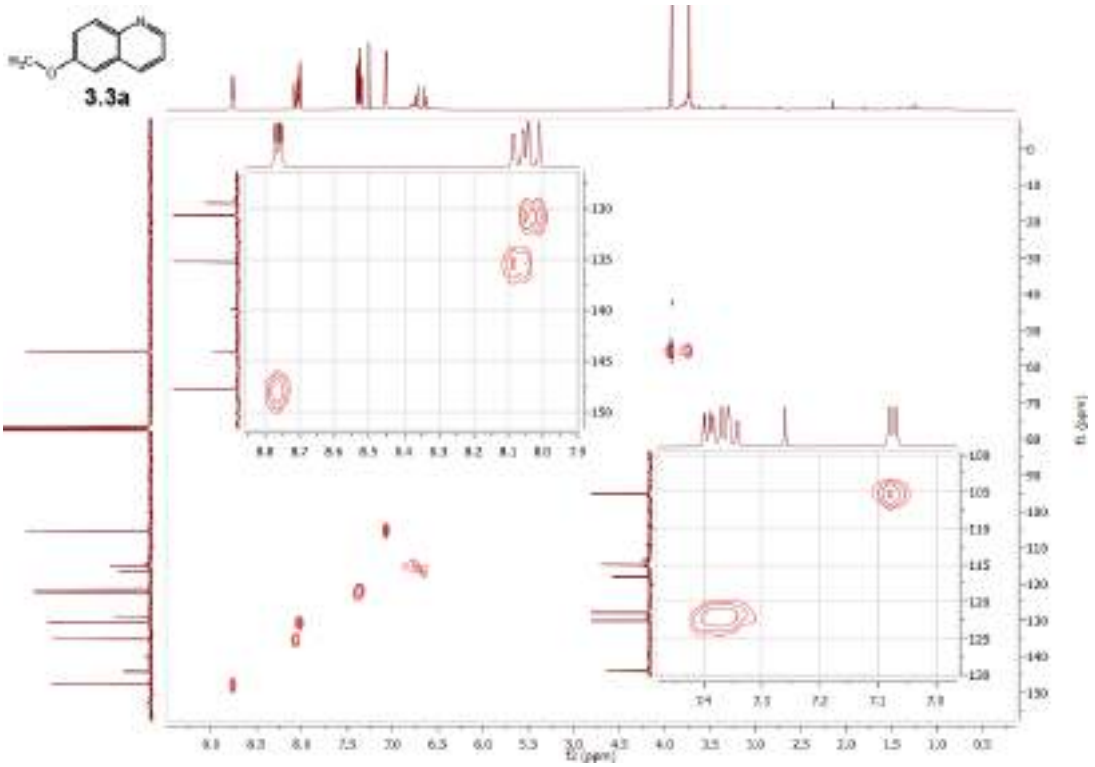

Figure A18. HMQC spectra of **3.3a**

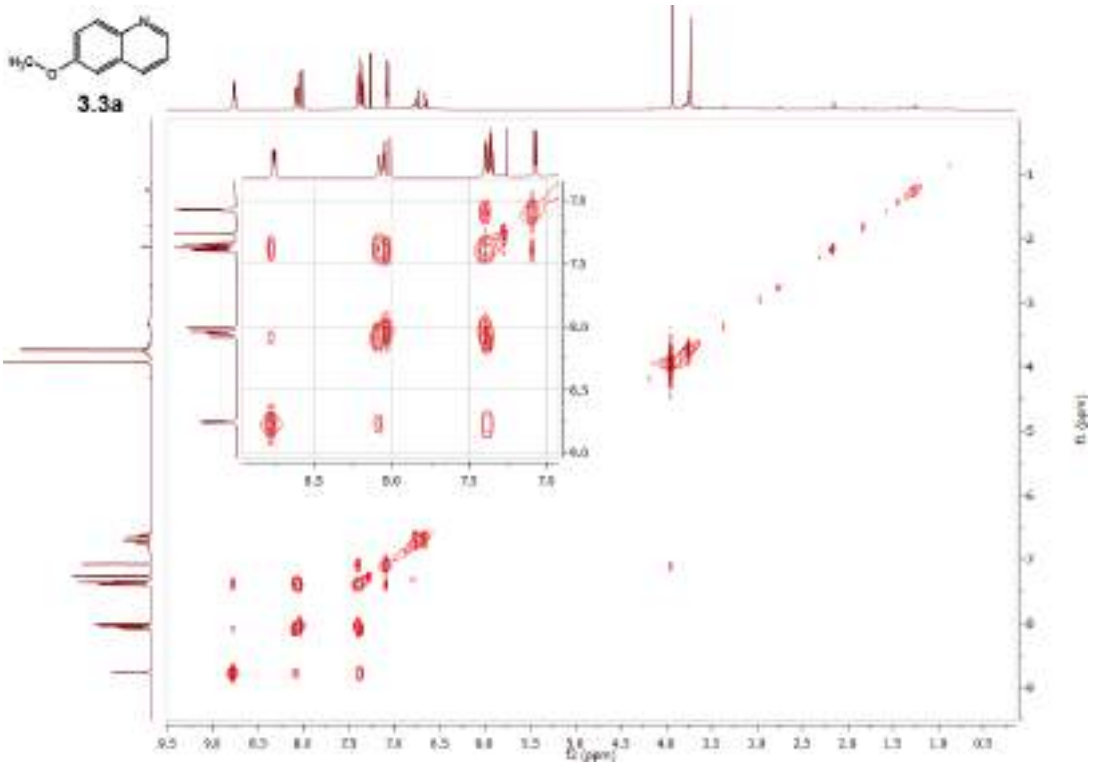

Figure A19. COSY spectra of **3.3a**

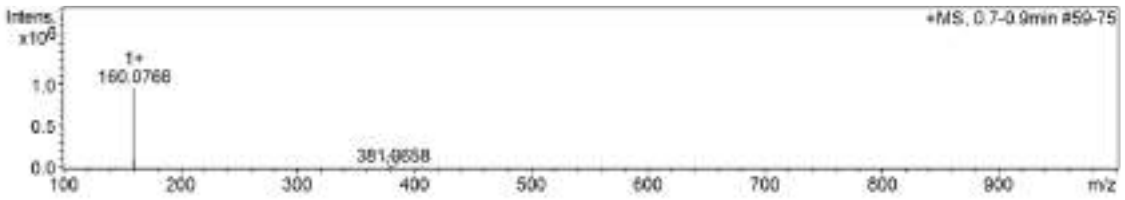

Figure A20. Mass spectra of **3.3a**

Mass (Most Intense MS Peaks) *m/z*: 161.0789 (11.2), 160.0766 (100.0).

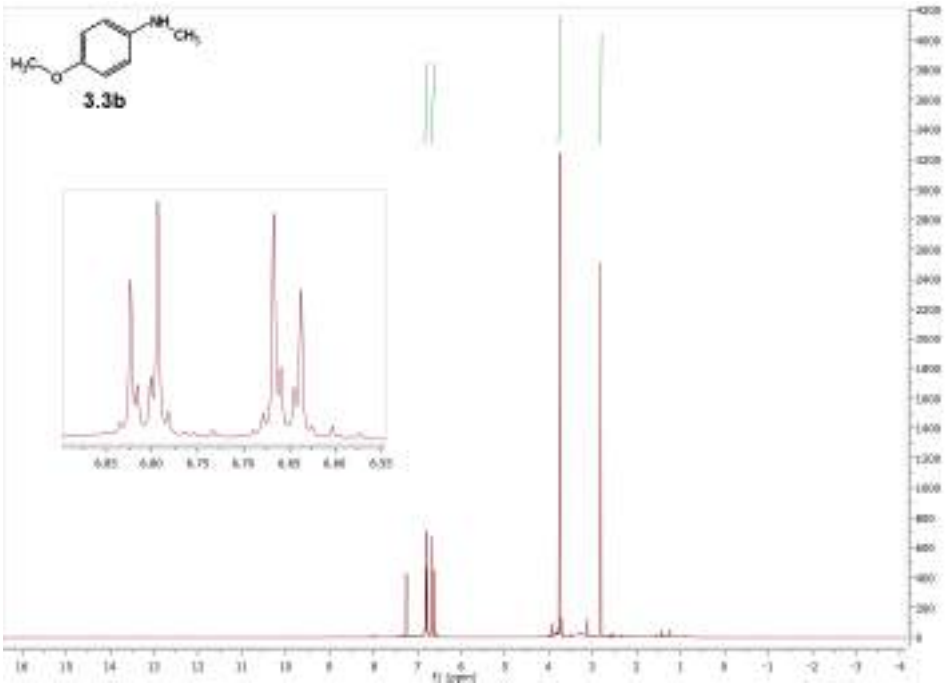

Figure A21. ^{1}H NMR spectra of **3.3b**

^{1}H NMR (300 MHz, $CDCl_3$) δ 6.84 – 6.78 (m, 2H), 6.69 – 6.62 (m, 2H), 3.76 (s, 3H), 2.82 (s, 3H).

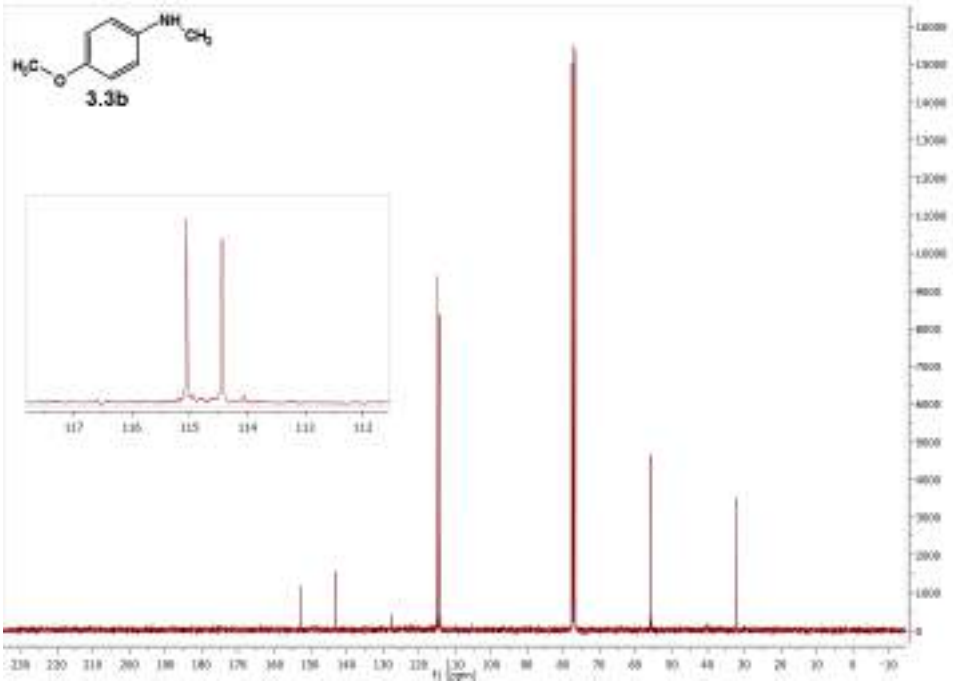

Figure A22. ^{13}C NMR spectra of **3.3b**

^{13}C NMR (75 MHz, $CDCl_3$) δ 152.7, 142.9, 115.1, 114.4, 55.98, 32.2.

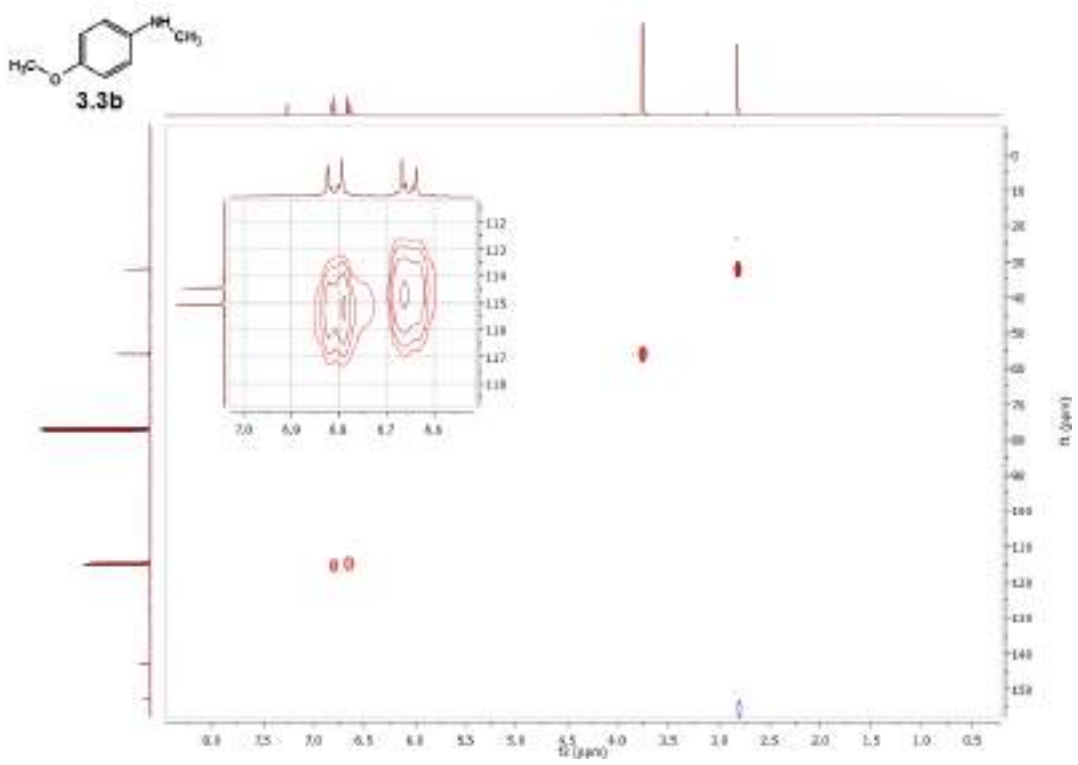

Figure A23. HMQC spectra of **3.3b**

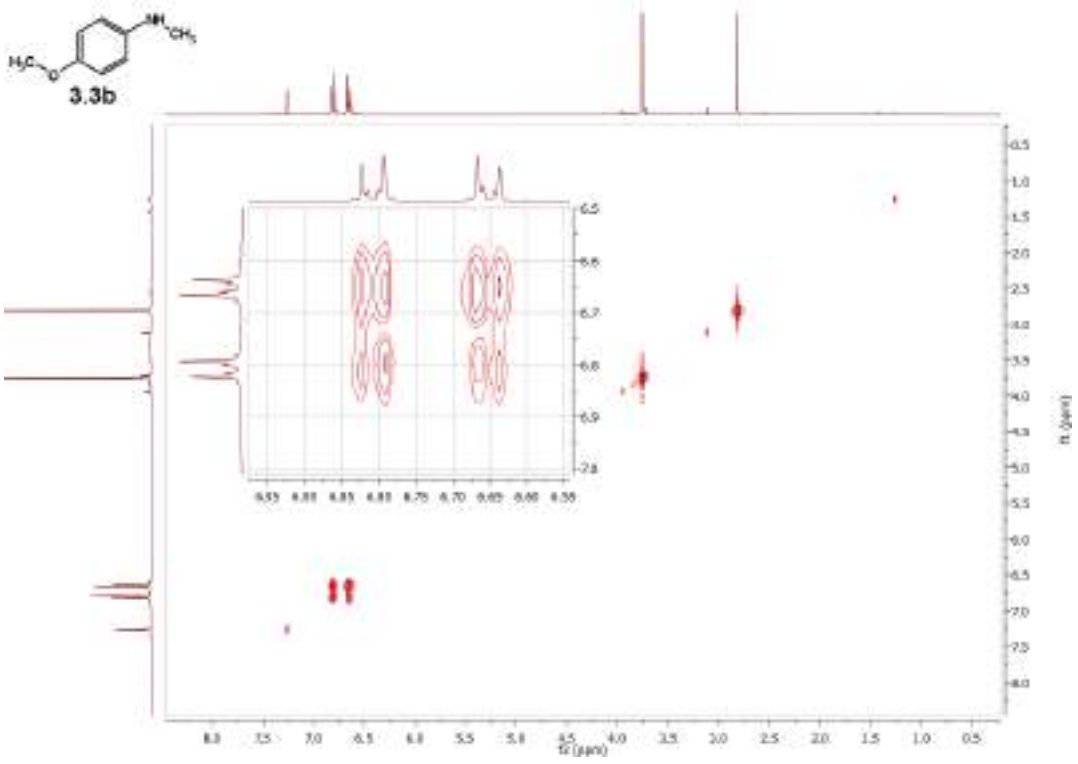

Figure A24. COSY spectra of **3.3b**

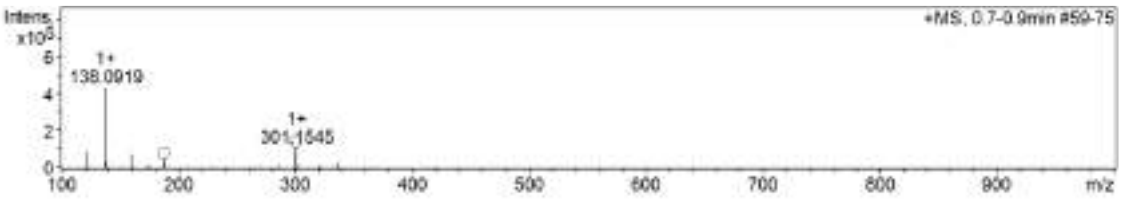

Figure A25. Mass spectra of **3.3b**

Mass (Most Intense MS Peaks) *m/z*: 301.1545 (25.2), 188.1068 (11.3), 160.0756 (18.3), 138.0919 (100.0), 123.0679 (20.5).

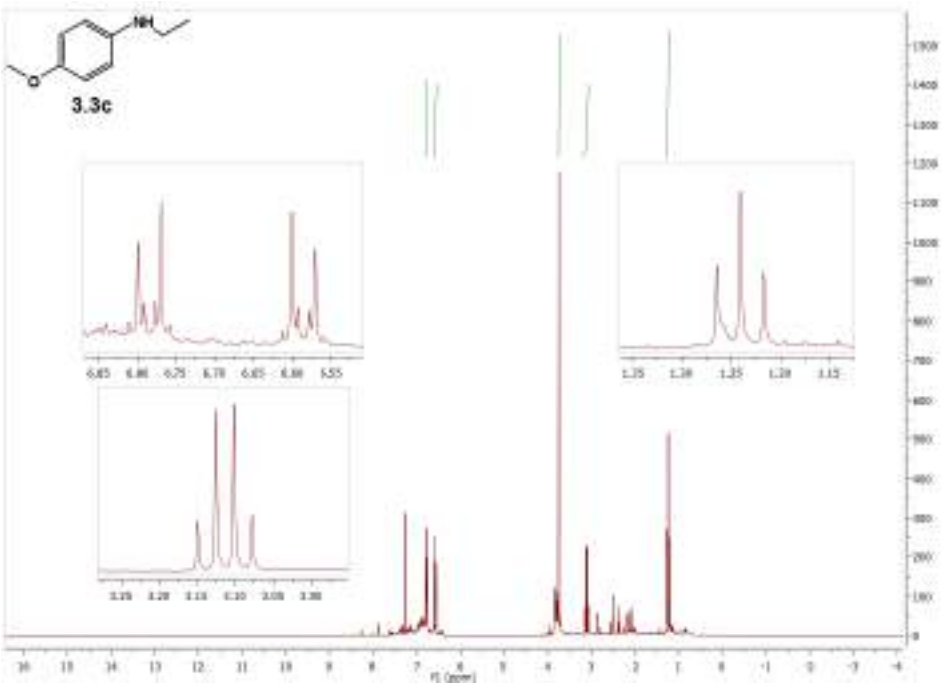

Figure A26. ^{1}H NMR spectra of **3.3c**

^{1}H NMR (300 MHz, $CDCl_3$) δ 6.82 – 6.75 (m, 2H), 6.62 – 6.55 (m, 2H), 3.75 (s, 3H), 3.11 (q, J = 7.1 Hz, 2H), 1.24 (t, J = 7.1 Hz, 3H).

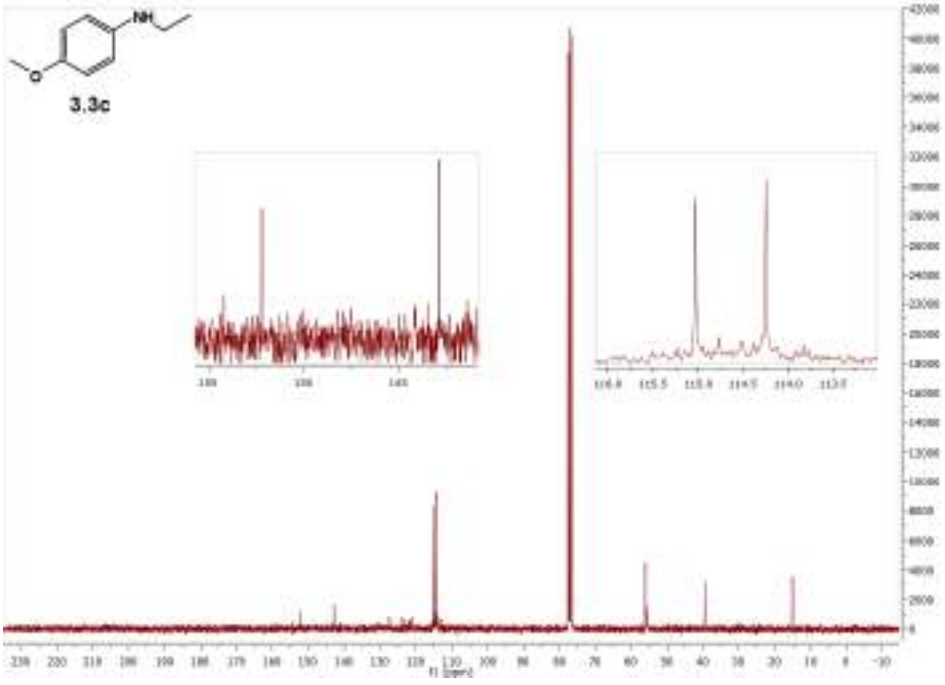

Figure A27. ^{13}C NMR spectra of **3.3c**

^{13}C NMR (75 MHz, $CDCl_3$) δ 152.19, 142.91, 115.04, 114.25, 55.98, 39.60, 15.16.

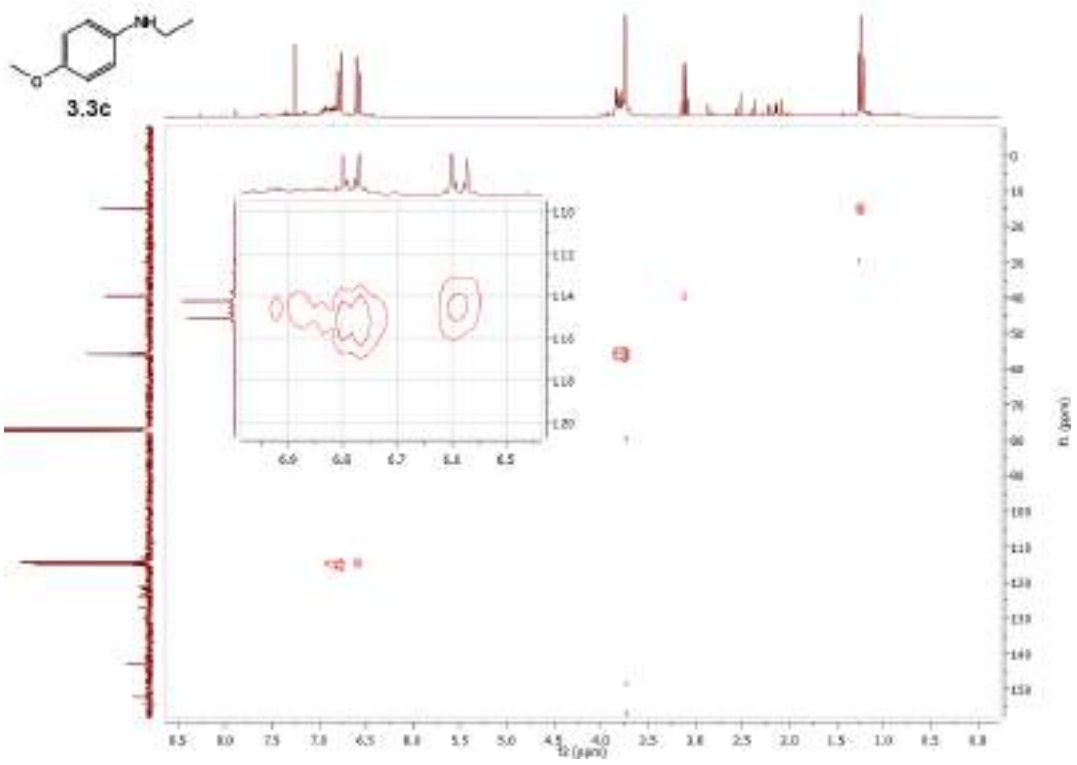

Figure A28. HMQC spectra of **3.3c**

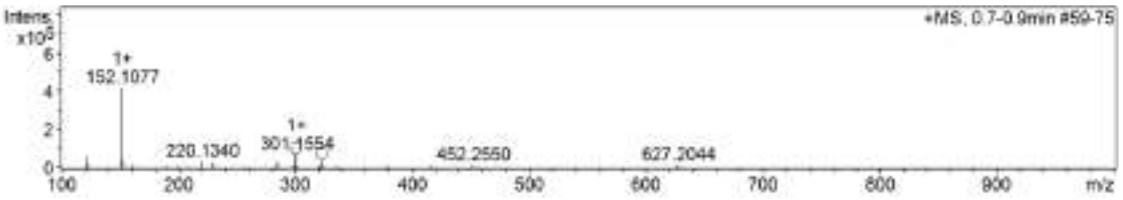

Figure A29. Mass spectra of **3.3c**

Mass (Most Intense MS Peaks) *m/z*: 323.1751 (11.4), 301.1554 (17.2), 153.1104 (10.), 152.1077 (100.0), 123.0680 (15.5).

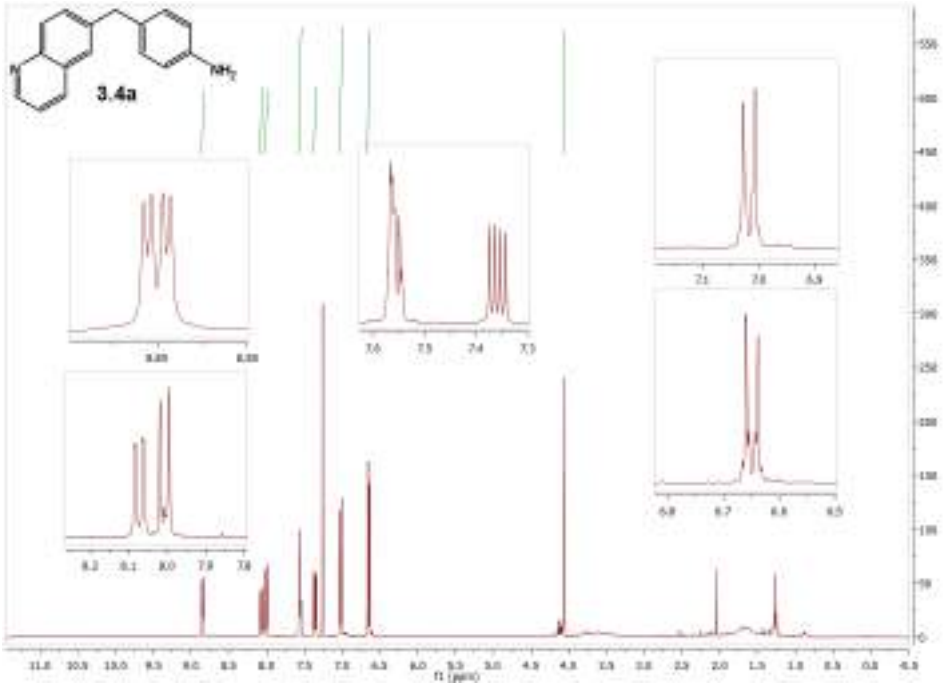

Figure A30. ^{1}H NMR spectra of **3.4a**

^{1}H NMR (400 MHz, $CDCl_3$) δ 8.85 (dd, J = 4.3, 1.7 Hz, 1H), 8.07 (dd, J = 8.3, 1.8, 1H), 8.01 (d, J = 9.2, 1H), 7.58 – 7.54 (m, 2H), 7.36 (dd, J = 8.3, 4.2 Hz, 1H), 7.02 (d, J = 8.3 Hz, 2H), 6.67 – 6.63 (m, 2H), 4.06 (s, 2H).

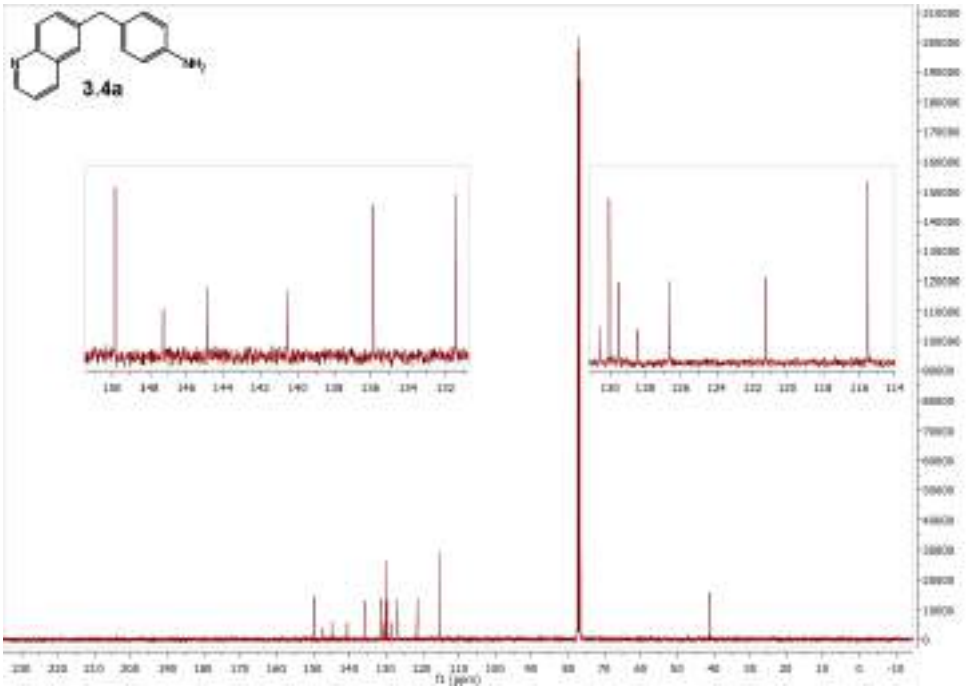

Figure A31. ^{13}C NMR spectra of **3.4a**

^{13}C NMR (100 MHz, $CDCl_3$) δ 149.9, 147.3, 144.9, 140.7, 135.9, 131.4, 130.6, 130.1, 129.5, 128.5, 126.6, 121.2, 115.5, 41.2.

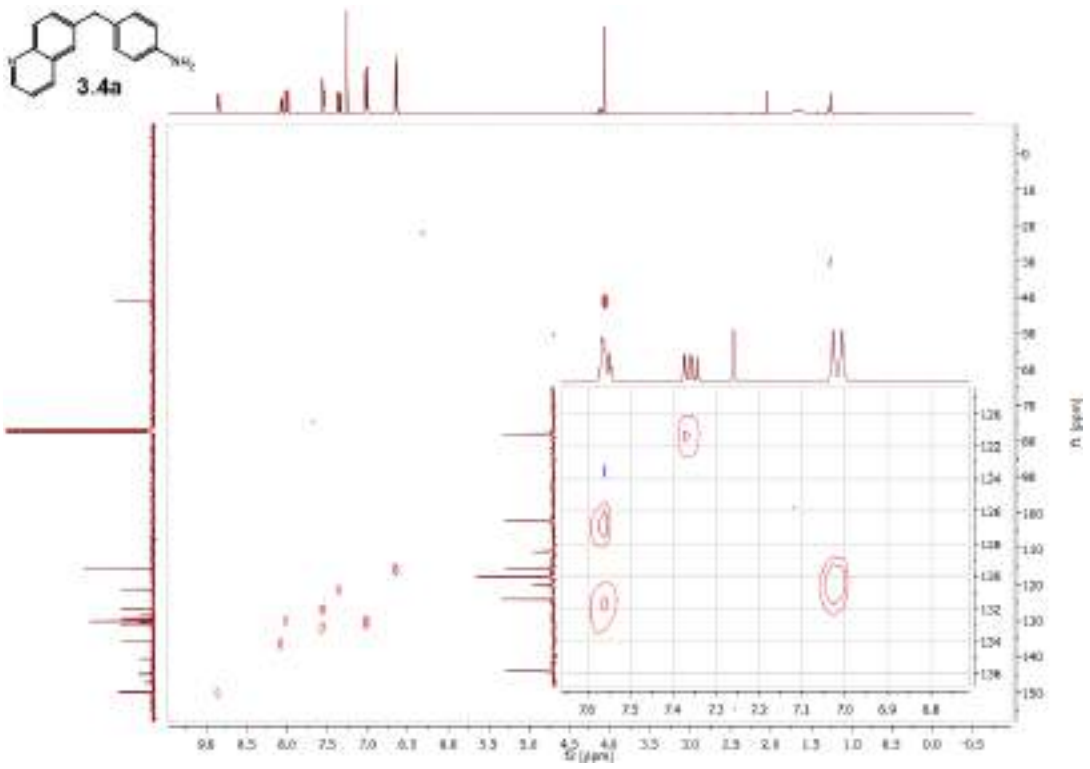

Figure A32. HMQC spectra of **3.4a**

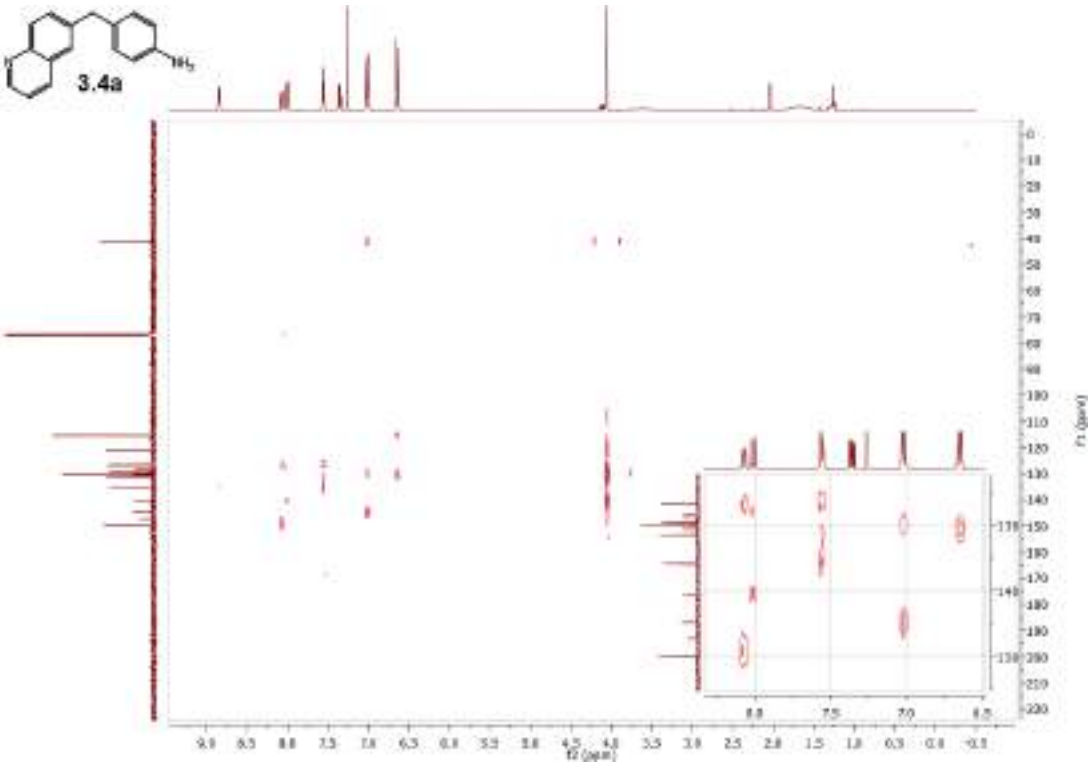

Figure A33. HMBC spectra of **3.4a**

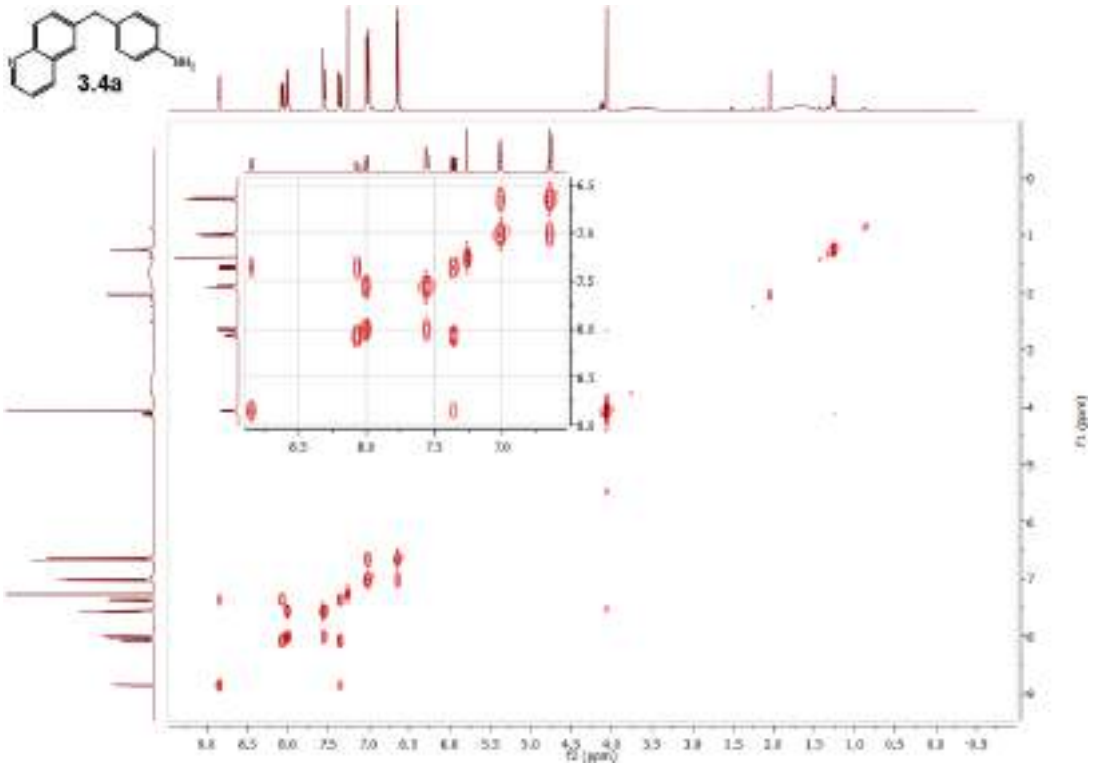

Figure A34. COSY spectra of **3.4a**

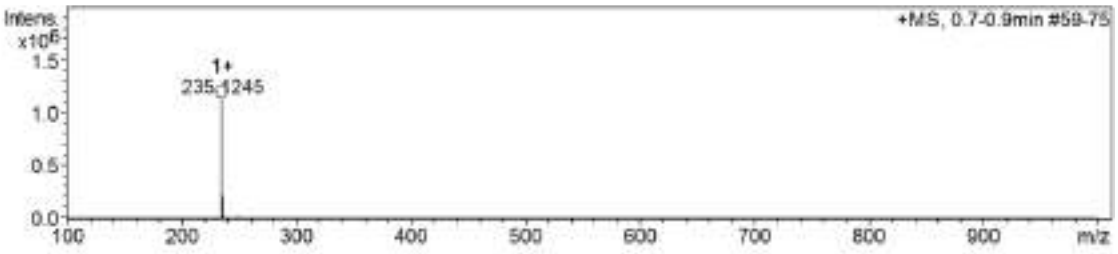

Figure A35. Mass spectra of **3.4a**

Mass (Most Intense MS Peaks) *m/z*: 236.1273 (18.8), 235.1245 (100.0).

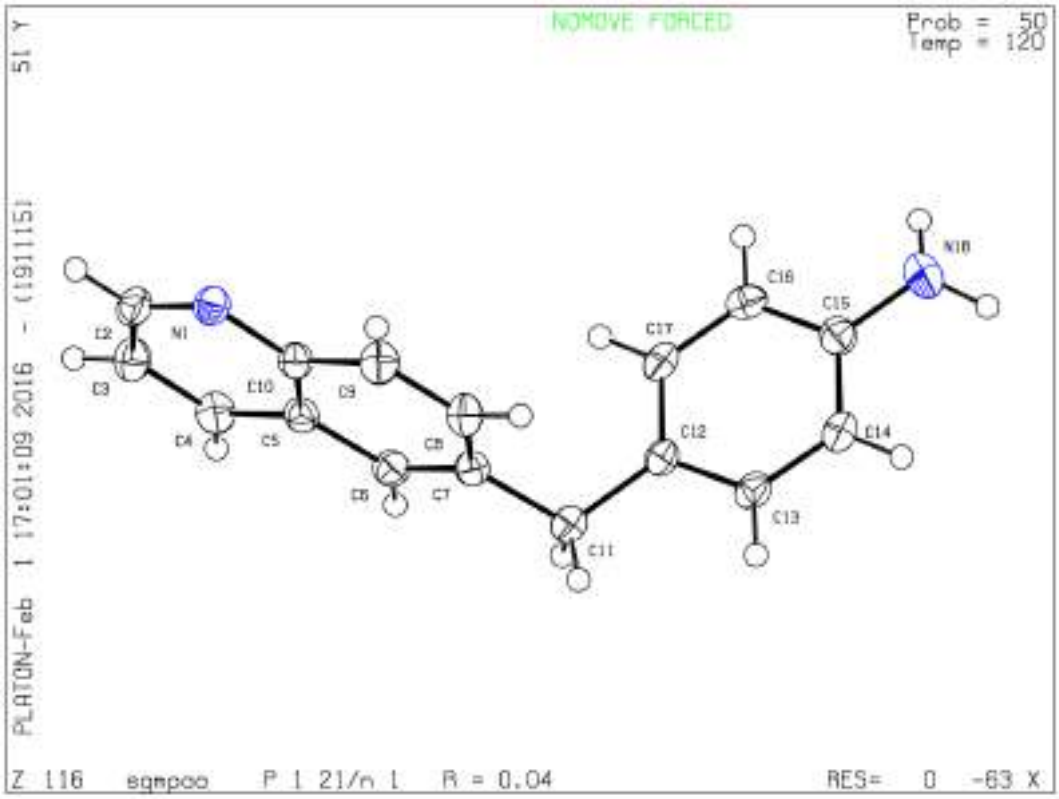

Figure A36. Crystal structure of **3.4a**

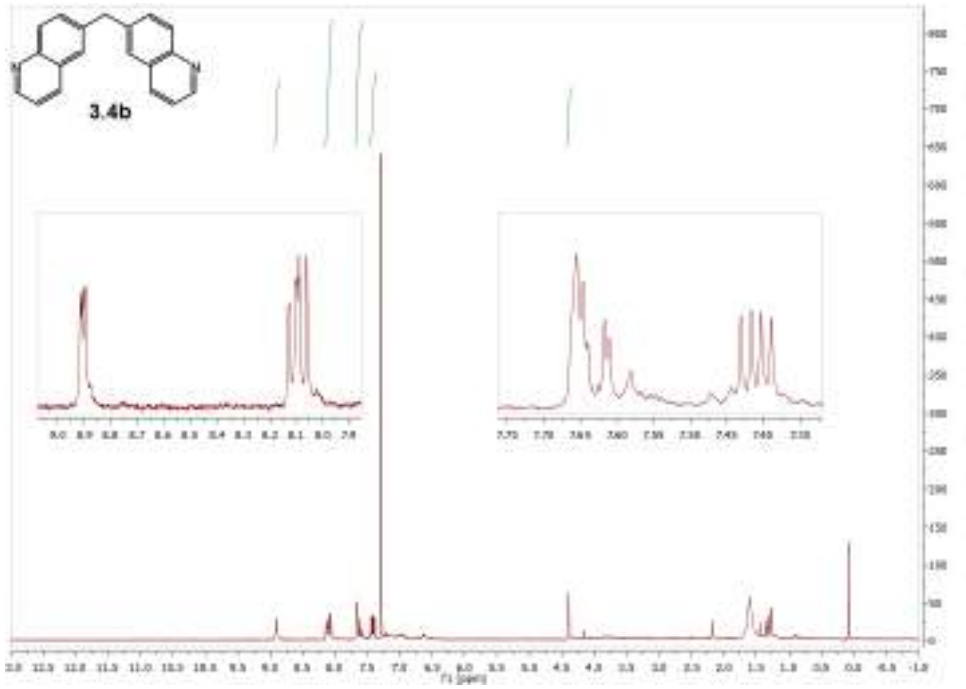

Figure A37.^{1}H NMR spectra of **3.4b**

^{1}H NMR (300 MHz, $CDCl_3$) δ 8.91 (dd, J = 4.3, 1.7 Hz, 2H), 8.09 (m, 4H), 7.70 – 7.57 (m, 4H), 7.41 (dd, J = 8.3, 4.2 Hz, 2H), 4.39 (s, 2H).

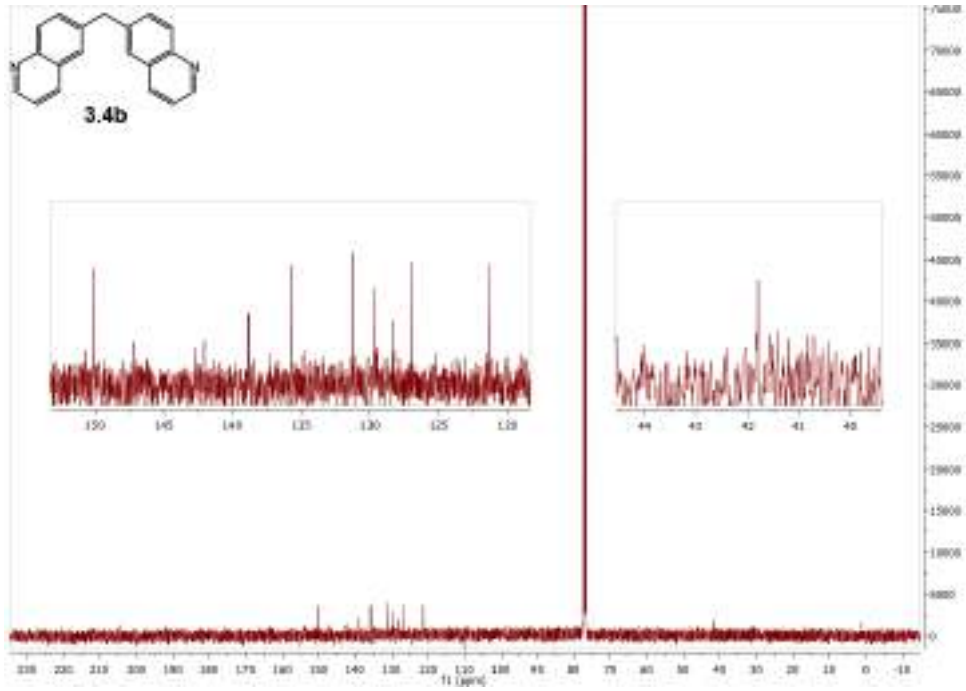

Figure A38. ^{13}C NMR spectra of **3.4b**

^{13}C NMR (100 MHz, $CDCl_3$) δ 150.1, 147.3, 138.9, 135.7, 131.2, 129.8, 128.4, 127.1, 121.3, 41.8.

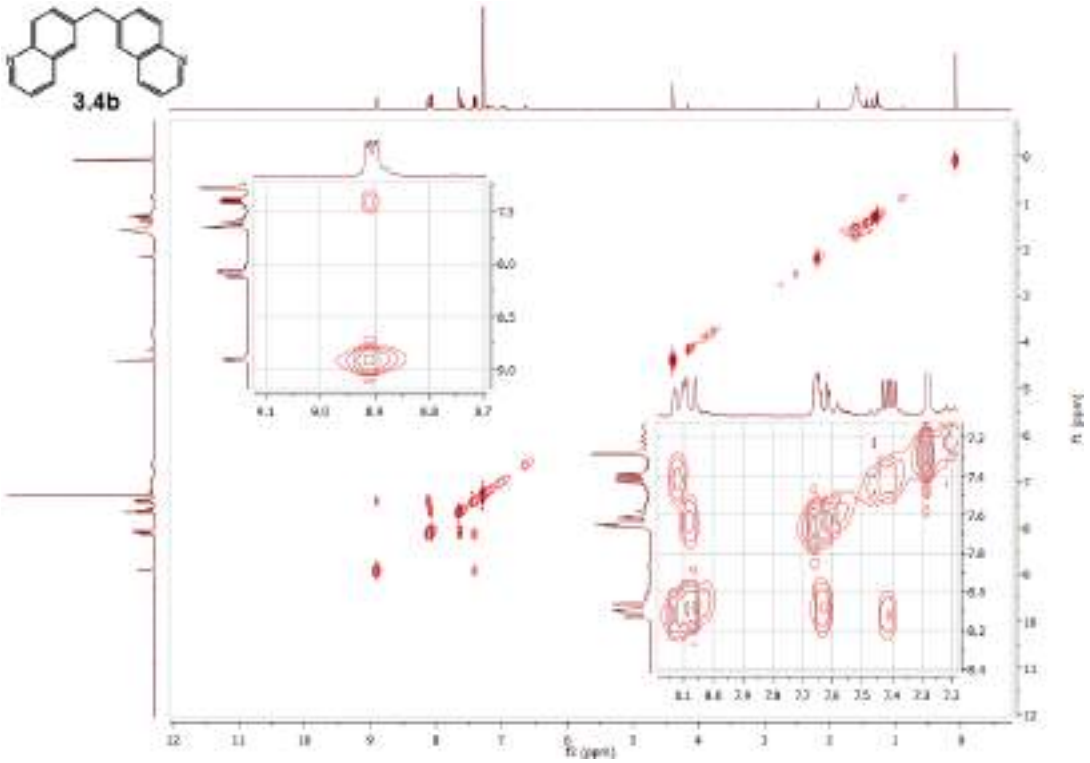

Figure A39. COSY spectra of **3.4b**

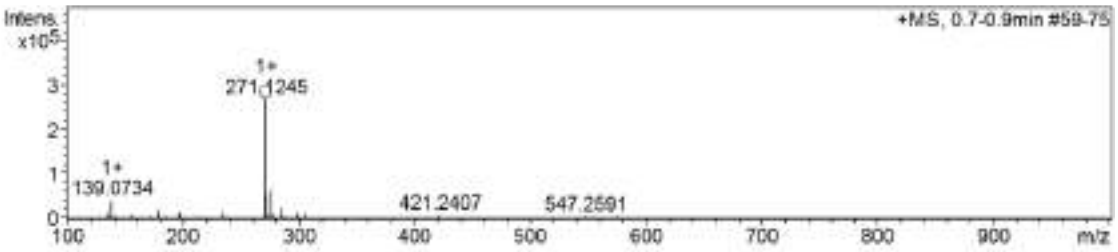

Figure A40. Mass spectra of **3.4b**

Mass (Most Intense MS Peaks) *m/z*: 277.1343 (24.0), 272.1270 (19.9), 271.1245 (100.0), 139.0734 (15.4).

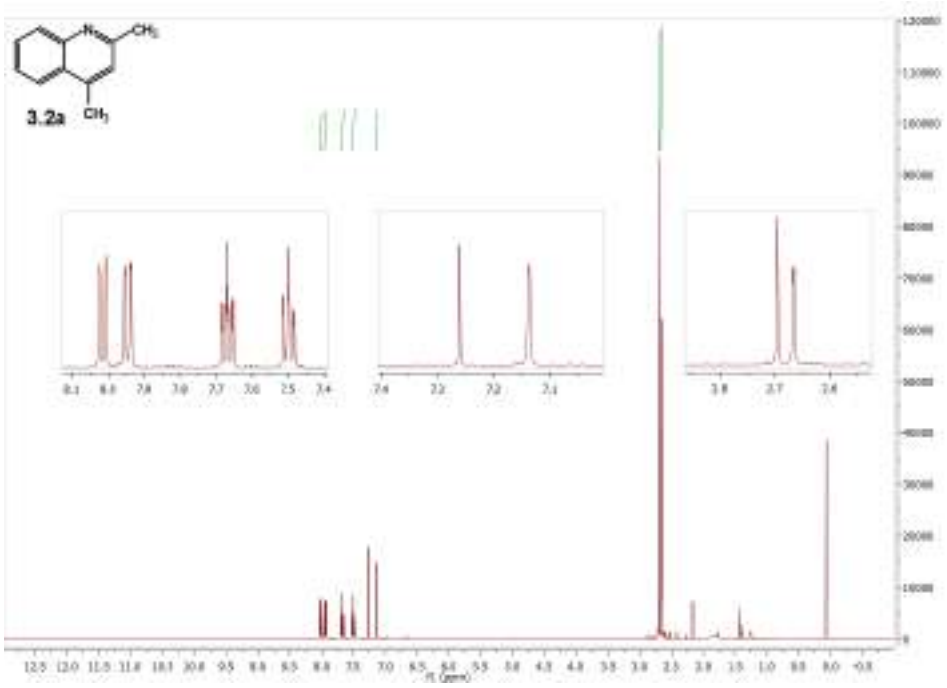

Figure A41. ^{1}H NMR spectra of **3.2a**

^{1}H NMR (500 MHz, $CDCl_3$) δ 8.02 (d, J = 8.5, 1H), 7.95 (dd, J = 8.3, 1.4 Hz, 1H), 7.67 (ddd, J = 8.4, 6.8, 1.4 Hz, 1H), 7.50 (ddd, J = 8.2, 6.9, 1.3 Hz, 1H), 7.14 (d, J = 1.1 Hz, 1H), 2.70 (s, 3H), 2.67 (d, 3H).

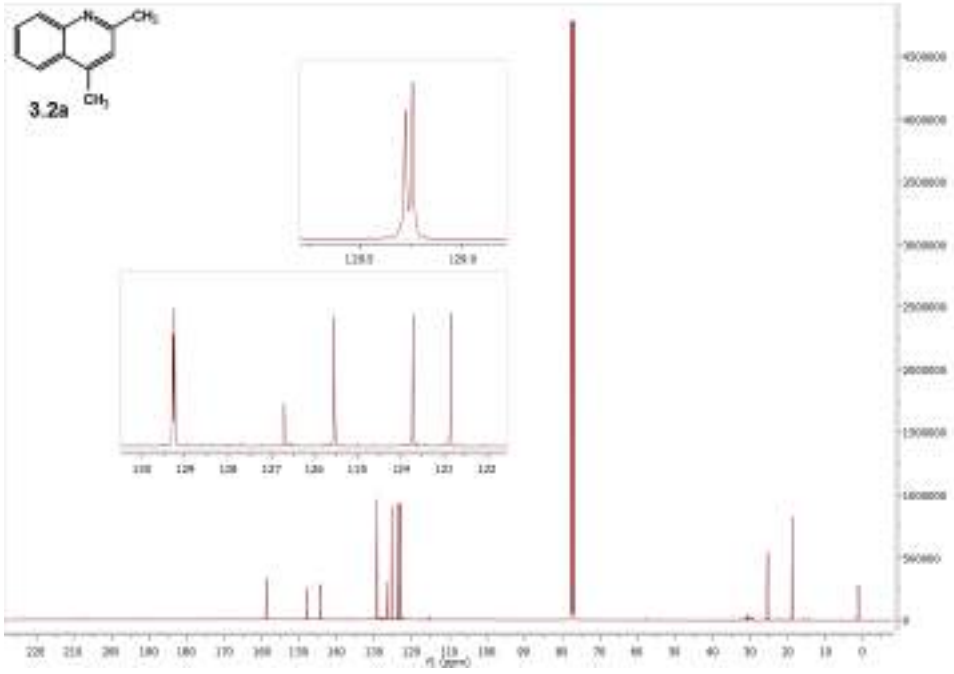

Figure A42. ^{13}C NMR spectra of **3.2a**

^{13}C NMR (126 MHz, CDCl3) δ 158.80, 147.84, 144.32, 129.28, 129.24, 126.70, 125.55, 123.72, 122.86, 25.38, 18.74

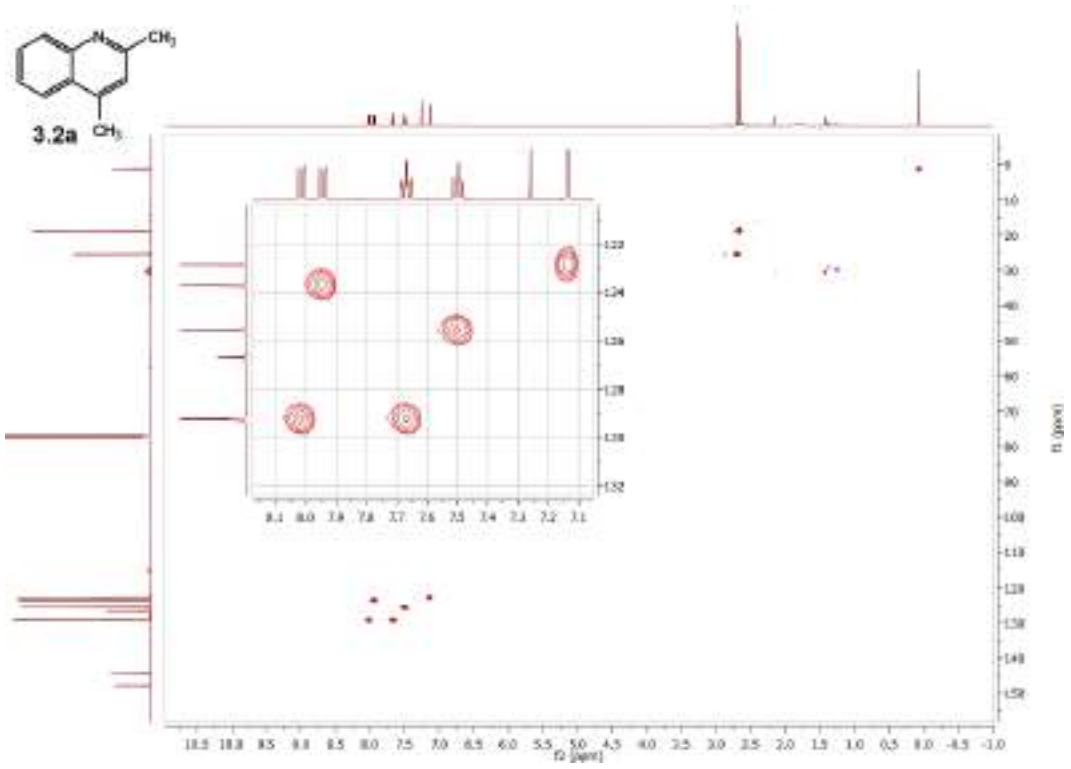

Figure A43. HMQC spectra of **3.2a**

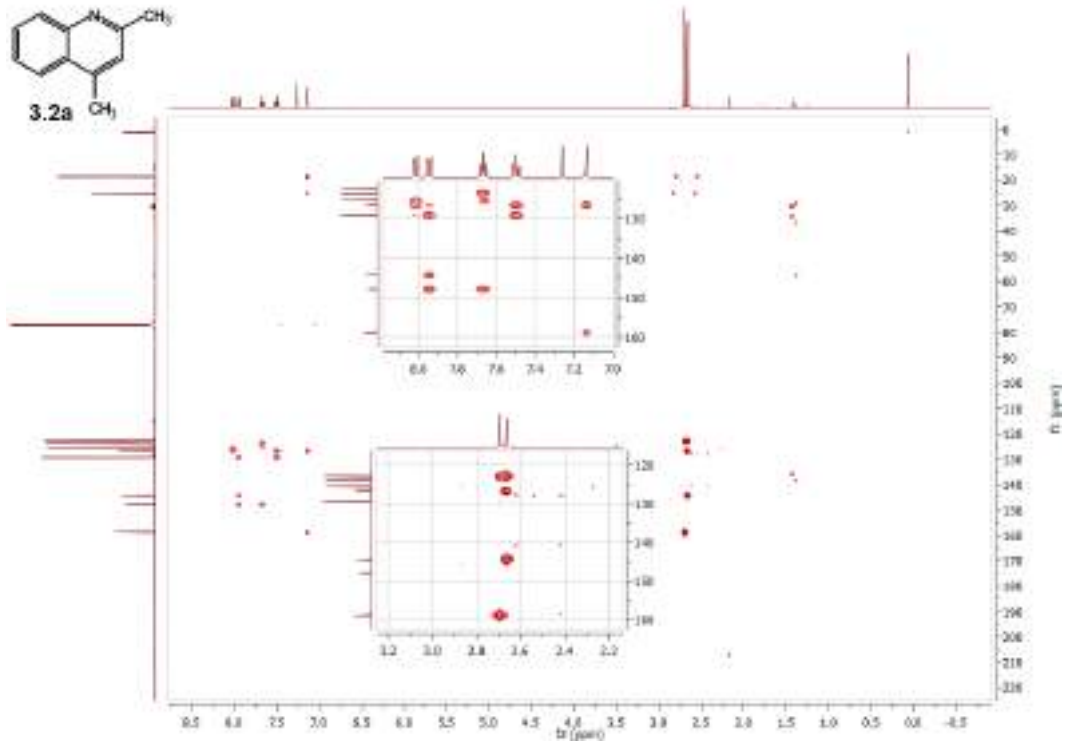

Figure A44. HMBC spectra of **3.2a**

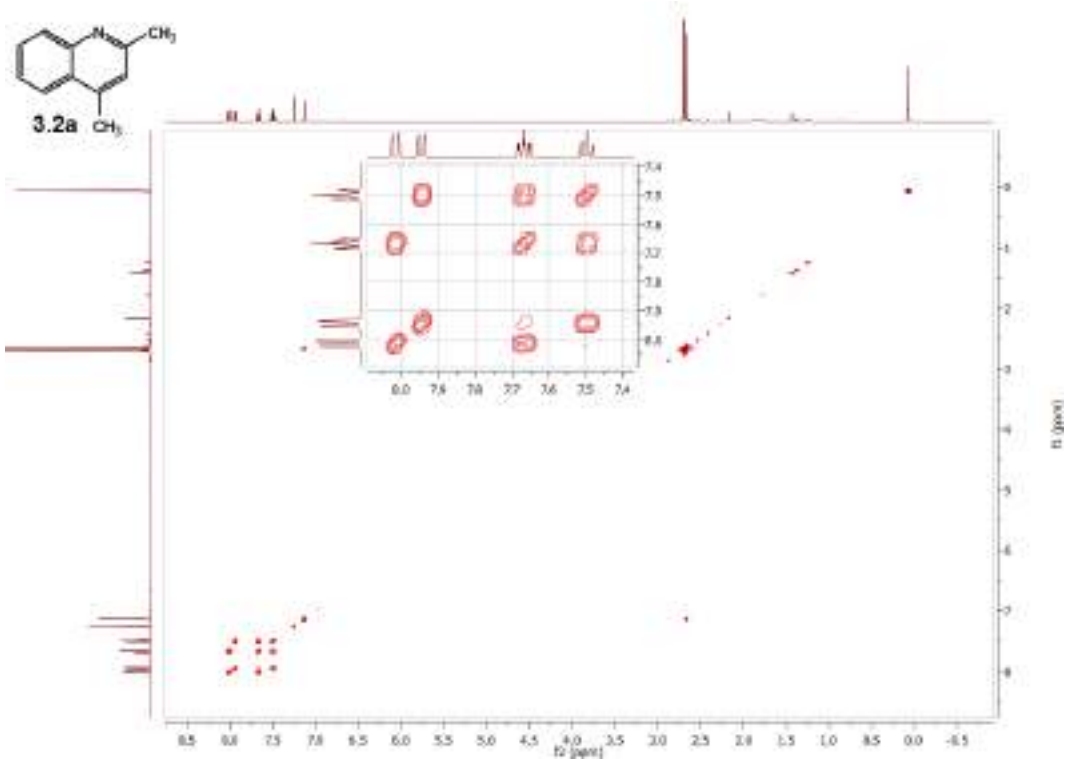

Figure A45. COSY spectra of **3.2a**

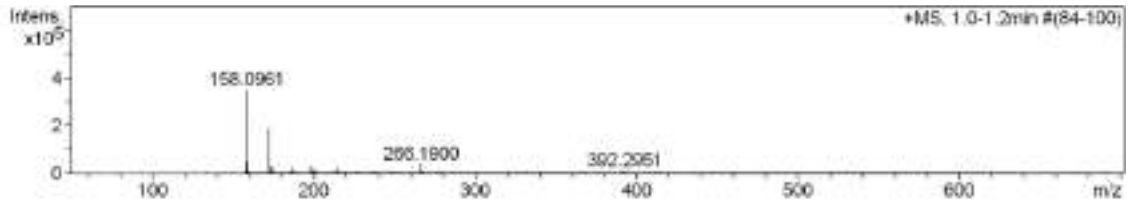

Figure A46. Mass spectra of **3.2a**

Mass (Most Intense MS Peaks) *m/z*: 266.1900 (10.7), 172.1123 (53.1), 159.0992 (12.9), 158.0961 (100.0).

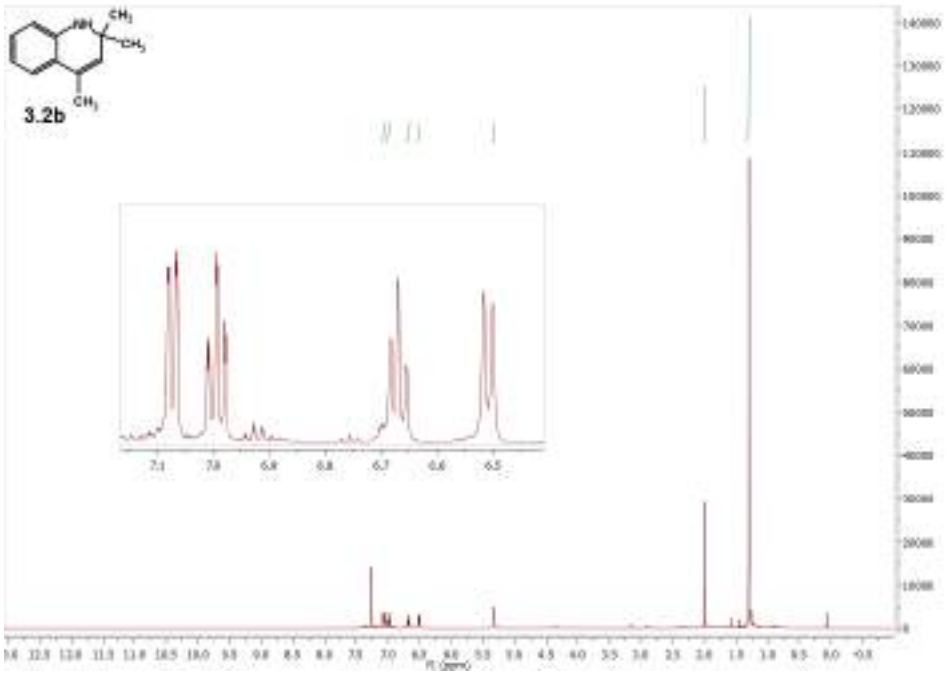

Figure A47. ^{1}H NMR spectra of **3.2b**

^{1}H NMR (500 MHz, $CDCl_3$) δ 7.07 (dd, J = 7.6, 1.5 Hz, 1H), 6.99 (td, J = 7.6, 1.5 Hz, 1H), 6.67 (td, J = 7.5, 1.3 Hz, 1H), 6.53 – 6.49 (d, 1H), 5.32 (d, J = 1.5 Hz, 1H), 1.99 (d, J = 1.4 Hz, 3H), 1.30 (s, 6H).

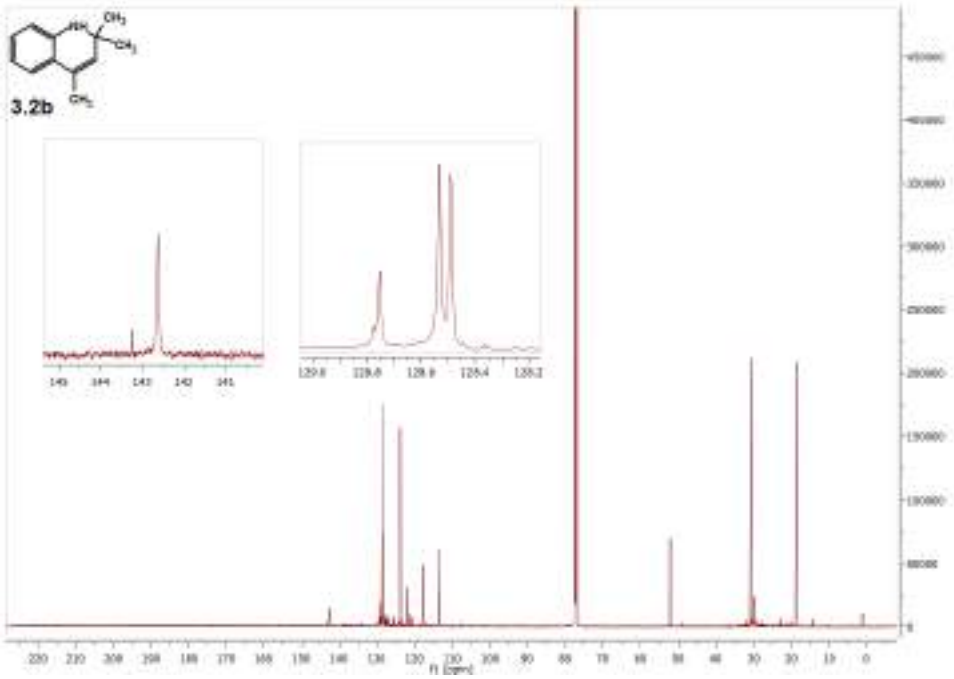

Figure A48. ^{13}C NMR spectra of **3.2b**

^{13}C NMR (125 MHz, $CDCl_3$) δ 142.63, 128.75, 128.53, 128.49, 123.78, 122.06, 117.89, 113.58, 52.17, 30.82, 18.71.

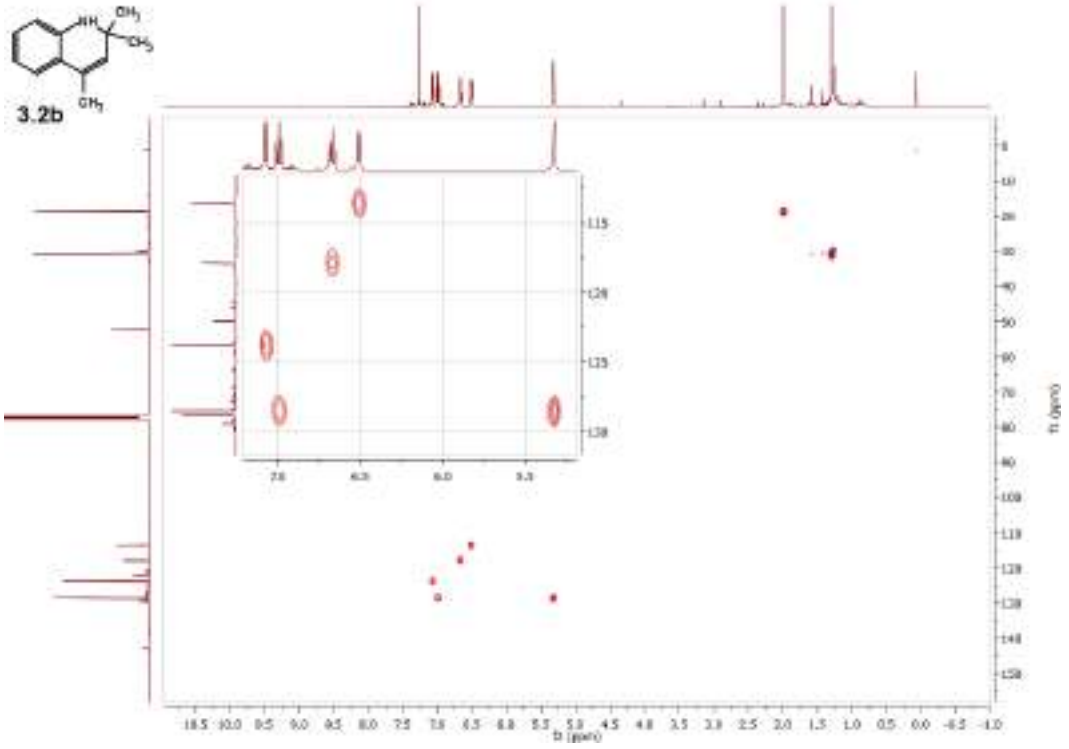

Figure A49. HMQC spectra of **3.2b**

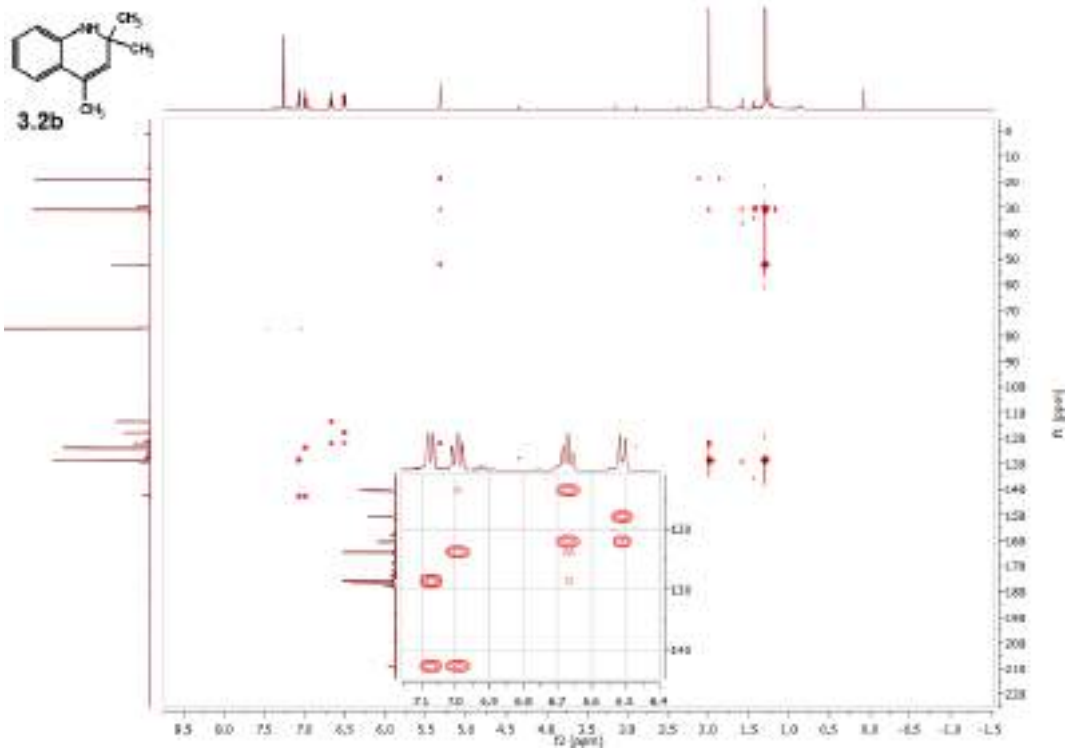

Figure A50. HMBC spectra of **3.2b**

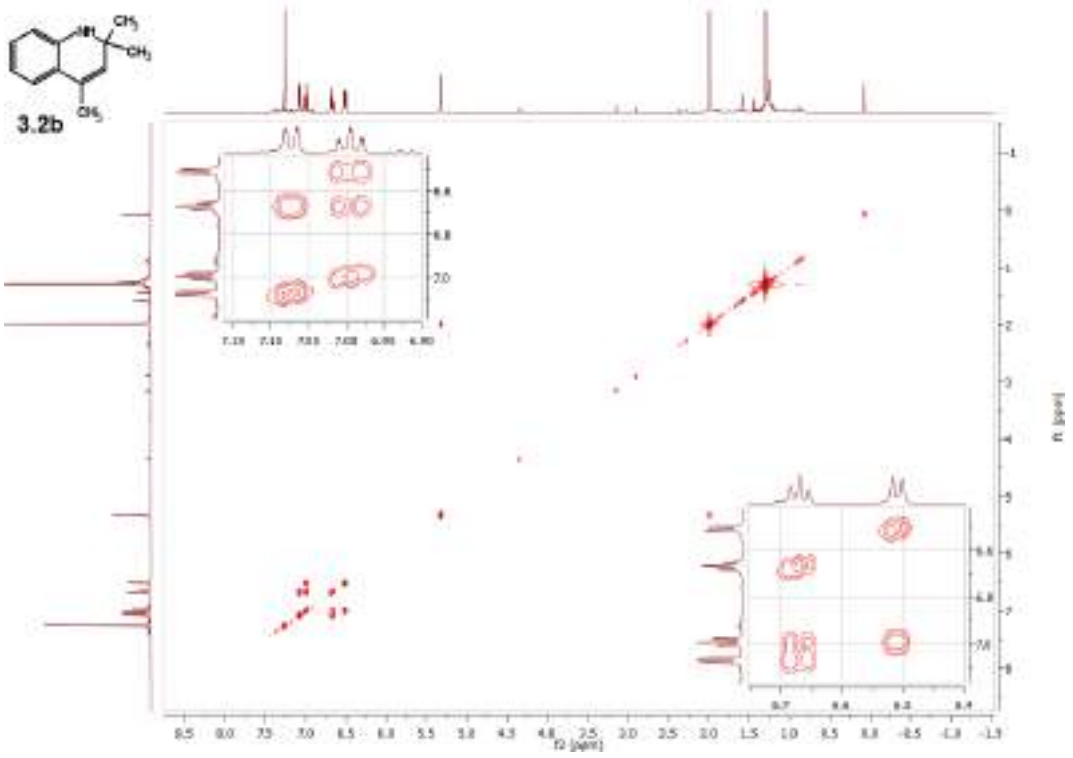

Figure A51. COSY spectra of **3.2b**

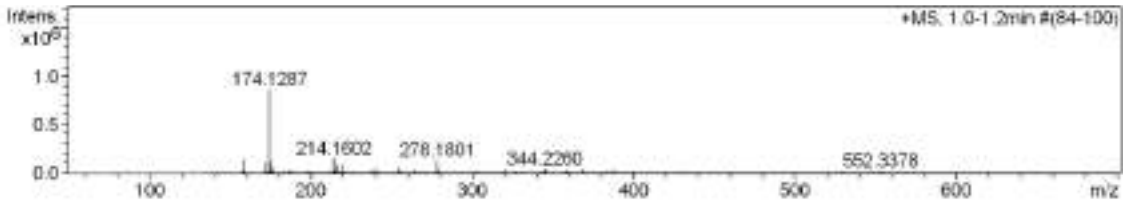

Figure A52. Mass spectra of **3.2b**

Mass (Most Intense MS Peaks) *m/z*: 278.1801 (15.0), 214.1602 (16.7), 175.1316 (13.6), 174.1287 (100.0), 172.1126 (12.3), 158.0962 (15.9).

6.3 Catalyst-free transesterification (chapter 4)

6.3.1 GC calibration curve

A GC calibration curve for GlyF was obtained using *n*-tetradecane (C_{14}) as external standard. Four different solutions of the commercial GlyF isomers in ethyl acetate were prepared at 0.08, 0.06, 0.04 and 0.02 M concentration. In particular 406, 302, 207 and 101 mg of GlyF were used. To each solution, the same quantity of *n*-tetradecane was added. Figure A53 shows the results of the calibration test.

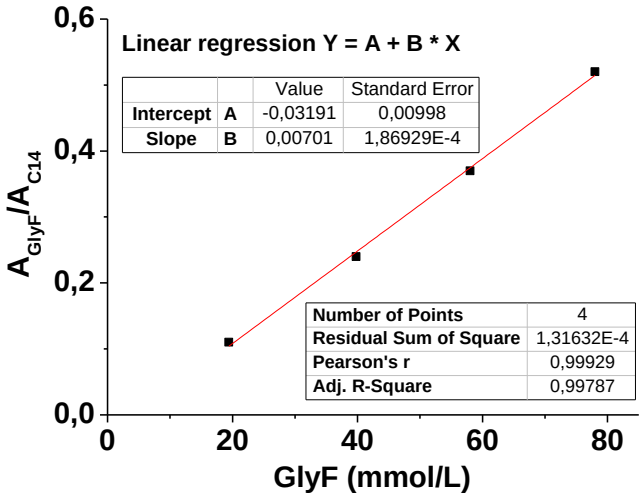

Figure A53. Calibration curve for GlyF. *n*-tetradecane (C_{14}) was used as standard. A_{GlyF}/A_{C14} was the ratio of GC area responses of GlyF and C_{14}.

6.3.2 NMR and mass analyses

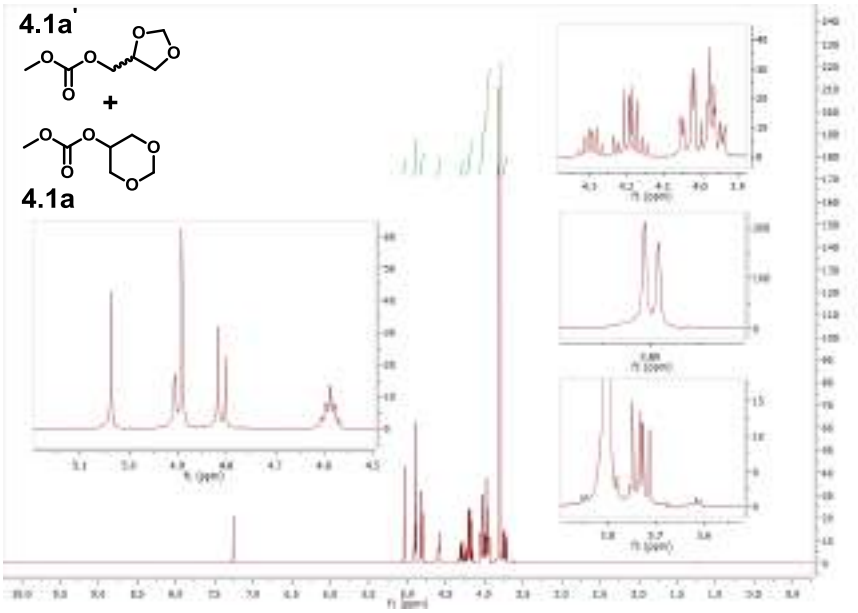

Figure A54. ^{1}H NMR spectra of mixture product **4.1a+4.1a'**

^{1}H NMR ($CDCl_3$, 400MHz) δ (ppm): 5.04 (s, 1H), 4.89 (m, 2H), 4.81 (d, *J* = 6.2 Hz, 1H), 4.59 (m, 1H), 4.30 (qnt, 1H), 4.25 – 4.13 (m, 2H), 4.07 – 3.92 (m, 5H), 3.80 (s, 3H), 3.79 (s, 3H), 3.73 (dd, *J* = 8.5, 5.4 Hz, 1H).

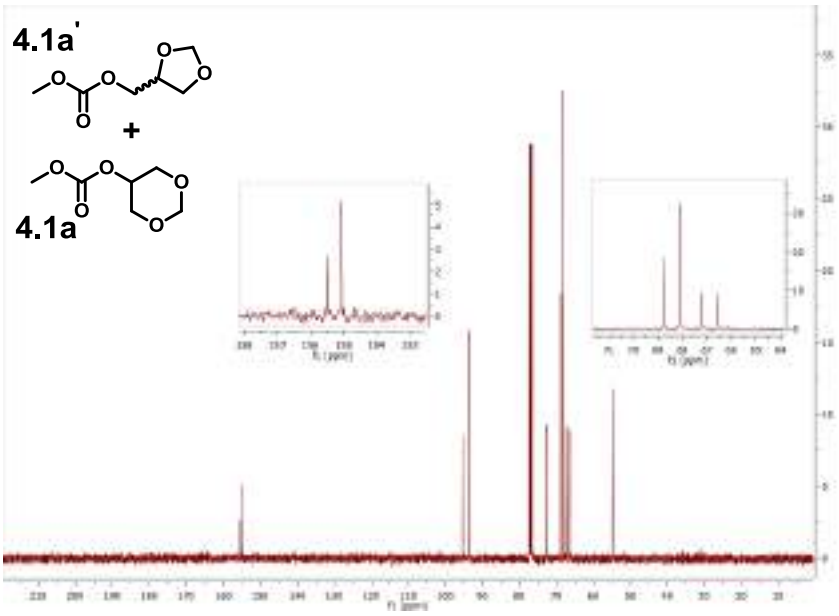

Figure A55. ^{13}C NMR spectra of mixture product **4.1a+4.1a'**

^{13}C NMR ($CDCl_3$, 100MHz) δ (ppm): 155.5, 155.1, 95.4, 93.5, 72.8, 68.8, 68.1, 67.2, 66.6, 54.9.

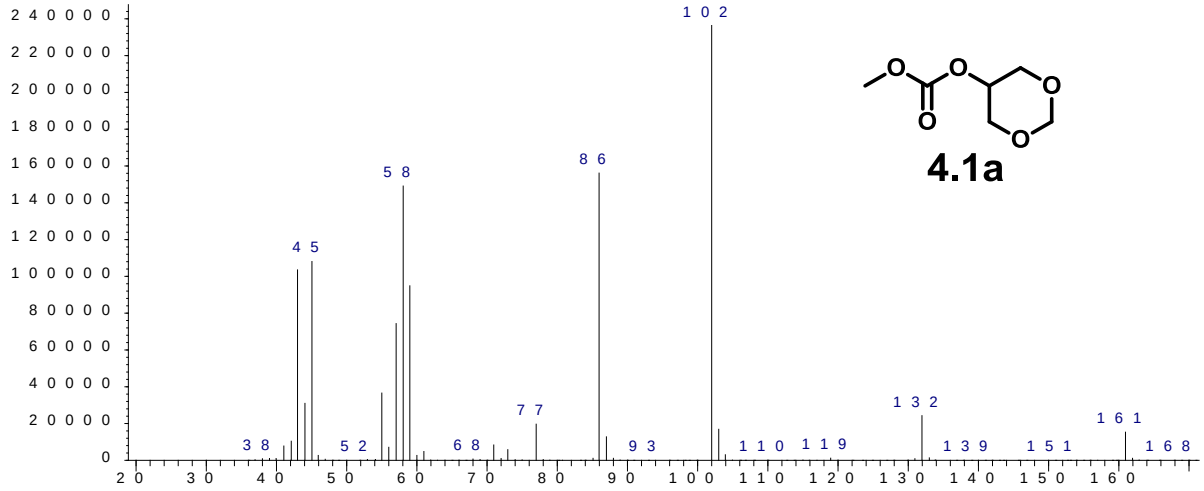

Figure A56. MS spectra of product **4.1a**

GC/MS (relative intensity, 70eV) *m/z*: 162 (M^+, <1%), 161 ($[M-H]^+$, 6), 132 (10), 102 (100), 86 (63), 59 (38), 58 (60), 57 (30), 55 (15), 45 (44), 44 (12), 43 (42).

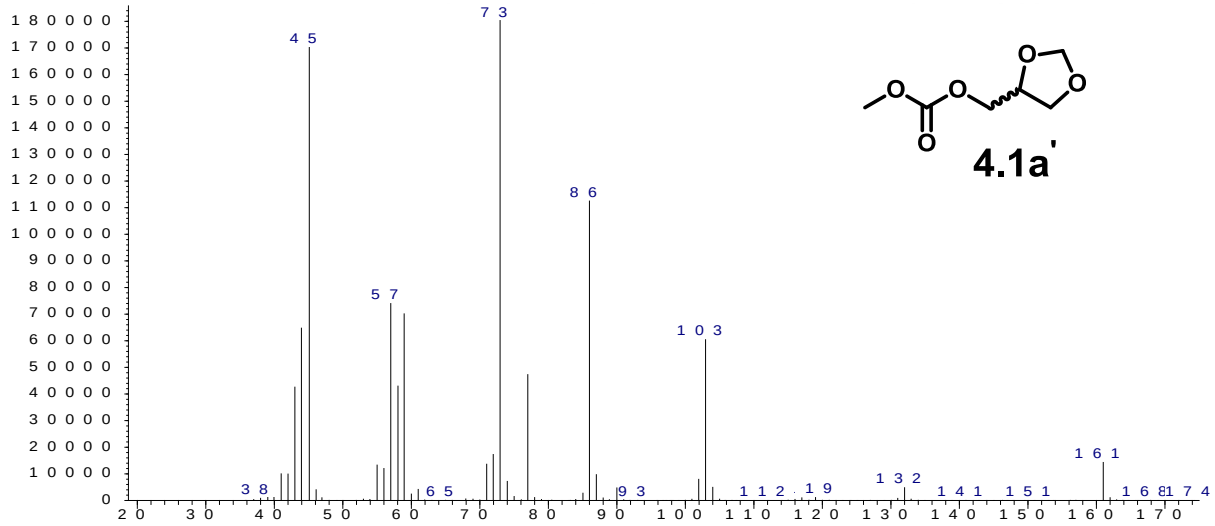

Figure A57. MS spectra of product **4.1a'**

GC/MS (relative intensity, 70eV) *m/z*: 162 (M^+, <1%), 161 ($[M-H]^+$, 8), 103 (32), 86 (61), 77 (25), 73 (100), 59 (38), 58 (23), 57 (40), 45 (92), 44 (35), 43 (23).

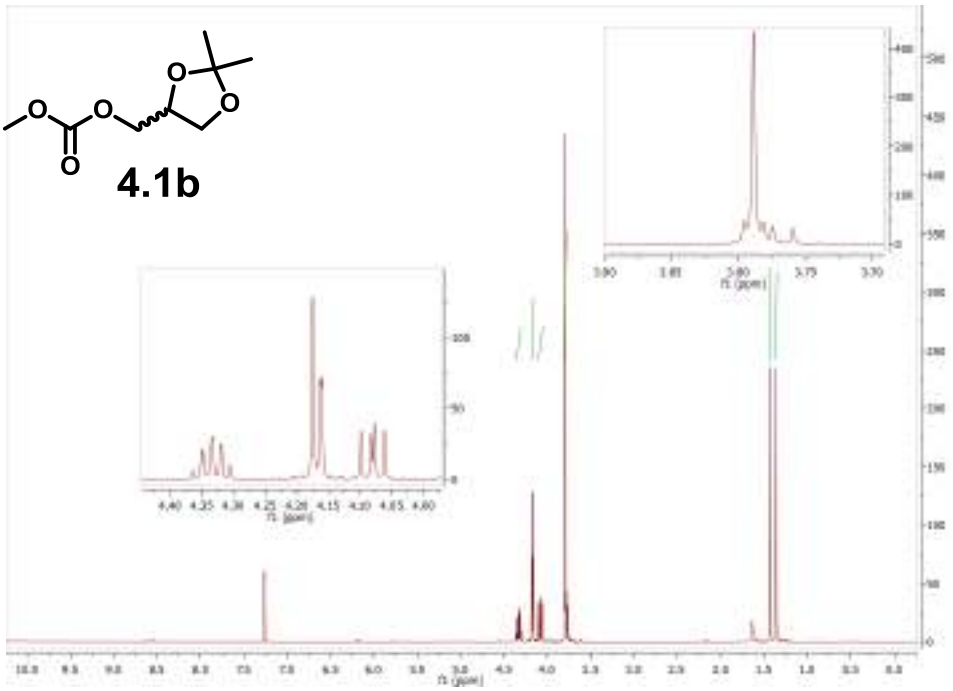

Figure A58. ^{1}H NMR spectra of product **4.1b**

^{1}H NMR ($CDCl_3$, 400MHz) δ (ppm): 4.38 – 4.29 (m, 1H), 4.19 – 4.15 (m, 2H), 4.08 (dd, *J* = 8.6, 6.4 Hz, 1H), 3.81 – 3.75 (m, 4H), 1.43 (s, 3H), 1.36 (s, 3H).

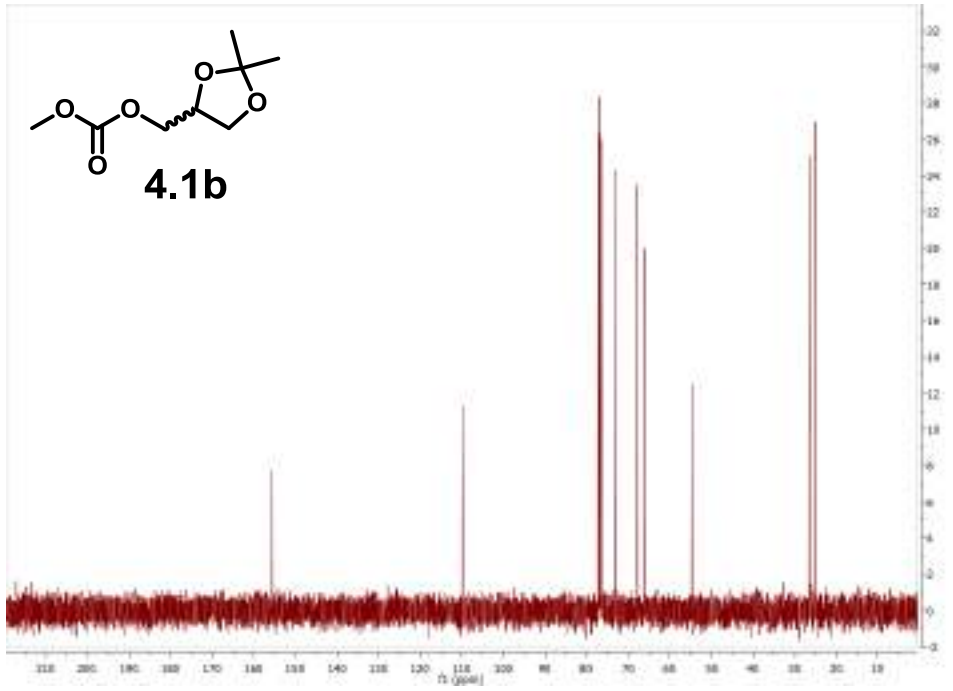

Figure A59. ^{13}C NMR spectra of product **4.1b**

^{13}C NMR ($CDCl_3$, 100MHz) δ (ppm): 155.5, 109.8, 73.2, 67.9, 66.2, 54.9, 26.6, 25.2.

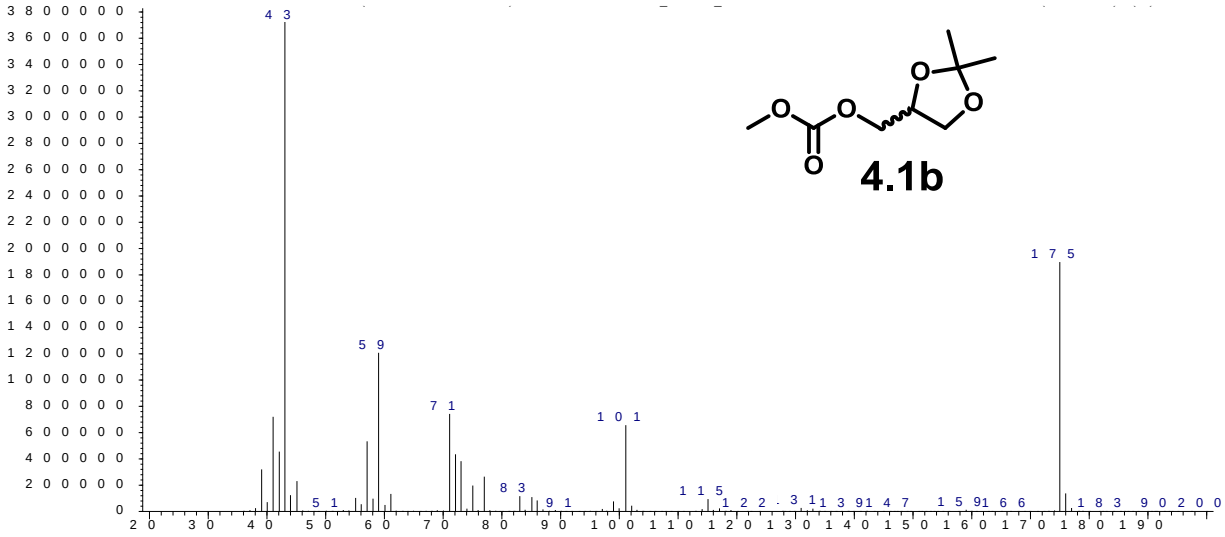

Figure A60. MS spectra of product **4.1b**

GC/MS (relative intensity, 70eV) *m/z*: 190 (M^+, <1%), 175 (50), 101 (17), 73 (10), 72 (11), 71 (19), 59 (31), 57 (14), 43 (100), 42 (12), 41 (19).

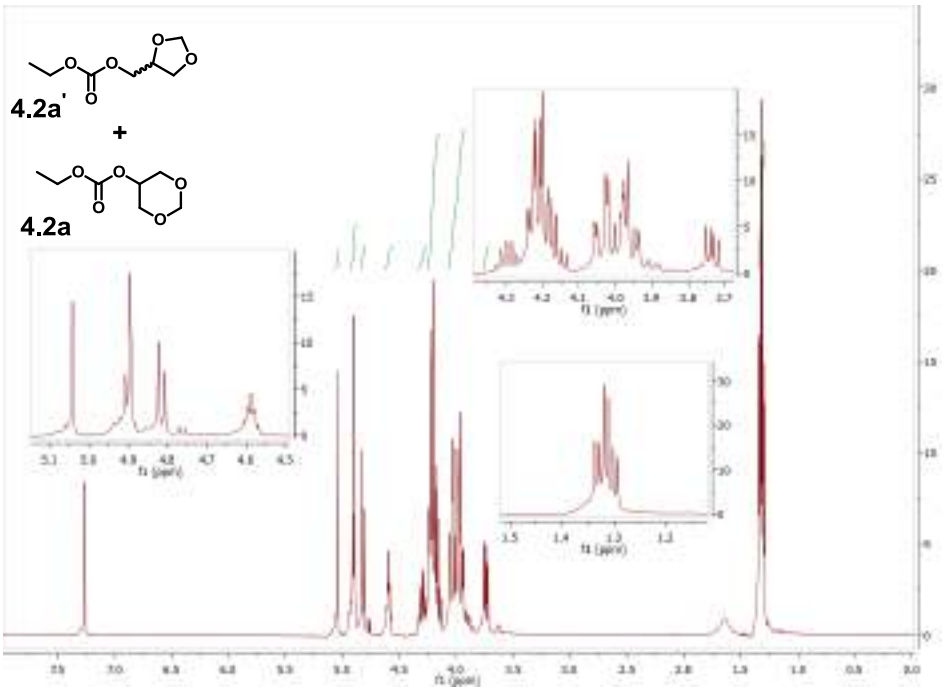

Figure A61. ^{1}H NMR spectra of mixture product **4.2a+4.2a'**

^{1}H NMR ($CDCl_3$, 400MHz) δ (ppm): 5.0 (s, 1H), 4.9 – 4.9 (m, 2H), 4.8 (d, *J* = 6.2 Hz, 1H), 4.6 (m, 1H), 4.3 (qnt, 1H), 4.3 – 4.1 (m, 6H), 4.1 – 3.9 (m, 5H), 3.7 (dd, *J* = 8.5, 5.4 Hz, 1H), 1.3 (dt, *J* = 7.1, 3.3 Hz, 6H).

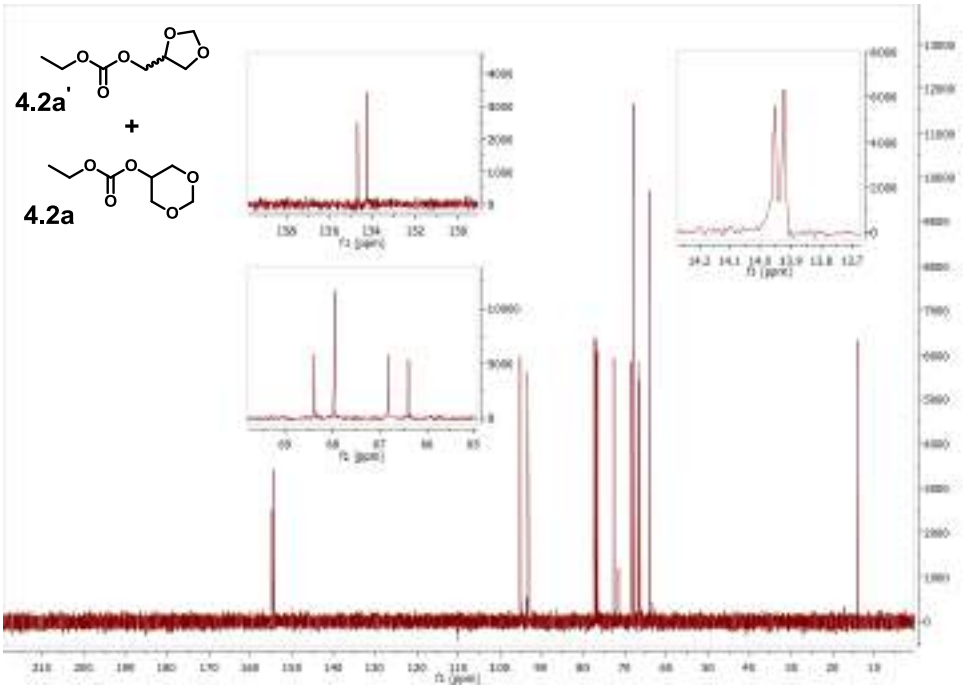

Figure A62. ^{13}C NMR spectra of mixture product **4.2a+4.2a'**

^{13}C NMR ($CDCl_3$, 100MHz) δ (ppm): 154.7, 154.3, 95.2, 93.3, 72.7, 68.4, 68.0, 66.8, 66.4, 64.1, 14.0, 13.9.

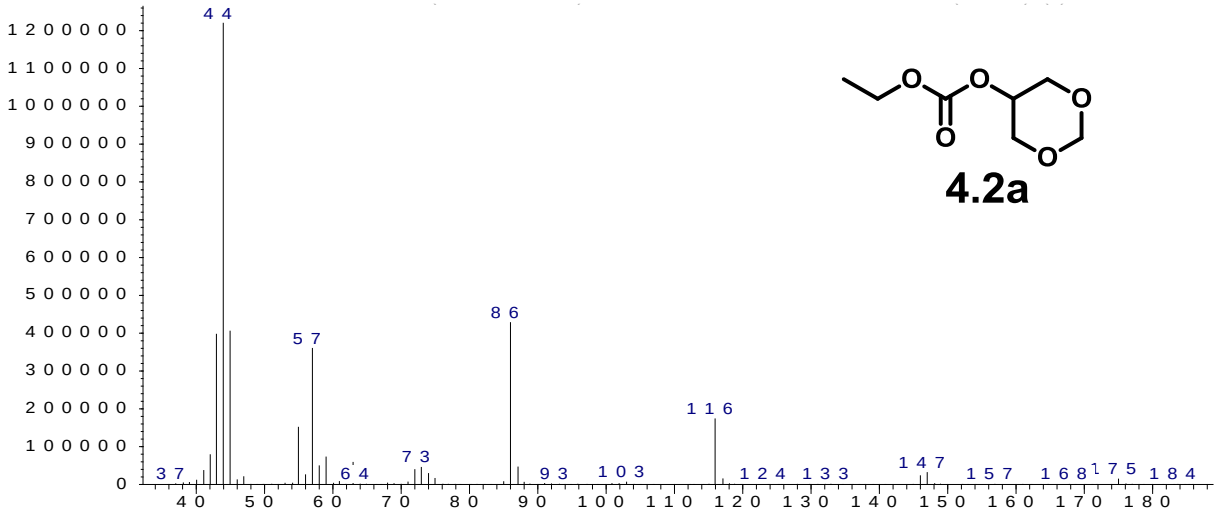

Figure A63. MS spectra of product **4.2a**

GC/MS (relative intensity, 70eV) *m/z*: 176 (M^+,<1%), 175 ($[M-H]^+$, 1), 116 (14), 86 (34), 57 (28), 55 (12), 45 (32), 44 (100), 43 (31).

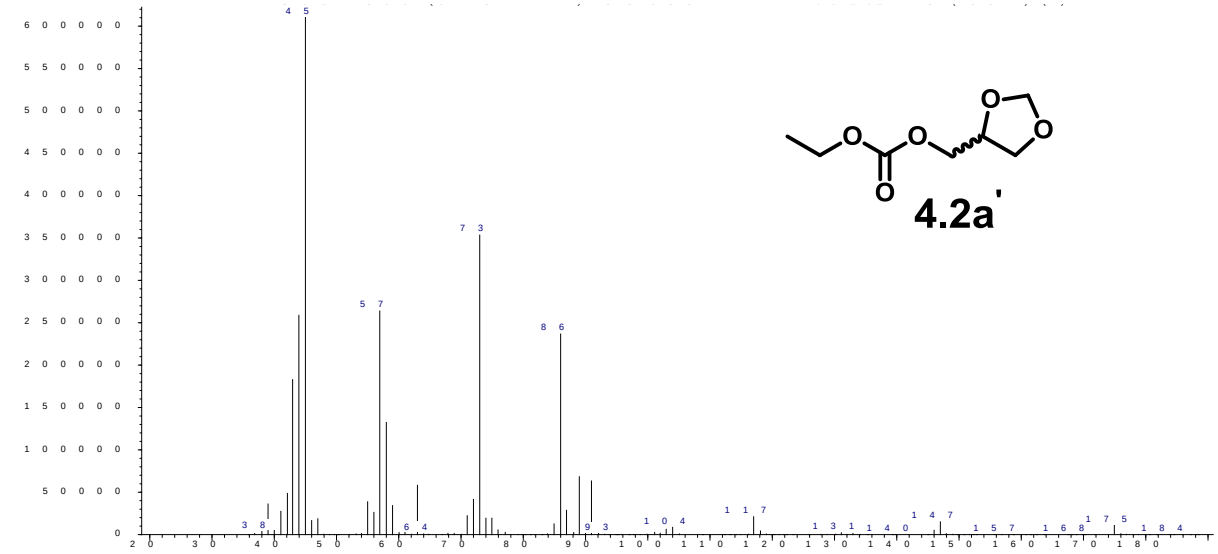

Figure A64. MS spectra of product **4.2a'**

GC/MS (relative intensity, 70eV) *m/z*: 176 (M^+, <1%), 175 ($[M-H]^+$, 2), 91 (10), 89 (11), 86 (38), 73 (57), 58 (21), 57 (42), 45 (100), 44 (42), 43 (29).

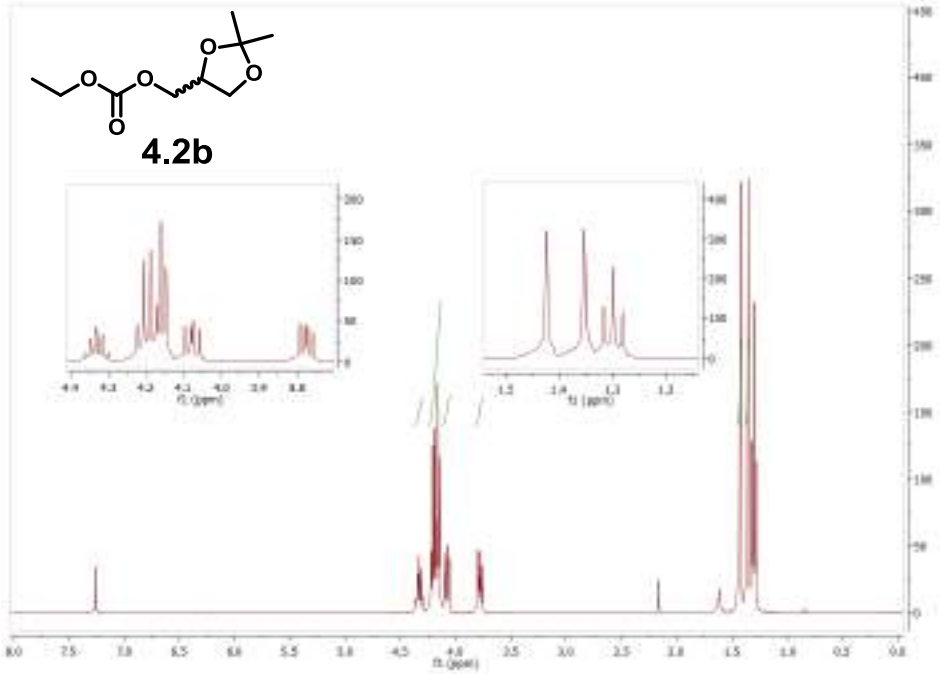

Figure A65. ^{1}H NMR spectra of product **4.2b**

^{1}H NMR ($CDCl_3$, 400MHz) δ (ppm): 4.33 (m, 1H), 4.24 – 4.13 (m, 4H), 4.08 (dd, *J* = 8.5, 6.4 Hz, 1H), 3.78 (dd, *J* = 8.5, 5.8 Hz, 1H), 1.42 (s, 3H), 1.35 (s, 3H), 1.30 (t, *J* = 7.1 Hz, 3H).

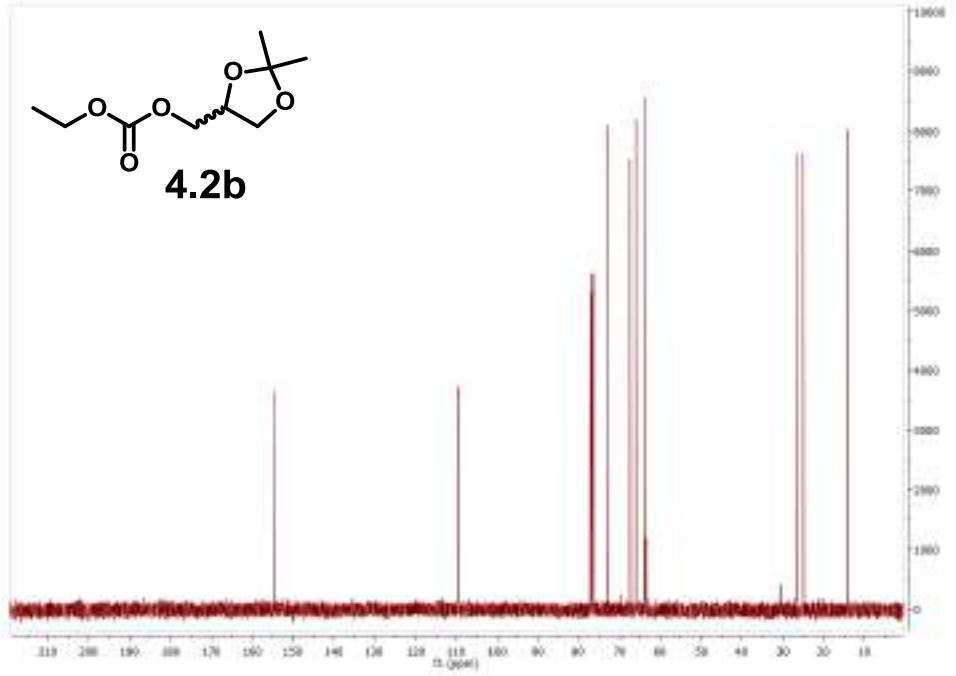

Figure A66. ^{13}C NMR spectra of product **4.2b**

^{13}C NMR ($CDCl_3$, 100MHz) δ (ppm): 154.7, 109.6, 73.1, 67.5, 66.0, 64.0, 26.4, 25.1, 14.0.

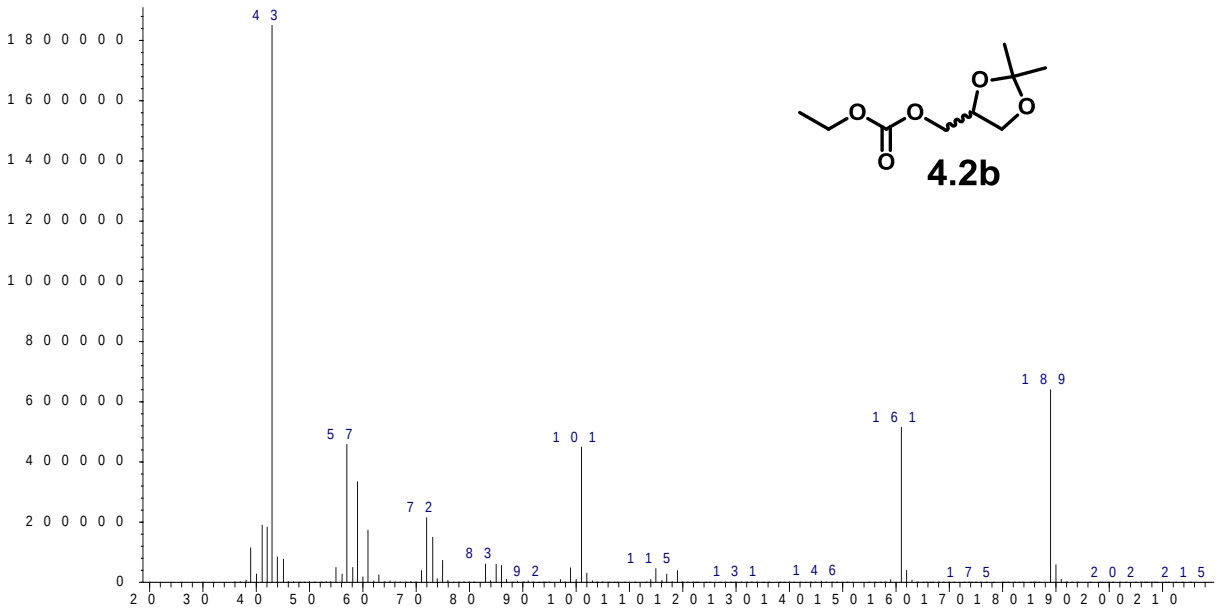

Figure A67. MS spectra of product **4.2b**

GC/MS (relative intensity, 70eV) *m/z*: 204 (M^+,<1%), 189 (39), 161 (31), 101 (27), 72 (12), 61 (10), 59 (18), 57 (25), 43 (100), 42 (10).

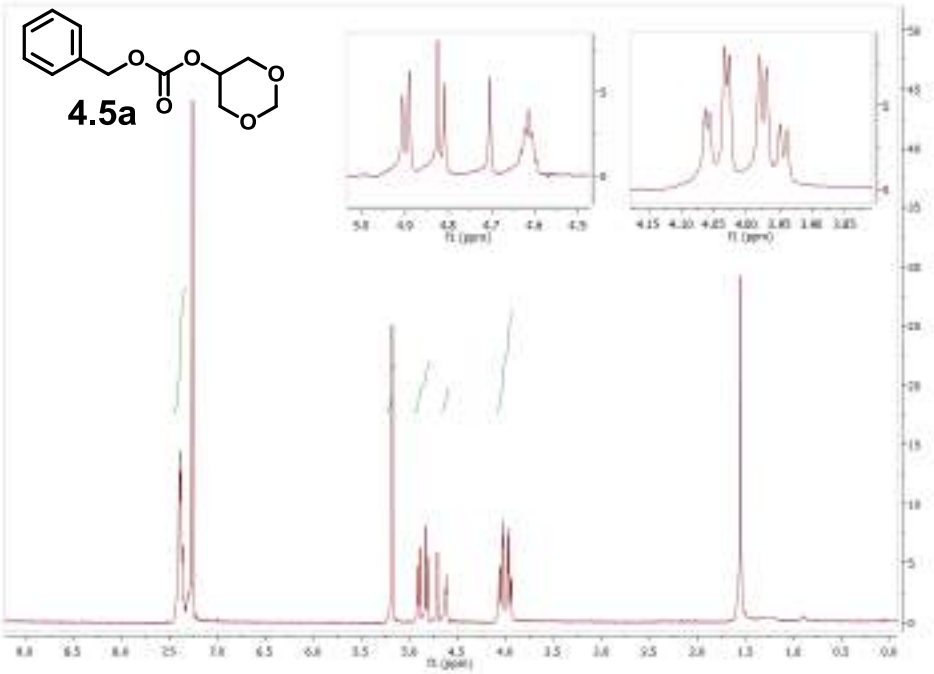

Figure A68. ^{1}H NMR spectra of product **4.5a**

^{1}H NMR ($CDCl_3$, 400MHz) δ (ppm): 7.5 – 7.3 (m, 5H), 5.2 (s, 1H), 4.9 (d, *J* = 6.2 Hz, 1H), 4.8 (d, *J* = 6.3 Hz, 1H), 4.7 – 4.6 (m, 1H), 4.0 (dd, *J* = 12.1, 2.8 Hz, 1H), 4.0 (dd, *J* = 12.1, 4.3 Hz, 1H).

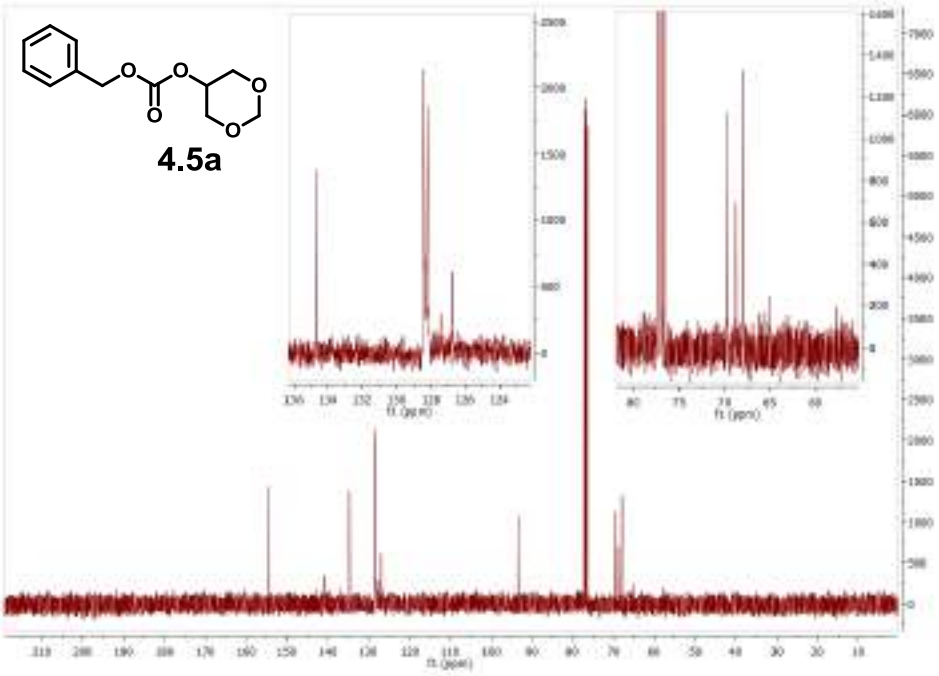

Figure A69. ^{13}C NMR spectra of product **4.5a**

^{13}C NMR ($CDCl_3$, 100MHz) δ (ppm): 154.3, 140.8, 134.7, 128.4, 128.2, 93.4, 69.8, 68.8, 68.0.

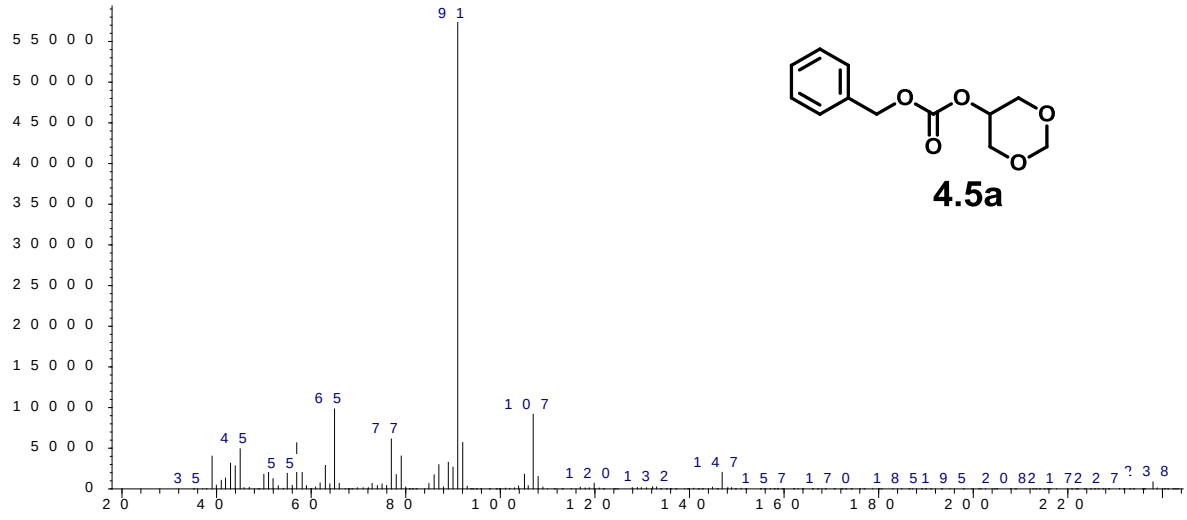

Figure A70. MS spectra of product **4.5a**

GC/MS (relative intensity, 70eV) *m/z*: 238 (M^+, 1%), 107 (15), 92 (10), 91(100), 77 (10), 65 (17), 57(10).

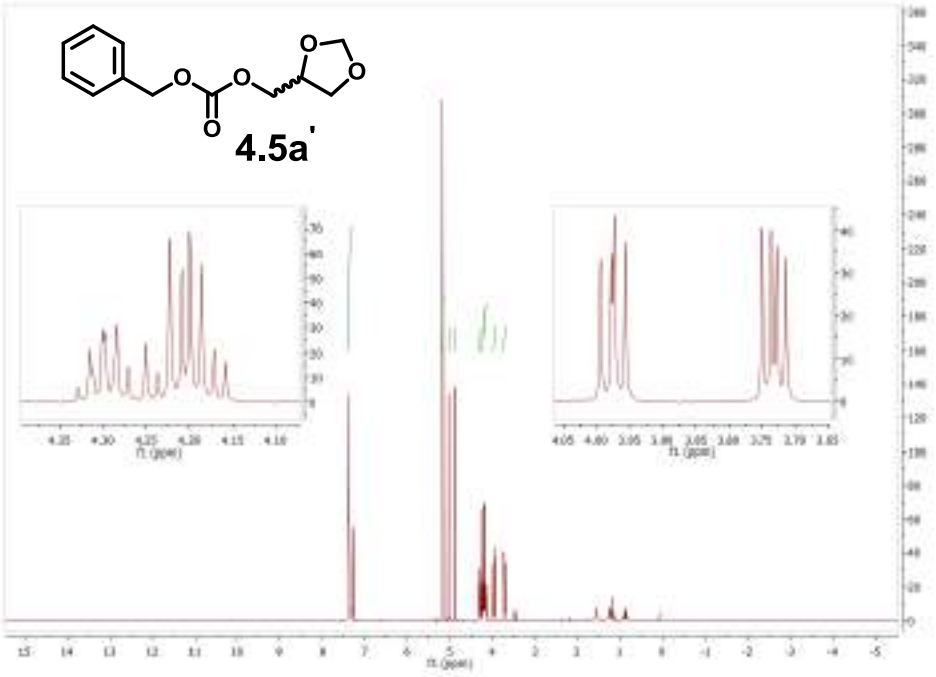

Figure A71. ^{1}H NMR spectra of product **4.5a'**

^{1}H NMR (400 MHz, $CDCl_3$) δ(ppm): 7.5 – 7.3 (m, 5H), 5.2 (s, 2H), 5.0 (s, 1H), 4.9 (s, 1H), 4.3 (m, 1H), 4.3 – 4.2 (m, 2H), 4.0 (dd, *J* = 8.5, 6.7 Hz, 1H), 3.7 (dd, *J* = 8.5, 5.4 Hz, 1H).

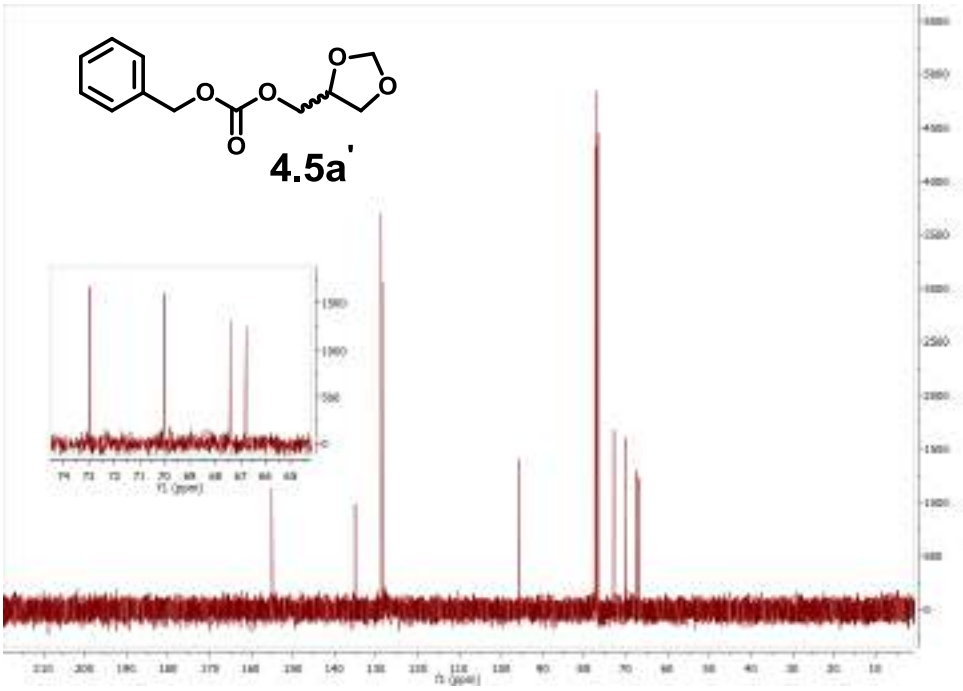

Figure A72. ^{13}C NMR spectra of product **4.5a'**

^{13}C NMR ($CDCl_3$, 100MHz) δ (ppm): 155.0, 135.1, 128.7,128.7, 128.5, 95.6, 73.0, 70.0, 67.4, 66.8.

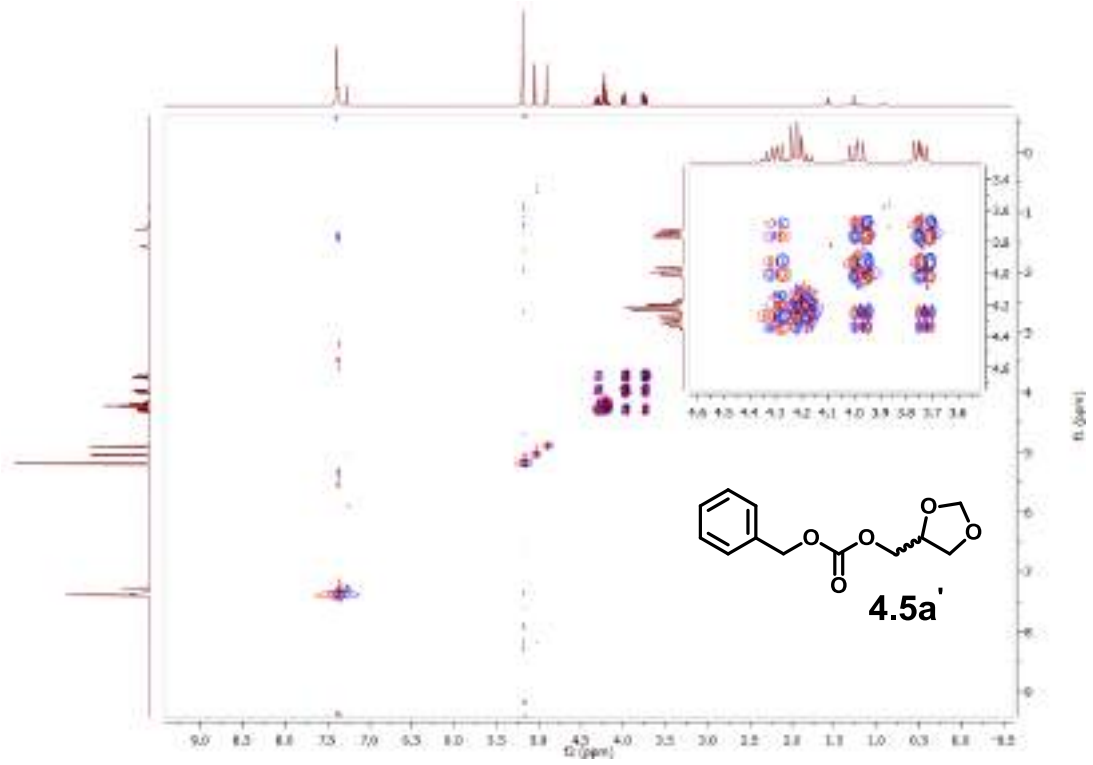

Figure A73. DQFCOSY spectra of product **4.5a'**

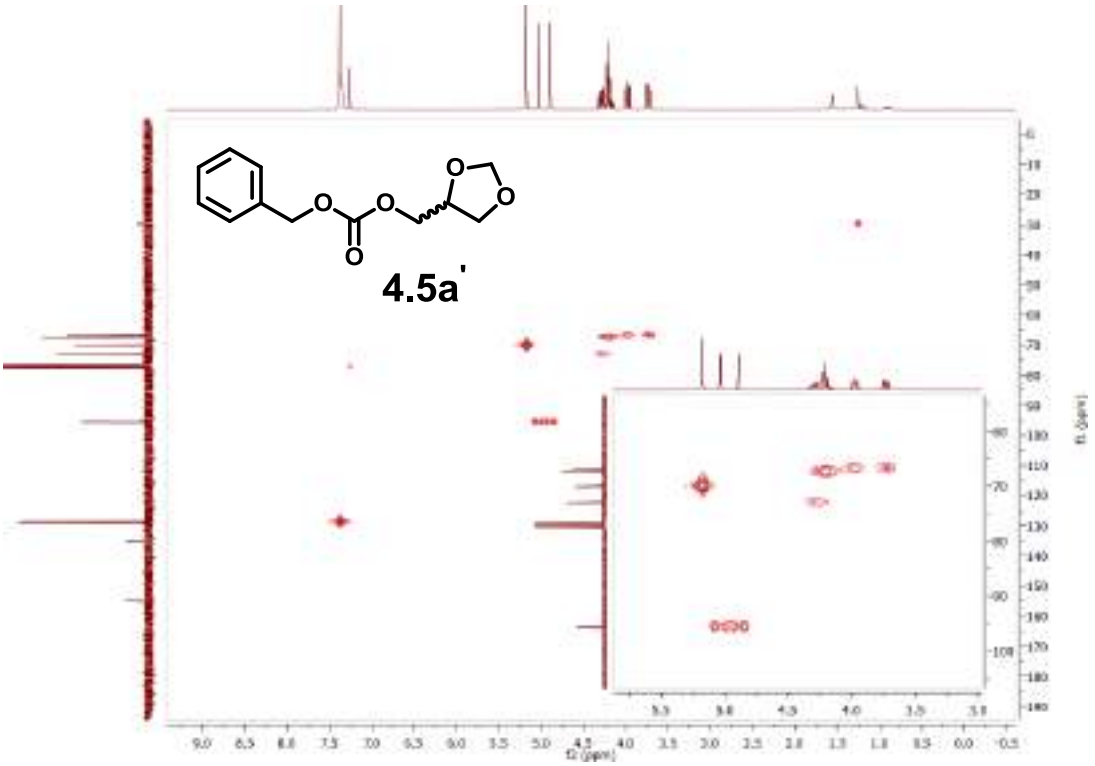

Figure A74. HMQC spectra of product **4.5a'**

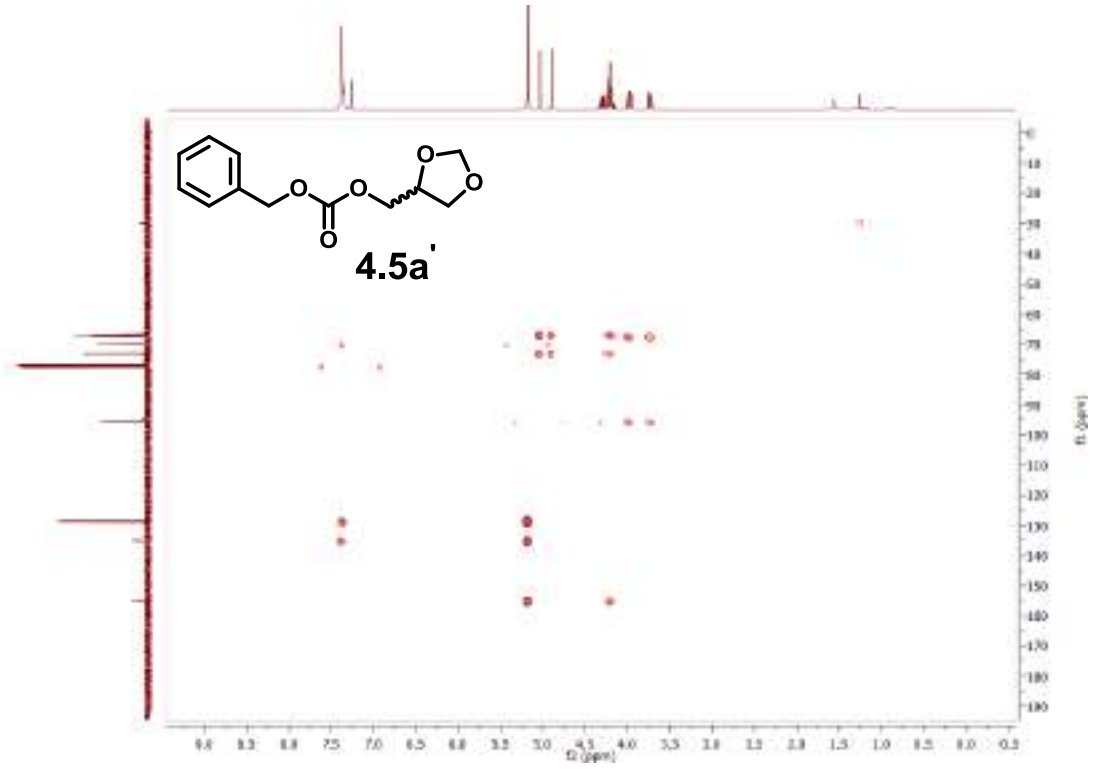

Figure A75. HMBC spectra of product **4.5a'**

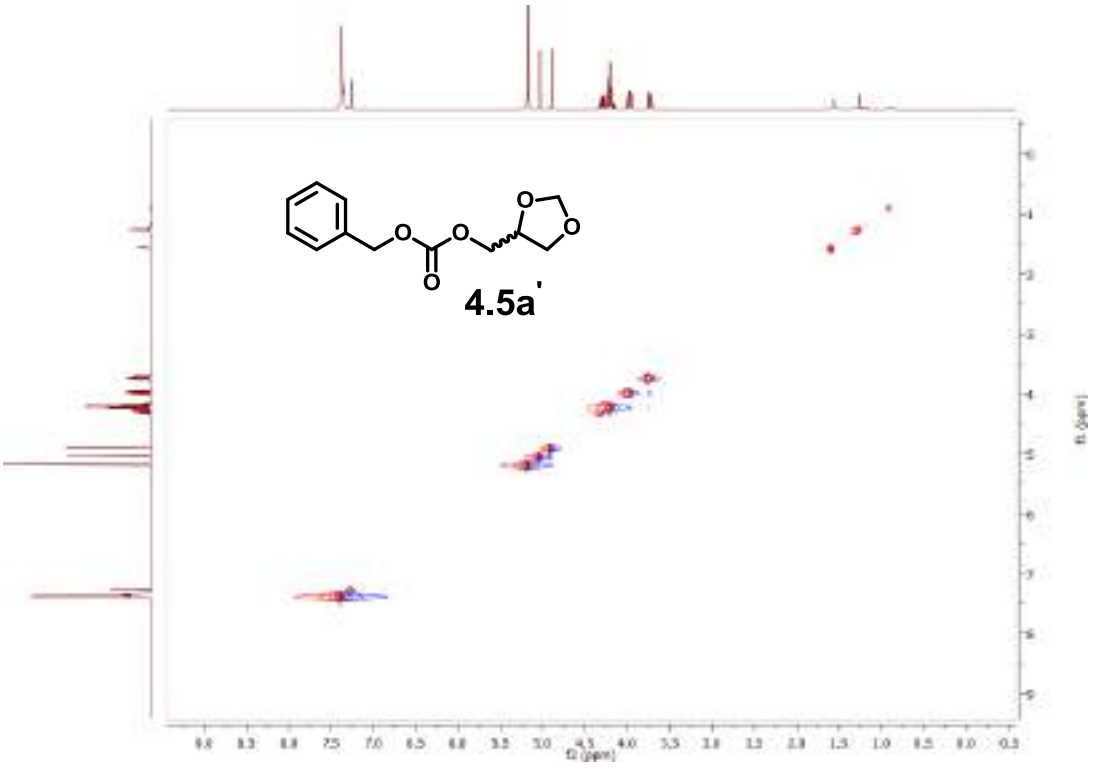

Figure A76. NOESY spectra of product **4.5a'**

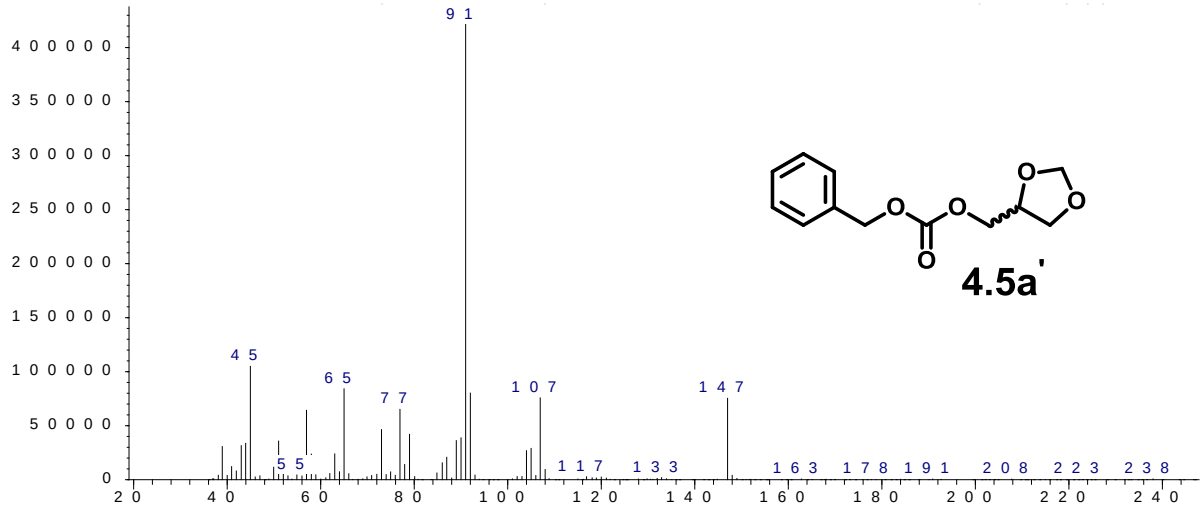

Figure A77. MS spectra of product **4.5a'**

GC/MS (relative intensity, 70eV) *m/z*: 238 (M^+, <1%), 147(17), 107(17), 92 (18), 91(100), 79 (10), 77 (15), 73 (11), 65 (19), 57 (15), 45 (24).

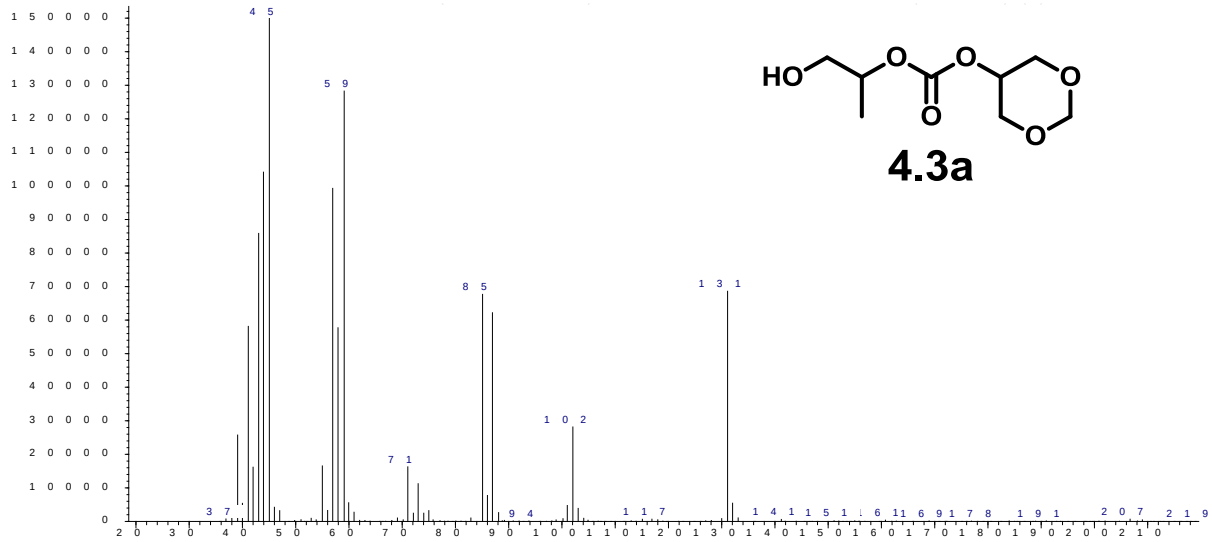

Figure A78. MS spectra of product **4.3a**

GC/MS (relative intensity, 70eV) *m/z*: 206 (M^+, <1%), 131 (45), 102 (18), 87 (41), 85 (44), 71 (11), 59 (84), 58 (38), 57 (65), 55 (11), 45 (100), 44 (68), 43 (56), 42 (11), 41 (38), 39 (17).

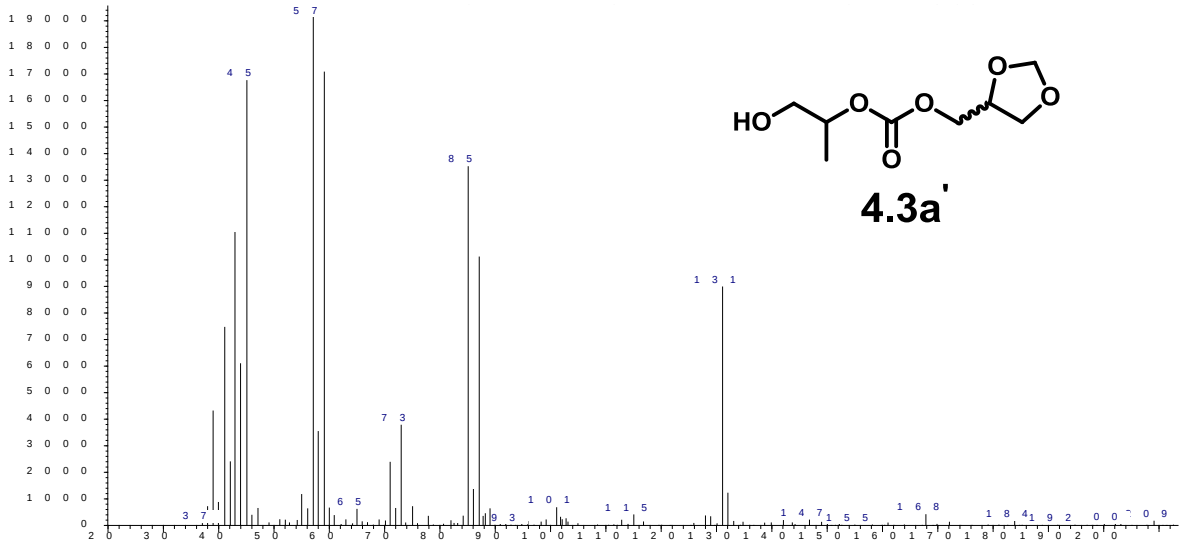

Figure A79. MS spectra of product **4.3a'**

GC/MS (relative intensity, 70eV) *m/z*: 206 (M^+, <1%), 131 (46), 87 (52), 85 (69), 73 (19), 71 (12), 59 (87), 58 (18), 57 (100), 45 (86), 44 (31), 43 (56), 42 (12), 41 (38), 39 (22).

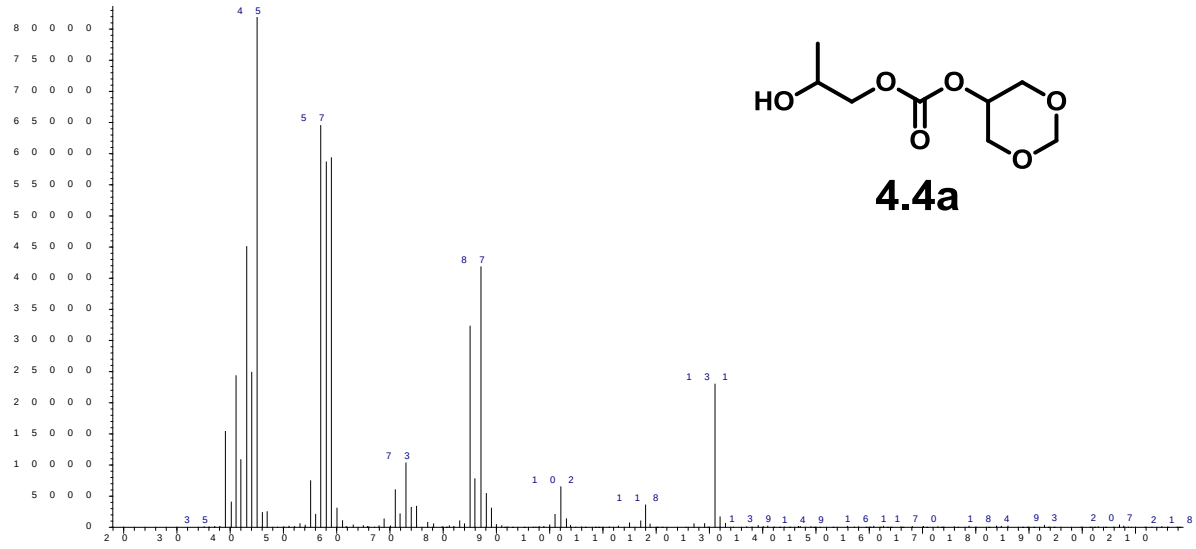

Figure A80. MS spectra of product **4.4a**

GC/MS (relative intensity, 70eV) *m/z*: 206 (M^+, <1%), 131 (27), 87 (50), 85 (39), 73 (12), 59 (71), 58 (70), 57 (77), 45 (100), 44 (30), 43 (54), 42 (13), 41 (29), 39 (18).

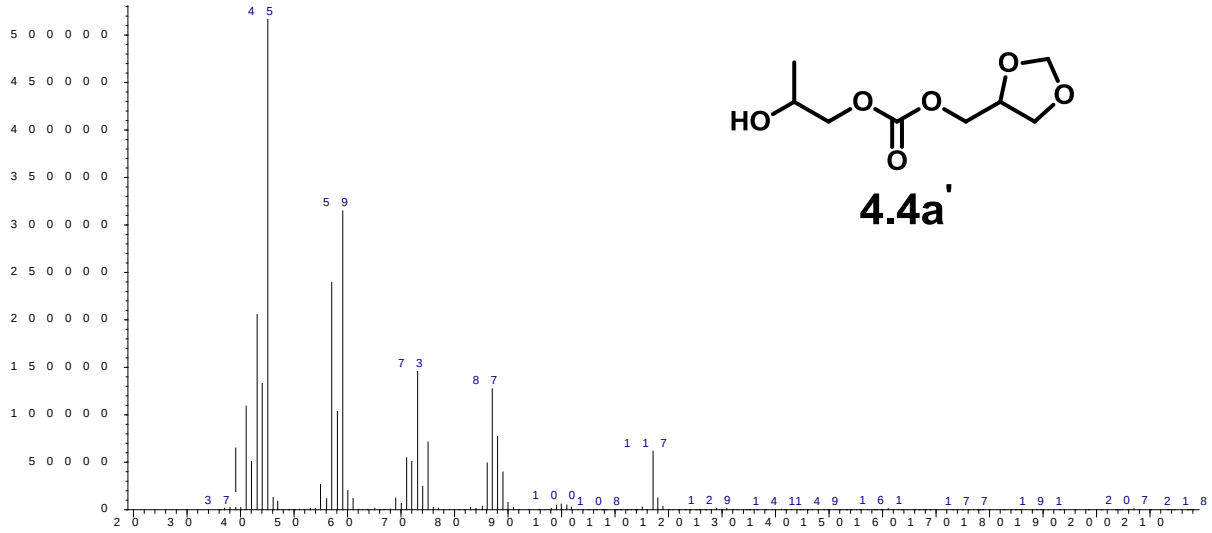

Figure A81. MS spectra of product **4.4a'**

GC/MS (relative intensity, 70eV) *m/z*: 206 (M^+, <1%), 117 (12), 88 (15), 87 (24), 75 (13), 73 (27), 72 (10), 71 (10), 59 (59), 58 (19), 57 (45), 45 (100), 44 (25), 43 39), 42 (10), 41 (21), 39 (12).

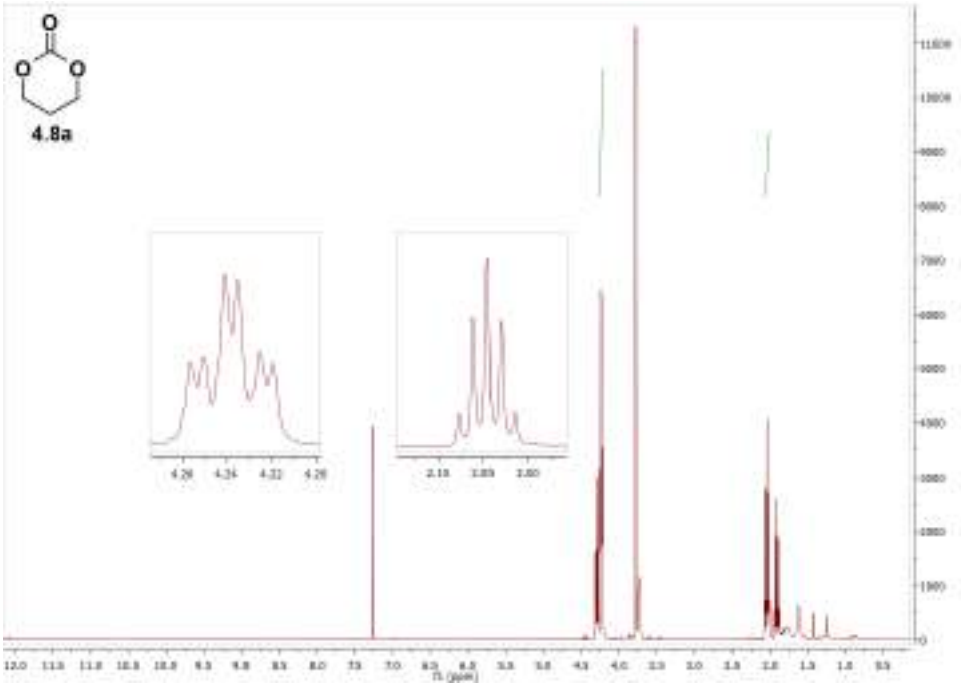

Figure A82. ^{1}H NMR of **4.8a+4.8b**

^{1}H NMR ($CDCl_3$, 400 MHz) δ: 4.24 (td, J = 6.2, 2.3 Hz, 4H), 2.05 (quint, J = 6.2 Hz, 2H).

The other signals correspond to compound **4.8b** (see Figure A84) and traces of DMC.

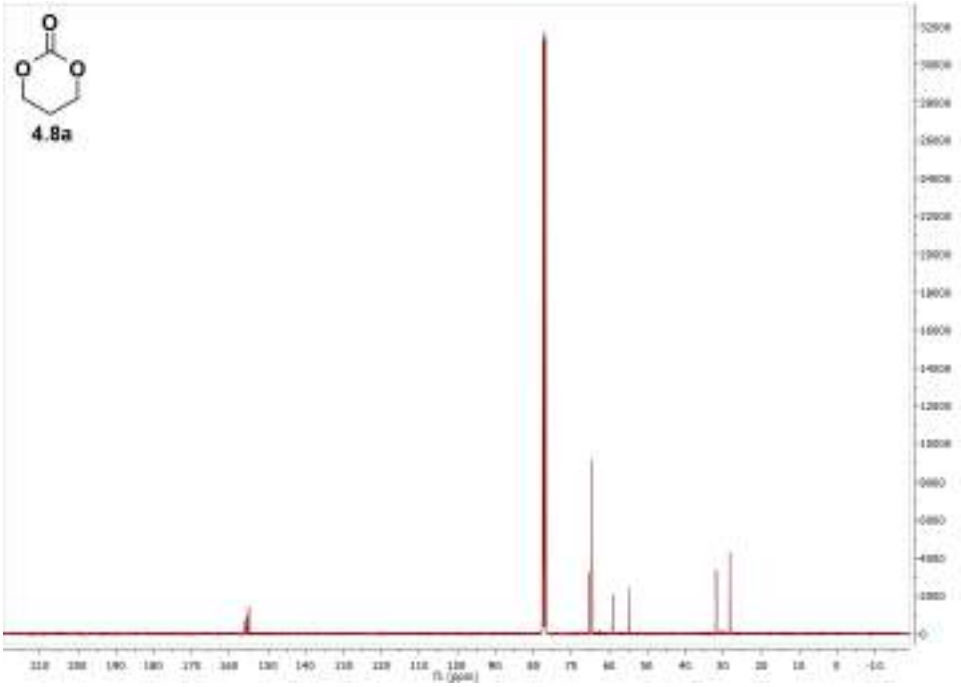

Figure A83. ^{13}C NMR of **4.8a+4.8b**

^{13}C NMR ($CDCl_3$, 100 MHz) δ: 155.06, 64.43, 28.20.

The other signals correspond to compound **4.8b** (see Figure A85) and traces of DMC.

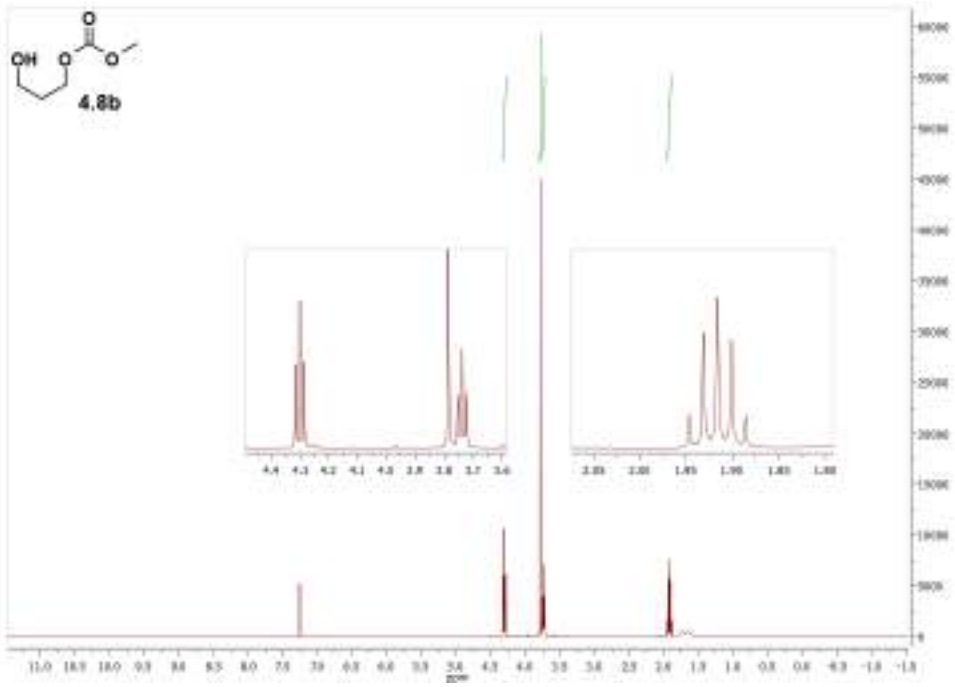

Figure A84. ^{1}H NMR of **4.8b**

^{1}H NMR ($CDCl_3$, 400 MHz) δ: 4.30 (t, *J* = 6.2 Hz, 2H), 3.79 (s, 3H), 3.74 (t, *J* = 6.0 Hz, 2H), 1.92 (m, 2H)

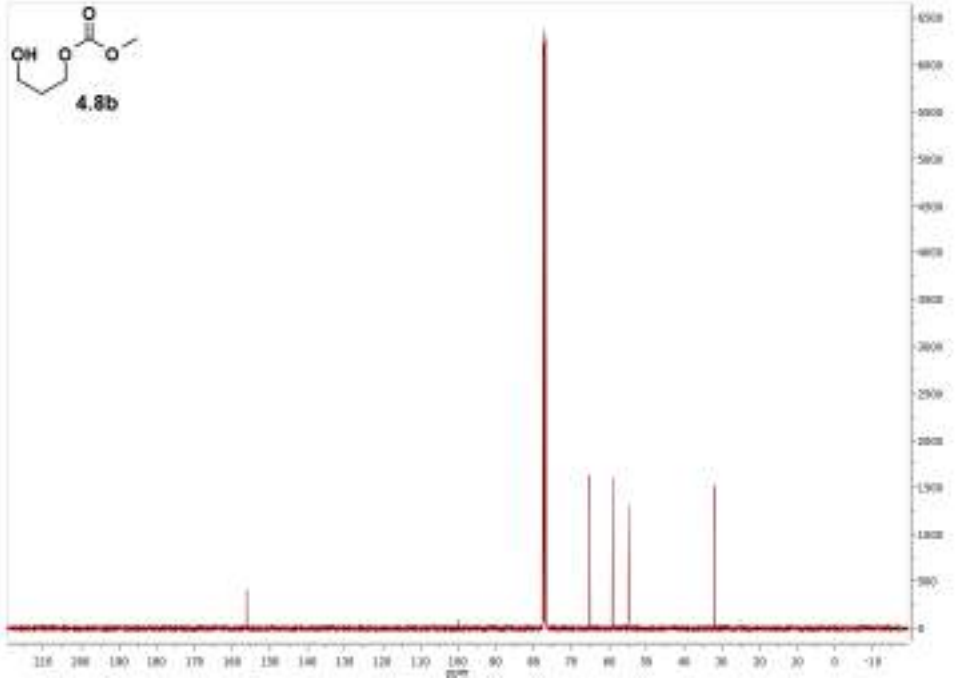

Figure A85. ^{13}C NMR of **4.8b**

^{13}C NMR ($CDCl_3$, 100 MHz) δ: 156.21, 65.18, 59.18, 54.97, 31.82.

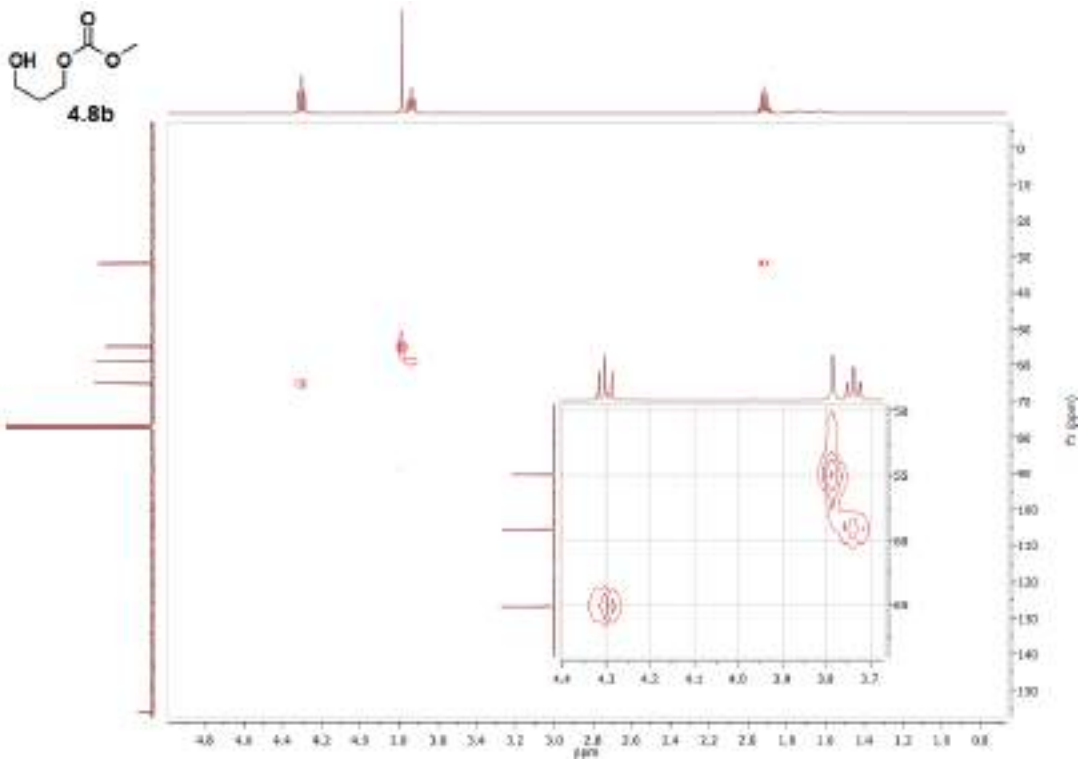

Figure A86. HMQC spectra of **4.8b**

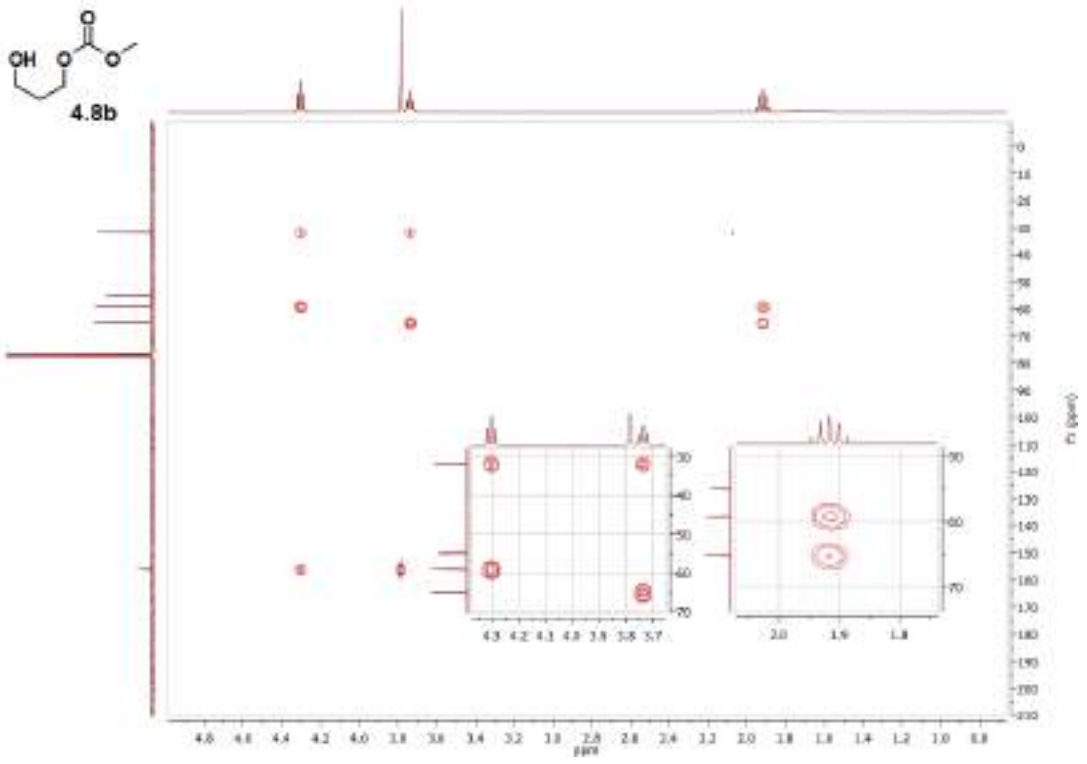

Figure A87. HMBC spctra of **4.8b**

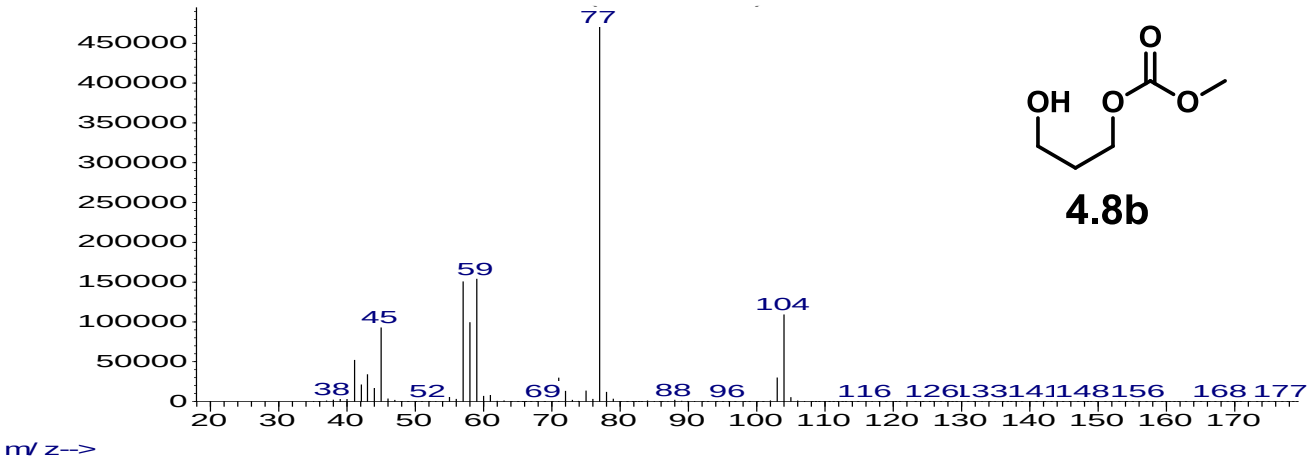

Figure A88. Mass spectra of **4.8b**

GC/MS (relative intensity, 70 eV) m/z: 134 (M^+, ≤1); 104.00 (22); 77.00 (100); 59.00 (31); 58.00 (20); 57.00 (30); 45.00 (19); 41.10 (10).

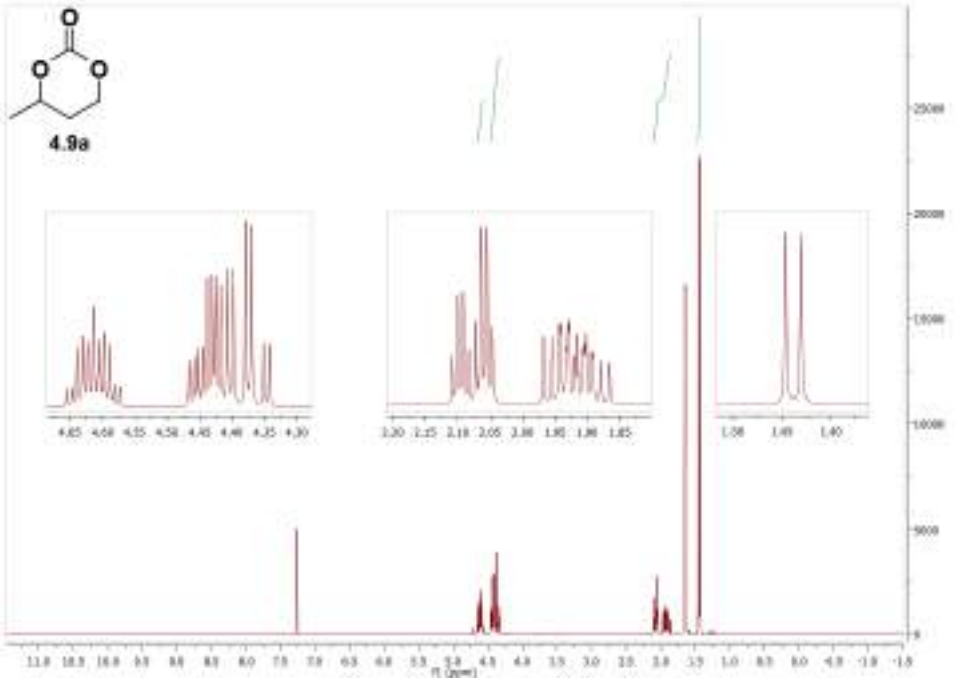

Figure A89. ^{1}H NMR of **4.9a**

^{1}H NMR ($CDCl_3$, 400 MHz) δ: 4.61 (m, 1H), 4.47 – 4.34 (m, 2H), 2.12 – 1.86 (m, 2H), 1.44 (d, *J* = 6.3 Hz, 3H).

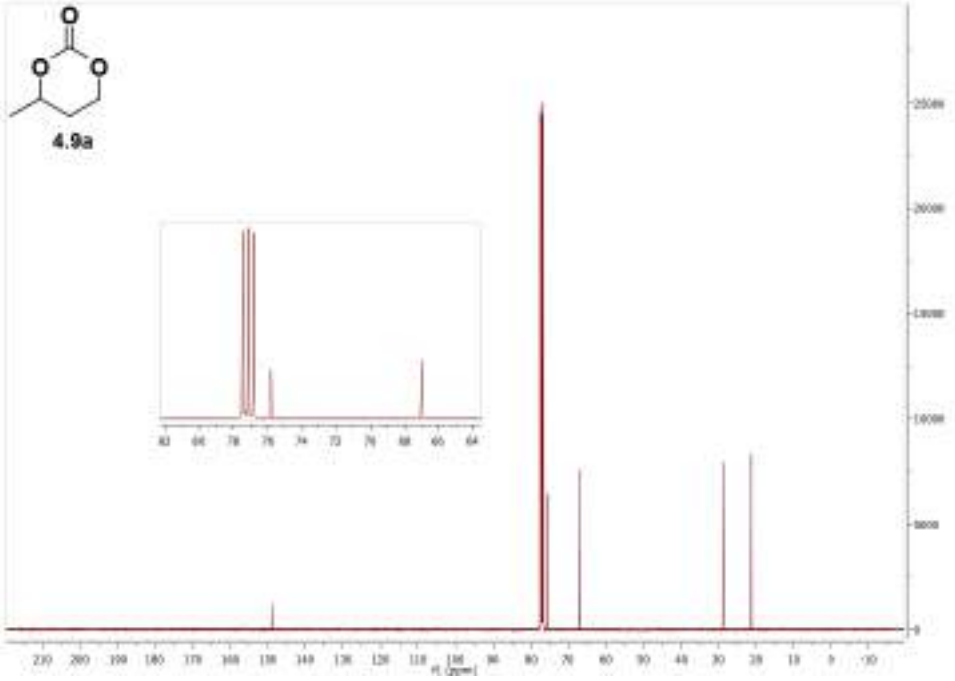

Figure A90. ^{13}C NMR of **4.9a**

^{13}C NMR ($CDCl_3$, 100 MHz) δ: 149.07, 75.83, 66.99, 28.81, 21.26.

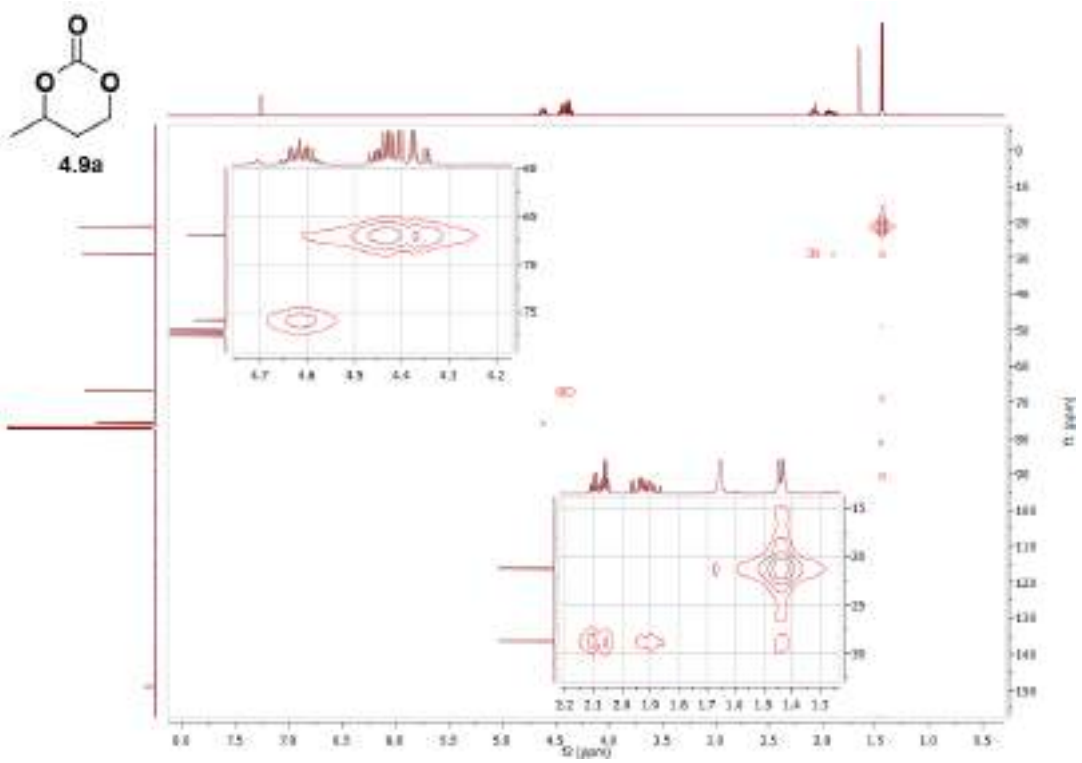

Figure A91. HMQC of **4.9a**

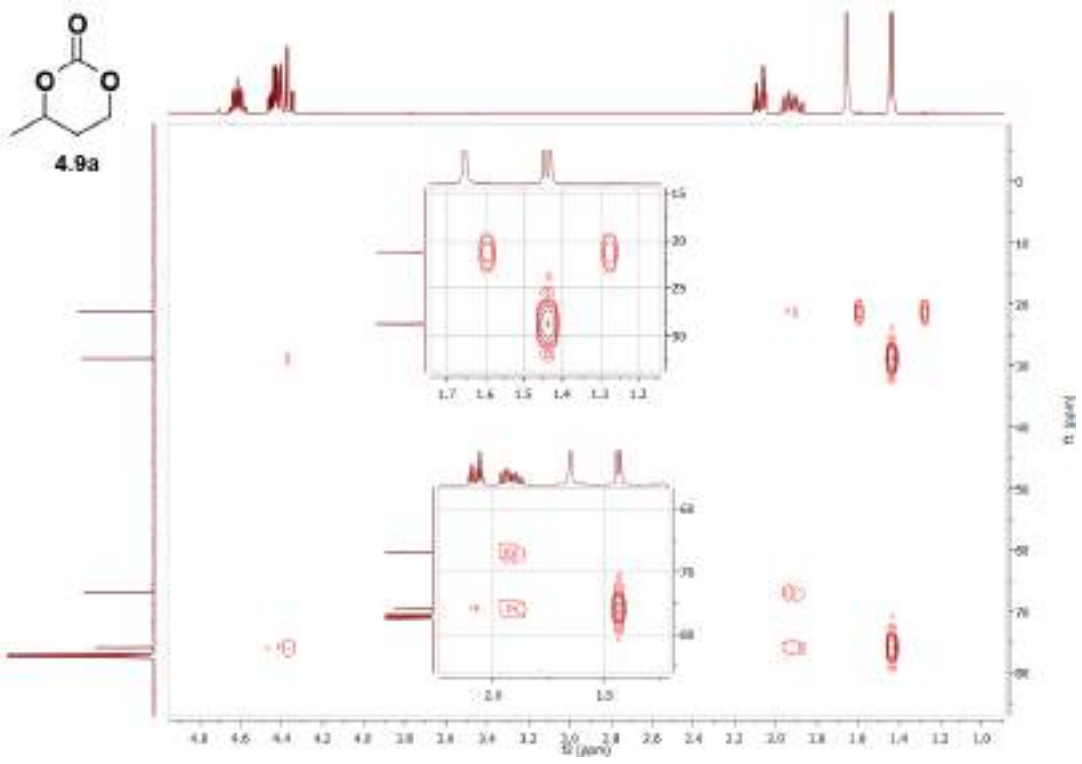

Figure A92. HMBC of **4.9a**

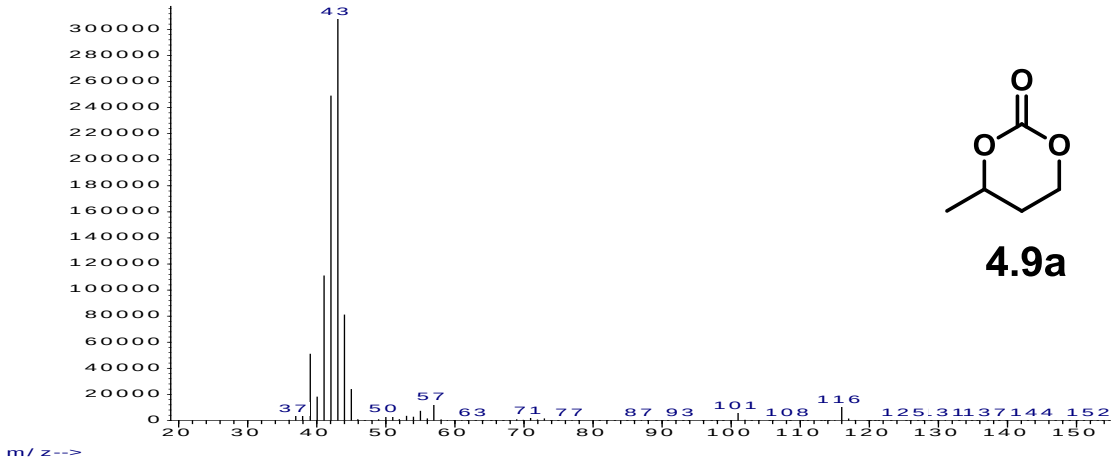

4.9a

Figure A93. Mass spectra of **4.9a**

GC/MS (relative intensity, 70 eV) m/z: 116.00 (M^+, 3); 44 (25); 43 (100); 42 (78); 41 (35); 39 (16).

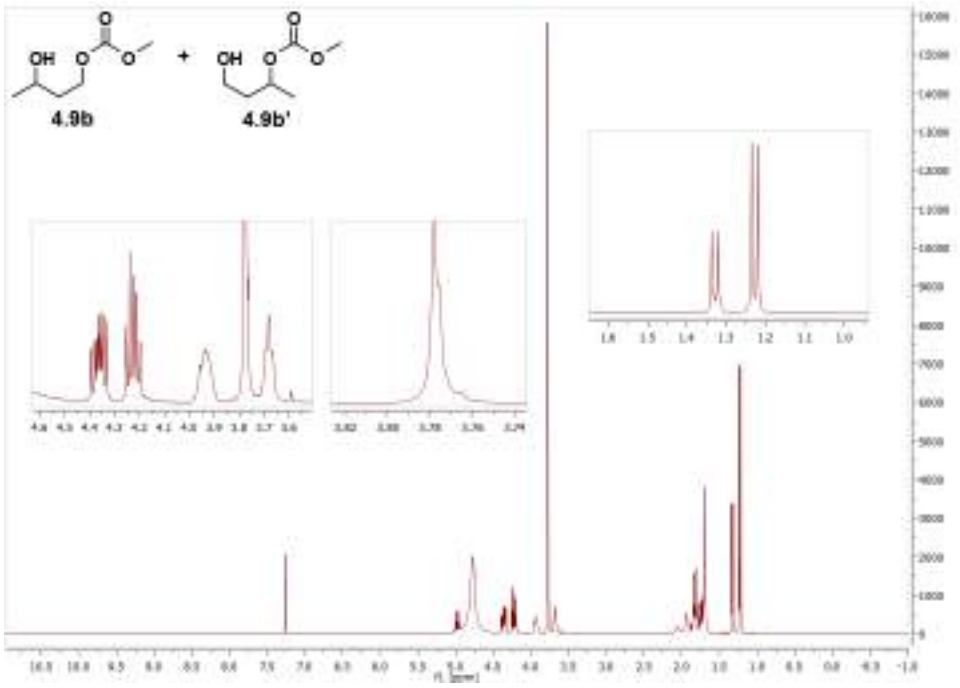

Figure A94. ^{1}H NMR of **4.9b+4.9b'**

Characteristic signals are the doublets of the methyl groups δ=1.35 – 1.2 and the two singlets of the methyl groups at almost the same δ = 3.78.

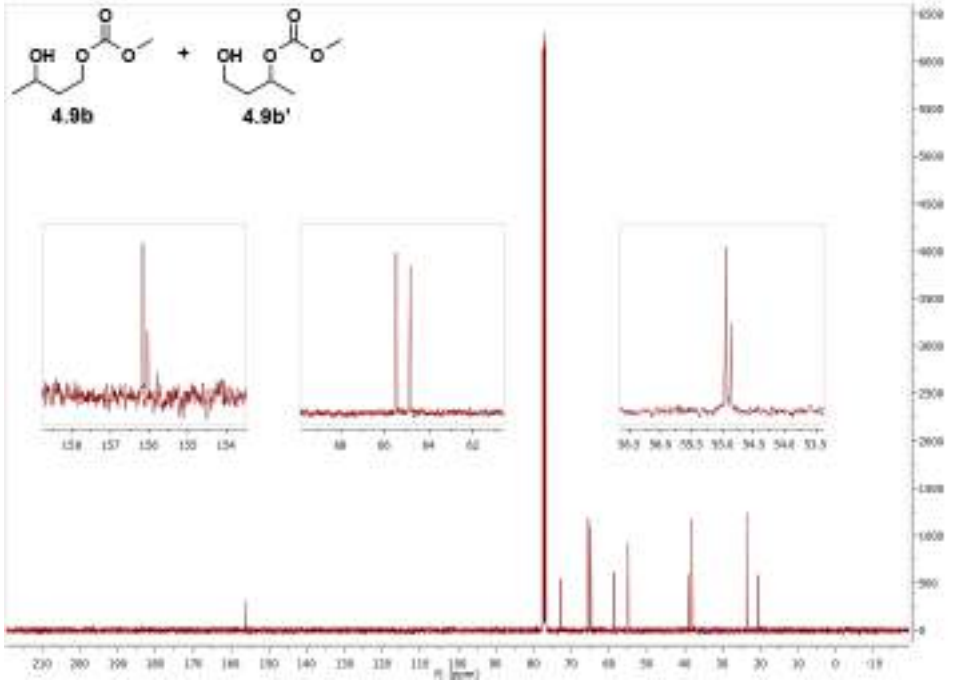

Figure A95. ^{13}C NMR of **4.9b+4.9b'**

^{13}C NMR ($CDCl_3$, 100 MHz) δ: 156.17, 156.04, 72.80, 65.48, 64.86, 58.90, 54.96, 54.87, 39.03, 38.08, 23.72, 20.47.

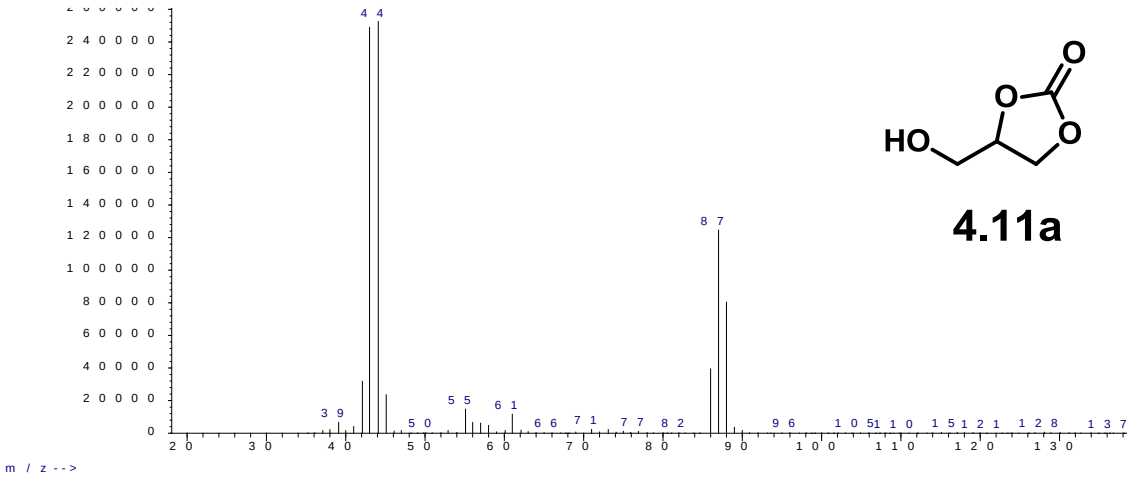

Figure A96. Mass spectra of **4.11a**

GC/MS (relative intensity, 70 eV) m/z: 118 (M+, ≤1); 88 (38); 87 (40); 86 (15); 45 (9); 44 (100); 43 (94).

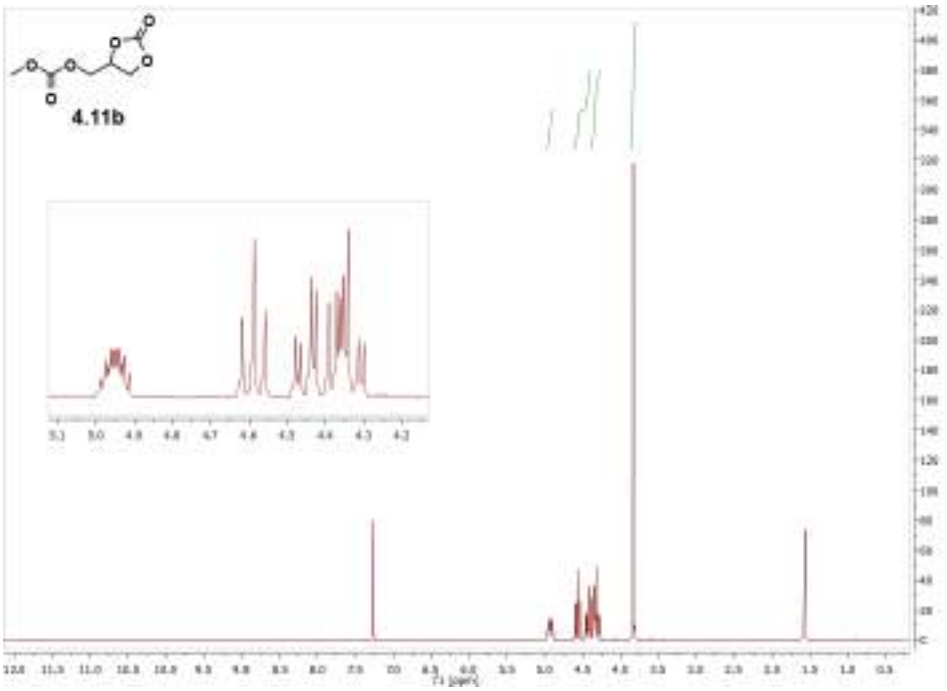

Figure A97. ^{1}H NMR of **4.11b**

^{1}H NMR ($CDCl_3$, 400 MHz) δ: 4.93 (m, 1H), 4.65 – 4.40 (t, 2H), 4.39 – 4.27 (m, 2H), 3.83 (s, 3H).

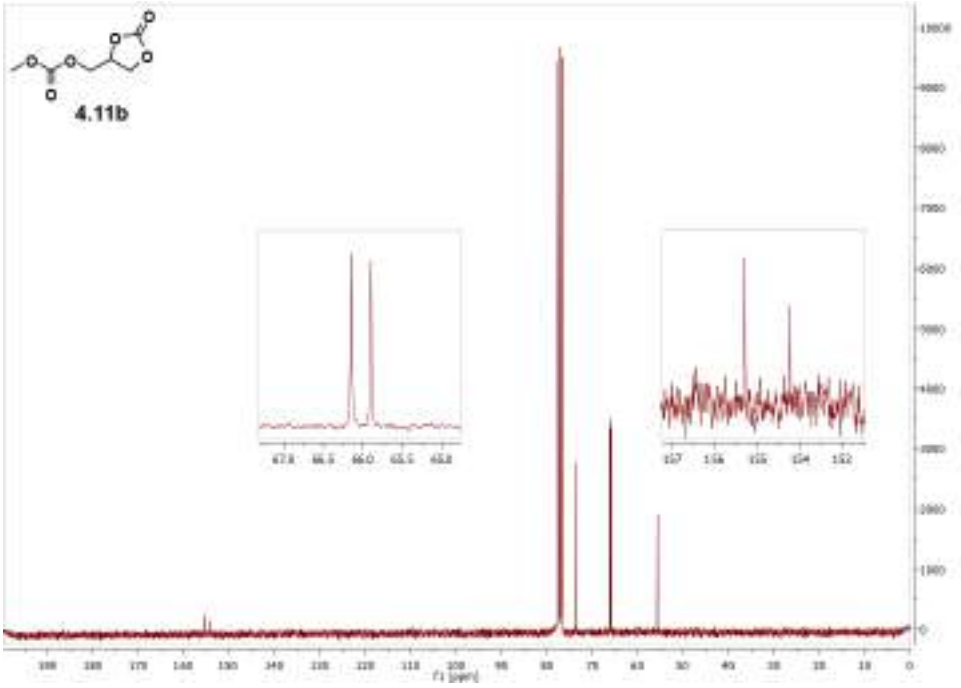

Figure A98. ^{13}C NMR of **4.11b**

^{13}C NMR ($CDCl_3$, 100 MHz) δ: 155.31, 154.24, 73.51, 66.15, 65.90, 55.61.

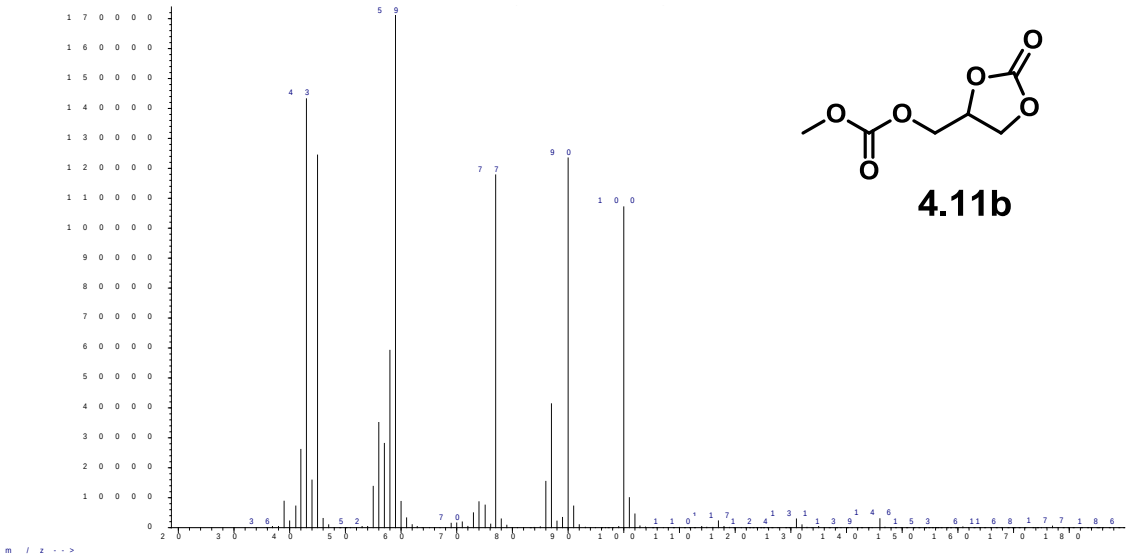

Figure A99. Mass spectra of **4.11b**

GC/MS (relative intensity, 70 eV) m/z: 176 (M+, ≤1); 100 (61); 90 (71); 87 (24); 86 (9); 77 (67); 59 (100); 58 (34); 57 (16); 56 (20); 55 (8); 45 (71); 44 (9); 43 (82); 42 (15).

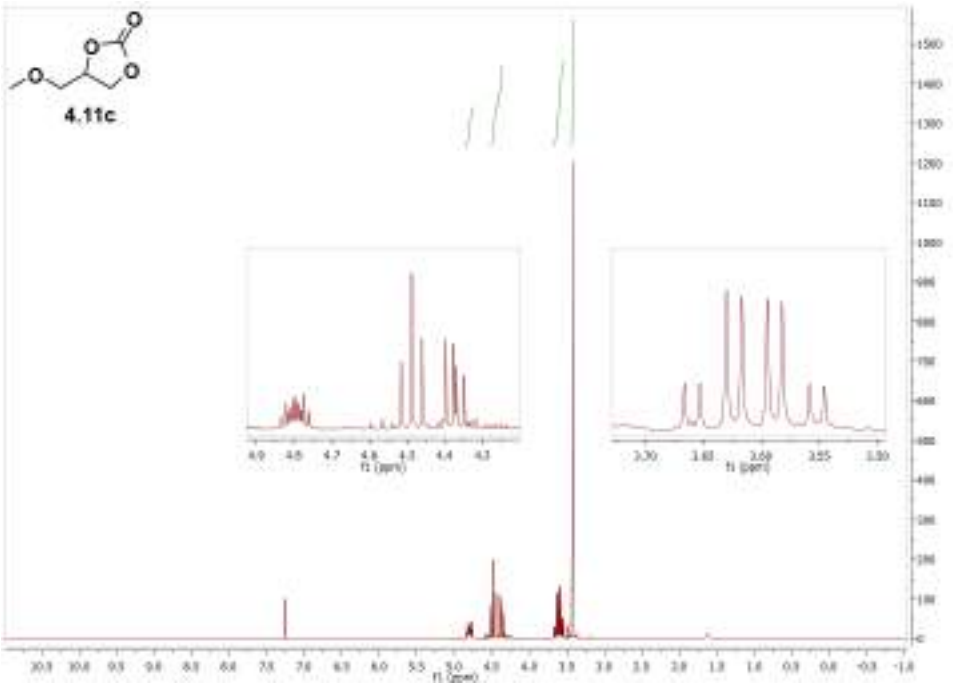

Figure A100. ^{1}H NMR of **4.11c**

^{1}H NMR ($CDCl_3$, 400 MHz) δ: 4.80 (m, 1H), 4.53 – 4.31 (m, 2H), 3.61 (m, 2H), 3.43 (s, 3H).

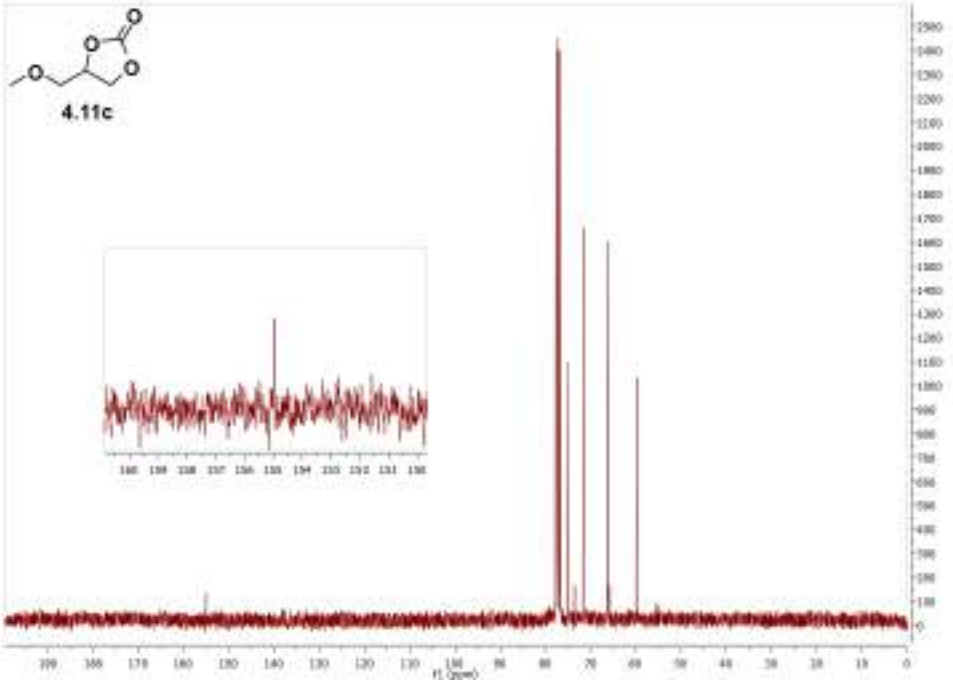

Figure A101. ^{13}C NMR of **4.11c**

^{13}C NMR ($CDCl_3$, 100 MHz) δ: 154.98, 75.05, 71.62, 66.32, 59.81.

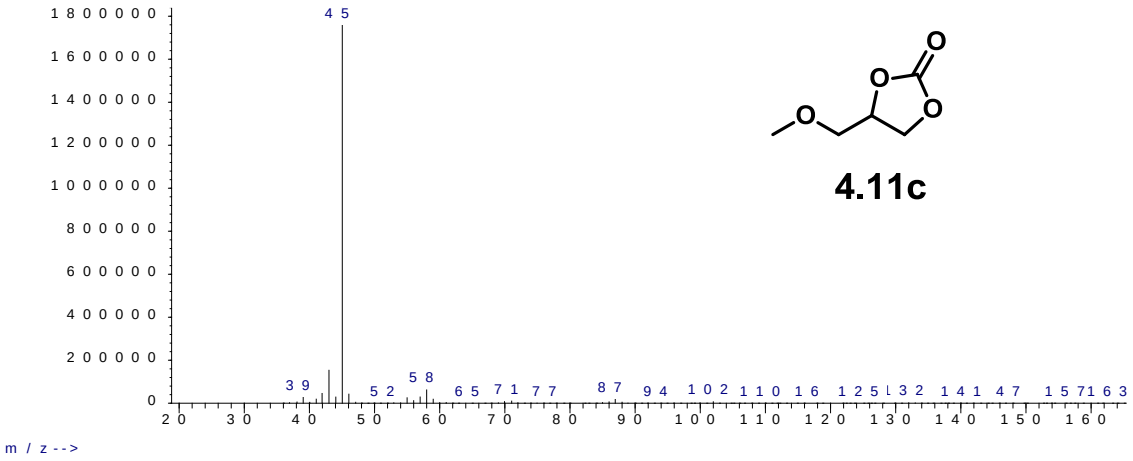

Figure A102. Mass spectra of **4.11c**

GC/MS (relative intensity, 70 eV) m/z: 132 (M+, ≤1); 45 (100); 43 (8).

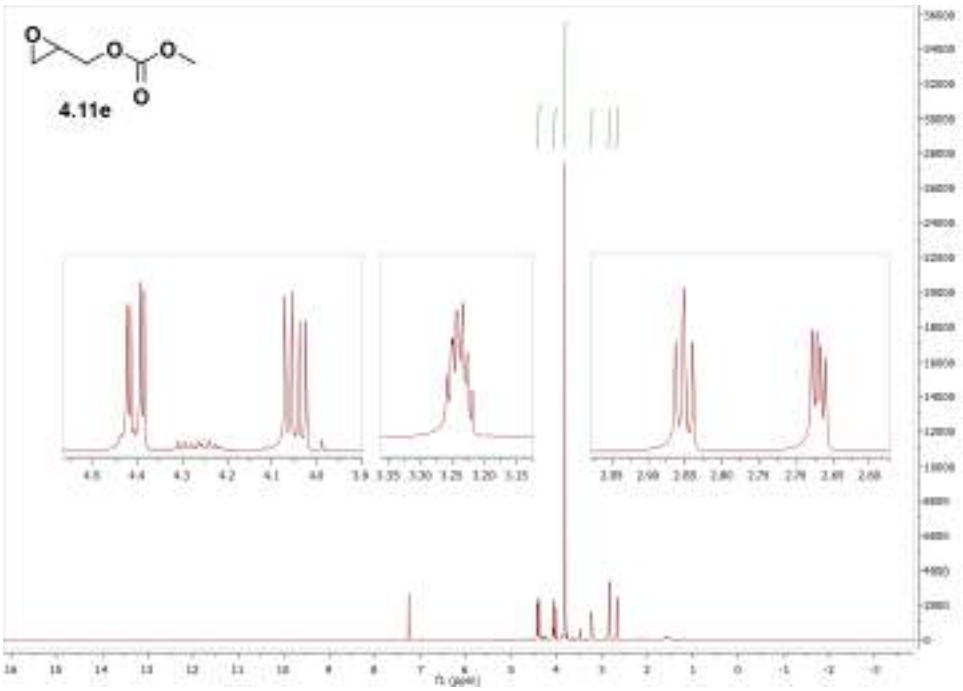

Figure A103. ^{1}H NMR of **4.11e**

GC/MS ($CDCl_3$, 400 MHz) δ: 4.40 (dd, J = 12.1, 3.3 Hz, 1H), 4.05 (dd, J = 12.0, 6.1 Hz, 1H), 3.83 (s, 3H), 3.27 – 3.21 (m, 1H), 2.85 (dd, J = 4.9, 4.1 Hz, 1H), 2.67 (dd, J = 4.9, 2.6 Hz, 1H).

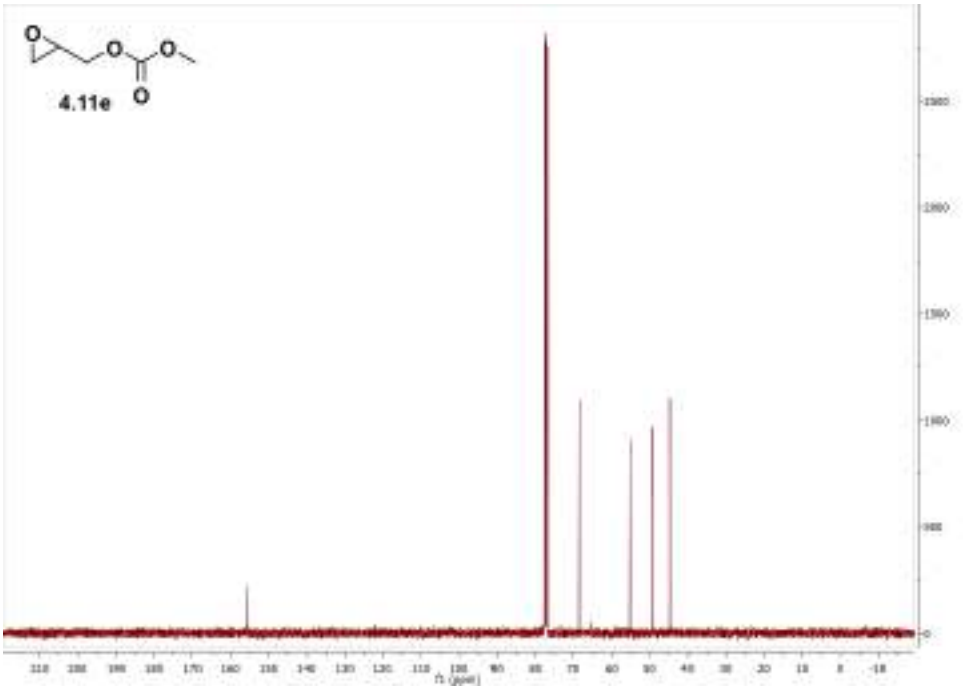

Figure A104. ^{13}C NMR of **4.11e**

^{13}C NMR ($CDCl_3$, 100 MHz) δ: 155.69, 68.39, 55.19, 49.18, 44.71.

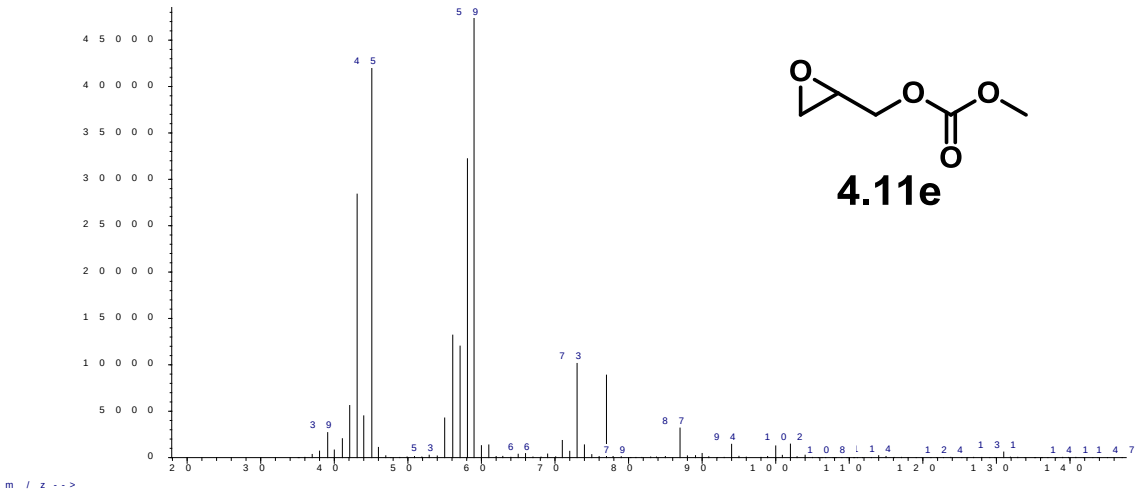

Figure A105. Mass spectra of **4.11e**

GC/MS (relative intensity, 70 eV) m/z: 132 (M+, ≤1); 77 (16); 73 (20); 59 (100); 58 (67); 57 (23); 56 (26); 55 (8); 45 (89); 44 (7); 43 (62); 42 (12).